Promotors:    Prof. dr. ir. Steven Sleutel

              Department Environment

              Faculty of Bioscience Engineering

              Ghent University, Belgium


              Prof. dr. Mohammed Abdul Kader

              Department of Soil Science

              Bangladesh Agricultural University

              Mymensingh, Bangladesh



Dean:     Prof. dr. ir. Marc Van Meirvenne

Rector:   Prof. dr. ir. Rik Van de Walle

Masuda Akter

# Linkage between subtropical paddy soil nitrogen supply and iron and manganese reduction

Thesis submitted in fulfilment of the requirements for the degree of Doctor (PhD) in Applied Biological Sciences

Dutch translation of the title:

Verband tussen stikstof levering in subtropische paddy rijstbodems en ijzer en mangaan reductie

Illustration on the front cover:

Landscape of wet season's paddy fields and experimental site (Melandoho)

## Acknowledgement

Ghent, November 2017
Masuda Akter

# <u>Table of Contents</u>

# Summary

Indigenous paddy soil nitrogen (N) supply dominantly meets lowland rice's N-requirement, with only 30-40% of seasonal uptake provided by applied fertilizers. Detailed insight into controls of organic N mineralization in paddy soils is then crucial to optimize N use efficiency and minimize adverse impacts of excessive N on the environment. Multifold soil properties and interconnected processes co-determine availability of indigenous soil organic matter (OM) for N mineralization. In paddy soils, the capacity for $Fe^{3+}$-reduction and release of dissolved OM in particular could form rate limiting steps for the mostly anaerobic microbial activity. But it is still unclear whether young floodplain paddy soils with greater reducible $Fe^{3+}$ and $Mn^{4+}$ contents, and higher capacity to release dissolved OM (soil OC) also manifest higher net anaerobic N mineralization. We hypothesized that SOC to $Fe_{ox}$ ratio would controls anaerobic microbial activity and net mineral N supply at different management scales in young floodplain paddy soils. In this PhD potential links between net anaerobic N mineralization and dominant reductive processes and release of dissolved OM are studied on different scales for young floodplain paddy soils of Bangladesh and Sri Lanka. Next to controlling edaphic properties also several management impacts on net soil N supply and soil reduction are investigated.

Firstly we assessed the impact of the contents of reducible Fe and Mn on anaerobic N mineralization in five young floodplain paddy soils of Bangladesh. The soils were either untreated, amended with $Fe_2O_3$, or with Mn/Al mixed oxides and incubated anaerobically for 8 to 10 weeks. We found that the availability of these electron acceptors (reducible Fe and Mn) did not limit soil exchangeable-$NH_4^+$ accumulation but it did display convergence with trends in solution Fe. As soil Fe amendments were found to not well represent pedogenic (hydr-)oxides, a second aim was to instead study the dependency of soil N supply on availability of reducible Fe and Mn using a set of soils displaying natural variation in these and other soil properties. A Sri Lankan paddy field, known to be spatially heterogeneous in terms of soil N, OC, silt, clay, $pH_{KCl}$, oxalate-extractable Fe ($Fe_{ox}$) and Mn ($Mn_{ox}$), was selected. In total 50 spots within the field were sampled and anaerobically incubated for 6 weeks. The rates of change of soil redox potential (Eh), solution Fe, Mn, dissolved organic C (DOC) and N (DON), and gaseous C-emissions following submergence were measured. Soil OC content and magnitude of DON-release had the best predictive power of anaerobic N mineralization exceeding that of $Fe_{ox}$ and $Mn_{ox}$. The absence of correlations between Fe-reduction and C-emission would suggest that Fe's availability as electron-acceptor was thus not a confounding bottleneck for soil OM degradation. Instead net mineralized N did correlate with pH rise, Fe dissolution rate, and released DON. These correlations jointly would suggest that DON at least in part stems from release upon reductive dissolution of pedogenic oxides and pH-rise driven

desorption. Hence, we postulate that soil reduction indirectly promotes net soil N release through these two processes.

From lab incubations in chapters 2 and 3 we neglected that plant N uptake, aerenchyma $O_2$ transport and root exudation all impact establishment of reductive conditions as well as accumulation of soil mineral N. In a third step the linkage between mineral N release and reduction of $Fe^{3+}$ and $Mn^{4+}$ was investigated in soil with growing plant. Transplanted rice was grown for 72 days firstly under continuous and later on intermittent flooding in the greenhouse in four Bangladeshi paddy soils. Mössbauer spectroscopy revealed ferrihydrite and goethite in all four soils to be likely source minerals of dissolved Fe after reduction. An electron ($e^-$) balance calculation with $e^-$ donation based on total C-emission rates suggested reductive Fe and Mn dissolution to be lesser $e^-$ accepting processes. However, removal of dissolved $Fe^{2+}$ via exchange with $Ca^{2+}$ and $Mg^{2+}$ and precipitation with carbonates, phosphates and sulphates were not taken into account. Ion exchange was indeed confirmed to be large in these soils in ancillary anaerobic incubation experiments. We estimated that initial $e^-$ balance calculations likely underestimated pedogenic-$Fe^{3+}$ reduction by a factor two and then its importance as $e^-$ accepting process was confirmed. Most soil $Fe^{3+}$ was present in chlorites, vermiculite and their interstratified forms. We postulate that biogenic phyllosilicate Fe reduction could also have supported anaerobic microbial activity. During the flooding phase again a close synchrony was found between solution Fe and soil exchangeable N. The rate of net mineral N supply in these four Bangladeshi paddy soils positively correlated with solution Fe release rate but, unlike in Chapter 3, not with soil OC and N. Also, the rates of solution Fe release and net soil mineral N supply were positively related to release rates of DOC and $CO_2+CH_4$-C emission rates. Both observations make that we could not conclude if net soil N supply was tied directly to Fe-reduction, i.e. as $e^-$-acceptation process or indirectly, i.e. via co-release of DOM upon reductive dissolution of pedogenic Fe. A combination of both seems likely.


The strong controls of solution Fe and DOC release rates on net mineral N supply during earlier (2-4 weeks) flooding with still minor plant N demand (Chapter 4) may or not exist in field set-ups throughout a rice growing season. In the field with more heterogeneity soil mineral N supply may also strongly be influenced by rice plant growth and varying management and changing environmental factors, next to solution Fe and DON release. Furthermore, rice plant's N and soil mineral N status at different growth stages may impact net mineral N supply from soil and fertilizer, and N fertilizer use efficiencies at real field-scale. As a next step, in Chapter 5 the co-evolution of soil net mineral N supply with release of solution Fe and DON, as well as N fertilizer use efficiencies were investigated for a set of farmers' fields *in-situ*.

During the 2016 Aman (wet) season 6 field experiments were conducted in north-central Bangladesh with or without urea application. Synchronous asymptotic rises in soil exchangeable $NH_4^+$-N, solution Fe, Mn and DON were re-confirmed and among the 6 soils, large variation existed in net seasonal mineral N supply (inferred from soil + plant N). The latter positively correlated with %silt, $Fe_{ox}$, SOC, TN, and DON, while DON was found to strongly correlate with soil $NH_4^+$-N per time step and with TN overall. Hence, next to soil OM content, level of DON and reducible Fe ($Fe_{ox}$), indicative of OM quality and availability of alternative $e^-$ acceptors, respectively, were predictors of net soil N supply. N fertilizer recovery ($RE_N$), agronomic ($AE_N$) and physiological ($PE_N$) efficiencies were neither influenced by net mineral N supply nor by plant available P, K, Fe and Mn. So, other constraints to rice growth than N availability, such as differences in water supply, insect-pest and disease management between the six investigated fields likely overridingly controlled N use efficiencies. The unresponsiveness of soil exchangeable $NH_4^+$-N and DON to N-fertilization demonstrates the quick storage of fertilizer N in other N pools, likely in equilibrium with plant available N.

Finally, in Chapter 6 we investigated impact of three irrigation managements on depth profiles of soil moisture and Eh, reductive dissolution of Fe and Mn, and gross microbial activity and relations with net soil N-supply in a young floodplain paddy field. Despite some fluctuations in puddle layer's Eh, the solution C, Fe and Mn, total C emission, net soil N-supply and yield remained comparable under alternate wetting and drying (AWD) and continuous flooding (CF). More aerobic conditions under direct seeded rice (DSR) lead to a nearly doubled net C-emissions and lower net soil N-supply compared to AWD and CF. A higher fertilizer N recovery efficiency was found for CF (42%) than AWD (32%) and DSR (25%). This single season's outcome suggests that in terms of N availability and soil OM degradation, AWD could be safely adopted for rice cultivation during dry (Boro) season in Bangladesh, but long-term adoption of AWD requires more research.

In conclusion, the most likely processes responsible for co-buildup of solution Fe and DOC or DON are the release of OM bound to Fe(hydr-)oxides or mineral surfaces through Fe-reductive dissolution and/or by pH rise. However, because of multiple parallel unconsidered relations between pedogenic Fe reduction and soil N transformations, it was not yet possible to infer causality. Use of ^{15}N-labeled DON bound to pedogenic Fe would elucidate the relevance of reductive Fe and Mn dissolution as intermediate step to final soil net N supply. The relevancy of reduction of octahedral $Fe^{3+}$ in chlorites, vermiculite and their interstratified forms also needs to be confirmed. Clay interlayer $NH_4^+$ defixation's contribution to net soil N supply and on the opposite its role in removal of added fertilizer N was not clarified yet for Bangladeshi paddy

soils and still needs to be experimentally assessed with $^{15}$N-labeling of the fixed $NH_4^+$-pool. In sum, while pedogenic Fe reduction was not found to form a bottleneck for microbial activity, it still appears to co-determine net soil N supply via co-release of dissolved OM. A soil's ability to provide DON, indicative of soil OM quality and bio-availability was a predictor of net soil N supply for young floodplain Bangladeshi paddy fields. Lastly, the resilience of soil exchangeable $NH_4^+$ pool to major shifts in management like N-fertilizer application and change of irrigation scheme demonstrates that net paddy soil N supply cannot be entirely assessed by mere follow up of extractable mineral N. A full understanding only emerges from assessment of seasonal dynamics in various soil N pools in presence of growing rice.

# Samenvatting

De bodem stikstof (N) levering vanuit paddy rijstbodems vervult in hoofdzaak de N-behoefte van rijst aangezien slechts 30-40% van de opgenomen N afkomstig is uit toegediende meststoffen. Bijgevolg kan een beter inzicht van te verwachten seizoen organische N mineralisatie en daartoe bepalende factoren leiden tot een beter bemestingsbeheer met hogere efficiëntie van N-mestoffen en verminderde negatieve impact van overmatige N op het milieu.

Een waaier van bodem eigenschappen en onderling verbonden processen bepalen samen de mate waarin bodem organische stof (OS) wordt afgebroken met netto N mineralisatie als gevolg. De reduceerbaarheid van aanwezig driewaardig ijzer ($Fe^{3+}$) en de aanleg tot voorziening van opgeloste organische stof (DOM) zouden in het bijzonder beperkende processen kunnen vormen voor de voornamelijk anaerobe microbiële activiteit. Het is echter niet uitgeklaard of in jonge alluviale rijstbodems de anaerobe N mineralisatie daadwerkelijk hoger ligt met toenemend reduceerbaar $Fe^{3+}$ en ook $Mn^{4+}$. We veronderstellen dat de verhouding van bodem organische koolstof tot zwak kristallijn Fe (bodem $OC:Fe_{ox}$) bepalend is voor de anaerobe microbiële activiteit in en de N levering van deze bodems. In huidig proefschrift volgt een studie van de mogelijke verbanden tussen de netto minerale N levering, de belangrijkste reducerende processen en vrijstelling van DOM voor jonge alluviale rijstbodems uit Bangladesh en Sri Lanka op toenemende schaal (labo, potproeven, veldproeven). Naast de mediatie van bodemeigenschappen wordt ook de invloed van beheer (bemesting, irrigatie) op bodem N levering en redox processen onderzocht.

Eerst werd de beïnvloeding van de beschikbaarheid van reduceerbaar Fe en Mn op de bodem N levering bekeken in vijf jonge alluviale bodems uit Bangladesh. Hematiet ($Fe_2O_3$) of gemengde Mn/Al-oxiden werden toegediend en behandelde en controle bodems werden vervolgens 8 tot 10 weken anaeroob geïncubeerd. We vonden geen effect van de beschikbaarheid van deze alternatieve $e^-$ acceptoren op accumulatie van uitwisselbaar-$NH_4^+$, welke echter wel een synchroon verloop vertoonde met opgelost Fe (Hoofdstuk 2). Aangezien toediening van welke Fe vorm dan ook steeds slechts bij benadering een bodem met overeenkomstig hoger gehalte aan Fe-(hydr-)oxiden kan nabootsen was deze proefopzet niet geheel sluitend (oplosbaarheid en reduceerbaarheid van het toegediende Fe lag veel lager dan in situ in rijstbodems). Daarom werd een alternatieve opzet uitgewerkt met gebruik van natuurlijke variatie van pedogeen Fe en Mn bij gelijk beheer. Daartoe werden 50 afzonderlijke locaties van een gekend ruimtelijk heterogeen perceel in Sri Lanka (in bodem N, OC, leem%, klei%, $pH_{KCl}$, $NH_4$-oxalaat-extraheerbaar Fe ($Fe_{ox}$) en Mn ($Mn_{ox}$)) bemonsterd. Deze bodems werden vervolgens bij continue bevloeiing geïncubeerd gedurende 6 weken. Veranderingen

in bodem redox potentiaal (Eh), opgelost Fe en Mn en OC (DOC) en N (DON) werd naast gasvormige C-emissies opgevolgd. Bodem OC gehalte en mate van DON vrijstelling bleken de beste voorspellers van netto bodem minerale N levering, beter dan $Fe_{ox}$ en $Mn_{ox}$. Het gebrek aan een correlatie tussen Fe-oplossing door reductie en C-emissie duidt erop dat de beschikbaarheid van reduceerbaar Fe geen bepalende beperking vormde voor bodem OC afbraak. Er bestonden daarentegen wel correlaties tussen opgemeten pH-stijgingen, hoeveelheid vrijgesteld DON en de snelheid aan Fe-vrijstelling. Deze gezamenlijke correlaties suggereren ten minste dat DON ten dele werd vrijgesteld door reductieve oplossing van pedogeen Fe en voordien geboden OM of uit desorptie van DON door pH toename. We veronderstellen dus dat Fe-reductie bodem minerale N vrijstelling indirect bevordert langsheen deze twee omwegen.

In hoofdstukken 2 en 3 werd geen rekening gehouden met de normaal simultaan voorkomende N opname door de plant, met de aanvoer van $O_2$ langsheen het aerenchym en met wortelexudatie. Al deze processen kunnen zowel het plaatsvinden van reductiereacties in de bodems als de accumulatie van minerale N beïnvloeden en een heel wat realistischere proefopzet kan simpelweg gerealiseerd worden door uitvoeren van incubaties met groeiende rijstplanten. In hoofdstuk 4 werd het verband tussen netto minerale N levering en reductie van $Fe^{3+}$ en $Mn^{4+}$ verder bekeken in rijst potproeven in de serre. Rijst werd getransplanteerd in vier verschillende paddy bodems uit Bangladesh en gedurende 72 dagen geteeld onder eerst continue en daarna onderbroken bevloeiing. Mössbauer spectroscopie toonde aan dat ferrihydriet en goethiet in alle bodems de meest waarschijnlijke bronmineralen van opgelost Fe na reductie zouden moeten zijn. Een electronen ($e^-$) balans werd opgemaakt met $e^-$ donatie afgeleid uit bodem C-emissies. Deze ramingen wezen vooreerst aan dat pedogeen Fe en Mn slechts beperkt fungeerden als $e^-$ acceptor. Echter verwijdering van opgelost $Fe^{2+}$ door uitwisseling van $Ca^{2+}$ en $Mg^{2+}$ en neerslag met carbonaat, fosfaat en sulfaat werd daarbij niet verondersteld. Uit latere bijkomstige proeven bleek de $Fe^{2+}$ uitwisseling met ionen op bodemcolloïd oppervlakten echter substantieel en bijgewerkte $e^-$ balansen bevestigen dat een aanzienlijk deel van de bij anaerobe microbiële activiteit gedoneerde $e^-$ wel degelijk resulteerden in reductie van pedogeen $Fe^{3+}$. De initiële $e^-$ balansen onderschatten dit aandeel van pedogeen Fe reductie met een factor 2. Het meeste $Fe^{3+}$ was in de bodem echter aanwezig onder de vorm van structureel Fe in chloriet, vermiculiet en gelaagde vormen van beide. We postuleren dat gezien de niet sluitende $e^-$ balans met meename van meest gangbare terminale $e^-$ acceptoren en het algemeen voorkomen van phyllosilicaat $Fe^{3+}$ de biogene reductie daarvan ook ten dele anaerobe microbiële activiteit faciliteert in de bestudeerde bodems. In hoofdstuk 4 constateerden we weer een dichte gelijkenis tussen het verloop van opgelost Fe en uitwisselbaar $NH_4^+$. De reactiesnelheden van beide processen

correleerden onderling en tevens met vrijstelling DOC en emissie van $CO_2$ en $CH_4$, maar in tegenstelling tot hoofdstuk 3 niet met het bodem OC en N gehalte. Uit het geheel van deze observaties kan echter nog steeds niet besloten worden of het verband tussen bodem N voorziening en Fe-reductie direct is, langsheen de betrokkenheid van $Fe^{3+}$ als $e^-$ acceptator, of indirect via gelijktijdige vrijstelling van DOM bij reductie van pedogeen Fe. Wellicht echter opereren beide mechanismen.

De uit voorgaande hoofdstukken gesuggereerde controle van Fe reductie en DOM op netto bodem minerale N vrijstelling relatief kort na bevloeiing (2-4 weken) met slechts beperkte gewasopname kan al dan niet bestaan in het veld gedurende een teeltseizoen. Bij vergelijking van veldpercelen zal er daartussen een grotere variatie bestaan in toegepast beheer per perceel, in bodemcondities en omgevingsfactoren (zoals Fe end DON oplossing) en in de groei van de rijstplant. Bovendien zal het tijdsverloop in gewas N opname en bodem uitwisselbaar N verschillen tussen velden en dit kan dan ook een invloed hebben op N-meststof efficiëntie en netto bodem N levering. Daarom werd in hoofdstuk 5 de analyse van de co-evolutie van minerale N, opgelost Fe en DON uitgebreid naar veldschaal, naast een studie van de N-bemestingsefficiëntie van ureum. Tijdens het natte Aman seizoen werden 6 veldproeven uitgevoerd in centraal Noord-Bangladesh steeds met of zonder toediening van 60 of 80 kg N $ha^{-1}$ onder de vorm van ureum. Het gelijktijdig asymptotisch verloop van uitwisselbaar $NH_4^+$-N, opgelost Fe, Mn en DON werd herbevestigd in de 6 percelen, zij het met onderlinge verschillen in netto seizoen N levering afgeleid uit de som van bodem $NH_4^+$ en plant N. De netto N levering correleerde positief met leem%, $Fe_{ox}$, bodem OC en N en gemiddelde DON concentratie, waarvan het tijdsverloop eveneens correleerde met uitwisselbaar $NH_4^+$-N. Bijgevolg bleken de gehalten aan DON gehalte en reduceerbaar Fe, indicatief voor OM kwaliteit en beschikbaarheid van $e^-$ acceptoren, voorspellers van netto bodem N levering. De N-opname ($RE_N$), agronomische ($AE_N$) and fysiologische ($PE_N$) efficiëntie werden noch door netto bodem N levering noch door bodemgehalten aan P, K, Fe en Mn bepaald.  Bijgevolg werd de N-gebruiksefficiëntie bepaald door andere beperkingen op rijstgroei dan N beschikbaarheid, zoals verschillen tussen de percelen in beschikbaarheid van water voor irrigatie en beheer van insectplagen en plantenziekten. De beperkte invloed van N-bemesting op verloop van uitwisselbaar $NH_4^+$-N en DON demonstreren de snelle overdracht van N uit toegediende meststof naar niet gemeten bodem N fracties die zich in een evenwicht bevinden met uitwisselbaar $NH_4^+$-N.

Tenslotte onderzochten we in Hoofdstuk 6 de impact van irrigatie schema op de diepte verdeling van bodem vocht, Eh, oplossing van Fe en Mn door reductie, bodem microbiële activiteit, en verbanden met de netto bodem minerale N levering d.m.v. een veldproef. Ondanks fluctuatie van Eh in de bouwvoor bij niet-continue irrigatie 'alternate wetting and

drying (AWD)', bleven het verloop van opgeloste C, Fe en Mn, de bodem $CO_2$ en $CH_4$-emissie en de netto bodem minerale N-levering ongewijzigd t.o.v. permanent bevloeide percelen. De meer aerobe toestand van de bodem bij directe inzaai 'direct seeded rice (DSR)' leidde tot een bijna verdubbelde bodem C-emissie en een verminderde netto minerale N levering t.o.v. AWD en CF. De N-bemestingsefficiëntie was groter in geval van CF (42%) en verminderde bij AWD (32%) en DSR (25%) irrigatie. De uitkomst van huidig veldexperiment suggereren bijgevolg dat AWD tijdens het Boro seizoen kan worden geïmplementeerd zonder negatieve invloed op bodem N levering en bodem OC afbraak. Deze resultaten zijn slechts gebaseerd op één groeiseizoen en de lange-termijn invloed van AWD vergt dus nog voortgezet onderzoek.

In conclusie zijn de stijging in pH en oplossing van pedogeen Fe de meest waarschijnlijke mechanismen die leiden tot gezamenlijke accumulatie van opgelost Fe en DOC en DON. Maar causaliteit kon nog niet worden aangetoond ten gevolge van het parallel voorkomen van een aantal niet-begrootte linken tussen N transformaties en Fe reductie. Het gebruik van ^{15}N-gelabeled DON eerst gesorbeerd aan pedogeen Fe zal vereist zijn om onweerlegbaar het belang van Fe-oplossing door reductie aan te tonen als tussenstap binnen het globale N mineralisatie proces. De relevantie van reductie van $Fe^{3+}$ in chlorieten, vermiculiet en hun onderling gelaagde vormen moet nog worden bevestigd. De bijdrage $NH_4^+$ defixatie uit de klei inter-lammelaire ruimte tot netto bodem minerale N levering vergt eveneens verdere opmeting daarvan gedurende gehele groeiseizoenen. Ook de rol van dit proces in de meestal plotse verwijdering van N uit meststoffen zou moeten worden uitgeklaard a.d.h.v. proeven met ^{15}N-gemerkte meststof en opvolging van de opname en afgifte daarvan.

We concluderen dat reductie van pedogeen Fe geen beperking vormt voor algemene microbiële activiteit in jonge alluviale paddy rijstbodems van Bangladesh, maar dat dit proces wel medebepalend is voor netto N-levering langsheen de gekoppelde vrijstelling van DOM. Bijgevolg blijkt het vermogen van een bodem om DON te leveren, indicatief voor de bio-beschikbaarheid van bodem OM, een voorspeller te zijn voor netto N levering aan rijst in deze bodems. Tenslotte toont het gebrek aan respons van het uitwisselbaar $NH_4^+$ bij toediening van minerale N via bemesting in tegenstelling tot plant N-opname nogmaals aan dat de netto N levering uit rijstbodems niet gecapteerd kan worden door de klassieke opvolging van extraheerbaar minerale N. Een beter begrip kan enkel resulteren uit bepaling van de dynamiek van meerdere betrokken bodem N poelen (DON, microbiële N, gefixeerde N, uitwisselbare N, plant opgenomen N), steeds in aanwezigheid van groeiende rijst.

## List of abbreviations and symbols

BAU — Bangladesh Agricultural University

BRRI — Bangladesh Rice Research Institute

AEZ — Agro-ecological zone

SOM — Soil organic matter

SOC — Soil organic carbon

TN — Total N

$NH_4^+$ — Ammonium

$NO_3^-$ — Nitrate

$Fe^{3+}$ — Ferric iron

$Fe^{2+}$ — Ferrous iron

$Mn^{3+/4+}$ — Manganic ion

$Mn^{2+}$ — Manganous ion

DOC — Dissolved organic carbon

DOM — Dissolved organic matter

DON — Dissolved organic nitrogen

MBC — Microbial biomass carbon

MBN — Microbial biomass nitrogen

Eh — Redox potential

CBD — Citrate bicarbonate dithionite

$Fe_{ox}$ — Ammonium-oxalate extractable Fe

$Mn_{ox}$ — Ammonium-oxalate extractable Mn

RSMS — Rhizon soil moisture sampler

$CO_2$ — Carbon dioxide

$CH_4$ — Methane

CEC — Cation exchange capacity

$N_t$ — Modeled mineral N or DON amount in soil plus plant (mg kg$^{-1}$) at 't' days

$N_a$ — Amount of potentially mineralizable N (mg kg$^{-1}$)

$k_f$ — First-order N mineralization rate constant

$k$ — Zero-order N mineralization rate constant

HYV — High yielding variety

AWD — Alternate wetting and drying

DSR — Direct seeded rice

CF — Continuous flooding

# Chapter 1
## General Introduction

## 1.1. Rice production and its role in food security of South Asia and Bangladesh

Agriculture is traditionally a dominant sector in South Asian economy, employing about 60% of the labor force and contributing 22% of the regional GDP (Bishwajit et al., 2013). Rice is staple food for the majority of 1.7 billion (~70%) South Asian people and a basis of livelihood for more than 50 million households. Besides, rice provides 60-70% of calories and 50-55% of protein intake for South Asian people, hence rice security in this region is necessarily a reflection of food security. Rice production in South Asia has risen three times since the start of the Green Revolution in late 1960s, and currently it is the world's second largest rice producing region (Bishwajit et al., 2013). In this region rice is grown on 60 million ha land and produced around 225 million tons paddy in 2013, accounting for 37.5% and 32% global rice area and production, respectively (http://irri.org/rice-today/rice-in-south-asia). Bangladesh is also an agrarian country where agriculture contributes 19.3% of the country's gross domestic product (GDP) and agricultural activities involve about 48% of the total manpower (Shelley et al., 2016). Bangladesh has a long history of rice farming because the country's climatic conditions (rainfall, temperature) appropriate year-round rice cultivation. Rice is grown throughout the country except in the southeastern hilly areas. Among the South Asian countries, Bangladesh is one of the largest producers and consumers of rice with high per capita consumption (153 kg rice person$^{-1}$ year$^{-1}$) and is ranked the world's 6th largest rice producer (Bishwajit et al., 2013).

Despite an increasing Asian rice production the projected population will exceed two billions by 2030, with 300 million additional mouths to feed. Rice production in Bangladesh has also tripled from 1971-72 to 2013-14 (Fig. 1.2A), and the country has recently reached self-sufficiency in rice production (Shelley et al., 2016). However, the cultivable land is declining at a rate of 1% year$^{-1}$ due to construction of industries, factories, houses, roads and highways, and there is no possibility of horizontal expansion by bringing new area under rice cultivation (Shelley et al., 2016). Furthermore population growth rate is 2 million year$^{-1}$ and if such rate will continue, the expected population will be 238 million by 2050. Hence, demand for rice is continually increasing and being met from limited resources. Moreover, Bangladesh, India and Sri Lanka are disaster prone-countries and rice production is affected greatly by recurrent or erratic floods, cyclones, earth quake, landslides and drought. Many other uncertainties like growing water shortages, imbalanced fertilization, competition of rice land with nonagricultural uses and biofuel crops, increasing frequency of extreme weather, and emerging pest outbreaks due to climate change aggravate the situation. Self-sufficiency in rice production will be of crucial importance for national food security in several South Asian countries, including Bangladesh. Combination of appropriate policy reforms,

development and dissemination of resource-conserving technologies such as climate-smart rice varieties (e.g. flood, drought, and salinity tolerant), improved management practices including site-specific nutrient management, water-saving irrigation management, and direct-seeded rice need to ensure food security at present and future.

## 1.2. Present status of rice cultivation in Bangladesh

*1.2.1. Agro climatic conditions (rainfall and temperature), rice seasons, calendar and cultivars*

Bangladesh is located in the sub-tropical monsoon climatic regime between 20.57ºN to 26.63ºN and 88.02ºE to 92.68ºE (Khatun et al., 2016). The climate is characterized by wide seasonal variations in rainfall, moderately warm temperatures (Fig. 1.1A) and high humidity with less regional differences. Annual mean precipitation is 2498 mm, unevenly distributed across seasons (Rahman, et al., 2012). Four meteorological seasons are recognized: summer or pre-monsoon (Mar-May), southwest monsoon (Jun-Sep), autumn or post-monsoon (Oct-Nov) and winter or northeast monsoon (Dec-Feb). The pre-monsoon season is characterized by a mean temperature of 23-30°C (Fig. 1.1 A) and occurrence of only 19% of total annual rainfall, though the highest maximum temperature varied from 36-40ºC in northwestern and southwestern districts. The monsoon season typically represents more than 71% of total annual rainfall with widespread cloud coverage and high humidity. The post-monsoon season is a transition between the summer monsoon and winter with substantial declines in rainfall (incidence of only 8% of total annual rainfall) and temperature (Fig.1.1A), with minimum temperature generally still above 10°C. The winter is characterized by a mild temperature (18-22°C), dry weather, clear to occasionally cloudy sky with fog, and incidence of only 2% of total annual rainfall (Khatun et al., 2016). Rice cultivation in Bangladesh is generally focused into three season, viz. Aus, **Aman** and **Boro**, and grown under four ecosystems viz. irrigated rice (Boro), rain fed or partially irrigated (transplanted Aus and Aman) rice, rain fed upland (direct-seeded Aus) rice and deep water (broadcast Aman) rice. In the pre-monsoon season Aus rice is mostly grown under rainfed condition, either by direct seeding or broadcasting from March to April and harvested between July and August (Fig. 1.1B). Aman is the monsoon season rainfed (occasionally supplementary irrigated) rice, either directly seeded with Aus (Mar-Apr) or transplanted between July and August, and harvested between November to December (Fig. 1.1B). Boro is dry-season irrigated rice, usually planted from December to early February and harvested between April and June (Shelley et al., 2016), though in low-lying areas Boro rice is transplanted in early November after recession of floodwater and harvested from April to May (Fig. 1.1B).

3

In Bangladesh rice area and production was about 9.3 million ha and 9.8 million ton in 1971-72, which increased notably to 11.4 million ha and 34.4 million ton in 2013-14, respectively (Fig. 1.2A). This progress in rice production was instigated mostly from the shift of low-yielding traditional to high-yielding modern rice varieties (HYV) alongside development of irrigation facilities (Hossain et al., 2006). The area under rain fed Aus rice has therefore gradually been switched into irrigated Boro (Fig.1.2B). Consequently the individual contribution of Aus, Aman and Boro season rice to total national rice production were 24, 58 and 18% in 1971-72, but moved to 7, 38 and 55%, respectively in 2013-14, despite greater area coverage by Aman rice. At present around 80% of the rice area in Bangladesh is covered by BRRI (Bangladesh Rice Research Institute) developed modern rice varieties (85 high yielding rice varieties comprising 79 inbreeds and 6 hybrids), contributing 91% of total rice production (BRRI, 2017).
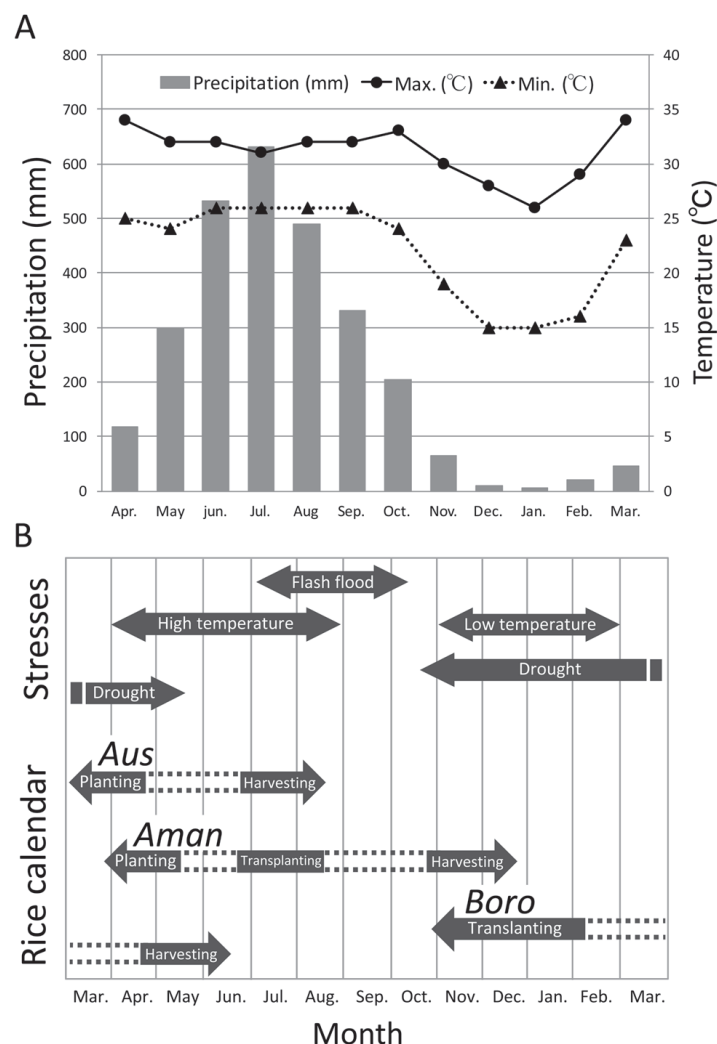


Fig. 1.1 Distribution of mean monthly rainfall, maximum and minimum surface air temperature (A), rice calendar and different stresses induced by agroclimatic parameters throughout year (B), in Bangladesh (Shelley et al., 2016)

4
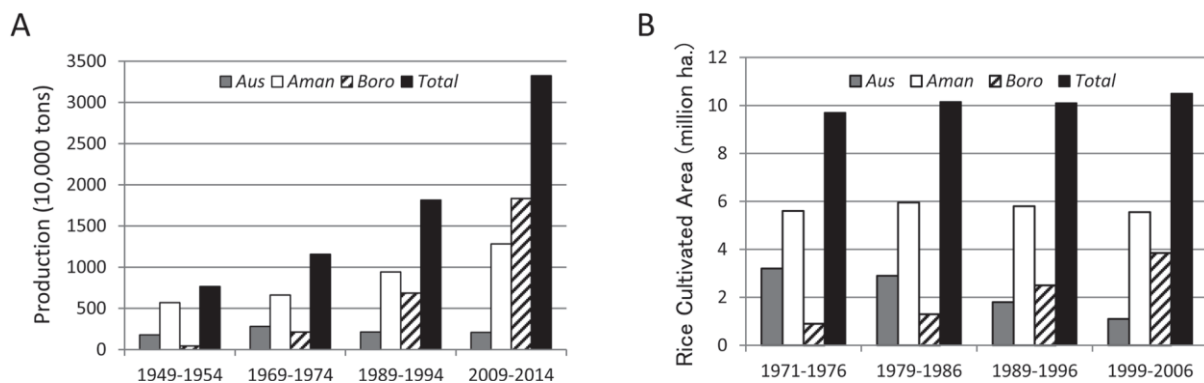
Fig. 1.2 Total rice production (A) and cultivated area (B) in different rice growing seasons in Bangladesh over time (Shelley et al., 2016)

### 1.2.2. Soil type

Bangladesh is one of the world's largest deltaic countries, categorized into three broad physiographic units belonging to three distinct geological ages, viz. Tertiary hills (occupying 12% of total area), Pleistocene terraces (covering 8% of total area) and **recent floodplain soils** (spreading about 80% of total area). Soils in Bangladesh are grouped into 21 General Soil Types (GST) based on identical mode of formation (similar environmental factors such as climate, physiography and drainage) and morphological appearances (Fig. 1.3) (Huq et al., 2013). Fourteen GSTs were recognized in floodplain soils, six on terrace soils and one on hilly areas (Huq et al., 2013). Among the floodplain soils calcareous and non-calcareous groups constitute about 87% of total floodplain soils and agricultural production in Bangladesh greatly depends on these soils (Alam et al., 1994). In total 465 soil series (US soil taxonomy) have been identified, fitting into five soil orders viz. Inceptisols, Entisols, Ultisols, Histosols and Mollisols (Huq et al., 2013) or 35 FAO-UNESCO soil units (mostly Fluvisols, Gleysols, Leptosols, Arenosols, Cambisols, Luvisols, Planosols, Alfisols, Histosols and Anthrosols). Foodplain soils are very fertile and suitable for rice cultivation, although during the rainy season rice can also be grown on terrace soils. Soils used in this thesis mostly belong to non-calcareous dark grey floodplain soils (Fig. 1.3), representing 13% of total area, except for two terrace soils (Noaddah and Chhiata). Soil Types (Soil Taxonomy) of the most studied soils were Aeric Haplaquepts (Sonatala-1 and Sonatala-2, BAU long-term experimental soil), Aeric Fluvaquents (Melandoho), Mollic Haplaquepts (Balina) and Ultic Ustochrepts (Noaddah-1 and 2) (Kader, 2012).
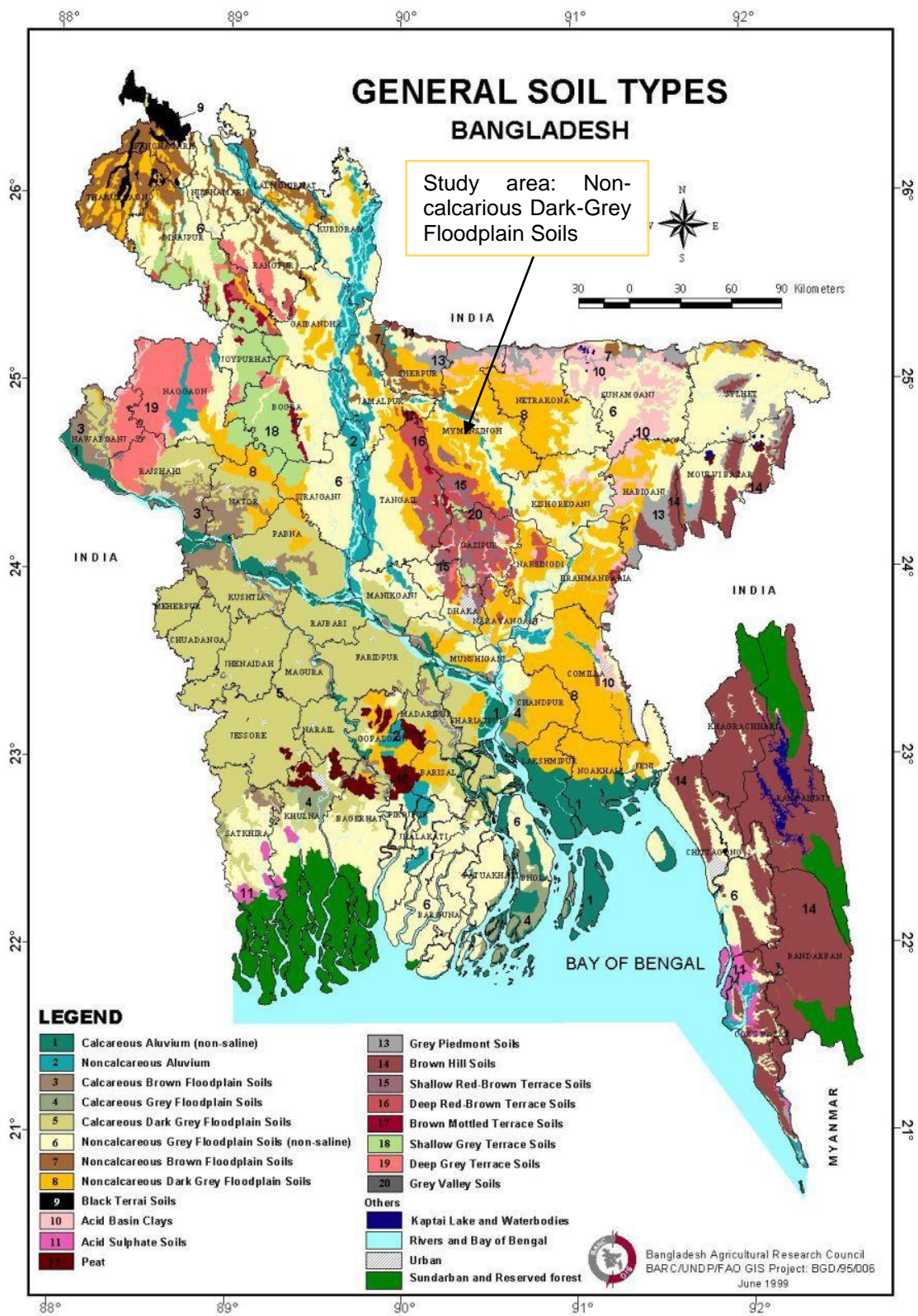
Fig. 1.3 General soil types in Bangladesh (Source: BARC, 1999)

## 1.3. Problems and major nutrients (N, P, K, S and Zn) management for rice cultivation in Bangladesh

### 1.3.1. Constraints in rice production

Despite a tripling of rice production by technological progress since the Green Revolution, South Asian countries including Bangladesh are still confronting food insecurity due to socio-economic, abiotic, biotic and management related constraints (John and Fielding, 2014; Fig. 1.1B). Socio-economic constraints account for more than 22% of rice yield loss in South Asian countries. In Bangladesh about 89% of total farm-holdings are below 2.49. There exists a wide-ranging gap between potential and farm level yield (0.6-2.2 t ha$^{-1}$ during 1994-95) (Alam and Hossain, 1998). Surprisingly, the predominance of small and marginal farms did not obstruct adoption of HYVs (Shelley et al., 2016). Hence, the yield gap is rather caused by several abiotic constraints and insustainable management out of which water shortage, inappropriate use of fertilizers (N, P, K), soil fertility depletion, inappropriate weed-insect-disease management, shortage of quality seed, crop damage by flood/typhoon/cyclone, and high or low temperature stress are the most important (John and Fielding, 2014; Fig. 1.1B). Water stress, soil fertility depletion and N deficiency are together responsible for an average 15.7% rice yield loss in South Asian countries including Bangladesh (John and Fielding, 2014). Estimated yield loss due to biotic (insect pests, diseases and weeds) and abiotic (water stress, submergence, heat-cold and soil related stress) constraints is about 28% (equivalent to ~7.8 million tons) of farm level yields in Bangladesh (Alam and Hossain, 1998).

Yield reduction by water stress is substantial (5% of farm level yield accounting for 18% of total yield loss) for rice cultivation under both rainfed and irrigated ecosystem in Bangladesh (Alam and Hossain, 1998; Shelley et al., 2016). Although water stress may hamper rice growth at any stage it will lead to complete crop failure or immense yield reduction (37-73%) during anthesis (reproductive) stage of Aman (late September to end of October) and Boro (late March and April) rice (Alam and Hossain, 1998; Fig. 1.1B; Shelley et al., 2016). About 40% of land in Bangladesh goes under water during monsoon season and excessive submergence causes 7% yield loss, contributes 26% of total yield loss (Alam and Hossain, 1998). Rice grows optimally between a critical temperature of 20°C and 35°C, (Yoshida, 1981). Aman rice experiences high temperature and rainfall at vegetative stage (Fig. 1.1B), but low temperature along with drought in reproductive (flowering) stage causes spikelet sterility, consequently lowers yield. Early Boro rice often faces low temperature stress at

vegetative and reproductive stage and late Boro often encounter high temperature stress at reproductive stage, hence would decline rice productivity in Bangladesh.

### 1.3.2. Soil Fertility

Generally, soil fertility level for most of the AEZs in Bangladesh is low to medium (BARC, 2012) and is moreover declining due to intensive land use (191% cropping intensity), imbalanced use of fertilizers, limited or no use of organic manures, and limited return of crop residues. **Soil organic matter (SOM)** content, a key indicator of soil fertility, is usually less than 1.0 to 1.5% for most soils of Bangladesh. Soil OM content has mainly declined under wheat-rice (aerobic-anaerobic) and high or medium high land conditions, but may have slightly increased under double rice cropping (BARC, 2012), though accurate figures are unavailable.

Most of the soils (almost all AEZs) in Bangladesh are deficient in several essential **plant nutrients** particularly N, P, K, S and Zn, with nitrogen (N) often most limiting (BARC, 2012). Recently, Mg and B have also been found limiting in many areas of Bangladesh. After 28 years of continuous triple rice cropping, annual grain yield with fertilizer (NPKSZn) application sustained almost at 10 t ha$^{-1}$ for triple rice cropping, but strongly declined to 1.77 t ha$^{-1}$ in unfertilized plots (BRRI, 2008-09). A rice yield gap analysis by Alam and Hossain (1998) reported that soil related stress is responsible for 5% of rice yield loss at farm level contributing almost 18% of total yield loss.

Since horizontal expansion of rice (irrigated) areas are limited, further rice production increase will largely require reducing yield losses and increasing efficiencies of inputs mostly water and fertilizers (N).

### 1.3.3. Management of major nutrients (N, P, K, S and Zn) in rice cultivation

Paddy soils in Bangladesh are commonly deficient in N, P, K, S and Zn, and exclusion of any nutrient by fertilizer application in continuous rice cropping will lead to deficiency (BARC, 2012; BRRI, 2008-09). Hence, sustainable rice production with high-yield targets necessitates balance between nutrient inputs to soil and output by crops. The apparent balances for rice based cropping patterns in Bangladesh are highly negative for N and K, and slightly positive for P (Fig 1.4). Negative N and K balances are mostly related to high cropping intensity with substantial N (24-122 kg N ha$^{-1}$ season$^{-1}$) and K (27-160 kg K ha$^{-1}$

season$^{-1}$) uptake, as opposed to little or no addition of organic manures and mostly removal of crop residues (Saha et al., 2007). Likewise, triple cropping systems exhibit even more negative balances for N and K (Fig 1.4). Inorganic fertilizers constitute the most important source of nutrients to Bangladeshi paddy soils as application of farmyard manure, composts and crop residues has steadily declined due to their use as fuel and fodder for cattle by rural people (Saha et al., 2007).
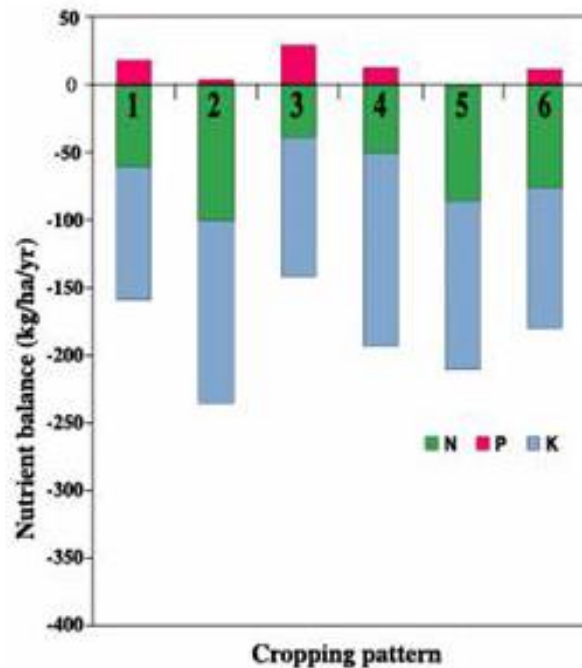


Fig. 1.4 Nutrient balance for rice based cropping patterns in Bangladesh (BARC, 2012)

1. Boro-Fallow-T. Aman; 2. Boro-T.Aus-T. Aman; 3. Boro-Green manure-T. Aman;

4. Mustard-Boro-T. Aman; 5. Wheat-T.Aus- T. Aman; 6. Wheat-Mungbean-T. Aman

The use of chemical fertilizers (N, P, K) as a supplemental source of nutrients has been introduced in the early 1950s in Bangladesh already and their use has been increasing gradually from mid 1960s with introduction of modern varieties and irrigation facilities, and is still increasing, particularly so for urea-N (BARC, 2012). The urea fertilizer use was 0.56 million ton in 1980-81 and increased to 2.7 million ton in 2010-11 (BARC, 2012). N, P, K, S and Zn are usually applied as urea, triple/single super phosphate, muriate of potash (MoP), gypsum and zinc-sulphate, respectively. Because of low K availability but high uptake and depletion in paddy soils (Saha et al., 2009), K fertilizer application has been proposed before each rice growing season. Rice straw removal causes negative K balance (-11 to -76 kg K

9

ha$^{-1}$ year$^{-1}$) even in appropriately K fertilized research rice fields (Saha et al., 2009). About 66 kg K ha$^{-1}$ season$^{-1}$ might be saved by addition of 4.5 t rice straw ha$^{-1}$ (BRRI, 2008-09). The existence of a residual effect for succeeding crops has resulted in the recommendation that P fertilizer application may be reduced by 30-50% for next two crops (BARC, 2012). Low S and Zn availability in wetland rice soils has prompted the advice to apply doses countering their fully expected crop uptake, though with 50% reduced Zn rate for the succeeding crop. Prilled urea N RE$_N$ in paddy soils of Bangladesh has been found to range from 13 to 63% (Saha et al., 2012; Gaihre et al., 2016), indicating huge loss of urea N to water bodies and the atmosphere. This signified indigenous soil N supply by organic N mineralization as an important N source for rice plant. Rising input costs including fertilizers, the government's ample subsidy on fertilizers mostly for urea (consists ~60% of total fertilizers use), the quest for food security and prerequisite to mitigate adverse impacts on environment, have prompted efficient N fertilizers use for sustainable rice production.

## 1.4. Paddy soil

Paddy fields are flooded parcels of arable land used for growing rice and other semi-aquatic crops. Irrigated rice is focused on alluvial floodplains, terraces, inland valleys and deltas in humid and sub-humid, sub-tropics and humid tropics of Asia. About 80% of total rice growing area in Asia is managed as paddy soils, corresponding to 139.6 million ha in 2008 (IRRI, 2000). Traditionally rice is transplanted and grown, whilst keeping a submerged environment from crop establishment to prior to harvest, since it is sensitive to water shortage (Gong, 1983). After rice production water is usually drained and paddy soils face multiple drying-re-wetting cycles during and in between rice-growing seasons (Nishimura et al., 2004). The management-induced change of oxic and anoxic conditions results in temporal and spatial variations in redox reactions, affecting the dynamics of organic and mineral soil constituents (Cheng et al., 2009).

Intensive lowland rice systems differ markedly from upland crop systems in their physical, chemical and trophic properties, which affect C and N cycling processes, often coupled to iron (Fe$^{3+}$-Fe$^{2+}$) redox cycling. Preferential accumulation of organic matter (OM) has typically been observed in submerged rice soils compared to aerobic soils due to lessened and incomplete soil OM decomposition (Sahrawat, 2003; Kögel-Knabner, et al., 2010). Consequently, the prolonged and submerged rice cultivation (from 50 to 2000 years) enhanced total N stocks in the paddy topsoil (0-20 cm) by 1.3 times than that of non-paddy fields (Roth et al., 2011). This increase in paddy topsoil N stock is mostly driven by the biomass inputs from growing vegetation and the restricted transport of OM to subsoil by the development of dense ploughpan.

Components of the flooded paddy soil-water system are floodwater, oxidized surface soil, reduced soil, rhizosphere-oxidized soil, plow pan and oxidized or reduced subsoil (Dobermann and Witt, 2000) (Fig. 1.5). The rice plant has the capacity to transport atmospheric $O_2$ through its stem (aerenchyma) to the roots and this $O_2$ diffuses into the adjacent soil layer, enabling rice plants to survive in an anaerobic environment (Reddy and Patrick, 1984). The aerobic soil layer supports aerobes and provides a site for $O_2$ required N transforming processes, while the anaerobic layer supports anaerobes and provides site for reactions occurring in absence of $O_2$ (Reddy, 1982). After submergence, $O_2$ supply greatly declines as the diffusivity of $O_2$ in water or saturated soil is 10,000 times lower than in air (Armstrong, 1979). Moreover, $O_2$ present in water is rapidly consumed for aerobic microbial respiration, and facultative and obligate anaerobes then dominate (Takeda and Furusaka, 1970).
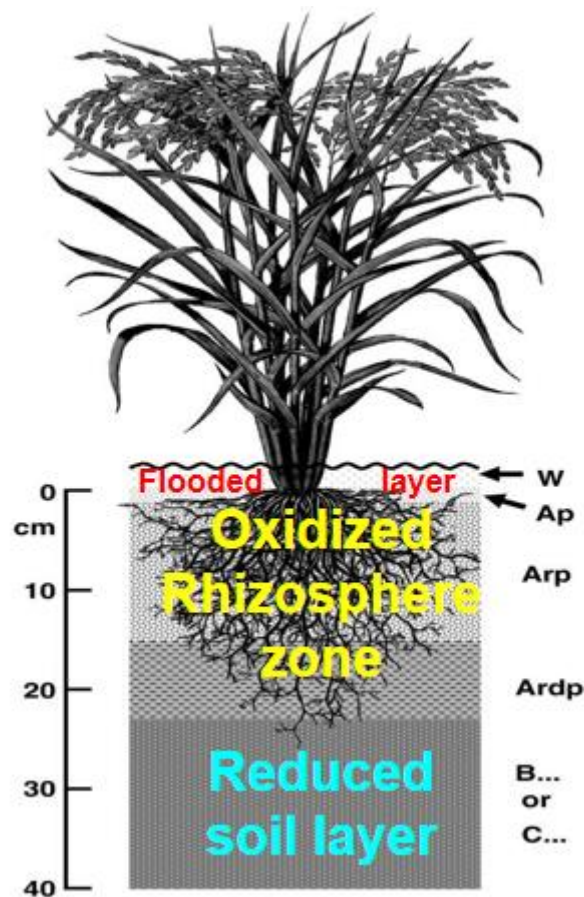


Fig. 1.5 Components of flooded paddy soil-water system (Source: Kögel-Knabner et al., 2010)

## 1.5. Nitrogen and its cycling in paddy soils

Nitrogen is a major component of many important structural, genetic and metabolic compounds in plant cells, such as chlorophyll, proteins, amino acids, enzymes, DNA, ATP etc. Total N uptake by widely cultivated wet (BR11) and dry (BRRI dhan29) season rice cultivars ranges from 33-59 kg N ha$^{-1}$ and 45-87 kg N ha$^{-1}$ with grain yields of 2.1-3.7 t ha$^{-1}$ and 3.2-5.1 t ha$^{-1}$, respectively (Saha et al., 2007). Nitrogen in flooded soils and sediments exists as inorganic forms but predominantly as organic forms (e.g. amide-N, α-amino-N, hexosamine-N, unknown-N and non-hydrolyzable-N (Yonebayashi and Hattori, 1986a). Inorganic forms ($NH_4^+$, $NH_3$, $NO_3^-$, $NO_2$) are taken up by the plants and microbes (Reddy and Patrick, 1984). Microbially mediated mineralization of organic N compounds into simpler inorganic N forms via extra-cellular enzyme activity is a prerequisite to release mineral N in paddy soils. In flooded paddy fields a multitude of biotic and abiotic N transformation processes occur, such as ammonification, immobilization, nitrification, denitrification, volatilization, nitrogen fixation and leaching (Fig. 1.6). Soil redox status greatly impacts N transformation reactions in wetland soils, hence different N transformation processes dominate in different zones (Fig. 1.6).

Ammonification, i.e. biological conversion of organic N to $NH_4^+$, is the dominant N mineralization process (Sahrawat, 1983) in anoxic soils, where $NH_4^+$ production during OM decomposition occurs through hydrolytic deamination of amino acids and peptides, degradation of nucleotides and metabolism of methylamine by methanogens (King et al,. 1983). $NH_4^+$ accumulates by organic N mineralization under anaerobic conditions since lower $O_2$ levels limit oxidation of $NH_4^+$ to $NO_3^-$ (Keeney and Sahrawat, 1986). This $NH_4^+$ can be converted back to organic N (immobilization) after being taken up by microbes and plants. Sources of $NH_4^+$ in the surface aerobic soil layer are fertilizers, organic N mineralization and release of $NH_4^+$ from clay interlayers. In flooded soils, N transport occurs through ion diffusion ($NH_4^+$ diffusion from anaerobic soil layers and $NO_3^-$ diffusion from aerobic soil layers due to their concentrations gradients), leaching, interflow and surface runoff. Positively charged $NH_4^+$ ion are adsorbed by negatively charged clay particles, whereas negatively charged nitrite and nitrate ions are usually lost from the field via leaching (Cho et al., 2010) and/or through nitrification-denitrification. By diffusion to the aerobic zone, $NH_4^+$ may either be nitrified to $NO_3^-$ or lost through $NH_3$ volatilization. In fact 13-40% of applied N fertilizer to rice is presumably subjected to loss through $NH_3$ volatilization (Dong et al., 2012; Yao et al., 2017), largely depending on soil and flood water pH that dertermine the $NH_3/NH_4^+$ ratio. $NO_3^-$ formed in the aerobic zone may transport rapidly to the anaerobic layer via diffusion (the diffusion coefficient of $NO_3^-$ movement is six fold higher than that for $NH_4^+$ in

water-saturated soil) and then quickly removed through denitrification (Patrick and Reddy, 1976). The N removal through nitrification-denitrification accounts for ~0.4 to 10% and ~2.5 to 39% of the applied N under continuously and intermittently flooded paddy fields *in-situ*, respectively (Dong et al., 2012; Zhou et al., 2012). Atmospheric $N_2$ can be fixed into the paddy soil-flood water system through biological nitrogen fixation (BNF). The estimated BNF inputs to the soil-floodwater system account for 15-70 kg N ha$^{-1}$ rice cycle$^{-1}$ depending on N fertilizer application (Cassman et al., 1996; Yoshida and Ancajas, 1973; Craswell and Vlek, 1983). Lastly, up to 40% of surface broadcasted urea N could be immobilized by algae growing in floodwater during the first week after fertilizer application but may be re-mineralized and utilized by the crop later on (Craswell and Vlek, 1983).

Hence, the net N supply for rice plants may be approximated balance between input through soil organic N mineralization, urea hydrolysis and BNF, and output via biotic immobilization, plant N-uptake, clay fixation, and losses by leaching, volatilization and nitrification-denitrification (Fig. 1.6). Since more than 50% of rice plant N-uptake usually originates from soil N pools, regardless of fertilizer application, indigenous soil N supply remains the central driving process for wetland rice productivity.
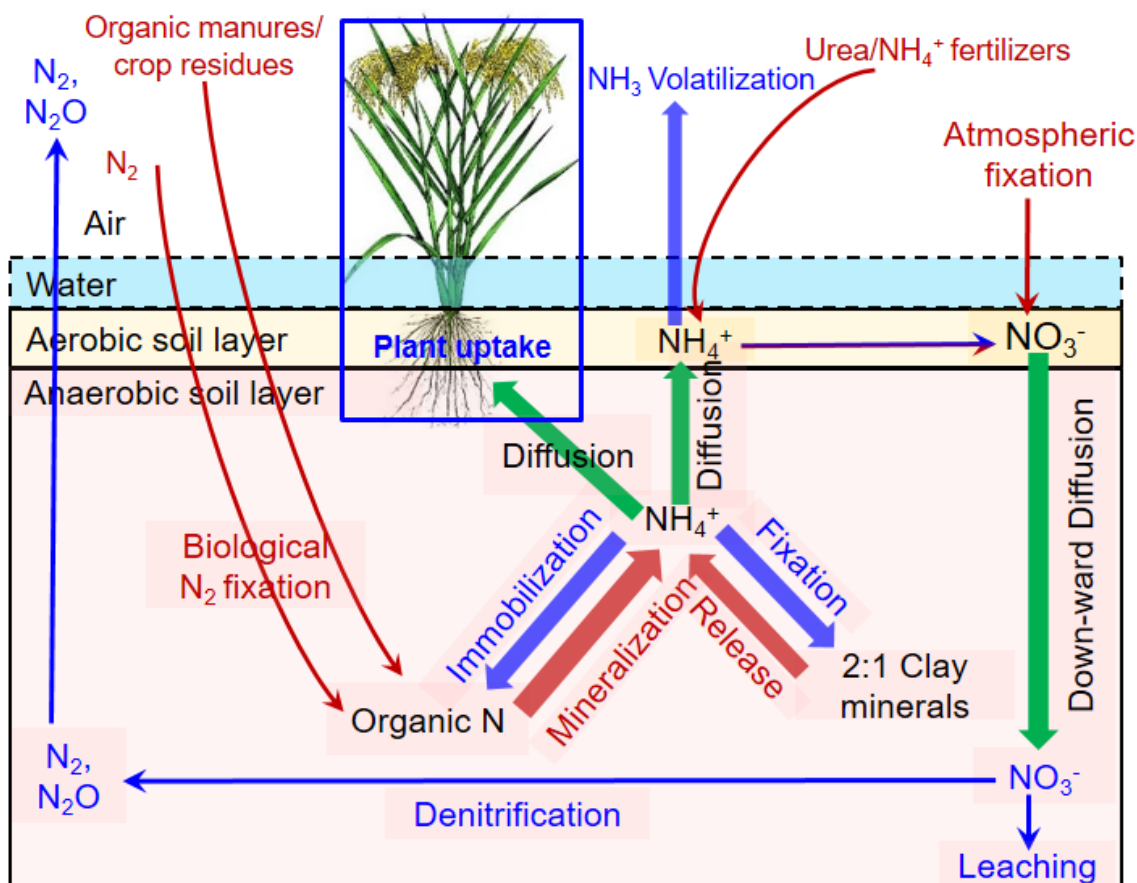
Fig. 1.6 Nitrogen transformation processes in paddy soils (Source: Buresh et al., 2008)

## 1.6. Controls of paddy soil organic N mineralization

Organic N mineralization is influenced by multifold factors such as soil moisture, temperature, clay mineralogy, soil OC and N content, cation exchange capacity, levels of pedogenic oxides, availability of terminal electron ($e^-$) acceptors, gross microbial activity and biochemical processes impacting soil Eh, pH and dissolved OM. Soil OM breakdown is typically slower in submerged than aerobic soil (Villegas-Pangga et al., 2000), because anaerobic bacterial microflora operate at lower energy level and at lower efficiency than aerobes. This results in incomplete decomposition and lower microbial cell synthesis per unit degraded OC (Reddy and Patrick, 1984). As a result of this inefficient OM oxidation at low Eh, OM tends to accumulate with time in water-logged soils due to **lack of $O_2$ and other terminal $e^-$ acceptors** (like $Fe^{3+}$, $Mn^{3+/4+}$, $SO_4^{2-}$) (Sahrawat, 2004b). Both lower gross N mineralization and immobilization in submerged soils, however, often resulted in a higher net N mineralization and inorganic N release compared to aerobic soils (Buresh et al., 2008). On

the contrary, Devevre and Horwath (2000) found the larger and sustained microbial biomass with more likely N immobilization under anaerobic than aerobic conditions. In wetland soils organic N mineralization is accomplished by a wide variety of heterotrophic microorganisms (White and Reddy, 2001). Accordingly, net N mineralization rate, $NH_4^+$-N, microbial biomass C (MBC) and N (MBN) are correlated, indicating that soil microbial biomass mediates a considerable part of net soil N release (Zhang et al., 2009). The average $NH_4^+$-N released in Chinese paddy soils under anaerobic incubation was 86 mg $kg^{-1}$ 161days$^{-1}$ (Zhang et al., 2017). Yonebayashi and Hattori (1986b) observed net N releases of 75-112 mg N $kg^{-1}$ during four weeks of anaerobic incubation, coming down to ~5 to 12% of total N in tropical and temperate paddy soils. In an *in-situ* study soil $NH_4^+$-N remains at higher levels (e.g. ~20 mg $kg^{-1}$) initially and then declines to below ~10 mg $kg^{-1}$ with advancement of rice growth (tillering till maturity: 24-100 DAT) (Zhang et al., 2009).

**Clay mineralogy** is important to abiotic preservation and release of $NH_4^+$ in flooded rice soils and hence can play a decisive role in the N cycle, efficiency of N fertilizer and rice plant's N nutrition (Steffens and Sparks, 1999; Juang et al., 2001). A substantial part of $NH_4^+$ formed by mineralization is transferred to non-exchangeable form in presence of sufficient expandable 2:1 clay minerals (Schneiders and Scherer, 1998) and can become available to succeeding rice crops. In a vermiculite rich soil, releases of 100 kg fixed $NH_4^+$-N $ha^{-1}$ during the rice growing season were reported by Keerthisinghe et al. (1984). Soil Eh usually influences the cycle of $NH_4^+$ fixation and release by affecting charge conditions of clay minerals, mostly through iron redox reactions (Scherer and Zhang, 1999; Stucki et al., 1984; Schneiders and Scherer, 1998).

**Soil OC and N content** are typically expected to positively impact accumulation of $NH_4^+$ or rice plant N uptake and have often been proposed as index of soil N supplying capacity (Cassman et al., 1996; Narteh and Sahrawat, 1997; Zhang et al., 2017). Nevertheless, other studies have found poor, insignificant or even negative correlations between N mineralization and soil OC and N content (Cassman et al., 1996; Adhikari et al., 1999; Kader et al., 2013). They explicitly assumed that SOM quality instead of quantity, stabilization of applied OM and fertilizer N into stabilized (humic) SOM fractions, and accumulation of phenolic-lignin compounds binding nitrogenous compounds into recalcitrant forms may decline soil N supply, with consequent poor relations with SOC and TN. So, chemical composition and **nature of soil OM** seems to be a critical factor with biologically available fractions (e.g. dissolved OM) more susceptible to decomposition and contributing to net soil N mineralization (Li et al., 2010). Kader (2012) found that the anaerobic N mineralization rate only positively correlated with N in several physio-chemical SOM fractions for highly

15

weathered soils, but not for young floodplain paddy soils of Bangladesh. Anaerobic N mineralization in the latter soils only correlated positively with pyrophosphate-extractable Fe and negatively with soil $pH_{KCl}$ out of several studied soil properties (Kader et al., 2013). This suggests that next to SOM content and quality indices, other inorganic predictors of the availability of alternative $e^-$ acceptors (mostly reducible $Fe^{3+}$) co-determine OM decomposition in subtropical paddy soils.

Although $O_2$ is the first most preferred and efficient $e^-$ acceptor during OM degradation, it becomes undetectable within a day of submergence via respiration by aerobes and plant roots (Ponnamperuma, 1972). Then facultative and obligate anaerobes sequentially or simultaneously use $NO_3^-$, $Mn^{4+}$, $Fe^{3+}$, $SO_4^{2-}$, $CO_2$, $N_2$ and even $H^+$ as $e^-$ acceptors to mediate SOM decomposition and $NH_4^+$ production in flooded paddy soils (Ponnamperuma, 1972; Gao et al., 2002) (Fig. 1.7). Redox potential (Eh) typically (ranges from +700 to -300mV) reflects reduction intensity and provides an indication of dominant $e^-$ acceptors availability (Inglett et al., 2005) (Fig. 1.7) and Eh drops in the puddle layer to a fairly stable range of +200 to -300mV, depending mostly on soil OM content and reducible elements (Sahrawat, 2012; Ponnamperuma, 1972). Near neutral pH, reduction of $Mn^{3+/4+}$, $Fe^{3+}$ and $SO_4^{2-}$ takes place over a wide range of Eh while reduction of dissolved $O_2$ and $NO_3^-$ only occur at higher and narrower Eh ranges. In submerged soils $NO_3^-$ is extremely unstable and bulk of $NO_3^-$ disappears through respiration within a few days (Ponnamperuma, 1972). $Mn^{4+/3+}$ reduction is an important process and Mn oxides act as preferred $e^-$ acceptor prior to $Fe^{3+}$ and so usually at very early rice growing stage (Gao et al., 2002). Solubility of Mn oxides in water is very low and a limited number of bacteria participate in their reduction. Next to Mn, $Fe^{3+}$ reduction begins within a few days after submergence at Eh less than +180 to +150mV (Patrick and Reddy, 1978) with gradual increases in soil solution $Fe^{2+}$ concentration (Gao et al., 2002; Jahan et al., 2013). In flooded rice soils reduction of inorganic $e^-$ acceptors produces $CO_2$ with OM acting as $e^-$ donor and $CO_2$ emission reaches its maximum value with depletion of these $e^-$ acceptors. Afterwards methanogenesis (conversion of acetate and $H_2/CO_2$ to $CH_4$ by obligate methanogens) initiates as terminal step and can ultimately dominantly participate in anaerobic degradation of SOM (up to 73% of C mineralization) in paddy soils (Jackel and Schnell, 2000a) (Fig. 1.7 and 1.8). The Fe redox systems nevertheless are nearly always dominant to other inorganic $e^-$ acceptors for OM oxidation (contributes in 42-84% of OM oxidation) and $NH_4^+$ production in flooded paddy soils (Reddy and De Laune, 2008; Yao et al., 1999; Jackel and Schnell, 2000).
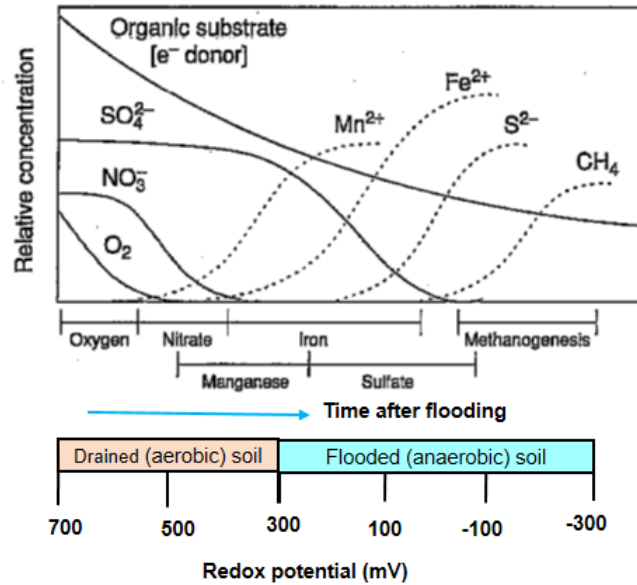
Fig. 1.7 Sequential reduction of oxidants and accumulation of reductants in wetland soils
(Source: Inglett et al., 2005)

## 1.7. Fe redox cycling and its linkage to paddy soil organic N mineralization

Iron in paddy soils remains as $Fe^{3+}$ oxides, oxyhydroxides and in the structure of clay minerals (Stucki, 1988), with amorphous $Fe^{3+}$-oxides acting as the predominant source (~35-50% of Fe is reducible) of reducible Fe (van Bodegom et al., 2003). Both microbial and chemical $Fe^{3+}$ reduction take place in wetland rice soils. But most $Fe^{3+}$ reduction is carried out by a wide variety of microbes and $Fe^{3+}$ reducing bacteria that gain $e^-$ from organic substrates, then transfer $e^-$ to $Fe^{3+}$ (Fig. 1.8) and produce $Fe^{2+}$ (Yi et al., 2012). In brief, complex OM is enzymatically hydrolyzed into sugars, amino acids, long-chain fatty acids and aromatics (Fig. 1.8). Long-chain fatty acids and aromatics are then further oxidized to $CO_2$ and $H_2O$ by $Fe^{3+}$ reducers. Fermentative microbes ferment sugars and amino acids into short-chain fatty acids and $H_2$, which are then oxidized by $Fe^{3+}$ reducers. The intensity of $Fe^{2+}$ production increases with decrease in crystallinity of $Fe^{3+}$ (hydr-)oxides and increase in easily mineralizable organic substances (Ponnamperuma, 1972).

17
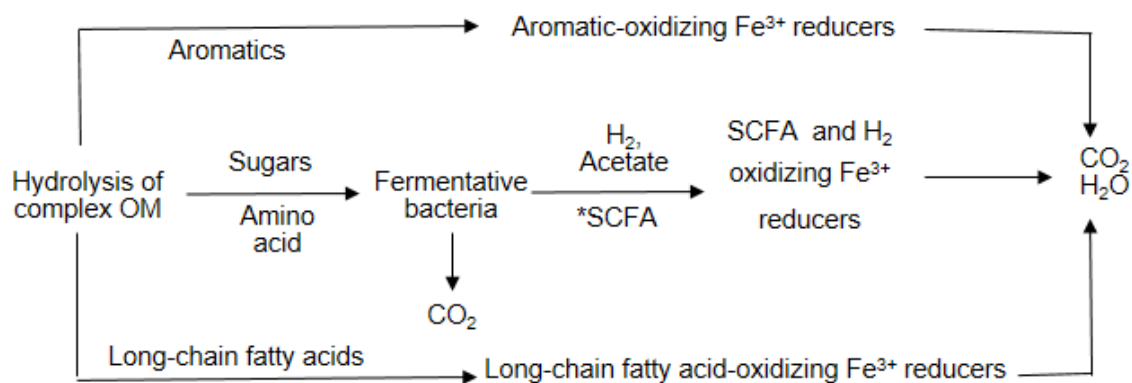
Fig. 1.8 Simplified model for the microbial oxidation of OM in anaerobic soil or sediment with Fe$^{3+}$ serving as electron acceptor (SCFA: Short-chain fatty acid) (Source: Li et al., 2012)

A study by Narteh and Sahrawat (1997) with diverse West African paddy soils found that extractable Fe is not directly related to NH$_4^+$ production under anoxic condition, but its inclusion in multiple regression analysis improved prediction of NH$_4^+$ production. While in another study with flooded paddy soils Sahrawat and Narteh (2001) reported significant correlations of mineralizable N with organic C (r=0.79) and Fe extracted by EDTA (r=0.86) or ammonium oxalate (r=0.75). They also found high mineralizable N in soils with high organic C and reducible Fe, and relatively lower mineralized N in soils having low organic C or reducible Fe (Sahrawat and Narteh, 2003).

The Fe$^{3+}$-Fe$^{2+}$ redox cycle is considered to interactively link to OM oxidation and C and N cycling under reductive environment (Fig. 1.9) in various ways.

Next to acting as e$^-$ acceptor, the Fe$^{3+}$-Fe$^{2+}$ redox cycle influences OM decomposition and N mineralization in submerged paddy soils by multiple mechanisms. Firstly, Fe$^{3+}$ reduction may be intimately linked to NH$_4^+$ fixation and release in flooded paddy soils (Fig. 1.9). Reductive dissolution of Fe (hydr-)oxides coatings on clay minerals' surface at low Eh, promotes NH$_4^+$ diffusion into or out of the interlayers depending on exchangeable NH$_4^+$ concentrations (Scherer and Zhang, 1999; Said-Pullicino et al., 2014). Moreover, decreasing Eh in flooded paddy soils may lead to reduction of structural Fe$^{3+}$, as such increases net negative charge of certain clay minerals and enhances NH$_4^+$ fixation (Stucki et al., 1984). Secondly, in flooded soils dissolved OM (DOM) release upon reductive dissolution of Fe- and Mn- (hydr-)oxides or by desorption due to pH rise, may importantly contribute to mineral N supply either by acting as an intermediate pool of organic N mineralization and/or subsequent mineralization after co-release (Li et al., 2010; Grybos et al., 2009). Thirdly, NO$_3^-$ reduction

coupled to $Fe^{2+}$-oxidation is ubiquitous in flooded paddy soils and 16-33% of $e^-$ could be donated to denitrification by $Fe^{2+}$-oxidation (Wang et al., 2016). Both biotic and abiotic $NO_3^-$ reduction coupled $Fe^{2+}$-oxidation may take place in wetland soils, and produced $NO_2^-$ then reacts with DOM and forms DON complexes (Fig. 1.9). Fourth, anaerobic $NH_4^+$-oxidation coupled to $Fe^{3+}$ reduction may fuel a substantial loss of N in paddy soils enriched in microbially reducible $Fe^{3+}$ and has been ascribed 8-61 kg $NH_4^+$ loss $ha^{-1}$ $year^{-1}$ (Ding et al., 2014). To sum, soil OM and reducible $Fe^{3+}$ content are two decisive factors in the soil N cycle, possibly impacting efficiency of applied N fertilizer, crop N uptake and N nutrition of wetland rice.
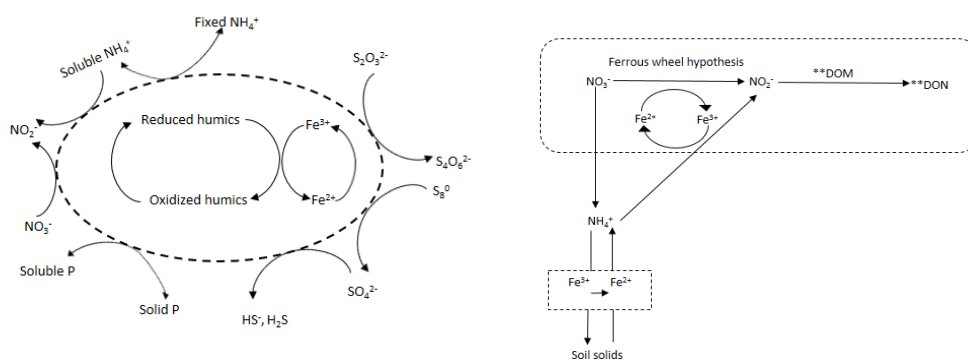


Fig. 1.9 Conceptual models illustrating relationships between $Fe^{3+}$– $Fe^{2+}$ redox wheel and N cycling in anaerobic soil or sediment (Source: Li et al., 2012)

## 1.8. Research hypotheses, aims and outline of the thesis

Estimation and prediction of N supply in paddy soils is crucial to optimize N use efficiency and minimize adverse impacts of excessive N on environment. Both are complicated since net soil N supply is influenced largely by multiple interrelated and co-occurring soil properties and biochemical processes. An extensive number of studies has evaluated predictor variables and relations of soil N supplying capacity to paddy soil properties (Cassman et al., 1996; Kader et al., 2013; Sahrawat and Narteh, 2003; Manguiat et al., 1996; Zhang et al, 2017). Several studies proposed soil OC and N as index of N mineralization in paddy soils, while other studies did not derive any single predictor, including SOC and TN. Kader (2012) already explored soil organic matter content and quality, edaphic properties, crop rotation, historical fertilizer management and clay mineralogy as predictors of anaerobic N mineralization in young floodplain paddy soils in Bangladesh but only derived significant relations with $Fe_{ox}$ and $pH_{KCl}$. It was then concluded that availability of $e^-$ acceptors, likely

primarily $Fe^{3+}$, might crucially limit anaerobic microbial activity and net N supply in abundantly present young floodplain paddy soils of Bangladesh.

The line of thought that Fe-reduction would be a rate-limiting process for anaerobic microbial activity in young floodplain paddy soils forms the starting point of the present PhD research.

Firstly, we hypothesized that restricted availability of alternative electron acceptors may form a bottleneck for anaerobic N-mineralization in these soils. Therefore, a first objective of this PhD thesis was **(O1)** to assess influence of content of alternative $e^-$ acceptors, particularly $Fe^{3+}$ and $Mn^{4+}$ on anaerobic N mineralization in young floodplain paddy soils by artificial addition of $Fe_2O_3$ or Mn/Al mixed oxides.

Experimental manipulation of available oxidants would probably not represent natural conditions. Therefore we expanded our first experimental approach by study of influence of natural variation in edaphic factors within a single paddy field on net soil N supply. A first key requirement was the existence of meaningful within-field variation of the ratio of SOC to pedogenic Fe and Mn. A known heterogenous paddy field in Atalle Sri Lanka was chosen based on these criteria. Size and activity of microbial biomass, content and reducibility of oxidants, and dynamics of DOC and DON were considered potential relevant indicators of anaerobic microbial activity. So, a second objective was to assess short- to medium term rates of change in soil pH, Eh, solution Fe, Mn, DOC and DON and gaseous C-emissions to predict anaerobic N mineralization relative to edaphic factors using within-field- spatial variation **(O2)**.

Thirdly we expanded bare soil incubations approach in several ways: i) by the introduction of a growing rice plant; and ii) by an attempt to identify dominant $e^-$ accepting $Fe^{3+}$-bearing minerals. Hence, a third objective was to assess linkage of mineral N release to reduction of $Fe^{3+}$ and $Mn^{4+}$, as primary terminal $e^-$ acceptors in a rice growth pot experiment with recording of ancillary information on soil Eh, reduction, and soil Fe mineralogy **(O3).** This rice pot growth experiment was confounded to a selection of 4 Northern Bangladeshi paddy soils.

In a field setting, however, losses of N may also become more pertinent and soil processes take place in an even more heterogeneous spatial environment in terms of temporal and depth-gradients in Eh, temperature, and root growth. The question then emerges if and how in a field setting net mineral N release relates to Fe/Mn-reduction, changes in solution pH

and DOC/DON release. Next to validating the lab and greenhouse-scale findings, a field-scale approach allows addressing other related research questions like elucidating low N fertilizer efficiency, common in Bangladesh. Thus a fourth objective was to validate co-evolution of mineral N release with solution Fe and DON release attained by the lab incubations and rice growth pot experiments in six farmers' fields *in-situ* and evaluate N fertilizer use efficiency **(O4).**

Increasing adoption of water-saving irrigation in rice production is strongly gaining ground throughout Asia. At present this transition has only started in Bangladesh while systems like alternate wetting and drying and mid-season drainage have become widespread in the Phillipines and China, respectively. Non-continuous flooding should at least temporarily alter depth profiles of soil moisture, Eh and microbial activity. Under such circumstances it is even difficult to forward hypotheses on the impact on soil N supply to the rice plant and on the N use efficiency. While much attention has gone to the impact of irrigation management on the greenhouse gas balance, experimental study of N-supply and its relation to Fe-reduction is still pending. Therefore, a fifth objective was to investigate changes in depth profiles of soil moisture and redox potential, reductive dissolution of Fe and Mn, gross anaerobic microbial activity next to net soil N supply to rice plant under continuous and intermittent flooding irrigation management in a Bangladeshi paddy field **(O5).**

The above objectives this thesis may be summarized as following main five **research questions**:

**Q1**: Does the availability of alternative electron acceptors form a bottleneck for anaerobic N-mineralization?

**Q2a**: Do rate of change in soil pH, Eh, solution Fe, Mn, DOC and DON and gaseous C emission relate to anaerobic N mineralization? **Q2b**: Does the power of these indicators of anaerobic microbial activity to predict net soil N supply exceed that of common soil properties?

**Q3a**: Do explored relations between $Fe^{3+}$ and $Mn^{4+}$ reduction and net soil mineral N supply observed in the lab still hold in presence of a growing rice plant firstly under continuous then intermittent flooding? **Q3b**: What are dominant Fe-bearing minerals acting as oxidant in North-Bangladeshi paddy soils?

**Q4**: To what extent do connections between mineral N release to $Fe^{3+}$ and $Mn^{4+}$ reduction and DON observed under controlled conditions hold *in-situ* during a rice growing season with or without N fertilizer application?

**Q5**: How are soil N supply and anaerobic microbial activity impacted by adoption of water-saving irrigation?

Next to the introductory **Chapter 1**, this thesis comprises five other chapters addressing these research questions. We hypothesized that the limited availability of pedogenic Fe ($Fe_{ox}$) would control anaerobic N mineralization in young floodplain paddy soils in Bangladesh. To test this hypothesis **Chapter 2** presents an investigation of progressive dissolution of Fe and Mn and buildup of $NH_4^+$ in five young floodplain paddy soils collected from Bangladesh. The soils were either untreated, amended with $Fe_2O_3$, or with Mn/Al mixed oxides and were anaerobically incubated (**Q1**). The starting point for **Chapter 3** was to alternatively to Chapter 2's approach instead make use of natural variation in the relative contents of SOC (electron donor) and pedogenic Fe and Mn (presumably dominant terminal electron acceptors). An incubation study on soil collected from 50 locations within a single Sri Lankan paddy field was carried out to address **Q2a & Q2b**. In **Chapter 4** the linkage between mineral N release and $Fe^{3+}$ and $Mn^{4+}$ reduction was further investigated in a greenhouse rice growth pot experiment (**Q3a**) with four farmers' fields paddy soils with a more detailed characterization of Fe-bearing minerals present (**Q3b**). **Chapter 5** evaluates N fertilizer use efficiency and links between net N supply with releases of dissolved Fe, Mn and ON during wet rice growing season in six farmers' fields of north-central Bangladesh (**Q4**). Detailed study on the depth profiles of soil moisture, Eh, reductive processes, microbial activity and total C emission under continuous or intermittent flooding would assist to comprehend irrigation-impacts on paddy soil net N supply (**Q5**). A field experiment with three irrigation management (CF, AWD and DSR) throughout dry (Boro) season were investigated and discussed in **Chapter 6**.

# Chapter 2

# Control of Fe and Mn availability on nitrogen mineralization in subtropical paddy soils



**After:**

Akter, M., Kader, M. A., Pierreux, S., Gebremikael, M.T., Boeckx, P. and Sleutel, S., 2016. Control of Fe and Mn availability on nitrogen mineralization in subtropical paddy soils. Geoderma. 269, 69-78.

**Abstract**

The availability of alternative electron acceptors like $Fe^{3+}$ and $Mn^{4+}$ may form a bottleneck to anaerobic SOM mineralization and thereby $NH_4^+$-release in flooded paddy soils. We assessed the influence of availability of soil Fe and Mn on anaerobic N mineralization in lab incubation experiments. Collected paddy soils from Bangladesh either untreated, amended with $Fe_2O_3$, or with Mn/Al mixed oxides were anaerobically incubated. In a first 8 weeks incubation with 5 treatments from a long-term field experiment (Control, N, NP, NPK and N+FYM) we found no considerable differences in evolution of soil solution Fe and Mn between the control and $Fe_2O_3$ treated soils. Whereas, the soil solution contents of Fe were lower and Mn were higher in Mn/Al mixed oxides treated soils. Similar observations were made for dissolved Fe and Mn in a second 10-weeks incubation experiment with four farmers' fields soils. Evolution of KCl-extractable $NH_4^+$ was not affected by $Mn^{4+}$ or $Fe^{3+}$ application and we therefore conclude that availability of electron acceptors was not limiting release of $NH_4^+$ in the studied soils. The large and rapid increase of exchangeable-$NH_4^+$ at the onset of the incubations provoked the question whether part of it derived from release of fixed-$NH_4^+$. A third experiment revealed, however, instead a small significant increase of the fixed-$NH_4^+$ within four weeks. In addition, the microbial biomass carbon already plateaued after two weeks. Both results suggest that released mineral N was mainly derived from biotic anaerobic N mineralization and not from defixation of $NH_4^+$. Finally, while not directly dependent on Fe and Mn application, there was a remarkable convergence in the buildup of soil exchangeable-$NH_4^+$ and soil solution Fe concentrations. This warrants further investigation and still suggests involvement of reductive Fe and Mn-oxide dissolution in $NH_4^+$-release, e.g. through release of bound organic N after reduction of these oxides.

## 2.1. Introduction

Rice grain yield is highly sensitive to an excess or a deficiency of nitrogen (N) at both vegetative and reproductive growth phases (Ponnamperuma, 1977) and paddy rice removes 16 to 17 kg N for the production of one ton rough rice, including straw (Choudhury et al., 1997). Therefore, N is the most limiting nutrient in intensive paddy rice cultivation. The urea-N use efficiency of lowland rice is, however, very low (30-40% or lower) (Choudhury et al., 2002) due to rapid losses via ammonia volatilization, denitrification, leaching (Cassman et al., 1998) and greater immobilization (Said-Pullicino et al., 2014). In a large part of South-East Asia (Bangladesh, Myanmar, India, Laos) at present the N uptake of wetland rice is by half to two-thirds derived from the soil N pool, even in N fertilized fields (Ando et al., 1992; Manguiat et al., 1994). Therefore, soil N mineralization, dominantly resulting in $NH_4^+$

accumulation, remains a key process for nutrition of lowland rice (Sahrawat and Narteh, 2001). Consequently, reliable estimation of mineralizable N is essential to determine the dose and time of N fertilizer application, optimize N use efficiency as well as minimize adverse impacts of excessive N on the environment (Watanabe et al., 1987; Mikha et al., 2006, Sharifi et al., 2007). However, N mineralization in wetland soils is influenced by several physicochemical factors including the C/N ratio of soil organic matter (SOM), size and activity of the microbial biomass pool, temperature, pH, contents of alternative electron acceptors etc. (White and Reddy, 2001). All these factors complicate the estimation of anaerobic N mineralization and their relative importance is insufficiently known for subtropical paddy soils.

Different efforts have been undertaken to predict N mineralization in lowland paddy soils (Watanabe et al., 1987; Narteh and Sahrawat, 1997). SOM content has been proposed as an evident index of available N in submerged paddy soils, based on significant correlation between soil C and N, and mineralizable N (Narteh and Sahrawat, 1997; Sahrawat, 2006). However, other studies have found poor, insignificant or even negative correlations with soil C and N (Cassman et al., 1996; Adhikari et al., 1999; Sahrawat, 2010; Kader et al., 2013). Possibly, the quality of SOM instead of its content should be considered. Indeed, anaerobic decomposition of crop residues under continuous flooded rice systems promotes accumulation of phenolic-lignin compounds, which covalently bind nitrogenous compounds into recalcitrant forms and decrease soil N supply (Olk et al., 2006). This, for one, may explain why the relation between soil N content and anaerobic N mineralization is not straightforward. Kader (2012) found significant positive correlations between the soil N mineralization rate and N in several physiochemical SOM fractions in highly weathered paddy soils, whereas the relationship was insignificant or even negative in young floodplain soils of Bangladesh. Therefore, not only SOM quality but also other inorganic factors appear to control N mineralization in subtropical paddy soils.

In waterlogged paddy soils, microbes utilize reducible species ($O_2$, $NO_3^-$, $Mn^{4+}$, $Fe^{3+}$, $SO_4^{2-}$ and $CO_2$) successively as terminal electron acceptors to mediate SOM decomposition (Ponnamperuma, 1972; Gao et al., 2002) and $NH_4^+$ production. Both $Mn^{4+}$ and $Fe^{3+}$ serve as good acceptors for electrons released during anaerobic respiration of organic compounds and are present in anoxic soils as oxides, hydroxides and as structural parts of clay minerals (Stucki, 1988; Nealson and Myers, 1992). Ferric iron reduction has been estimated to support oxidation of SOM for 58-79% by Yao et al. (1999) and 66-84% by Inubushi et al. (1984). Hence, the unavailability of reducible iron may decline SOM oxidation and mineralization (Sahrawat, 2003). Likewise, Sahrawat and Narteh (2001) postulated

mineralizable N and $NH_4^+$ production to be greatly influenced by the relative contents of reducible iron and organic C in flooded paddy soils. Kader et al. (2013) found that anaerobic N mineralization was significantly positively correlated with pyrophosphate-extractable Fe content and negatively with soil $pH_{KCl}$, but not with a myriad of other soil properties for a set of 25 farmers' fields paddy soils. The connection between reductive Fe dissolution and $NH_4^+$ release is in fact multifold: next to serving as electron acceptor, Fe-(hydr)oxides are also major binding surfaces for SOM. Leinweber and Schulten (2000) revealed a substantial part of proteinaceous and heterocyclic N to be selectively bound to pedogenic oxides. Thirdly, $NH_4^+$-fixation and release in tropical rice soils was also correlated with reducible-Fe (Sahrawat, 1979; Sahrawat, 2004a), possibly because reductive dissolution of Fe-(hydr-)oxides coatings on clay surfaces was required to enable defixation of $NH_4^+$.

We hypothesized that restricted availability of alternative electron acceptors forms a bottleneck for anaerobic N-mineralization. To address this hypothesis, we assessed if addition of Fe(III)- and mixed Mn(IV)/Al-oxides promotes anaerobic N mineralization. We studied the progressive dissolution of Fe and Mn as well as buildup of $NH_4^+$ in five young floodplain paddy soils of North-Bangladesh. We also estimated the relative contribution of abiotic release of fixed-$NH_4^+$ to the buildup of soil exchangeable-$NH_4^+$, next to biotic anaerobic N-mineralization in these soils. Next to soil type, long-term nutrient application management may moderate the relation between soil exchangeable $NH_4^+$ release and availability of reducible Fe and Mn. Firstly, because it determines SOM level and quality and hence rate of microbial SOM decomposition and demand for alternative electron acceptors. Secondly, because CNP stoichiometry of soil microorganisms is quite homeostatic (Griffiths et al., 2012), N or P limitation may result in lowered microbial use efficiency, i.e. a larger donation of electrons per unit of $NH_4^+$ released. Lastly, K competes with $NH_4^+$ for clay interlayer space and soil K-deficiency could affect abiotic release of $NH_4^+$ from the fixed-$NH_4^+$-pool, and thus requirement for Fe or Mn reduction per unit of $NH_4^+$ released. A second objective was to explore if long-term (30y) nutrient application (N, P, K) in a field experiment controls soil $NH_4^+$ supply's dependency on availability of alternative electron acceptors.

## 2.2. Materials and Methods

### 2.2.1. Site description and soils

Five representative paddy soils (from 4 farmers' fields and from the Bangladesh Agricultural University (BAU) long-term fertilizer and organic matter application field experiment) were collected from the Northern (24°43′ N, 90°25′ E) district of Bangladesh (Table 2.1). Five

Table 2.1 Selected properties of paddy soils used for incubation experiments

| Soils | Texture | Extraction Methods | | | | | | | | pH-KCl | SOC | Total N | Exchangeable K+ | CEC | Exchangeable $NH_4^+(NO_3^-)$ |
|---|---|---|---|---|---|---|---|---|---|---|---|---|---|---|---|
| | | DCB | | 0.5M HCl | | Na-pyrophosphate | | $NH_4^+$-oxalate | | | | | | | |
| | | $(g\ kg^{-1})$ | | $(g\ kg^{-1})$ | | $(g\ kg^{-1})$ | | $(g\ kg^{-1})$ | | | $(g\ kg^{-1})$ | $(g\ kg^{-1})$ | $(mg\ kg^{-1})$ | $(cmol_c\ kg^{-1})$ | $(mg\ kg^{-1})$ |
| | | Fe | Mn | Fe | Mn | Fe | Mn | Fe | Mn | | | | | | |
| **Farmers' fields** | | | | | | | | | | | | | | | |
| Sonatala-1 | Silt Loam | 12.2 | 0.3 | 7.5 | 0.3 | 1.0 | 0.1 | 5.4 | 0.2 | 4.9 | 21.4 | 2.1 | 26 | 44 | 7(13) |
| Sonatala-2 | Silt Loam | 9.9 | 0.2 | 7.7 | 0.2 | 0.9 | 0.1 | 4.9 | 0.1 | 4.7 | 16.3 | 1.7 | 15 | 35 | 5(14) |
| Melandoho | Silt Loam | 8.2 | 0.1 | 3.3 | 0.1 | 1.2 | 0.0 | 3.3 | 0.1 | 3.7 | 8.2 | 0.9 | 78 | 25 | 23(12) |
| Noaddah | Silty Clay | 14.2 | 0.1 | 3.8 | 0.1 | 2.8 | 0.0 | 6.2 | 0.1 | 3.8 | 9.2 | 1.0 | 65 | 36 | 39(6) |
| **BAU long-term field experiment** | | | | | | | | | | | | | | | |
| Control | Silt Loam | 10.7 | 0.2 | 6.5 | 0.2 | 0.7 | 0.1 | 4.0 | 0.4 | 5.7 | 15.1 | 1.6 | 17 | - | 6(11) |
| N | Silt Loam | 11.0 | 0.2 | 6.4 | 0.2 | 0.6 | 0.1 | 4.2 | 0.4 | 5.9 | 15.3 | 1.6 | 15 | - | 6(14) |
| NP | Silt Loam | 11.3 | 0.2 | 6.7 | 0.2 | 0.8 | 0.1 | 4.5 | 0.4 | 5.7 | 15.8 | 1.8 | 17 | - | 6(11) |
| NPK | Silt Loam | 10.9 | 0.2 | 6.1 | 0.2 | 0.8 | 0.1 | 4.3 | 0.4 | 5.7 | 17.0 | 1.8 | 17 | - | 6(15) |
| N+FYM | Silt Loam | 10.6 | 0.2 | 7.1 | 0.2 | 0.7 | 0.1 | 4.4 | 0.4 | 5.7 | 16.6 | 1.8 | 19 | - | 5(15) |

treatments of the BAU experiment were included, i.e. unfertilized control; N:100 kg N ha$^{-1}$; NP:100 kg N ha$^{-1}$ + 20 kg P ha$^{-1}$; NPK:100 kg N ha$^{-1}$ + 20 kg P ha$^{-1}$ + 19 kg K ha$^{-1}$; N+FYM:100 kg N ha$^{-1}$ + 5 Mg FYM ha$^{-1}$. Crop residues were exported at harvest, except for roots and 3-5cm of the aboveground stubble. During each year's dry season farmyard manure (FYM: cowdung mixed with rice straw) was applied in the N+FYM treatment at a rate of 5 Mg ha$^{-1}$ as fresh material.

The area is dominated by Rice-Fallow-Rice cropping systems with a subtropical monsoon climate. The annual mean temperature and rainfall are 25.8°C and 2427mm, respectively (BMD, 2015). Samples collected from the 0-15cm depth layer (i.e. the puddle layer) were mixed, broken, air dried, ground and sieved (2mm). Details of relevant soil properties are presented in Table 2.1. The four farmers' fields soils were selected for their variation in Fe and Mn extracted by different methods, total C and N and pH-KCl. The ratio of SOC:Fe extracted by dithionite citrate bicarbonate (DCB), varied between 0.6 and 1.8. XRD-analysis (Sleutel et al., 2013) revealed that the clay of the five soils were composed of variable admixtures of 2:1 phyllosilicates, with no smectites present. Instead, mica, vermiculite, chlorite, kaolinite, quartz, feldspars and interstratified mica-chlorite were identified in all soils. The Noaddah soil contained lepidocrocite and the Sonatala-1 and Melandoho soils contained goethite. A vermiculite-chlorite intergrade was detected in the Melandoho soil.

*2.2.2. Soil incubation methods*

Three controlled laboratory soil incubation experiments were set up. In the first two, soils were either 1° untreated ($T_1$), 2° amended with $Fe_2O_3$ powder (MW: 159.69g; 99% assay; particle size: <5μm; $NH_4$-oxalate extractable Fe: 4.5%; perchloric-nitric acids digested Fe: 44%) ($T_2$) or 3° amended with mixed Mn/Al-oxides ($NH_4$-oxalate extractable Mn and Al: 10 and 21% respectively) ($T_3$), synthesized by a modified method from Schwertmann and Cornell (1991). The application dose of Fe in $Fe_2O_3$ was set to half (Experiment 2.2.2.1) or the total (Experiment 2.2.2.2) content of $NH_4$-oxalate Fe present in the four soils on average. The dose of mixed Mn/Al oxides in both experiments were set equal to the average $NH_4$-oxalate extractable Mn content. The Mn/Al-ratio matched that of Bangladeshi paddy soils (Kader, 2012). In a third incubation experiment only untreated farmers' field soils were used (Experiment 2.2.2.3).

*2.2.2.1. Experiment I: Changes in pH, soil solution Fe, Mn and dissolved OC in relation to fertilizer management and Fe or Mn addition*

A first lab soil incubation experiment was set up covering 5 fertilizer treatments × 3 pre-treatments × 3 field replicates of the long-term BAU field experiment. Soils from these treatments were incubated for 8 weeks. Three pre-treatments, viz. $T_1$: Control, $T_2$: $Fe_2O_3$ at a rate of 2g $kg^{-1}$ soil and $T_3$: Mn/Al mixed oxide at a rate of 3.04g $kg^{-1}$ soil were included. The intent was to see whether Fe- and Mn-availability affect reductive dissolution of Fe and Mn, microbial activity and production of dissolved organic carbon (DOC) in relation to fertilizer management history. One hundred and twelve grams dry soil was filled to 5cm in 5.1cm inner diameter 10cm high PE-recipients to a bulk density of 1.1 Mg $m^{-3}$. The soils were oversaturated with deionized water to a standing water level of 2cm, after which the micro-rhizon soil moisture samplers (RSMS) (Rhizosphere Research Products, The Netherlands) were vertically inserted into each soil column cautiously. Soil solution at 0-5cm depth was sampled regularly by RSMS. Each RSMS was outfitted with a 5cm and 2.5mm OD porous part (pore size: 0.12-0.18 μm), stainless steel strengthener wire, a 12 cm PE/PVC tube, male luer lock and syringe needle. All soil columns were then kept in an incubation cupboard at 20°C. Every week, soil pore water (9ml each) was extracted by connecting a glass 10ml vacuum tube to each RSMS via the syringe needle. The collected soil pore solutions were analyzed for their Fe, Mn, and dissolved organic carbon (DOC) concentration and pH. Soil $CO_2$ and $CH_4$ emissions were monitored incrementally over the incubation. Gas emissions were assessed by placing each soil core inside a 2L glass jar, fitted with a septum, inside an incubation cupboard. After 2h, a 12ml gas sample was withdrawn from the jars' headspace by connecting 12ml pre-evacuated glass exetainer vials (Labco Limited Lampeter UK: 738W) via double sided needles. At the end of the 8-week incubation, the soil was analyzed for exchangeable-$NH_4^+$ content by 1M KCl-extraction, for microbial biomass C (MBC) content and for pH-KCl.

*2.2.2.2. Experiment II: Influence of Fe and Mn availability on anaerobic N mineralization in four paddy soils*

In a second incubation experiment, the parallel evolutions of KCl-extractable $NH_4^+$, pH-KCl, and dissolved Fe- and Mn-contents were compared in unamended and Fe or Mn/Al mixed oxides amended farmers' field soils for 10 weeks. All soils were incubated anaerobically in small PE pots (6.8cm height and 3.4cm inner diameter). The amount of dry soil per pot was 36g for Sonatala-1 and Sonatala-2 (1 Mg $m^{-3}$) soils and 45g for the Noaddah and Melandoho soils(1.2 Mg $m^{-3}$), matching the actual bulk density in the field at a 4cm soil depth. Three

treatments were again laid out, viz. an unamended control ($T_1$), addition of $Fe_2O_3$ at a rate of 7.2g $kg^{-1}$ ($T_2$) and addition of Mn/Al (0.08 ratio) mixture at a rate of 1g $kg^{-1}$ soil ($T_3$). All pots were kept in an incubation room at constant temperature (20°C) and deionized water was regularly added to maintain a standing water level of 2cm. Per treatment, two tubes were sampled destructively at 1, 2, 4, 6, 8 and 10 weeks after the start of the experiment. The soil in each tube was mixed properly by hand shaking and the soil paste was transferred into 85ml Nalgene centrifuge tubes and centrifuged at 8000rpm for 3 minutes. Thereafter, the supernatant was filtered through a Whatman (GF/C) glass microfibre filter fitted in a vacuum holder. The filtrate was then analyzed for Fe and Mn content. The soil residue of each sample was again homogenized and analyzed for 1M KCl extractable $NH_4^+$, pH-KCl and soil moisture content. A minor part of soil exchangeable $NH_4^+$ (about 5%) was extracted by the supernatant and was not quantified here.

*2.2.2.3. Experiment III: Short-term evolution of fixed-$NH_4^+$ content and MBC in paddy soils*

In a third incubation experiment, the contributions of abiotic defixation of $NH_4^+$ and biotic anaerobic N mineralization to anaerobic mineral N release were assessed in the four farmers' field soils. The soils were prepared and incubated in the same way as described in experiment-II, but only for four weeks. Twelve soil samples (4 soils × 3 replicates) were taken out biweekly and analyzed destructively for MBC and soil moisture content. In addition, soil material of each tube was dried in the oven at 25ºC for 72 hours, ground, sieved at 50µm mesh size and analyzed for fixed-$NH_4^+$-content (see 2.2.3).

*2.2.3. Soil chemical analysis*

Soil pH-KCl was measured by glass electrode in a 1:2.5 soil:KCl suspension. The pH of soil pore solution was measured directly by inserting the glass electrode in the soil solutions collected by RSMS in PE vials. Prior to incubation, contents of Fe, Al and Mn of air dried soils were determined by various extraction methods including ammonium oxalate (Blakemore et al., 1987), Sodium-Pyrophosphate (Blakemore et al., 1987), Dithionite-citrate-bicarbonate (Blakemore et al., 1987) and 0.5M HCl (Loveley and Phillips, 1986). Soil pore solutions and extracts were analyzed for their Fe, Al and Mn concentration by Inductively Coupled Plasma-Atomic Emission Spectroscopy on a radial plasma iCAP 6300 series spectrometer (Thermo Scientific, US). For the determination of exchangeable-$NH_4^+$, 15g of homogenized moist soil, equivalent to about 10g dry soil, was weighted in a 250ml Erlenmeyer and 50ml 1M KCl was added. The slurries were shaken for 2 hours and filtered through Ø150mm filter paper and collected KCl-extracts were stored in the freezer. The

extracts were analyzed for their $NH_4^+$-N concentration with a continuous flow auto analyzer (Skalar, The Nederlands). The dissolved organic carbon content in the collected soil solutions were determined by means of a TOC-analyzer (TOC-VCPN, Shimadzu Corporation, Kyoto, Japan) with separate measurement of total C and inorganic C after acidification with 2M HCl.

Non-exchangeable-$NH_4^+$ was determined on dried soil samples according to the Silva and Bremner (1966) method. In this method soil sample was treated with alkaline potassium hypobromite (KOBr-KOH) to eliminate exchangeable $NH_4^+$ and $NH_4^+$ released through decomposition of organic N. After that the soil residue was treated with 5M HF-1MHCl to decompose minerals containing non-exchangeable $NH_4^+$. The released $NH_4^+$ was determined via steam distillation of the soil-acid mixture with KOH and subsequent titration. Soil microbial biomass C on fresh soil was determined by the chloroform-fumigation-extraction method according to Vance et al. (1987) and resulting $K_2SO_4$ extracts were analyzed for their C content with the Shimadzu TOC-analyzer.

*2.2.4. Analysis of gas samples*

$CH_4$ and $CO_2$ concentrations of collected gas samples in exetainers were analyzed by a Trace Ultra GC (Interscience: Thermo Electron Corporation), equipped with packed columns and a flame ionization detector for $CH_4$ and a thermal conductivity detector (TCD) for $CO_2$. The production rate ($\mu g \ g^{-1}$ dry soil $h^{-1}$) of $CH_4$ and $CO_2$ was calculated by accounting for gas density and headspace volume. The relative fraction of $CH_4$-C to total C ($CH_4$-C+ $CO_2$-C) emitted from each soil sample was computed as a measure of soil anaerobicity.

*2.2.5. Data analysis*

All data were processed using SPSS. One-way and two-way ANOVA were used to detect for significant differences in KCl-extractable $NH_4^+$, dissolved Fe and Mn, $CH_4$ production rate, pH-KCl, MBC and non-exchangeable-$NH_4^+$ at the different sampling times.

**2.3. Results**

*2.3.1. Evolution of pH, Fe and Mn in field experimental soils (Experiment I) and farmers' fields soils (Experiment II)*

Generally the soil solution's pH of the five soils (only unfertilized control presented here) from the BAU field experiment (Fig. 2.1) and the soil KCl-extract based pH of all four farmers' fields soils (data not shown) increased over time, with or without addition of $Fe_2O_3$ or the Mn/Al-oxides mixture. Differences among the treatments ($T_1$, $T_2$ and $T_3$) per soil were always minor and insignificant.
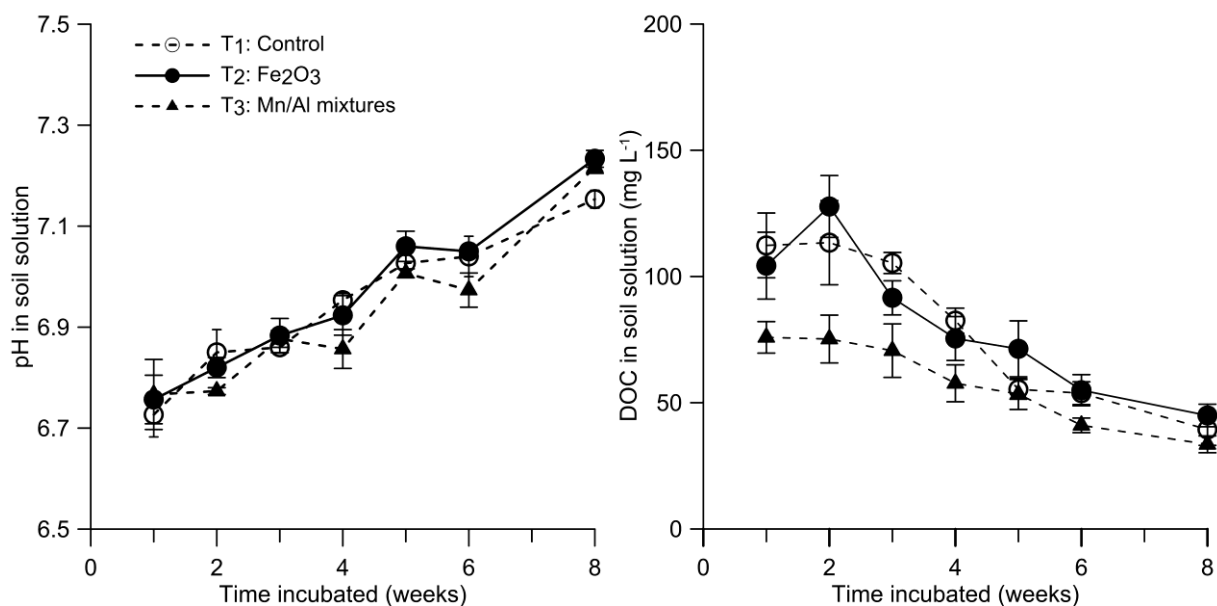


Fig. 2.1 Changes of pH and DOC in control soils from BAU long-term field experiment either amended with $Fe_2O_3$ or mixed Mn/Al oxides or left untreated (vertical bars indicate the standard errors of the means)

*2.3.1.2. Water soluble Fe*

In case of all five BAU field fertilizer treatments, the Fe in soil solution of $Fe_2O_3$ or Mn/Al-mixed oxides treated and untreated ($T_1$) soils increased steeply after two weeks (9 to 16mg $L^{-1}$) and peaked at the 4th week since onset of submergence (11 to 18 mg $L^{-1}$) (Fig. 2.2). Elevated Fe concentrations continued until the 5th week of inundation (10 to 17 mg $L^{-1}$) and decreased gradually in subsequent weeks. For all the five field experimental treatments, $Fe_2O_3$ addition ($T_2$) significantly lifted ($p < 0.05$) the soil solution Fe concentration compared to control treatments $T_1$, but only for week-6. On the opposite, soil amendment with mixed Mn/Al oxides ($T_3$), lowered the Fe concentration by 2 to 48% for week 1 to 5 when compared to $T_1$. Water soluble Fe content varied among the four farmers' fields paddy soils. However,

32

per soil the trend of soluble Fe was analogous in case of control ($T_1$) and $Fe_2O_3$ ($T_2$) treated soils (Fig. 2.2). In both Sonatala-1 and Sonatala-2 soils, the water soluble Fe content increased steadily, peaked after 4 weeks in $T_1$ and $T_2$, while for $T_3$ this maximum was already reached after 2 weeks. The increase in dissolved Fe was 12.3, 5.4, 13.9, 28.1 and 13.1 mg kg$^{-1}$ in the Sonatala-1, Sonatala-2, Melandoho, Noaddah and BAU soils, respectively. Subsequently, Fe concentration decreased gradually with time. In the Noaddah soil, dissolved Fe concentration increased linearly until 6 weeks of flooding and then leveled off. For the Melandoho soil in contrast, the Fe concentration only started to increase linearly 4 weeks after onset of submergence.



Fig. 2.2 Evolution of dissolved Fe in paddy soils either amended with $Fe_2O_3$ or mixed Mn/Al oxides or left untreated (vertical bars indicate the standard errors of the means)

*2.3.1.3. Water soluble Mn*

Over all five BAU field experimental treatments (here only two presented (Fig. 2.3) the evolution of soil solution Mn content over time was similar for the untreated and Fe amended soils but Mn content was clearly lifted by Mn/Al-mixed oxide application ($T_3$). In general, the concentration of soil solution Mn always went up gradually from its initial value of 0.0 mg L$^{-1}$

to a maximum after 2 weeks, followed by a slow decrease after 4 (in $T_3$) and subsequent weeks. The Mn contents after 2 weeks were significantly ($p<0.01$) higher in $T_3$ than in $T_1$ and $T_2$ and the content remained more or less at the same level until week-4. Similar to Fe, the evolution of water soluble Mn with time differed strongly among the four farmers' fields soils. Soil solution Mn contents were significantly ($p<0.05$) higher upon Mn/Al mixed oxides application ($T_3$) compared to the $T_1$ treatments (after 2 weeks for Sonatala-1 and Sonatala-2; after 10 weeks for Melandoho and Noaddah) (Fig. 2.3). The water-soluble-Mn content in both Sonatala-1 and Sonatala-2 soils went up sharply until the second week after submergence and declined rapidly to a stable range after 6 weeks. In contrast, the dissolved Mn content of the Melandoho soil remained at the initial level (2 mg $kg^{-1}$) in treatments $T_1$ and $T_2$ whereas in $T_3$ the concentration increased steadily from 2 to 8 mg $kg^{-1}$ over 10 weeks. Likewise, for the Noaddah soil, water extractable Mn went up gradually until 8 weeks for all treatments and concentrations were about double with soil Mn-amendment.
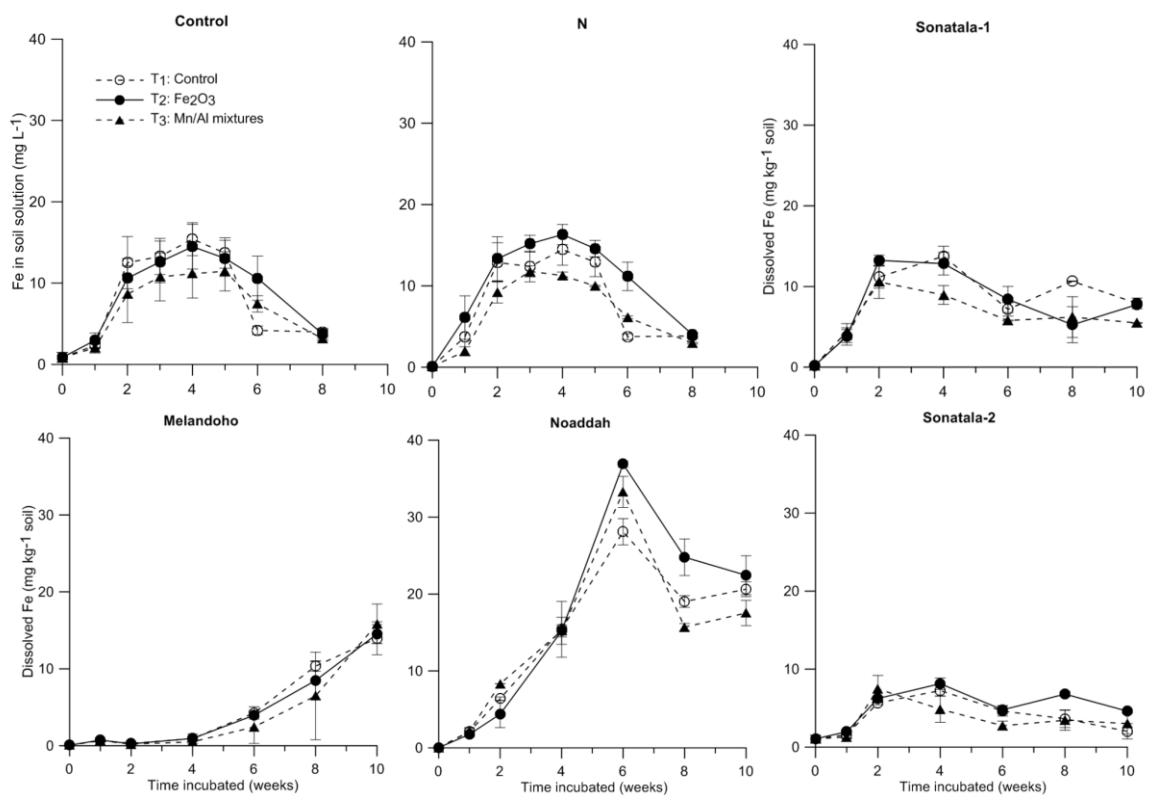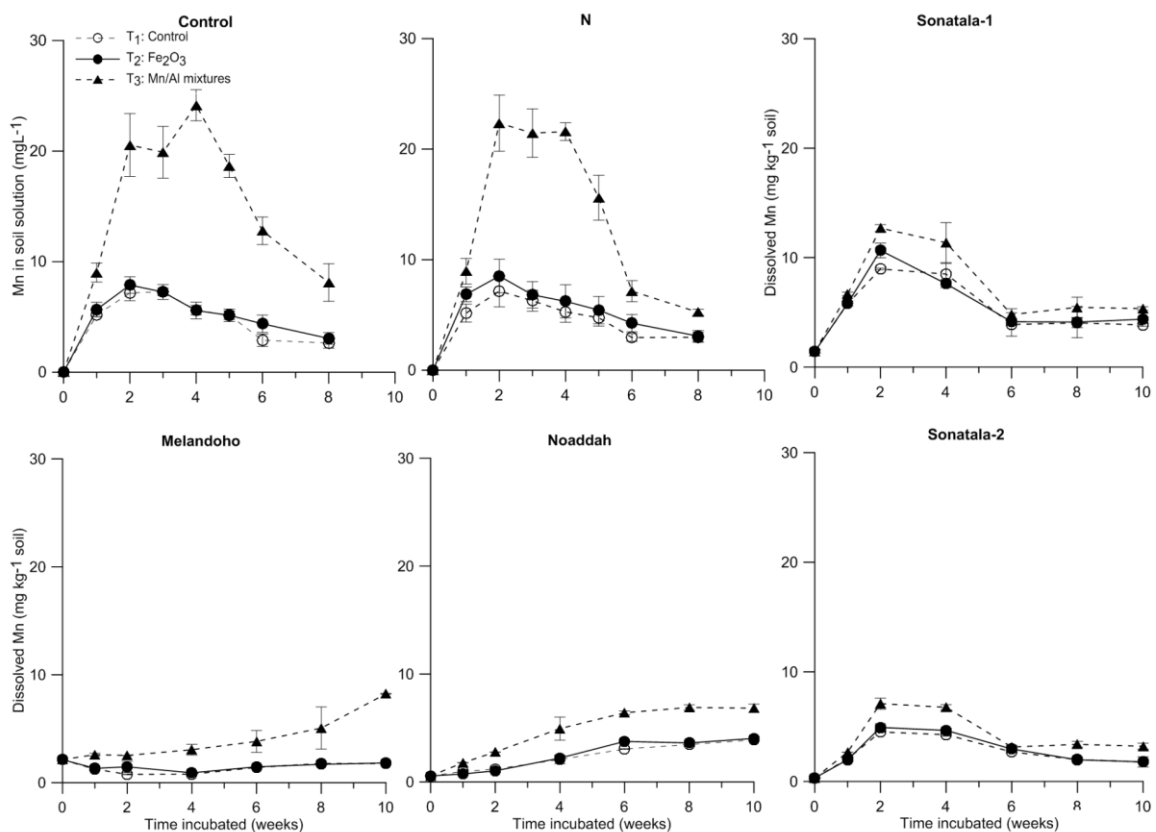


Fig. 2.3 Evolution of dissolved Mn in paddy soils either amended with $Fe_2O_3$ or mixed Mn/Al oxides or left untreated (vertical bars indicate the standard errors of the means)

## 2.3.2. Exchangeable ammonium (NH₄⁺) and microbial biomass carbon (MBC)

The initial 1M KCl extractable-$NH_4^+$ content was significantly lower in the N+FYM treated soil than in the other field experimental treatments (Table 2.2). The $NH_4^+$ contents increased after 8 weeks strongly by about 20 mg kg$^{-1}$ without any significant differences between the Mn or Fe treated and untreated soils (Table 2.2). Similar observations were made for the farmers' fields soils, with no dependency of $NH_4^+$ content on Fe or Mn amendment, regardless of their variation in initial soil exchangeable $NH_4^+$ content (Fig. 2.4). In both Sonatala-1 and Sonatala-2 soils exchangeable-$NH_4^+$ went up linearly from first sampling event to week 4, reached a maximum and maintained at a same level in the subsequent weeks. In the Melandoho and Noaddah soils, the exchangeable-$NH_4^+$ more or less remained at its initial value during the first 2 weeks and only then started to go up linearly until 10 weeks and 6 to 8 weeks, respectively. After 8 weeks of incubation, soil MBC in the five BAU long-term experimental soils ranged from 179 to 227 mg kg$^{-1}$, comprising 1.2 to 1.5% of SOC, irrespective of Fe or Mn amendment (data not shown). MBC measured after 2 weeks of incubation in third experiment differed strongly between the four farmers' fields soils (46 to 287 mg C kg$^{-1}$ soil), comprising 0.6-2.3% of SOC (data not shown)**.** In all soils the MBC-contents after 4 weeks of submergence were significantly ($P<0.05$) higher than after 2 weeks, except in the Noaddah soil.
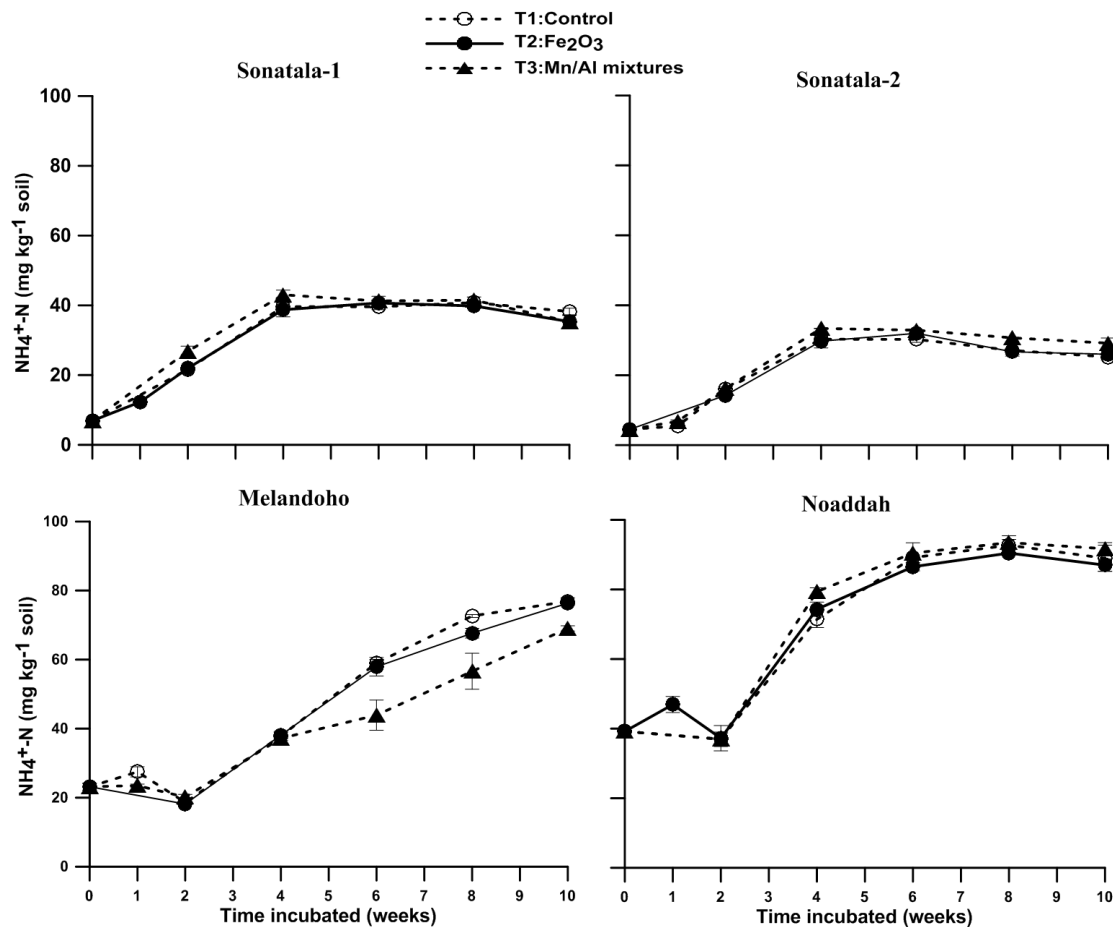
Fig. 2.4 Evolution of $NH_4^+$ content in paddy soils either amended with $Fe_2O_3$ or mixed Mn/Al oxides or left untreated (vertical bars indicate the standard errors of the means)

Table 2.2 The mean soil 1M-KCl extracted $NH_4^+$ content (mg kg$^{-1}$ soil) (± standard deviation), initially and after 8 weeks of flooding of BAU experimental treatments either amended with $Fe_2O_3$ or Mn/Al mixed oxides or left untreated

| Treatments | Control | N | NP | NPK | N+FYM |
|---|---|---|---|---|---|
| Week-0 | 5.88 ± 0.95b | 5.78 ± 0.42b | 5.85 ± 1.18b | 5.66 ± 0.85b | 4.55 ± 0.35a |
| Week-8 | | | | | |
| $T_1$(-) | 25.42 ± 6.27 | 29.50 ± 4.98 | 23.48 ± 2.28 | 28.71 ± 7.59 | 22.96 ± 5.23 |
| $T_2$ (Fe) | 23.59 ±5.74 | 29.67 ± 2.73 | 25.58 ± 3.76 | 30.42 ± 8.31 | 23.18 ± 9.12 |
| $T_3$ (Mn) | 23.94 ± 4.05 | 28.58 ± 2.03 | 22.82 ± 3.15 | 30.40 ± 11.28 | 25.28 ± 6.01 |
| ANOVA | NS | NS | NS | NS | NS |

* different lower case letters denote significantly different (P≤0.05) $NH_4^+$ concentration amongst the field experimental treatments according to Duncan's Multiple Range Post Hoc Test.

*2.3.3. Dissolved Organic Carbon (DOC) and $CO_2$ and $CH_4$ production from the BAU field experimental soils (Experiment I)*

The concentration of DOC was initially high in all five BAU soils and then decreased gradually during anaerobic incubation, irrespective of Fe or Mn-application treatment (Fig. 2.1, only unfertilized control shown here). The DOC concentration amounted 76-145 and 32-56 mg C $L^{-1}$ after 1 and 8 weeks, respectively. Over the entire 8-weeks period, the DOC concentrations in all Mn ($T_3$) amended soils, were 16 to 29% lower than those in $T_1$ treatments. DOC amounted 0.39 to 0.59% of SOC.

Seven incremental measurements of soil $CH_4$ and $CO_2$ emission were taken as indications of the onset of methanogenesis and depletion of Fe-reduction, rather to quantify soil $CO_2$ and $CH_4$ emitted. The relative fraction of C emitted as $CH_4$ to the total C-emission ($CH_4$-C+$CO_2$-C) was plotted against time for each of the five paddy soils (Fig. 2.5). Overall, the percentage of produced $CH_4$-C to total C was negligible until 5 weeks, and then increased rapidly to reach a maximum after 6 to 8 weeks of continuous submergence. Overall, the rate of $CH_4$ emission ($\mu$g $g^{-1}$ $h^{-1}$) from the Mn-treated soils ($T_3$) were significantly ($p<0.05$) lower compared to the $T_1$ treatments. Irrespective of Fe or Mn amendment, $CO_2$ emission ranged 0.8 to 6.1 $\mu$g $g^{-1}$ $h^{-1}$ after 1 week, and then decreased gradually to an almost stable value of 0.001 to1.2 $\mu$g $g^{-1}$ $h^{-1}$ after 6 weeks (data not shown).
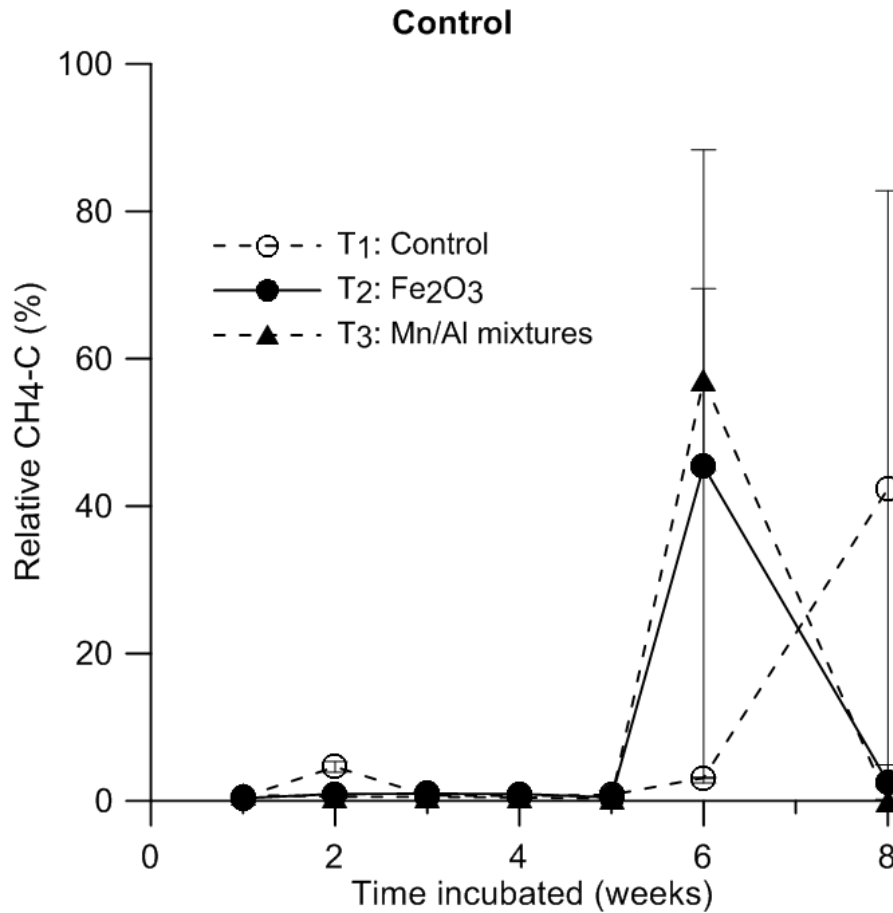
Fig. 2.5 Evolution of the relative $CH_4$-C emission ($CH_4$-C emission / ($CO_2$-C+$CH_4$-C emission) from soils of the BAU long-term field experiment, either treated with $Fe_2O_3$ or mixed Mn/Al oxides or left untreated (vertical bars indicate the standard errors of the means)

*2.3.4. Evolution of exchangeable and non-exchangeable $NH_4^+$ (Experiment III)*

After onset of submergence, exchangeable-$NH_4^+$ gradually increased in all four farmers' fields soils during the 4-week incubation, while non-exchangeable-$NH_4^+$ mainly exposed a sharper initial increase (Fig. 2.6). The amount of non-exchangeable-$NH_4^+$ differed significantly ($p<0.01$) per soil: Sonatala-1 (281-435 mg $kg^{-1}$), Sonatala-2 (201-319 mg $kg^{-1}$), Melandoho (239-289 mg $kg^{-1}$) and Noaddah (179-250 mg $kg^{-1}$). In all four soils, the non-exchangeable-$NH_4^+$ content after 2 and 4 weeks was significantly ($p<0.01$) higher than the initial content.
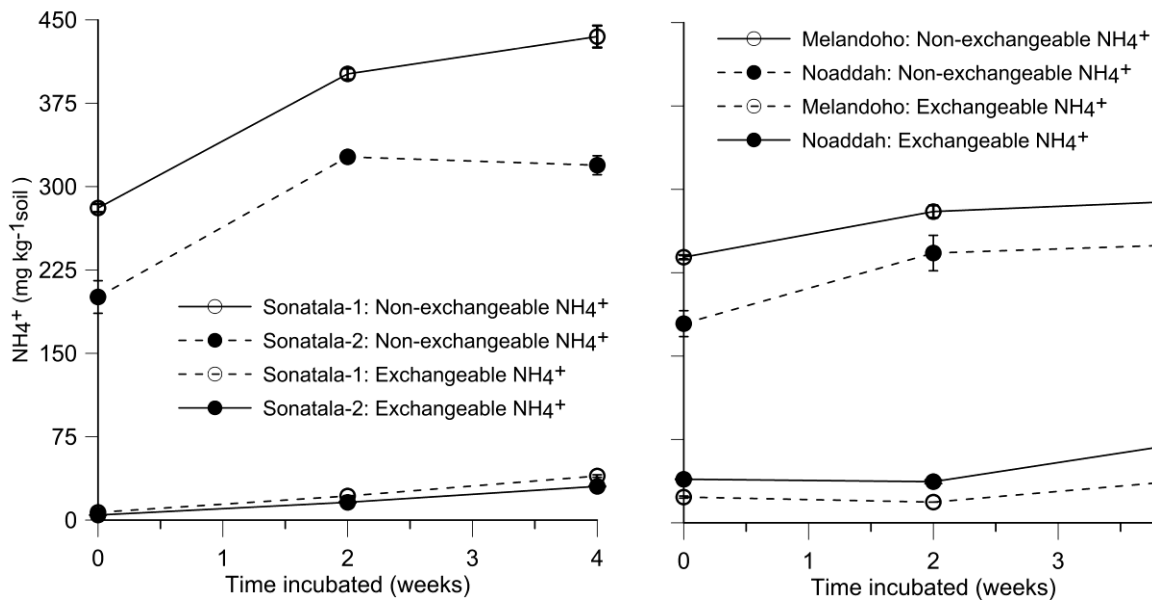
Fig. 2.6 Evolution of exchangeable and non-exchangeable-$NH_4^+$ in untreated farmers' fields paddy soils (vertical bars indicate the standard errors of the means)

## 2.4. Discussion

### 2.4.1. Detailed insight into soil solution chemistry, pH, MBC and $CO_2/CH_4$ in soils of BAU long-term field experiment

Iron reduction is one of the dominant processes in wetland paddy soils required to support mineralization of SOM (Van Bodegom et al., 2003; Qu et al., 2004). In all five soils, the increased soil solution Fe concentrations of $T_1$ and $T_3$ sustained from week-2 to week-5, whereas in $T_2$ this was until week-6. This indicates that iron-oxide addition to some extent prolonged the supply of $Fe^{3+}$ as alternative electron acceptor, yet only to a limited extent. The limited utilization of $Fe^{3+}$ as alternative electron acceptor from added hematite powder in $T_2$ was perhaps due to its higher crystallinity (only 4.5% of added Fe was $NH_4$-oxalate extractable). Alongside, after 8 weeks the soil pH-KCl and the pH in soil solution increased by 1.0 and 0.2-0.5 units, respectively, by reductive consumption of protons but this was irrespective of the Fe- or Mn-oxide application of the five paddy soils. The following decrease in Fe content after 5-6 weeks of incubation was likely due to precipitation of iron as $Fe_3O_4.nH_2O$ or $Fe_3(OH)_8$ and $FeS.nH_2O$, brought about by the increasing pH and declining partial pressure of dissolved $CO_2$ (Ponnamperuma et al., 1967) and reduction of $SO_4^{2-}$. Relatively lower concentrations of soil solution Fe in $T_3$ than $T_1$, are most likely due to a preferential reduction of the added Mn-oxides (Ponnamperuma, 1972; Munch and Ottow, 1980).

Analogous to Fe, increasing concentrations of water soluble Mn content after submergence of paddy soils primarily results from reduction of Mn(IV)(hydr-)oxides and a decrease Mn-concentration is usually due to removal of $Mn^{2+}$ by precipitation as $MnCO_3$, formation of insoluble organic complexes and cation exchange reactions (Ponnamperuma, 1972). Amendment of $Fe^{3+}$ did not affect the evolution of $Mn^{2+}$ concentrations in soil solution at all, probably since Mn is preferentially utilized as alternative electron acceptor compared to Fe. The evolution of soil solution Fe and Mn content did not differ noticeably among the five fertilizer treatments soils (viz. control, N, NP, NPK and N+FYM). Hence, Fe and Mn-reduction appeared to occur at the same rate, irrespective of 34 years of distinct fertilization management. But always higher soil solution Mn contents in the $T_3$ resulted from supplemental reduction of added Mn-oxides compared to the $T_1$ treatments. Thus, unlike amendment with $Fe^{3+}$, soil application of Mn(IV)-oxides did affect the sequence of soil redox reactions, and they served as important electron acceptors during 1 to 5 weeks of flooding. The $CH_4$ production started after about 5 weeks of continuous flooding, partly coinciding with the completion of $Fe^{3+}$ and $Mn^{4+}$ reduction. Decreased $CO_2$ emissions after several weeks of flooding probably resulted from increased reduction of $CO_2$ to $CH_4$, precipitation of $FeCO_3$ (Yao et al., 1999) and lower concentration of readily bio-available C source (DOC).

The concentration of DOC was higher initially and decreased with time in all soil/amendment combinations. This contrasts with a commonly observed gradual release of DOC in the soil solution following the onset of flooding, caused by several mechanisms. Grybos et al. (2009) stated that anaerobic incubation of wetland soils releases 2.5% of total SOC as DOC, which is mainly associated with rising pH from 5.5 to 7.4 and reduction of soil Mn and Fe. At higher pH, net positive surface charge of minerals decreases and organic molecules become more electronegative due to deprotonation. Decreasing DOC levels may also be explained by the formation of complexes between functional groups (carboxyl, hydroxyl) of DOC and metal ions such as $Fe^{2+}$ (Stumm and Sulzberger, 1992; Kraemer, 2004), which are gradually released into the soil solution following submergence. In accordance with this, Nierop et al. (2002) stated that precipitation of DOM by $Fe^{2+}$ under anaerobic conditions removed 75% of DOC from solution at an $Fe^{2+}/C$ quotient of 1. Furthermore, in all soils, DOC concentrations were relatively lower in Mn/Al mixed oxides treated paddy soils ($T_3$) than in case of the unamended control $T_1$. This appears to be linked with the higher soil solution $Mn^{2+}$ concentrations in $T_3$ than in the other two treatments, with a comparable enhanced formation of $Mn^{2+}$-DOC complexes. Alternatively, rapid mineralization of DOC, a readily biodegradable C pool (Hanke et al., 2013; Zhang et al., 2007), could also explain gradual lowering of DOC levels. Particularly so because contents of low ordered Fe-oxides, important sorbents of

SOC, were low and so DOC desorption from these surfaces, otherwise perhaps compensating decreasing DOC levels, might also have been limited. In all five field experimental treatments, the MBC after 8 weeks contributed 1.2 to 1.5% of the total SOC pool. MBC was not significantly different among the five BAU fertilizer treatments, in contrast to previous studies like e.g. Zhang et al. (2009), but this may be due to relatively small variation in SOC content amongst the field experimental treatments without any significant differences between the $Fe_2O_3$ or Mn/Al mixed oxides treated and untreated soils. Consequently, in line with observations for the evolution of DOC, Fe, and Mn we conclude that availability of $Mn^{4+}$ or $Fe^{3+}$ only had at most a modest control on microbial biomass in the studied paddy soils.

After 8 weeks the KCl extractable $NH_4^+$ content in all five BAU soils increased by 17 to 25 mg $kg^{-1}$ but the differences among the untreated and Fe or Mn-treated soils were not significant. This matches the observation that hematite ($Fe_2O_3$) powder addition ($T_2$) yielded a slight increase of Fe but MBC and onset and rate of $CH_4$ production were unaffected. The addition of Mn/Al mixed oxides, however, did result in increased soil solution Mn ($T_3$) and significantly lowered or delayed $CH_4$ emission. We should acknowledge, however, that lower $CH_4$ production in $T_3$ may have been linked either with the competitive consumption of $H_2$ produced from OM decomposition by Mn-reducing bacteria or with oxidation of $CH_4$ in a redox pair with $Mn^{4+}$ (Yao et al., 1999; Yu et al., 2007). Still, Mn-amendment had no effect at all on $NH_4^+$ accumulation. Nevertheless, it is striking that 33 years of distinct fertilizer amendment did not affect release of $NH_4^+$ between the BAU experimental treatments. N release in soil is logically determined by soil organic nitrogen quality as well. Said-Pullicino et al. (2014), for instance, demonstrated that much plant-available N comes from incorporated crop residues and content of crop-derived particulate organic matter has often been found most responsive to fertilizer and exogenous OM amendment. Consequently, we might expect a closer dependency of N-supply from crop residues, rather than from bulk SOM, and availability of alternative electron acceptors. At BAU, straw was, however, exported and sand fraction OM contents did not differ with fertilizer treatment and had C:N ratio of 14-16, i.e. not indicative of a large contribution of undecomposed plant-matter (Kader, 2012). Nor did sand N correlate with the anaerobic N mineralization rate (Kader, 2012). So in contrast to the field studied by Said-Pullicino et al. (2014), crop residues were likely a lesser source of $NH_4^+$ following mineralization and there is no indication of a stronger dependency on availability of electron acceptors than in case of bulk soil N mineralization.

Experiment I, however, covered just one soil type and we only measured exchangeable-$NH_4^+$ content at the end of the incubations. To confirm these findings the second experiment

with four farmers' fields soils and destructive soil sampling was performed to track exchangeable-$NH_4^+$ with time.

*2.4.2. Effect of Fe and Mn availability on mineral N release in farmers' fields soils*

Generally, as in the first BAU-soil experiment, water soluble Fe initially increased linearly, peaked and then slowed down in all farmers' field soils, except for Melandoho. Reductive dissolution of Fe(III)(hydr-)oxides and precipitation again logically explain these evolutions. The ranges in water soluble Fe content were soil specific and relatively higher in the Noaddah soil. The magnitude of $Fe^{3+}$ reduction logically varies from soil to soil depending particularly on the redox changes, SOM (electron donors) content, forms and degree of crystallinity of Fe-(hydr-)oxides, pH etc. (Ponnamperuma, 1972; Qu et al., 2004; Zhang et al., 2012). Reduced Fe has been found to be correlated with ammonium-oxalate extractable Fe, meaning that weakly crystalline Fe-(hydr-)oxides are probably the most important source of reduced Fe (Van Bodegom et al., 2003). We calculated the increase in soil solution Fe since onset of flooding until a maximum was reached and its temporal rate of change for all five soils. Neither magnitude nor rate of change in Fe correlated to $NH_4$-oxalate extractable Fe or to DCB-extractable Fe. But the magnitude of Fe-release correlated positively with Na-pyrophosphate extracted Fe (r=0.90; p=0.037). Though Na-pyrophosphate is often mistakenly assumed to exclusively isolate organically complexed Fe, it in fact partly extracts non- or poorly crystalline Fe in general (SSSA, 2008), i.e. indeed likely sources of dissolved Fe following reduction. For Bangladeshi floodplain paddy soils, Kader et al. (2013) furthermore found that anaerobic N mineralization as well only correlated positively with Na-pyrophosphate-extractable Fe, out of a substantial list of soil parameters. In our limited set of five soils, there was no correlation between anaerobic soil $NH_4^+$-release and Na-pyrophosphate extractable Fe (r=0.03, p=0.15). It should be noted that besides quantity, the quality of soil OM (SOC) might have overridingly controlled anaerobic soil net N mineralization and reduction of Fe. Higher levels of labile C may on the one hand result in fast depletion of readily reducible Mn and Fe. However, in general, Kader (2012) thus concluded a poor relation between soil OM quality and net mineral N release in young floodplain soils of Bangladesh. It thus seems unlikely that differences in OM quality overrulingly determined N release, obscuring potential relations between Fe-reduction and net soil N supply in the present study. It could be postulated though that with increasing OM loading onto pedogenic Fe-(hydr)oxides, these might become less reducible.

As in experiment 1, there were only minor differences in the contents of water soluble Fe between untreated and $Fe_2O_3$ amended soils. This would mean that either: 1° availability of reducible-Fe was already sufficient to cover consumption of electrons donated by microbial activity in all soils; or 2° the supplied $Fe_2O_3$ (hematite powder) was not adequately available for reduction due to its physical conformation. In line with the second explanation, Qu et al. (2004) proposed that the addition of ferric oxides like goethite, hematite etc. had no effect on dissolved $Fe^{2+}$ contents in paddy soil slurries compared to unamended controls, indicating no microbial mediated reduction of the added oxides. Indeed, Van Bodegom et al. (2003) also found that crystalline iron oxides were not substantial contributors of reducible-Fe, in contrast to non-crystalline pedogenic Fe.

Ammonium release patterns during anaerobic incubation were asymptotic for all four farmers' field paddy soils. Generally, the total amount of released $NH_4^+$ ranged from 25 to 54 mg $kg^{-1}$ during 10 weeks, analogous with that attained by Narteh and Sahrawat (1999), who reported $NH_4^+$ released varied between 3 to 74 mg $L^{-1}$ after 15 weeks of anaerobic incubation. Among the four soils, the maximum amount of $NH_4^+$ was produced in the Noaddah soil, followed by Melandoho. For all soils, there were only insignificant differences in $NH_4^+$ content among the treated ($T_2$ and $T_3$) and untreated ($T_1$) soils after 10 and 8 weeks. Consequently, this leads us to reject the main hypothesis that lack of available reducible-Fe or Mn would form a bottleneck for anaerobic microbial activity and net N mineralization in these Bangladeshi paddy soils. Again, the experimental setup (i.e. application of $Fe_2O_3$ as a powder) could have been inappropriate to fully reject this research's primary hypothesis. However, like in the BAU soils, the addition of amorphous mixed Mn/Al oxides ($T_3$) did significantly increase the concentration of dissolved-Mn and to some extent prolonged microbial Fe-reduction. Nonetheless, there was no influence on the final release of mineral N. From this it is in fact possible to justly conclude that a lack of available alternative electron acceptors did not limit anaerobic N mineralization. This does not mean that Mn- and Fe-reduction and mineral N-release are entirely decoupled. In fact, a positive correlation existed between content of exchangeable-$NH_4^+$ and soil solution Fe per measuring date in farmers' fields paddy soils (Sonatala-1: r=0.55 to 0.69 and p=0.13 to 0.20; Sonatala-2: r=0.34 to 0.68 and p=0.06 to 0.14; Melandoho: r=0.90 to 0.94 and p=0.002 to 0.01; Noaddah: r=0.77 to 0.92 and p =0.004 to 0.08) irrespective of soil amendments. Possibly, reductive dissolution of Fe and Mn-oxides releases bound organic N, which may then be mineralized into $NH_4^+$. This hypothesis requires verification through dedicated experiments. Lastly, soil N supply as here assessed from evolutions of soil exchangeable $NH_4^+$ depends on the balance between N mineralization and biotic immobilization and both processes are microbial and depend on

availability of an electron acceptor. Additional monitoring of the build-up of the microbial N pool would have been required to draw conclusions on the dependency of soil N mineralization on alternative electron acceptor availability.

*2.4.3. Exchangeable and non-exchangeable-$NH_4^+$ in farmers' fields*

The relative fast and substantial increase of exchangeable-$NH_4^+$ in the Sonatola-1, Sonatola-2 and Noaddah soils was striking. This prompted the question whether such a fast initial mineral N build-up can be entirely ascribed to microbial action. Alternatively, it could at least partly have resulted from abiotic fixed-$NH_4^+$ release. If release of fixed-$NH_4^+$ is substantial, then logically Fe and Mn addition should have no control at all on the exchangeable-$NH_4^+$ buildup in the studied soils. Content of fixed $NH_4^+$ differed between the four soils and roughly related to clay content for the Sonatala-1, Sonatala-2 and Melandoho soils, taking into account a higher abundance of vermiculite in the Sonatala-1 soil (Sleutel et al., 2013). However, the Noaddah soil had double clay content but lowest fixed $NH_4^+$ content, possibly because of its low abundance of vermiculite. Regardless of $NH_4^+$ content, in all four farmers' fields soils, the gradual increase of both exchangeable and non-exchangeable-$NH_4^+$ during the 4-weeks incubation actually indicated that flooding favored $NH_4^+$ fixation, rather than its net release. In line, Scherer and Zhang (1999) suggested that reduction and dissolution of Fe-(hydr-)oxides coatings on clay surfaces at low Eh may favors either release or fixation of $NH_4^+$ depending on $NH_4^+$ concentration in solution. Furthermore, Matsuoka and Moritsuka (2011) proved that the release and storage of weakly fixed $NH_4^+$ on exposed edges of layer phyllosilicates is controlled by content of exchangeable $NH_4^+$ in anaerobically incubated paddy soil. Said-Pullicino et al. (2014) also found that greater exchangeable $NH_4^+$ concentration in anaerobic soils slowed release of fertilizer-derived fixed N compared to oxic soils.

The buildup of exchangeable-$NH_4^+$ after two weeks therefore must have derived primarily from SOM decomposition. The MBC measurements matched this reasoning as there was but a small additional increase between week 2 and 4 since the onset of submergence and even a decrease in the Noaddah soil. In summary, these results on fixed-$NH_4^+$ and MBC indicated that there was no considerable abiotic release of $NH_4^+$ to an exchangeable pool, which instead must therefore have been biotical-derived, i.e. from anaerobic N mineralization.

## 2.5. Conclusions

Our study on five Bangladeshi paddy soils demonstrates that evolutions of exchangeable-$NH_4^+$, pH and Fe, Mn and DOC in soil solution during flooding remained similar with or without addition potential alternative electron acceptors. Although hematite powder-addition didn't influence reductive Fe dissolution, mixed Mn-oxide amendment did lead to higher soil solution Mn and lower DOC concentrations and delayed methane emission, pointing to additional microbially driven reduction of the applied Mn. Hence, together with the absence of an effect on exchangeable-$NH_4^+$ buildup in soil, our hypothesized dependency of the latter process on availability of alternative electron acceptors is rejected. The simultaneous buildup of exchangeable and fixed-$NH_4^+$ upon anaerobic incubation shows that this $NH_4^+$ must have been primarily biogenic. Reductive dissolution of Fe and net anaerobic N mineralization do, nonetheless, appear to be linked to each other, given the very similar temporal patterns of soil solution Fe and 1M KCl-extractable-$NH_4^+$ in each one of the studied soils. We hypothesize that reductive dissolution of pedogenic oxides releases organic N, which is then mineralized. A first step to elucidate this relationship could be to establish linear pe+pH/dissolved $Fe^{2+}$-curves, which could designate the origin of reduced Fe in these floodplain soils. In addition oxalate-, pyrophosphate- and DCB-extraction of soil N prior to and after multiple cycles of soil incubation might be used to confirm selective binding of organic N on such reducible pedogenic oxides. Additionally, advanced spectroscopic visualization of co-occurrence of Fe, Mn and N via new technology like nano-SIMS could be applicable for confirmation.

# Chapter 3

# A study of paddy soil N supply dependency on edaphic factors and biochemical responses to submergence using within-field spatial variation
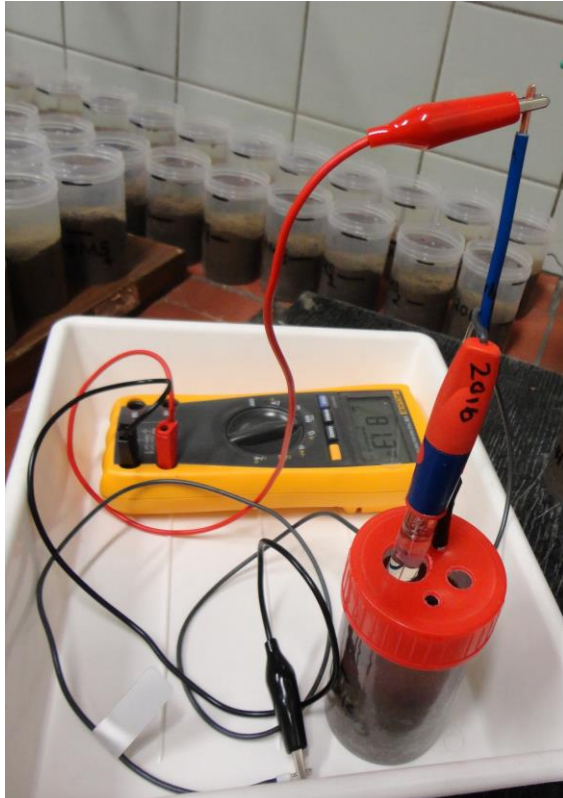
**Abstract**

Evidence across soils for a linkage between soil mineral N supply and processes like reductive Fe-dissolution or extent of pH and Eh changes after submergence is difficult to establish because multiple soil factors co-vary and often specific parts of soil C and Fe are involved in anaerobic microbial activity. We assessed 1° if as opposed to bulk soil contents, short- to medium term rates of change of soil redox potential (Eh), solution Fe, Mn, organic C (DOC) and N (DON) and gaseous C-emissions following submergence would be useful predictors of net anaerobic N mineralization; 2° if their predictive power exceeds that of common edaphic properties. To exclude substantial variation in soil mineralogy and recent management we made use of variation within a spatially heterogeneous paddy field in Sri Lanka in terms of soil N, OC, silt, clay, $pH_{KCl}$, oxalate-extractable Fe ($Fe_{ox}$) and Mn ($Mn_{ox}$) and collected soil from fifty spots. Changes in soil Eh, pH, $NH_4^+$ and $NO_3^-$, dissolved Fe, Mn, DOC and DON, microbial biomass C (MBC) and N (MBN), and total C emission were assessed in anaerobic incubation for 42 days in a single paddy field so as to keep land-use history and past management as constants. Generally, most variables increased linearly within first 14 days, stayed at higher level between 14-28 days, then declined during 28-42 days. The modeled net mineralized N ($N_t$) ranged from 20-86 mg $kg^{-1}$ i.e. 2.3-6.7% of TN with mineralization rate ($k_t$) of 0.02-2.86 mg $kg^{-1}$ $day^{-1}$. Principal component analysis indicated two clusters of variables: $N_t$ strongly ($p<0.01$) correlated with SOC (r = 0.79) and DON (r = 0.73), followed by DOC, MBC, TN, $CH_4$ efflux, MBN, Fe release rate and pH rise (r = 0.29 to 0.71; $p<0.05$). SOC alone explained about 62% variation in $N_t$, and excluding SOC, stepwise-regression found DON, MBC, Eh, MBN and $CH_4$ efflux to jointly explain 77% variability. In sum, SOC and DON played most important roles on the studied soils' net anaerobic N mineralization rather than $Fe_{ox}$ and $Mn_{ox}$ or other edaphic properties. Total C emission did not relate to $N_t$ and Fe rate. So it seems that Fe's availability as electron-acceptor may not have been a confounding bottleneck for SOM degradation and net N mineralization in the present paddy field. Instead, significant correlations between Fe rate, DOC, DON, and pH rise suggested release of DOM to at least partly stem from reductive dissolution of pedogenic oxides and desorption. The correlation between DON and $N_t$ may point out that DON release forms an intermediate step to final net anaerobic mineral N supply, but this requires verification using stable ^{15}N-isotope setups.

## 3.1. Introduction

Expansion of paddy production by cultivating fertilizer responsive high yielding varieties through subsidy schemes is a political priority to satisfy annual domestic rice requirement in rice producing Asian countries, e.g. in Sri Lanka (Ekanayake, 2009; Weerahewa et al., 2010). However, this goal is far from achieved as (sub-)tropical paddy soils are usually low in organic carbon (OC), pH (4.5-6.0) and cation exchange capacity (CEC) (<10 cmol kg$^{-1}$), and prevailing humid and high temperature further impedes storage of soil OC, leading to deterioration of soil fertility and crop productivity (Wijewardena, 2005). In addition frequent limited knowledge on soil N supply brings about overuse or misuse of N fertilizer and this lowers N use efficiency and emerges a direct economic loss for farmers, and adversely impacts the atmospheric environment and water quality. On the other hand blanket doses are justified by the fact that soil N supply remains difficult to predict, though it is well known that main rice plants uptake ~50 to 80% N which is not directly from fertilizers but from SOM mineralization (Zhang et al., 2017) and partly also from release of fixed $NH_4^+$. Native soil N supply is only often partly or weakly explained by general soil traits.

Several previous studies have examined linkage between anaerobic N mineralization and paddy soil properties but mostly inconsistent relations varying with soil type or region are derived (Narteh and Sahrawat, 1997; Kader et al., 2013; Zhang et al., 2017). For instance in West African paddy soils Narteh and Sahrawat (1997) found positive relations between anaerobic N mineralization and soil pH, OC, total N, clay and CEC, while in floodplain Bangladeshi paddy soils instead (Kader et al., 2013) these were either absent or even negative. Multifold explanations can be forwarded, one being that in nearly continuously submerged paddy soils, significant amounts of amide N may be bound to aromatic OM, readily limiting available soil N (Schmidt-Rohr et al., 2004) and explaining the often poor relation between paddy soil N and N supply. Just as important to understand soil N supply might be limited by the availability of alternative electron (e$^-$) acceptors such as $NO_3^-$, $Mn^{4+}$, $Fe^{3+}$, $SO_4^{2-}$ and $CO_2$ onto which soil microbial activity depends after flooding-caused depletion of $O_2$ and lowering of redox potential (Eh). Reducibility of $Fe^{3+}$, the main e$^-$-acceptor (Inubushi et al., 1984; Sahrawat, 2004a), may form a bottleneck for soil N mineralization but is hard to assess from common soil extraction-based measurement, though some authors did relate N supply and extractable Fe (e.g. by $NH_4$-oxalate or HCl) (Narteh, and Sahrawat, 1997; Zhang et al., 2017). Actual availability of oxidants and C and N to microbes is likely better understood by ambient levels of dissolved organic N (DON) and C (DOC), MBC and MBN, and release of Fe and Mn in soil solution, next to Eh and pH. Reduction and dissolution of Fe oxides coating on surface of clay minerals induced by low

Eh after flooding, may also favor either release or fixation of $NH_4^+$ by diffusion out of or into the interlayer of clay minerals depending on exchangeable $NH_4^+$ level (Scherer and Zhang, 1999).

Recently, Akter et al. (2016) observed co-evolution of solution Fe release and exchangeable $NH_4^+$-N in waterlogged paddy soils with diverse SOC to $Fe_{ox}$ ratio, possibly denoting Fe's connection to N mineralization. Moreover desorption of DOC and DON from clays and pedogenic Fe and Mn following flooding is either due to gradual lifting of pH to neutrality or/and reductive dissolution of Fe- and Mn- (hydr-)oxides (Grybos et al., 2009; Hanke et al., 2013). This release of DOC and DON may be pertinent for microbial degradation and contribute to mineral N release, though causality is not clear yet. Regardless, it is obvious that DOM provides a substrate for microbes, as was clearly seen from declined C and N mineralization approximately by 2 to 20% and 7 to 27% resp. in DOM-removed Chinese paddy soils (Li et al., 2010). Lastly, also the microbial N pools (MBN) usually temporarily immobilizes substantial amounts of initially available N (Cucu et al., 2014; Said-Pullicino et al., 2014) but then eventually re-mineralizes with release of $NH_4^+$.

In synthesis, we, as other did, postulate that in water-logged soils even more than under unsaturated conditions, available N is best represented by exchangeable mineral N, DON and MBN jointly, recognizing that soil N supply is the resultant of mineralization, immobilization and N loss processes (Cucu et al., 2014; Said-Pullicino et al., 2014; Wang et al., 2001). Alternative predictors of N mineralization thus may include the size and activity of microbial biomass, content and composition of oxidants, and levels of DOC and DON (Narteh and Sahrawat, 1997; Li et al., 2010; Akter et al., 2016; Zhang et al., 2017). Our objective was to assess indices of their evolutions alongside pH and Eh during incubation of submerged soil and compare their ability to predict soil N mineralization relative to edaphic factors. Since experimental manipulation of quality and availability of OM and of oxidants would probably not represent natural conditions study of natural variation across paddy fields seems a more viable approach. However, differences in recent management (fertilizer application, irrigation, crop rotation, use of exogenous OM and removal of residues) may then overridingly determine observed soil N release and it becomes impossible to fundamentally investigate connections with indices of microbial activity and availability of OM and oxidants. Alternatively, spatial variation of levels of OC, N, Fe and Mn, and texture within a single paddy field could be used to identify predictor-variables of anaerobic N mineralization. In our present investigation we sampled 50 locations from a spatially heterogeneous farmer's paddy field in Sri Lanka and monitored pH, Eh, solution Fe, Mn,

DOC and DON, total C ($CO_2$-C + $CH_4$-C) emission, MBC and MBN, next to $NH_4^+$-N release during 42 days of incubation and evaluated co-variations.

## 3.2. Materials and Methods

### 3.2.1. Study site, soil sampling and analysis of soil properties

Fifty soil samples characterized by wide spatial variations in properties (Table 3.1) were collected from a selected farmer's paddy field in Atalle, Sri Lanka (7°33'12" N, 80°26'15" E). The study area is representative of Sri Lanka's 'intermediate zone' with annual rainfall of 1000 to 2000 mm and temperature range of 21 to 34°C (Panabokke, 1996). The deep and poorly drained soil was derived from alluvial material and classified as a Typic Endoaquent according to USDA Taxonomy. The soil was annually flooded during the Maha or wet season and rain-fed rice was grown (Sep-Feb). Irrigated rice was also grown in the Yala or dry season (Mar-Aug). The field was divided into 50 grid cells and for each one random point (Fig. 3.1a) was assigned and sampled by spade till 15cm depth using a GPS receiver. After removal of root fragments, collected soil samples were broken, air dried and stored at room temperature. Details of general soil properties are presented in Table 3.1. Total C and N were directly determined by a Tru Mac CNS analyzer (LECO), while poorly crystalline-pedogenic Fe as predominant source for reducible Fe (van Bodegom et al., 2003) was determined by the ammonium oxalate extraction method. Before incubation soil pH-KCl and mineral N ($NH_4^+$-N and $NO_3^-$-N) were measured in 1:5 soil:1M KCl extracts by means of a glass electrode and a continuous flow auto analyzer (Skalar, The Nederlands), respectively. Spatial within-field variation of sand, silt and clay content determined by a previous sampling campaign and analysis with the pipette-sedimentation method (Gee and Or, 2002). The field site was explicitly selected for their wide spatial ranges in organic C (5.6-12.3 g $kg^{-1}$) (Fig. 3.1b), N (0.8-1.4 g $kg^{-1}$), oxalate extractable Fe ($Fe_{ox}$: 0.83-2.59 g $kg^{-1}$) and Mn ($Mn_{ox}$: 0.00-0.16 g $kg^{-1}$), resulting in gravimetric SOC to $Fe_{ox}$ ratio's between 3 to 14 and SOC to $Mn_{ox}$ ratio's 56 to 2191 (Table 3.1). The set of 50 soil samples also covered ranges in initial exchangeable mineral N ($NH_4^+$-N: 4-11 and $NO_3^-$-N: 0-7 mg $kg^{-1}$), exchangeable K (49-108 mg $kg^{-1}$) and pH-KCl (4.4 to 5.8, denoting strongly acidic pH range). Clear opposite gradients existed between silt and clay contents within the field i.e. % silt was increasing (10 to 19%) while % clay (18 to 4%) was declining from southeast to northwest. The texture for most soils was Sandy Loam with several soils being Loamy Sand while percentage of sand was nearly constant. Recent management and land-use history were uniform with paddy rice cultivation. Except $Mn_{ox}$ and $NO_3^-$-N, mean and median values were almost identical with

skewness values close to zero for other soil properties, indicating that data for most traits were normally distributed (Table 3.1).

Table 3.1 Selected properties and ranges of the studied biochemical processes in the paddy soil samples used for incubation experiment

| Soil ID | Minimum | Maximum | Mean | STDEV | Std error | Median | Skewness |
|---|---|---|---|---|---|---|---|
| SOC g kg$^{-1}$ | 5.6 | 12.3 | 8.8 | 1.6 | 0.2 | 9.1 | -0.2 |
| Total N g kg$^{-1}$ | 0.8 | 1.4 | 1.1 | 0.1 | 0.0 | 1.1 | 0.1 |
| Fe$_{ox}$ mg kg$^{-1}$ | 828 | 2585 | 1523 | 509 | 72 | 1352 | 0.5 |
| Mn$_{ox}$ mg kg$^{-1}$ | 4 | 172 | 33 | 33 | 5 | 22 | 2.5 |
| SOC:Fe$_{ox}$ | 3 | 14 | 6 | 2 | 0 | 6 | 1.0 |
| SOC:Mn$_{ox}$ | 56 | 2191 | 505 | 403 | 57 | 426 | 1.8 |
| pH-KCl | 4.4 | 5.8 | 4.8 | 0.3 | 0.0 | 4.8 | 1.2 |
| NH4-N mg kg$^{-1}$ | 3.9 | 10.6 | 6.2 | 1.4 | 0.2 | 6.0 | 1.1 |
| NO$_3^-$-N mg kg$^{-1}$ | 0.1 | 6.8 | 0.7 | 1.4 | 0.2 | 0.0 | 2.4 |
| C: N | 6 | 10 | 8 | 0.8 | 0.1 | 8 | -0.3 |
| Clay (%) | 4 | 18 | 9 | 2 | 0 | 9 | 0.8 |
| Silt (%) | 10 | 19 | 16 | 2 | 0 | 16 | -0.7 |
| pH rise | 0.5 | 1.7 | 1.2 | 0.2 | 0.0 | 1.2 | -0.2 |
| Mean Eh (0 to 21DAS, mV) | -332 | 122 | -73 | 124 | 18 | -26 | -0.3 |
| Fe release rate (mg l$^{-1}$ d$^{-1}$) | 0.7 | 9.8 | 3.2 | 1.8 | 0.3 | 2.9 | 1.2 |
| Mn release rate (mg l$^{-1}$ d$^{-1}$) | 0.0 | 1.2 | 0.2 | 0.2 | 0.0 | 0.2 | 2.7 |
| Total C emission (mg kg$^{-1}$) | 97 | 442 | 259 | 91 | 13 | 248 | 0.3 |
| Total DON, $N_t$ (mg kg$^{-1}$) | 2.3 | 9.6 | 5.5 | 1.6 | 0.2 | 5.1 | 0.5 |
| Mean DOC (mg kg$^{-1}$) | 47 | 106 | 64 | 14 | 2 | 60 | 1.4 |
| Mean MBC (mg kg$^{-1}$) | 128 | 538 | 316 | 89 | 13 | 313 | 0.0 |
| Mean MBN (mg kg$^{-1}$) | 30 | 137 | 89 | 23 | 3 | 87 | -0.1 |
| Parameters of 1st order N mineralization kinetics | | | | | | | |
| $k_f$ (mg kg$^{-1}$ d$^{-1}$) | 0.00004 | 2.9 | 0.4 | 0.8 | 0.1 | 0.1 | 2.2 |
| $N_t$ (mg kg$^{-1}$) | 20 | 103 | 47 | 20 | 3 | 43 | 0.8 |

|                 |       |
|:---------------:|:-----:|
| (a)             | (b)   |
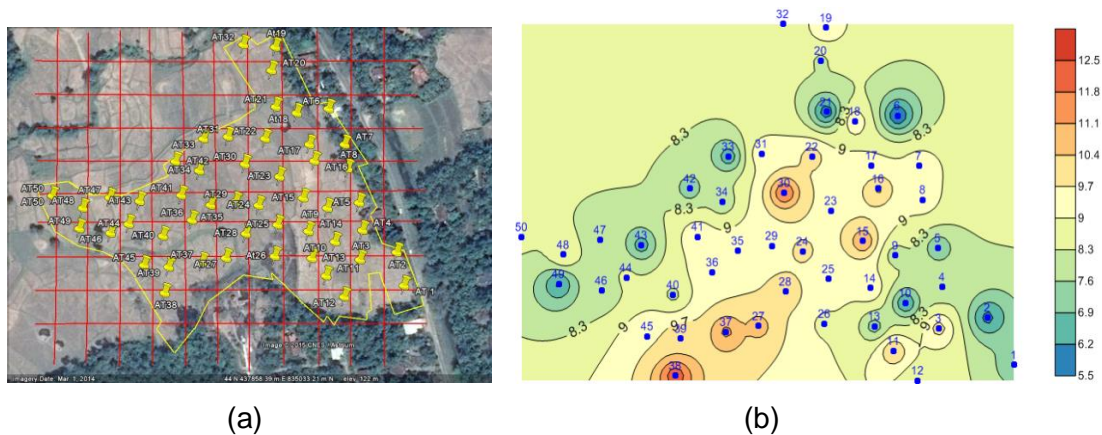
Fig. 3.1 Boundary with sampling scheme of the field in Atalle, Sri Lanka (a), and spatial distribution of top soil OC (b) (g kg$^{-1}$) in the studied soil set

### 3.2.2. Experimental method

A controlled (19 °C) laboratory incubation experiment covering 50 soils × 4 sampling events was set up for 42 days. The incubation period was based on previous findings that peak concentrations of solution Fe and Mn, and soil exchangeable $NH_4^+$ are usually reached in 2 to 4 weeks of anaerobic incubation (Akter et al., 2016). The intent was to attain detailed insight into evolutions of pH, Eh, solution Fe, Mn, DON and DOC, total C emission, MBC and MBN, as indicative of redox processes and microbial activity, and their linkage to anaerobic N mineralization. All soils were anaerobically incubated in small PE pots of 10cm height and 5.6cm inner diameter. Per pot 141g dry soil was filled forming a soil core of 4.4cm height, matching the actual bulk density in the field (1.3 Mg m$^{-3}$). Soils were then flooded to a standing water level of 4cm. This level was maintained by regular addition of degassed (by purging with $N_2$ gas for 1h) deionized water.

### 3.2.3. Assessment of soil Eh and pH

Frequent monitoring of soil redox potential (Eh) was carried out with in-house fabricated Pt-electrodes (Pt wire joined at the tip of insulated Cu wire with steel epoxy resin, Devcon Co., Netherlands), installed permanently at 3 cm below the soil surface in all 50 soils. Before installation each fabricated Pt eletrode was tested with standard redox buffers (125 and 250 mV) and AgCl reference electrode. In each pot, an AgCl reference electrode (3M KCl saturated with AgCl) was also installed at least 1.5h before measuring the redox potential (mV) by connecting both redox and reference electrode with a multi-meter. Eh was then recalculated by adding measured potential ($E_m$) and potential of Ag/AgCl reference electrode

($E_{ref}$) ($E_h = E_m + E_{ref}$). During incubation, pH was measured regularly by direct insertion of a glass electrode into the soil to depth of 2 to 3 cm.

*3.2.4. Collection and analysis of soil solution to track dissolved Fe, Mn, DOC and DON*

In a single set of soil cores of all 50 sampling locations a Rhizon soil moisture sampler (RSMS: pore size: 0.12-0.18 µm, 5 cm long, 2.5 mm Ø porous part) (Rhizosphere Research Products, The Netherlands) was vertically installed per pot to regularly collect soil pore solution. To monitor dissolved Fe and Mn, solution was extracted into 16.2 mg $K_3$EDTA-coated 9 ml plastic vacuum vials (Vacutest Kima srl : Arzergrande (PD), Italy) by piercing the vial's septum with RSMS's needle. $K_3$EDTA coated vials were used to avoid precipitation of solution Fe and Mn. The extracts were analyzed for their Fe and Mn concentration by ICP-OES with a radial plasma iCAP 6300 series spectrometer (Thermo Scientific, US). Log-normal models were used to describe the temporal evolutions of Fe and Mn concentration (*Fe(t)* and *Mn(t)*):

$$Fe(t) = Fe_{max}.e^{-c_{Fe}\left(1-\ln(\frac{t}{t_{max;Fe}})^2\right)}$$

$$Mn(t) = Mn_{max}.e^{-c_{Mn}\left(1-\ln(\frac{t}{t_{max;Mn}})^2\right)}$$

, with *$Fe_{max}$* and *$Mn_{max}$* the peak solution concentrations (in mg l$^{-1}$), and *$t_{max;Fe}$* and *$t_{max;Mn}$* the elapsed time in days after submergence (DAS) to reach these maxima in dissolved Fe and Mn. The parameters *$c_{Fe}$* and *$c_{Mn}$* describe the shape of the log-normal curve.

Per soil and per sampling time another aliquot of soil solution was sampled into a 9ml vacuum vial (Vacutest Kima srl: Arzergrande (PD), Italy) to track evolutions in dissolved organic carbon and nitrogen (DOC and DON). DOC concentrations were determined by a Shimadzu TOC-VCPN-analyzer (Shimadzu Corporation, Kyoto, Japan) with separate measurement of total C and inorganic C after acidification with 2M HCl. To determine DON, soil solution was oxidized first by alkaline per sulfate digestion method (Koroleff, 1983). Briefly, 2ml solution was taken into 12ml disposable culture tubes of 10cm height × 1.6cm diameter with 1mm wall thickness and GL18 neck (Duran Group, Germany). Then 3ml oxidizing reagent (mixture of purified $K_2S_2O_8$, $H_3BO_3$ and 3.75M NaOH) was added, and tubes were swirled and closed with caps (GL18, screw cap (PP) with rubber seal, Duran Group, Germany) instantly to avoid $NH_3$ lost from alkaline solution. Samples were then autoclaved for 30 minutes at 121°C temperature and $NO_3$ levels were measured by a continuous flow auto-analyzer (Skalar, The Nederlands). The rate of DON buildup was estimated by fitting a first-order kinetic model to its temporal evolution: $N_t = N_0 + N_d(1 - e^{-k_d t})$, where *t* is the time (in days), *$N_0$* is the initial DON content, *$N_{(t)}$* is

the amount of DON released at time $t$ (mg kg$^{-1}$), $N_d$ the potential amount of DON pool, and $k_d$ is the first-order DON release rate (mg kg$^{-1}$ d$^{-1}$).

### 3.2.5. Soil sampling to monitor buildup of mineral N and microbial biomass (MBC and MBN)

To follow-up soil mineral N (NH$_4^+$-N+NO$_3^-$-N) release, a single soil core was taken out per sampling location after 8, 15, 28 and 42 DAS. About 20g of each collected homogenized moist soil, equivalent to ~10g dry soil was weighted in a 250ml Erlenmeyer and extracted with 50ml 1M KCl (soil to 1MKCl ratio approximated at 1:5), by shaking for 2h and filtration of the extracts through Ø150mm filter paper (MN 616 1/4). Extracts were analyzed for their NH$_4^+$-N and NO$_3^-$-N concentration by a continuous flow auto-analyzer (Skalar, The Nederlands). To calculate anaerobic N mineralization rates, a first-order kinetic model was fitted (mean R$^2$ = 0.94) to the time series of mineral N: $N_t = N_0 + N_a(1 - e^{-k_f t})$, where $t$ is the time (in days), $N_t$ is the amount of mineral N released at time $t$, $N_0$ is initial mineral N, $N_a$ is the potentially mineralizable N (mg kg$^{-1}$), and $k_f$ is the first-order N mineralization rate constant. Simultaneous to mineral N, MBC and MBN on fresh soil were determined using chloroform-fumigation-extraction method (Vance et al., 1987). K$_2$SO$_4$ extracts were analyzed for their C content with Shimadzu TOC-analyzer and MBC was calculated by dividing the difference between C content in CHCl$_3$ fumigated and non-fumigated samples with $k_C$ factor of 0.45. To quantify MBN on same K$_2$SO$_4$ extracts the alkaline per sulfate digestion method (Koroleff, 1983) was used (see Section 3.2.4). MBN was then calculated by dividing the difference between N content in CHCl$_3$ fumigated and non-fumigated samples with $k_N$ factor of 0.54 (Zhang et al., 2009). For each sample gravimetric moisture content was determined by oven drying ~20g moist soil at 105°C for 24h which allows calculation of all concentrations on soil dry weight basis.

### 3.2.6. Gas sampling and measurement of headspace CH$_4$ and CO$_2$ fluxes to assess C mineralization

Carbon mineralization evolved as total C emission was assessed by collecting gas samples covering 50 soils × 8 sampling events over whole incubation period. Each sample was incubated for 1h at room temperature in 2L glass jar, fitted with a septum. Gas samples were then drawn at 0, 30 and 60 min from the jar's headspace by connecting 12ml pre-evacuated glass exetainer vials (Labco Limited Lampeter UK: 738W) by a double sided needle. The CH$_4$ and CO$_2$ concentrations in collected headspace air samples were measured by two Trace Ultra Gas Chromatographs (Thermo Electron Corporation, US), equipped with packed columns and a flame ionization detector for CH$_4$, and a thermal conductivity detector

connected with auto-sampler for $CO_2$. Gas concentrations were converted to mass based levels by the ideal gas law and linear regression was used to calculate the fluxes of $CO_2$ (average $R^2$: 0.62) and $CH_4$ (average $R^2$: 0.67). Then C-efflux rate (in mg $CO_2$-C + $CH_4$-C kg$^{-1}$ soil h$^{-1}$) was recalculated for all sampling points. Accumulated total C emission (in mg C kg$^{-1}$ soil) was computed and its temporal evolution was described by a zero-order kinetic model.

### 3.2.7. Data analysis and development of maps

Non-linear regression analysis was employed to estimate parameters of first-order models describing DON and mineral N build-up over time. Correlation (Pearson correlation coefficient) and stepwise linear regression analyses were performed to investigate co-variations of modeled amount ($N_t$) of net mineralized N on the one hand and static soil properties, pH rise, mean Eh during submergence, release rate of Fe and Mn, levels of DON, DOC, MBC and MBN, and total C emission. To further explore these relations principal component analysis (PCA) was also performed considering only the first and second canonical variables (PC1 and PC2 derived from PCA) as dependent variables in the regression analysis to identify predictor variables for modeled $N_t$. All statistical analyses were performed using SPSS 24.0 statistical package. Ordinary inverse distance weighted (IDW) maps were created for soil variables and processes using the Surfer11 software package.

## 3.3. Results

### 3.3.1. Characterization of soil biochemical properties during anaerobic incubation

In waterlogged paddy soils initially present $O_2$ is rapidly consumed by microbes launching anaerobic conditions and alternative e$^-$ acceptors are utilized by microbial populations during SOM decomposition. Such conditions could result changes in biochemical properties including soil pH, Eh, solution chemistry particularly dissolved Fe, Mn, DOC, DON, MBC and MBN, which could also influence soil organic C and N mineralization in paddy soil set with diverse properties. Thus the trends with expected changes and interrelations of all these parameters and total C emission by controlled laboratory anaerobic incubation experiment are outlined in this section. While changes in soil mineral N build-up and it's linkage with soil properties and aforementioned biochemical processes during incubation are presented in section 3.2.2 and 3.3.3, respectively.

### 3.3.1.1. Evolution of soil redox potential (Eh) and pH

Overall, soil Eh ranged widely from -368 to 312 mV in the first week of incubation (data not shown), and by 21DAS the mean Eh had declined to -322 to 122 mV (Table 3.1), indicating wide variation in establishment of degree of reductive conditions within the paddy field (Fig. 3.2a). We categorized all 50 locations into two broad classes- based on mean Eh level over 0-21DAS. In a first set of 28 soils (Soil ID: 27 to 50, excluding 35 but including 1, 7, 12, 14 and 23) Eh evolved to relatively higher potentials (mean Eh level 0-21DAS = -40 to 122 mV). In the other set there was an evolution to more reducing conditions (mean Eh level 0-21DAS = -40 to -340 mV) (Soil ID: 2 to 26, including 35 but excluding 1, 7, 12, 14 and 23) (Fig. 3.2a). Out of both categories, three representative soils were selected to demonstrate the evolutions of other studied biochemical variables further on (Soil ID 3, 11 and 22 vs. Soil ID: 28, 39 and 47) (Fig. 3.2b). After 21 days strong reductive conditions persisted in these soils and Eh stayed around -100 mV until 42 days. In the soil set with higher mean Eh level fluctuated within a range of -100 to 100 mV during 12 to 42DAS (Fig. 3.2b). As expected the pH for all 50 soils increased from 5.1-6.2 to 6.2-6.9 after 8DAS, and remained nearly neutral until 42DAS, i.e. an overall rise by 0.6-1.9 pH-units. The extent of pH rise was greater in the set of soils that evolved to lower Eh (1.5 unit) than for the soils with higher (-100 to +100mV) equilibrium Eh soils (1.2 unit). Overall pH rise significantly correlated ($p<0.05$) with initial soil pH KCl ($r = -0.76$), $Fe_{ox}$ ($r = 0.53$), SOC ($r = 0.32$), %silt ($r = -0.34$) and the ratio SOC to $Fe_{ox}$ ($r = -0.33$) (Table 3.3). Rise in pH also correlated ($p<0.05$) to release rate of solution Fe ($r = 0.54$) and Mn ($r = 0.30$), $CH_4$ efflux ($r = 0.47$), levels of DOC ($r = 0.39$) and DON ($r = 0.42$) (see section 3.3.1.2 and Table 3.2). On the contrary, mean Eh (0 to 21DAS) did not correlate with any of these soil properties, nor with derived kinetic parameters of monitored biochemical processes over time (see section 3.3.1.2 and Table 3.2 and 3.3).



**(a)**          **(b)**
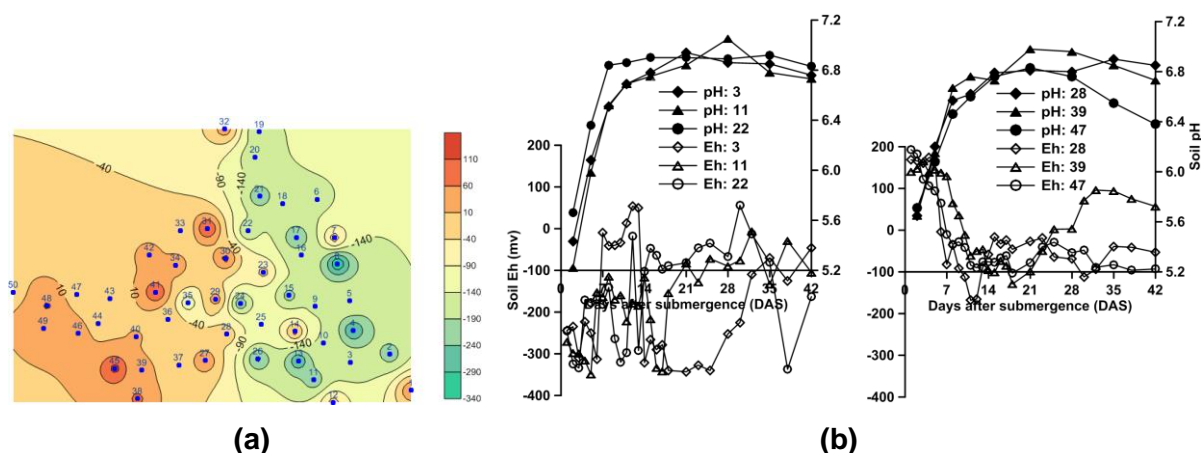
Fig. 3.2 Gradients in mean Eh during 0-21 DAS for all 50 locations (a), and temporal changes in Eh and pH of six sampling locations with three lower (-40 to -340mV; Soil ID 3, 11 and 22) and three higher (-40 to 122mV; Soil ID 28, 39 and 47) mean Eh level (b)

*3.3.1.2. Temporal evolutions of solution Fe and Mn, and their relations to soil properties and biochemical processes*

Typically for all 50 sampling locations dissolved Fe (0.04 to 125 mg $l^{-1}$) clearly exceeded Mn (0.1 to 12 mg $l^{-1}$) during the entire incubation, indicating a more prominent contribution of Fe reduction to sustain anaerobic microbial activity than Mn reduction. Temporal evolutions of Fe followed expected sigmoidal trends, with initial (on 2DAS) low levels (0-14 mg Fe $l^{-1}$), and maxima around 15DAS (12-78 mg $l^{-1}$) (Fig. 3.3a). After peaking both soil solution Mn and Fe subsequently gradually lowered until 42DAS. Resembled to Fe, solution Mn concentration in all soils (except for soil 27, 37, 40, 41 and 45 with greater Mn level) increased steadily form its low level of 0.1 -1.8 mg $l^{-1}$ on 2 DAS to 0.3-3.9 mg $l^{-1}$ on 8DAS, and stayed around same level until 21DAS, followed by lowering to initial low level on 42DAS (Fig. 3.3b). Log-normal models were well fitted to the temporal evolution of dissolved Fe (adjusted mean $R^2$ = 0.79) and Mn (adjusted mean $R^2$ = 0.72) (data not shown) and this disclosed substantial variations in maximal Fe and Mn concentrations reached (in mg $l^{-1}$) ($Fe_{max}$: 10 to 64 for the lower and 13 to 52 for higher equilibrium Eh classes, $Mn_{max}$: 0.2 to 4.6). Time (in days) required to reach maxima in dissolved Fe and Mn was variable as well ($t_{max;Fe}$: 8 to 18 and $t_{max;Mn}$: 6 to 16). Rates of initial Fe and Mn release (mg $l^{-1}$ $d^{-1}$) were calculated by dividing $Fe_{max}$ and $Mn_{max}$ with the respective $t_{max;Fe}$ and $t_{max;Mn}$ and ranged widely for both Fe (0.7 to 5.9) and Mn (0.03 to 0.4). Besides significant ($p<0.05$) correlations existed between Fe or Mn release rate and $Fe_{ox}$ and $Mn_{ox}$, respectively, both rates were also ($p<0.05$) correlated to the rise in pH and to the mean DOC level (Tables 3.2 and 3.3). Hence soils with more $Fe_{ox}$ and $Mn_{ox}$ released greater amounts of Fe and Mn, and this coincided with release of DOC, a higher $CH_4$ efflux and larger rise in soil pH.

Fig. 3.3 Temporal evolution of soil solution Fe (a) and Mn (b) of six sampling locations with three lower (Soil ID 3, 11 and 22) and three higher (Soil ID 28, 39 and 47) mean Eh level

*3.3.1.3. Changes in solution DOC and DON, and their linkage to soil properties and evolved biochemical processes*

Temporal evolutions of DOC and DON generally followed similar patterns for most soils and their concentrations differed greatly across the 50 sampling locations (Fig. 3.4). With time overall DOC and DON concentrations increased by 3 to 8% and 1 to 9% respectively, in soils with lower Eh due to more reduced state than higher Eh soils. For most locations including the 6-demonstrated soils (Fig. 3.4a), DOC concentrations (in mg $l^{-1}$) increased steadily from 89-254 (average 146) on 2 DAS to 109-345 (average 181) on 5DAS. These somewhat elevated DOC levels persisted until 35DAS (101-380 mg $l^{-1}$), and dropped on 42DAS (Fig. 3.4a). Compared to DOC, more pronounced asymptotic patterns of DON over time were observed for most sampling locations including the 6 demonstrated soils (Fig. 3.4b). DON concentrations ranged between 0.04 and 8.1 mg $l^{-1}$ on 2DAS, and increased quickly to 8-36 mg $l^{-1}$ on 21DAS, and nearly plateaued till 42DAS. Because of the limited changes in DOC with time the averaged DOC level was investigated as predictor of N mineralization and its relation to soil properties and biochemical processes. For DON estimated first-order kinetic model (adjusted mean $R^2$ = 0.73) parameters for DON release rate ($k_d$) and total amount ($N_t$) were instead used. The mean DOC level (47-106 mg $kg^{-1}$, ~119-270 mg $l^{-1}$) and total amount of DON released ($N_t$: 2 to 10 mg $kg^{-1}$, ~6-24 mg $l^{-1}$, Fig.

3.8b) depended on SOC and TN, as suggested from their strong mutual (p<0.01) correlations (Table 3.3). Besides both were significantly (p<0.01) and positively correlated to overall pH rise, Fe release rate, $CH_4$ efflux, mean MBC and MBN (see 3.3.1.4), but not with total soil gaseous C-efflux (Table 3.2).
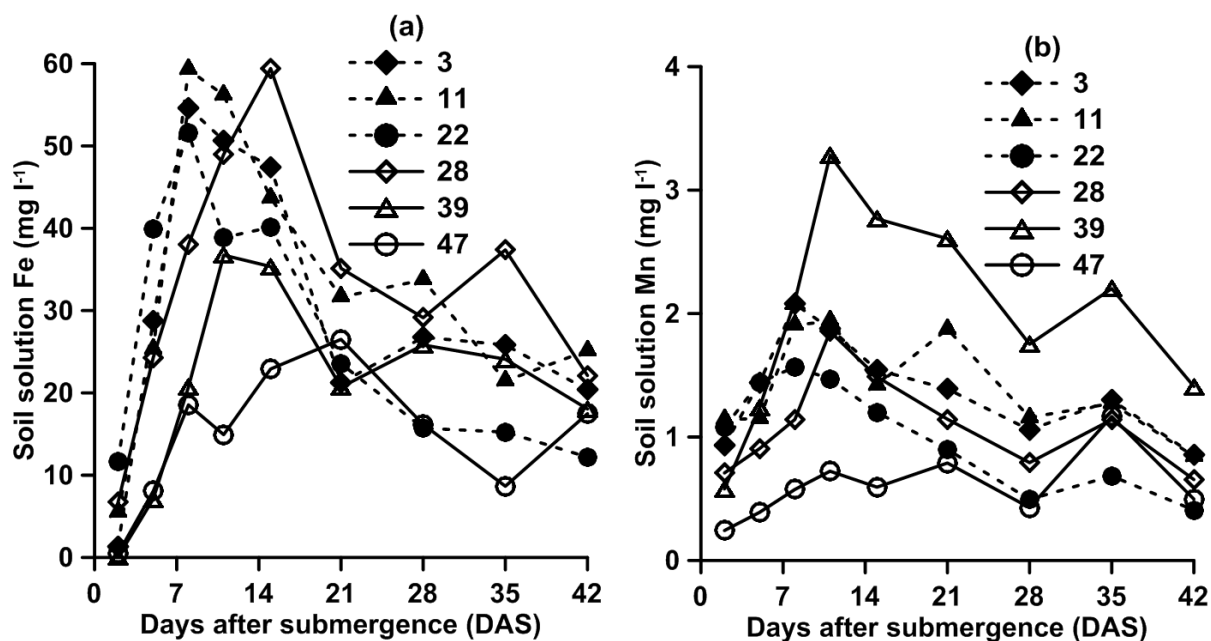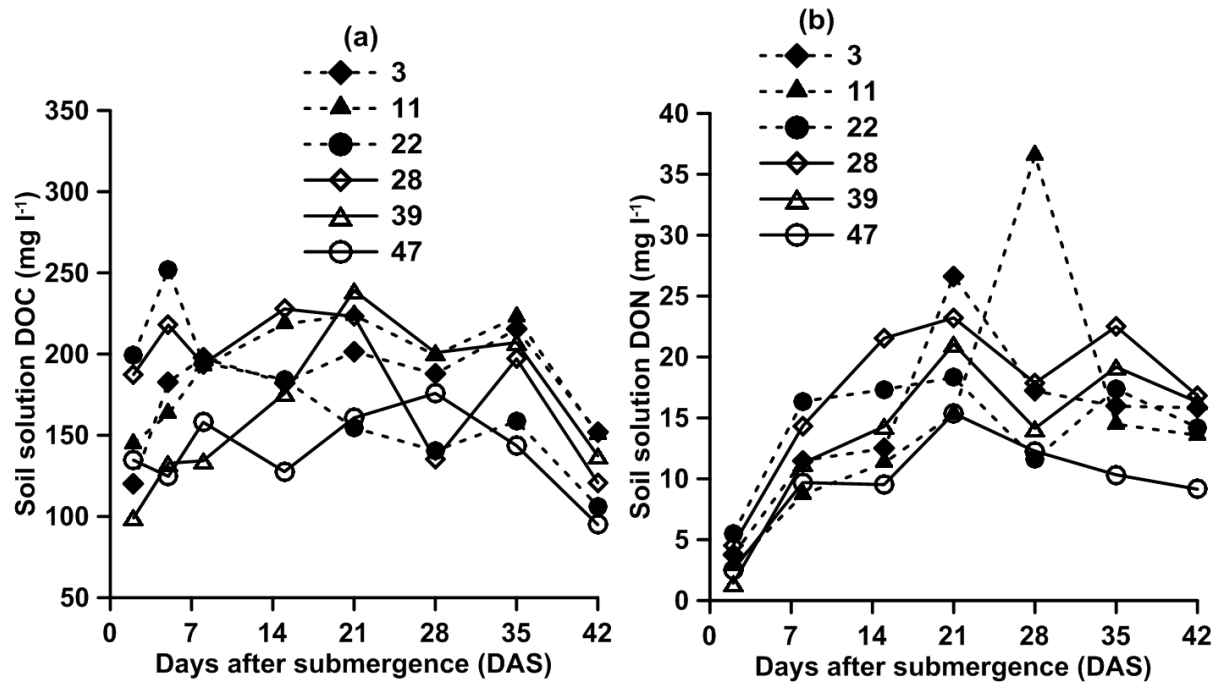


Fig. 3.4 Temporal evolutions of soil solution DOC (a) and DON (b) of six sampling locations with three lower (Soil ID 3, 11 and 22) and three higher (Soil ID 28, 39 and 47) mean Eh level

*3.3.1.4. Temporal changes in soil MBC and MBN*

Averaged over all four sampling events MBC and MBN ranged from 128 to 538 mg C $kg^{-1}$ and 26 to 127 mg N $kg^{-1}$, respectively (data not shown) and followed similar trends within soils which reached high or low equilibrium Eh (Fig. 3.5). A substantial buildup of MBC occurred within the first week of flooding to on average 316 mg $kg^{-1}$. Subsequent temporal fluctuations in MBC and MBN were more distinct in the group of high equilibrium Eh soils: the mean MBC dropped a little down to 267 mg $kg^{-1}$ around 14DAS and remained at a par (270 mg $kg^{-1}$ on 42DAS), with a marked short-lived increase on 28DAS (382 mg $kg^{-1}$). Consistent to MBC, MBN was also built up within the first week till on average 100 mg $kg^{-1}$. Afterwards the MBN in lower Eh soils slightly declined and plateaued to a range of 73 to 85 mg $kg^{-1}$ between 15 and 42 DAS. Just like with MBC, MBN in higher Eh soils plummeted to

means of 67 mg kg$^{-1}$ on 14DAS and 55 mg kg$^{-1}$ on 42DAS, but rose temporarily to 106 mg kg$^{-1}$ on 28DAS. Hence we considered mean values (of four sampling events, Fig. 3.5) for MBC and MBN to as predictor within a correlation analysis with soil properties, other monitored biochemical variables and soil mineral N kinetic parameters. MBC and MBN correlated with SOC and total N (r = 0.70 to 0.82; p<0.01), DOC and DON levels (p<0.01), and Fe release rate (p<0.05) (Tables 3.2 and 3.3).
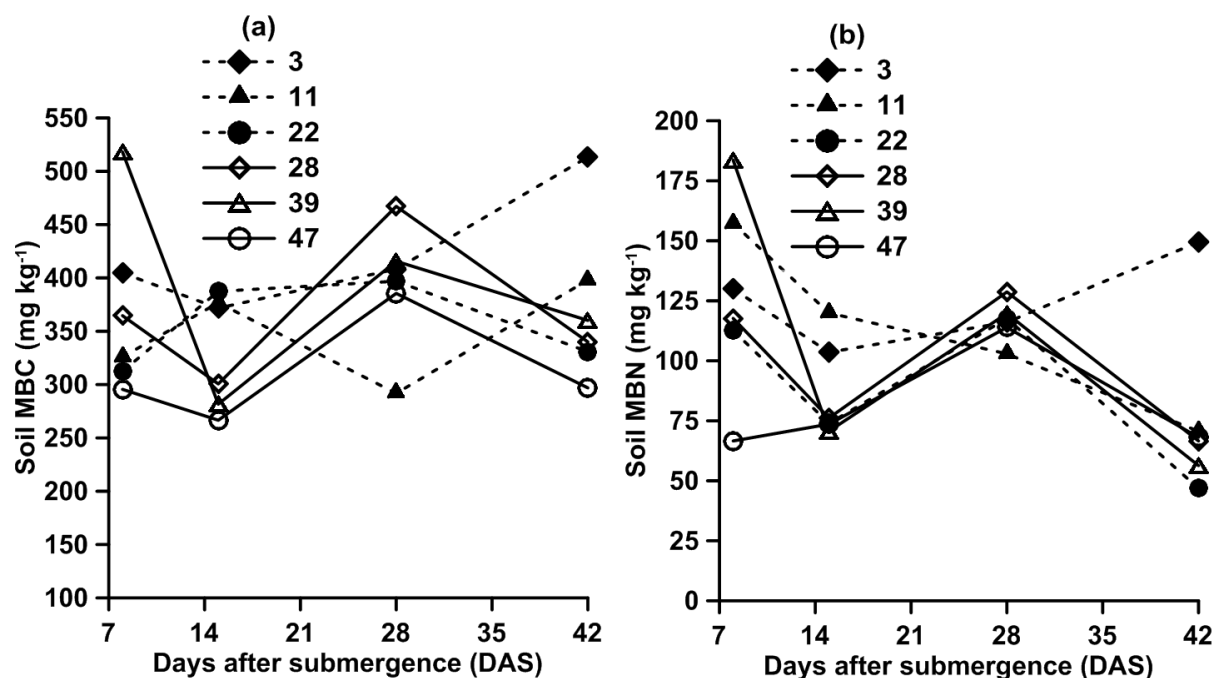


Fig. 3.5 Temporal evolutions of soil MBC (a) and MBN (b) build up of six sampling locations with three lower (Soil ID 3, 11 and 22) and three higher (Soil ID 28, 39 and 47) mean Eh level

*3.3.1.5. Total C (CH$_4$-C+CO$_2$-C) emission as proxy of anaerobic microbial activity and SOM decomposition*

Methane (CH$_4$) and CO$_2$ emissions were assessed (Fig. 3.6) during 42 days by regular headspace gas sampling to acquire quantitative insight in the overall variation in microbial activity between the 50 samples, rather than to monitor greenhouse gas emissions per se. The overall CH$_4$ efflux was minor (0 to 0.07µg g$^{-1}$ h$^{-1}$) with inconsistent temporal variation throughout the incubation period (Fig. 3.6a). Excluding remarkably greater CH$_4$ effluxes in the soil IDs 27, 28, 37 and 38, only minor differences existed in the average CH$_4$ efflux between the lower and higher Eh soils (Fig. 3.6a). Typically, the CH$_4$ efflux was initially (on 2DAS) at narrow range of 0-0.02 µg g$^{-1}$ h$^{-1}$ (mean 0.003), and gradually went up to a wider

range of 0-0.04 µg $g^{-1}$ $h^{-1}$ (mean 0.006) between 8 to 15DAS. In the lower Eh soils, this higher $CH_4$ efflux fluctuated at almost same level between 15 to 42DAS, while in the higher Eh soils $CH_4$ efflux declined to ~ 0.003-0.004 µg $g^{-1}$ $h^{-1}$ (mean) between 35 to 42DAS. Exceptions were sampling locations 27, 28, 37 and 38 where the $CH_4$ efflux was greater than other samples.  Due to overall large and inconsistent variations throughout incubation, the mean $CH_4$ efflux of all sampling events per soil (ranged 0.001-0.034 µg $g^{-1}$ $h^{-1}$) was used in the correlation/regression analysis. The mean $CH_4$ efflux positively correlated (r = 0.36 to 0.75) to DOC, DON, SOC, total N, pH rise and Fe and Mn release rates ($p<0.01$) (Tables 3.2 and 3.3, Fig. 3.9).

$CO_2$ emission rate principally (90.3-99.7%) constituted total C ($CO_2$-C + $CH_4$-C) emission (Fig. 3.6b). Overall the C efflux rate (in µg $g^{-1}$ $h^{-1}$) ranged from 0 to 1.3 (averaged: 0.1-0.4) throughout the incubation period (Fig. 3.6b). Total C efflux (in µg $g^{-1}$ $h^{-1}$) increased steeply and remained at maximum levels between 5 to 8DAS, within a range of 0-1.3 and mostly declined sharply and stabilized at ~0.1-0.2 µg $g^{-1}$ $h^{-1}$ between 15 to 42DAS. A later temporal rise was noticed in a number of soils on 28 and 35 DAS (Fig. 3.6b). A zero-order kinetic model plausibly fitted to the accumulated amount of mineralized C (mg $kg^{-1}$) over time ($R^2 \geq$ 0.80 to 1.00) (Fig. 3.6c and d), and the recalculated total C ($C_t$) emission after 42DAS was employed as variable in correlation/regression analysis with other properties and descriptors of dynamic biochemical processes. Unexpectedly, $C_t$ did not correlate to any of these, except with MBN and soil C:N ratio (r = 0.30; $p<0.05$). The 42-days cumulative emitted C varied in the range of 11-72 mg C $g^{-1}$ SOC (1.1-7.2% of SOC), at a C mineralization rate of 0.3 to 1.7 mg C $g^{-1}$ SOC $d^{-1}$.
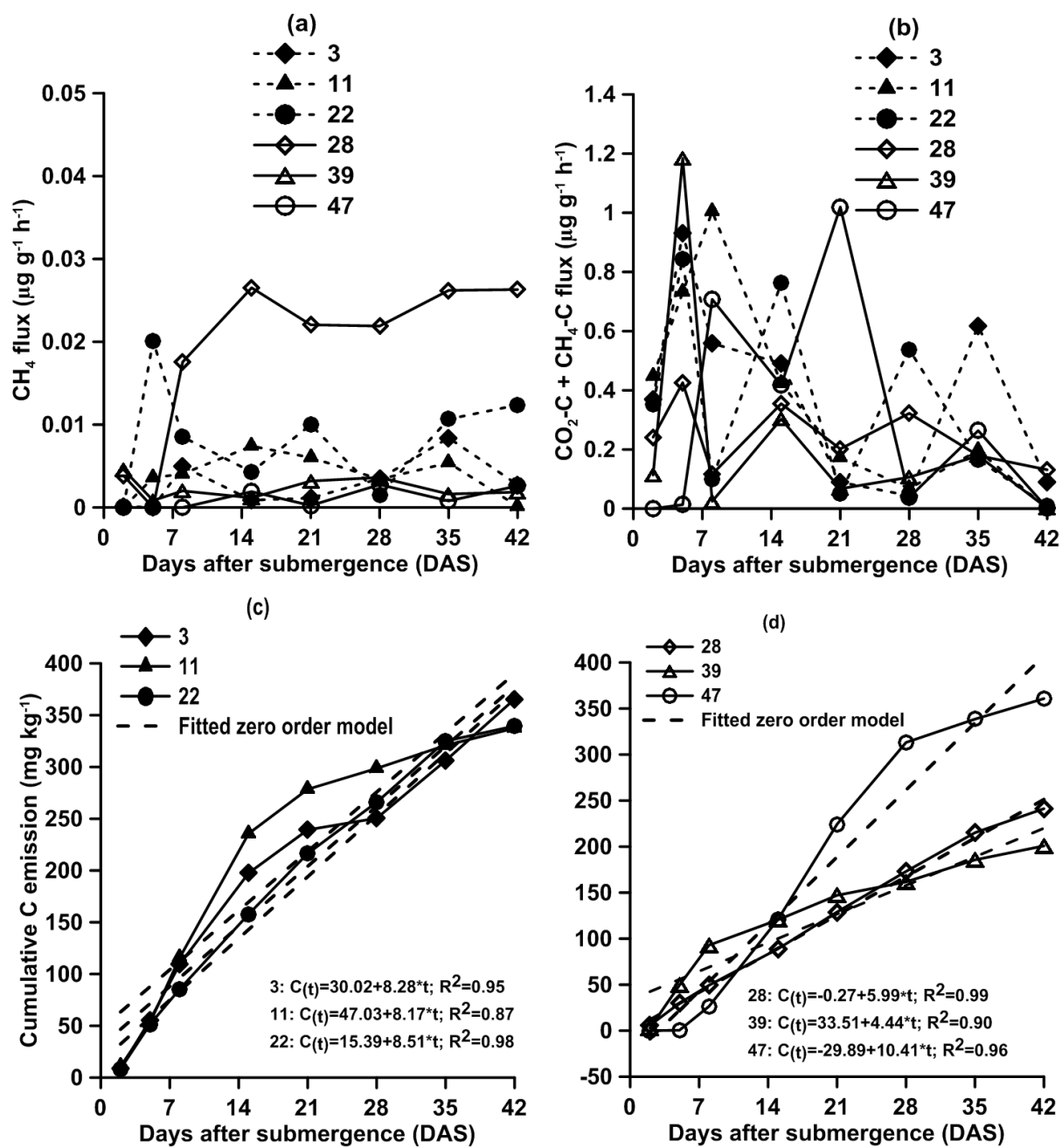
Fig. 3.6 Temporal changes in emission rates of $CH_4$ (a) and total C ($CO_2$-C+$CH_4$-C) (b), as well as cumulative C emission (c,d) of six sampling locations with three lower (Soil ID 3, 11 and 22) and three higher (Soil ID 28, 39 and 47) mean Eh level

Table 3.2 Pearson correlation coefficients (r) of the studied biochemical processes during 42 days anaerobic incubation

| Properties | Overall pH rise | Mean Eh (till 21DAS) | Fe release rate $(mg\ l^{-1}\ d^{-1})$ | Mn release rate $(mg\ l^{-1}\ d^{-1})$ | Total C emission $(mg\ kg^{-1})$ | Total DON release, $N_t$ $(mg\ kg^{-1})$ | Mean DOC $(mg\ kg^{-1})$ | Mean MBC $(mg\ kg^{-1})$ | Mean MBN $(mg\ kg^{-1})$ | Mean CH$_4$ flux $(\mu g\ g^{-1}\ h^{-1})$ |
|---|---|---|---|---|---|---|---|---|---|---|
| Overall pH rise | 1 | 0.00 | 0.54** | 0.30* | 0.15 | 0.42** | 0.39** | 0.06 | 0.17 | 0.47** |
| Mean Eh (till 21DAS) | 0.00 | 1 | -0.22 | 0.09 | -0.04 | -0.09 | -0.04 | -0.03 | 0.05 | 0.18 |
| Fe release rate (mg l⁻¹ d⁻¹) | 0.54**a | -0.22 | 1 | 0.56** | 0.19 | 0.67** | 0.77** | 0.37** | 0.32* | 0.64** |
| Mn release rate (mg l-1 d-1) | 0.30* | 0.09 | 0.56* | 1 | 0.15 | 0.13 | 0.50* | 0.10 | -0.01 | 0.40** |
| Total C emission (mg kg⁻¹) | 0.15 | -0.04 | 0.19 | 0.15 | 1 | 0.23 | 0.26 | 0.28 | 0.30* | 0.15 |
| Total DON release, $N_t$ (mg kg⁻¹) | 0.42** | -0.09 | 0.67** | 0.13 | 0.23 | 1 | 0.81** | 0.56** | 0.52** | 0.56** |
| Mean DOC (mg kg⁻¹) | 0.39** | -0.04 | 0.77** | 0.50* | 0.26 | 0.81** | 1 | 0.53** | 0.41** | 0.75** |
| Mean MBC (mg kg⁻¹) | 0.06 | -0.03 | 0.37** | 0.10 | 0.28 | 0.56** | 0.53** | 1 | 0.83** | 0.19 |
| Mean MBN (mg kg⁻¹) | 0.17 | 0.05 | 0.32* | -0.01 | 0.30* | 0.52** | 0.41** | 0.83** | 1 | 0.16 |
| Mean CH$_4$ flux (µg g⁻¹ h⁻¹) | 0.47** | 0.18 | 0.64** | 0.40** | 0.15 | 0.56** | 0.75** | 0.19 | 0.16 | 1 |

[a] *Significant at p = 0.05; ** Significant at p = 0.01

*3.3.2. Temporal evolution of apparent net N mineralization during anaerobic incubation*

The initial exchangeable mineral N (KCl-extractable) content (in mg kg$^{-1}$) ranged from 4 to 15 (mean of 7), the majority being $NH_4^+$ (4-11 mg $NH_4^+$-N kg$^{-1}$ with mean of 6) in all soils, while $NO_3^-$-N ranged between 0.1-6.8 mg N kg$^{-1}$ (mean: 0.7). $NO_3^-$-N was almost absent or negligible during 8-28DAS and an amount of 0.3-5.4 mg kg$^{-1}$ $NO_3^-$-N was detected on 42DAS only. Hence under flooded conditions soil mineral N build up was dominated by $NH_4^+$. Temporal evolutions of mineral N ($NH_4^+$-N + $NO_3^-$-N) followed clear but distinct general trends in high and low Eh soils (Fig. 3.7). In case of all lower Eh soils, mineral N content increased strongly in the first two weeks (Fig. 3.7a), and peaked either on 15DAS (in 13 soils out of 22) or 28DAS (in 9 soils out of 22). In the majority of higher Eh soils (25 out of 28) exchangeable N rose until 28 DAS (Fig. 3.7b). The maximum level of mineralized N ranged from 17-72 mg kg$^{-1}$ (mean of 40) in lower Eh soils and 22-85 mg kg$^{-1}$ (mean of 47) in higher Eh soils. From 28DAS onwards exchangeable N steadily declined to a level of 16-61 mg kg$^{-1}$ (mean of 30) in lower Eh soils and plunged by as much as 50% to a range of 4-68 mg kg$^{-1}$ (mean of 23) in higher Eh soils on 42DAS. In three higher Eh soils (soil ID 1, 7 and 12), exceptionally the exchangeable N content increased until 15DAS remained at a high level thereafter. The overall temporal trends of soil mineral N followed asymptotic course for most soils at least until 28DAS. A first-order kinetic model was hence fitted (average $R^2$ = 0.94) to the evolution of mineral N build-up with time course of 0-28DAS only for sampling locations 22 to 50 (high equilibrium Eh soils), due to rapid lowering between 28-42DAS. For the other (low Eh) soils the full 0-42DAS dataset was used to fit (Fig. 3.7). To explore the predictor variables of N mineralization from studied soil properties and biochemical processes, only modeled total amount of released mineral N ($N_t$) was further on used. The modeled N mineralization rate ($k_t$) was varied widely (0.02-2.86 mg kg$^{-1}$ day$^{-1}$) with in fact comparable final net mineralized N ($N_t$). Because of $k_t$'s very high sensitivity, this fitted parameter was not considered as a robust measure of actual microbial activity and was not further used in correlation analyses. The modeled $N_t$ ranged widely from 20-86 mg kg$^{-1}$ (mean of 43 mg kg$^{-1}$) i.e. 2.3 to 6.7% of total soil N was mineralized during 28-42 days (Fig. 3.8a).
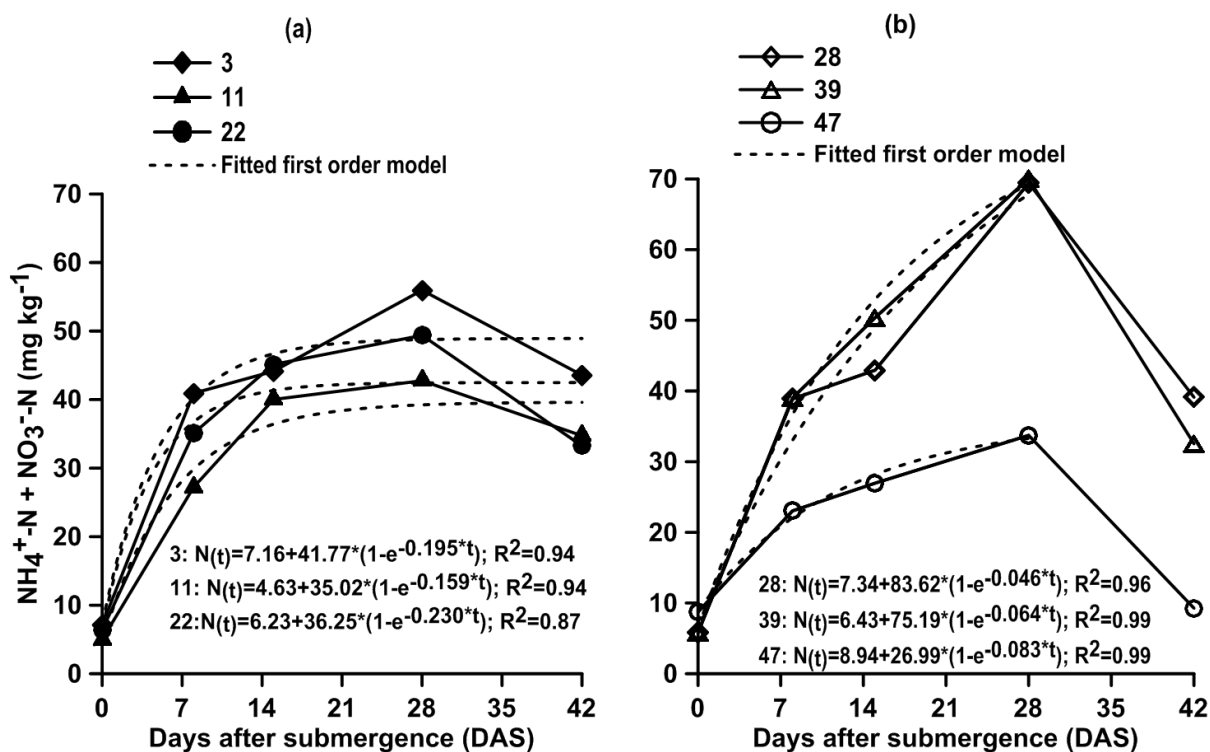
Fig. 3.7 Temporal changes in apparent net anaerobic N mineralization and fitted first-order kinetic model of six sampling locations with three lower (Soil ID 3, 11 and 22) and three higher (Soil ID 28, 39 and 47) mean Eh level

### 3.3.3. Correlation between modeled net mineralized N ($N_t$) and soil properties and indicators of dynamic biochemical processes

In the current study, the connections of the recalculated amount of modeled net mineralized N ($N_t$) to the studied soil properties and biochemical processes are firstly presented in a biplot of the first two PCA components (Fig. 3.9 and Table 3.3). Most variables (except $pH_{KCl}$, $Mn_{ox}$, % silt and clay) were clustered in the right quadrants of the PCA biplot with greater loadings on PC1, but a influence also imposed on PC2 (Fig. 3.9). Likewise, SOC, DON, DOC, $N_t$, TN, MBC, Fe rate, MBN, $CH_4$ efflux, pH rise, $C_t$ and $pH_{KCl}$ greater loaded PC1, which explained 30.9% of variation. $Fe_{ox}$, $SOC:Fe_{ox}$, silt (%), $SOC:Mn_{ox}$, clay (%), $Mn_{ox}$, Mn rate and mean Eh had dominantly loaded PC2, which explained 22.3% of variation.

Loading onto PC1 and 2 of modeled net mineralized N ($N_t$) matched that of SOC, DON, TN, MBC, MBN, DOC, $CH_4$ efflux, Fe release rate, pH rise, mean Eh and $C_t$ in the right quadrant

65

of the loading plot, indicating its possible positive linkages with all these variables. $N_t$ was furthermore ($p<0.05$) positively (r = 0.29 to 0.79) correlated with these variables, except $C_t$ and mean Eh (Table 3.3). Several significant ($p<0.01$) stepwise regression models were developed to predict the modeled amount of net mineralized N ($N_t$) from soil properties and evolved biochemical processes:

$$N_t \text{ (mg kg}^{-1}) = 6.8\text{SOC (g kg}^{-1}) + 666.3\text{CH}_4 \text{ efflux (µg g}^{-1} \text{ h}^{-1}) - 21.1 \ (R^2 = 0.67)............ (1)$$

$$N_t \text{ (mg kg}^{-1}) = 4.6\text{DON (mg kg}^{-1}) + 0.1\text{MBC (mg kg}^{-1}) + 0.04\text{Eh (mV)} -0.2\text{MBN (mg kg}^{-1}) + 508.9\text{CH}_4 \text{ efflux (µg g}^{-1} \text{ h}^{-1}) - 0.1 \ (R^2 = 0.77)................................................................. (2)$$

The model denoted that the modeled amount of net mineralized N ($N_t$) was explained by 67% by SOC and $CH_4$ efflux (Equation 1). Excluding SOC and soil N content as potential predictors, a stepwise regression model with DON, MBC, mean Eh, MBN and $CH_4$ efflux (Equation 2) was retained and this explained 77% of total mineralized N. The variables total N, DOC, Fe-buildup rate and pH rise were found to be redundant in the step-wise regression models, likely due to their co-linearity with SOC, DON and $CH_4$ efflux.



(a)                                              (b)
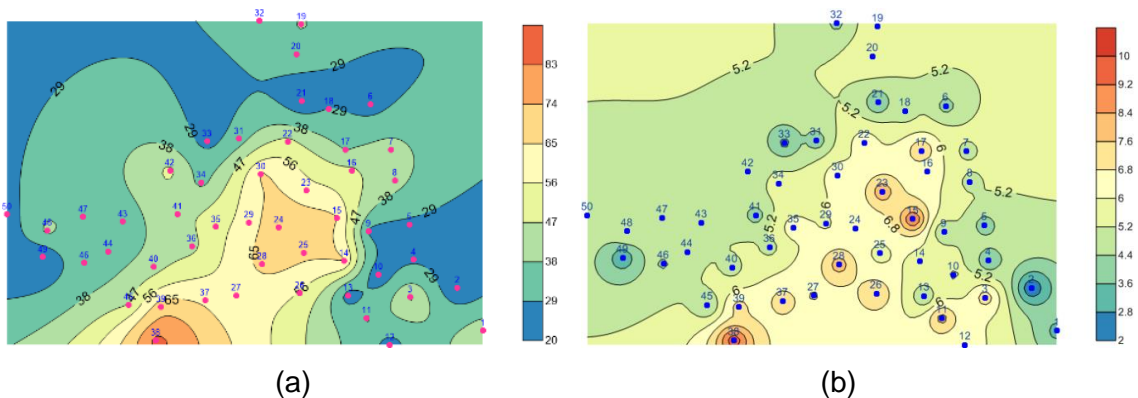
Fig. 3.8 Spatial distribution of modeled (first order kinetics) amount (in mg kg$^{-1}$ 42 days$^{-1}$) of apparent net mineralized N ($N_t$) (a) (in mg kg$^{-1}$ 42 or 28 days$^{-1}$), and DON released, $N_t$ (b) (in mg kg$^{-1}$ 42 days$^{-1}$) for the studied samples in Atalle, Sri Lanka
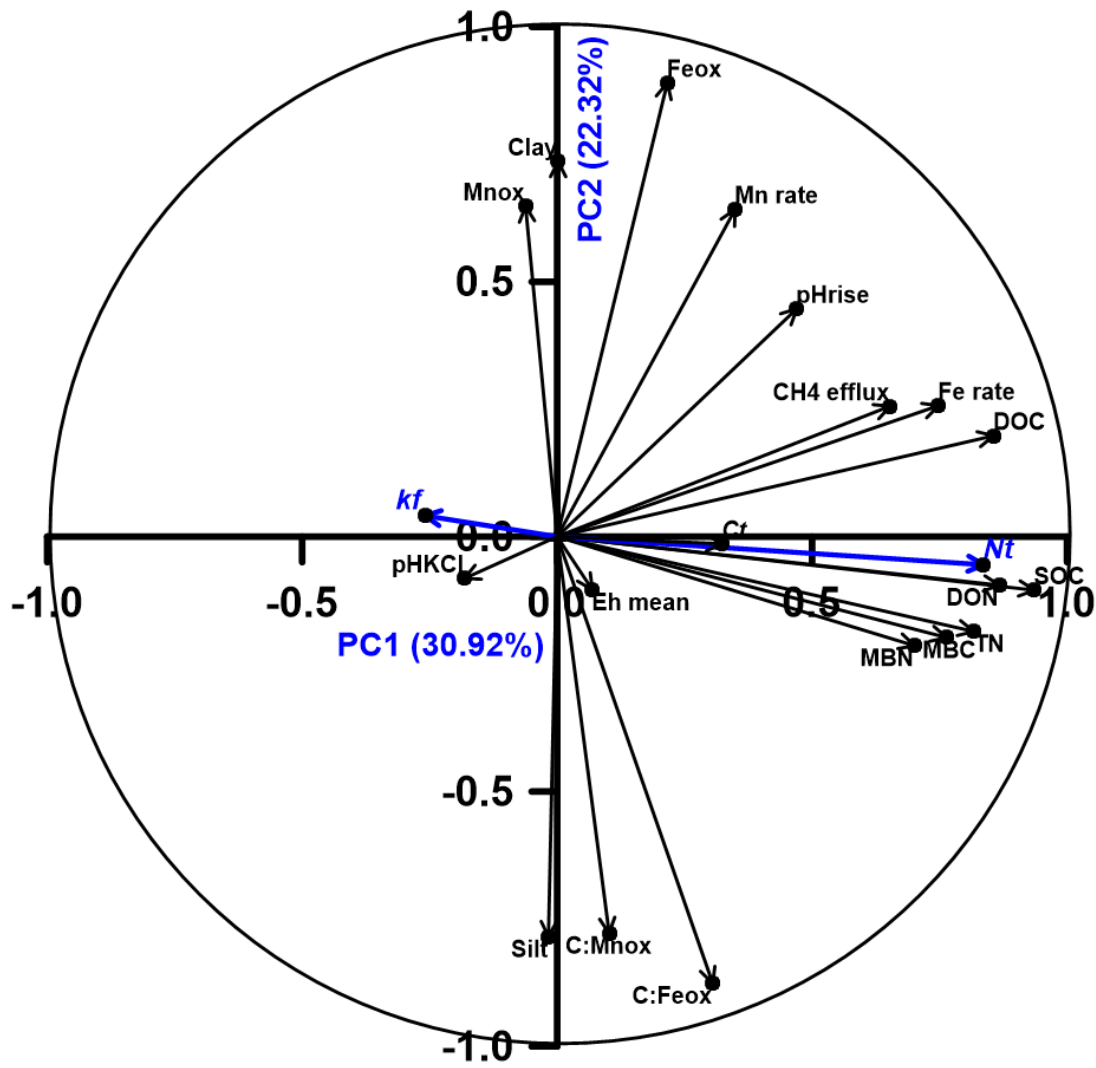
Fig. 3.9 Principal component analysis (PCA) biplot representing the first two principal components (PC1 and PC2) and distribution of studied soil properties and biochemical processes

Table 3.3 Pearson correlation coefficients (r) of the first order modeled apparent net N mineralization ($N_t$) during 28 days$^{-1}$ or 42 days$^{-1}$ with initial soil properties and evolved soil biochemical processes

| Properties | pH KCl | SOC (g kg$^{-1}$) | Total N (g kg$^{-1}$) | $Fe_{ox}$ (g kg$^{-1}$) | $Mn_{ox}$ (g kg$^{-1}$) | SOC to $Fe_{ox}$ | SOC to $Mn_{ox}$ | C:N | % silt | % clay | Modeled net mineralized N ($N_t$) (mg kg$^{-1}$) |
|---|---|---|---|---|---|---|---|---|---|---|---|
| Overall pH rise | -0.76**[a] | 0.32* | 0.19 | 0.53** | 0.00 | -0.33* | -0.12 | 0.36** | -0.34** | 0.23 | 0.29* |
| Mean Eh (till 21DAS) | -0.1 | 0.16 | 0.01 | -0.09 | 0.22 | 0.17 | 0.08 | 0.28* | 0.19 | -0.10 | 0.23 |
| Fe release rate (mg l$^{-1}$ d$^{-1}$) | -0.23 | 0.58** | 0.49** | 0.29* | -0.09 | 0.00 | -0.09 | 0.49** | -0.16 | 0.08 | 0.49** |
| Mn release rate (mg l$^{-1}$ d$^{-1}$) | 0.07 | 0.29* | 0.14 | 0.54** | 0.66** | -0.35* | -0.54** | 0.37** | -0.27 | 0.26 | 0.22 |
| Total C emission ($C_t$: mg kg$^{-1}$) | -0.15 | 0.24 | 0.11 | 0.06 | 0.10 | 0.09 | 0.06 | 0.29* | 0.05 | -0.12 | 0.22 |
| DON rate, $k_d$ (mg kg$^{-1}$ d$^{-1}$) | 0.25 | 0.21 | 0.28* | -0.59** | -0.37** | 0.60** | 0.37** | 0.07 | 0.55** | -0.54** | 0.05 |
| Total DON release, $N_t$ (mg kg$^{-1}$) | -0.13 | 0.76** | 0.69** | 0.08 | -0.26 | 0.32* | 0.22 | 0.58** | -0.02 | -0.04 | 0.73** |
| Mean DOC (mg kg$^{-1}$) | 0.05 | 0.72** | 0.57** | 0.26 | 0.07 | 0.11 | -0.11 | 0.63** | -0.12 | 0.09 | 0.71** |
| Mean MBC (mg kg$^{-1}$) | 0.06 | 0.82** | 0.77** | 0.08 | -0.03 | 0.38** | 0.11 | 0.62** | 0.14 | -0.03 | 0.66** |
| Mean MBN (mg kg$^{-1}$) | -0.11 | 0.75** | 0.70** | 0.13 | -0.13 | 0.31* | 0.17 | 0.56** | 0.09 | -0.14 | 0.50** |
| Mean CH$_4$ flux (µg g$^{-1}$ h$^{-1}$) | -0.16 | 0.47** | 0.36** | 0.20 | 0.05 | 0.05 | -0.06 | 0.41** | -0.23 | 0.16 | 0.56** |
| First order model parameters for N mineralization | | | | | | | | | | | |
| $N_t$ (mg kg$^{-1}$) | -0.01 | 0.79** | 0.62** | 0.08 | -0.04 | 0.34* | 0.07 | 0.72** | 0.04 | 0.08 | 1 |

[a] *Significant at p = 0.05; ** Significant at p = 0.01

## 3.4. Discussion

The used soils set in this study well covered quite comprehensively spanned diversity in several major soil properties, i.e. in SOC (0.6 to 1.23%), TN (0.08 to 0.14%), $Fe_{ox}$ (0.8 to 2.6g $kg^{-1}$), $Mn_{ox}$ (0.004 to 0.2g $kg^{-1}$), pHKCl (4.4 to 5.8) and clay (4 to 18%)  (Table 3.1, Section 3.2.1). These ranges are typical for cultivated paddy soils in South-East Asia (Kader et al., 2013; van Bodegom et al., 2003). SOM decomposition and N mineralization in submerged paddy soils have been previously found to be influenced by this multitude of factors, among which nature and content of reducing (SOM/C) and oxidizing agents particularly reducible $Fe_{ox}$, and pH are more intrinsic properties (Sharawat, 2004b; Minh Khoi, 2000; Inubushi et. al., 1984). Hence the spatial variability exhibited in these properties within the paddy field chosen for this research (Table 3.1; Fig. 3.1) should provide a useful experimental setup for identification of most relevant controls of anaerobic N mineralization.

*3.4.1. Soil biochemical processes during anaerobic incubation as influenced by spatial variations in soil properties*

*3.4.1.1. Soil Eh, pH and dissolution of Fe and Mn*

The overall Eh range (312 to -368 mV during 1-7DAS) demonstrates large temporal and spatial variations in initial microbial activity and establishment of reduced soil state (+200 to -400 mV) by reduction reactions, following disappearance of $O_2$ and $NO_3^-$ (Ponnamperuma, 1972). The observed Eh and pH (5.1 to 7.2) in the current study were primarily also in typical ranges for $Mn^{3+/4+}$ (300 to 200 mV) and $Fe^{3+}$ (300 to -100 mV at pH 5 to 8) reductions, and to a lesser extent as well in more reduced ranges with incidence of methanogenesis (< -150 to -280mV) (Patrick and Jugsujinda, 1986; Grybos et al., 2009; Minamikawa and Sakai, 2006; Wang et al., 1993). Both the nature and content of SOM and alternative $e^-$ acceptors along with flooding duration determine the extent of development of reducing conditions and trends of Eh evolutions, which usually followed asymptotic temporal courses in submerged soils (Ponnamperuma, 1972; Gao et al., 2002; Sahrawat, 2008), as also observed for the current set of sampled points (Fig. 3.2a). Mean Eh during 21DAS and cumulative C-emission did, however, not significantly correlate with SOC and most of the studied biochemical parameters and processes, except for weak positive relations to C:N ratio (r = 0.28 to 0.29; p<0.05) (Table 3.3). So it could then be logically hypothesized that the equilibrium Eh was rather depending on the availability of various oxidants. However, no correlations were found between Eh and Fe and Mn release rates nor with $Fe_{ox}$ and $Mn_{ox}$. Nevertheless, most soils

with release rates greater than 3.5 mg Fe $l^{-1}$ $d^{-1}$ and 0.2 mg Mn $l^{-1}$ $d^{-1}$ had almost negative mean Eh (~ below -90mV or lower) during first 21 days indicating more pronounced reductive dissolution of Fe- and Mn-(hydr-)oxides as compared to lower rates in soils with positive Eh (Fig. 3.2a, data not shown). Along with Eh (mainly stayed at $Fe^{3+}$ and $Mn^{3+/4+}$ reduction ranges) all these suggests that the quantity of reducible Fe and Mn partly would control drop of Eh. This reasoning is also supported when considering soil pH: there were significant correlations between pH rise and Fe and Mn release rates, and $CH_4$ emission (Table 3.2). Also, overall pH rise was steeper and greater in soils with lower initial $pH_{KCl}$ but higher $Fe_{ox}$ and SOC (Table 3.3 and Fig. 3.9). In contrast soils with already low initial pH and reducible Fe contents disclosed 0.3 unit smaller overall pH rise (see Section 3.3.1.) (Hanke et al., 2013). Hence, microbial accessibility of SOM and reducible $Fe^{3+}$(hydr-)oxides with acidic pH mostly regulated pH rise by reduction reactions in studied soils.

There were large variations in solution Fe and Mn concentrations and release rates (both measured and predicted) within the paddy field (see Section 3.3.1.2.) (Fig. 3.3). Next to lower Eh, low initial pH, resulting greater pH rise, quality and quantity of SOC and easily reducible $Fe_{ox}$ and $Mn_{ox}$ have previously been found to strongly influence Fe and Mn reductive dissolution (Inubushi et al., 1984; Ponnamperuma, 1972). The existing significant correlations of solution Fe release rate with overall pH rise, SOC, C:N and $Fe_{ox}$, and that of Mn with overall pH rise, SOC, C:N and $Mn_{ox}$ (Table 3.2 and 3.3) further supported the idea that both SOC and levels of pedogenic oxides determined Fe and Mn dissolution ( Fig. 3.9). The low reducible $Fe_{ox}$ and $Mn_{ox}$ contents compared to typical paddy soil levels (Hanke et al., 2013; Kader et al., 2013) would logically result in a dependency of Fe and Mn release to soil $Fe_{ox}$ and $Mn_{ox}$. Other processes like reduction of $SO_4^{2-}$ and $Fe^{3+}$ inside structural clay minerals (Pentráková et al., 2013; Brookshaw et al., 2016) might have also received $e^-$ concurrently, but we cannot confirm existence of these due to lack of data on $SO_4^{2-}$ reduction and clay mineralogy for the studied soils. The strong positive correlations of Fe and Mn release rates with DOC level (Table 3.2) further indicated that next to serving as $e^-$ acceptors, reduction of Fe- and Mn-(hydr-)oxides perhaps also led to release of DOM by reductive dissolution or by desorption due to the accompanied pH rise (Grybos et al., 2009; Pan et al., 2016). However at this stage a causal relation between buildup of DOC in soil solution and Fe and Mn reduction cannot be confirmed.

*3.4.1.2 Dissolved organic C (DOC) and N (DON)*

During entire experimental period, average DOC varied between 47 to 106 mg $kg^{-1}$ (~119-270 mg $l^{-1}$), exceeding more frequently reported DOC levels (4 to 69 mg $kg^{-1}$) in literature for

flooded paddy soils (Li et al., 2010; Hanke et al., 2013; Said-Pullicino et al., 2016). Yet the overall contribution of mean DOC level to SOC (0.5 to 1%) corresponded well to previous findings by Qiu, et al. (2006). The general higher concentrations of DOC in the studied paddy field may partly be explained by limited or incomplete decomposition of SOM and accumulation of water soluble intermediate metabolites under flooded conditions (Said-Pullicino et al., 2016). On the other hand, observed DON concentrations ranged between 0.01-14 mg kg$^{-1}$ (~0.04-36 mg l$^{-1}$) during 2-42 DAS, matching well to typical values (3-18 mg kg$^{-1}$) for subtropical paddy soils (Li et al., 2010). For all soils the estimated total net DON released during incubation ($N_t$) amounted 2-10 mg kg$^{-1}$ (~6-24 mg l$^{-1}$), contributed. e. 0.3 to 0.8% of TN. The coefficients of variation (CV) (21 to 29% for DOC and 27 to 44% for DON) suggest wide variations in their release within the paddy field sampling locations. Mean DOC and net DON released across the incubation most strongly correlated (p<0.01) (Tables 3.2 and 3.3) with SOC, TN, Fe and Mn release rates and pH rise, suggesting that variations in DOC and DON were mostly dependent on the quantity and quality of oxidizing (e.g. Fe$_{ox}$) and reducing agents (e.g. SOM). The linkage between DOC levels and Fe and Mn rates and pH rise could be indirect: i.e. faster and stronger anaerobic microbial activity leads to both more formation and accumulation of DOC, more Fe and Mn reductive dissolution, and rise in pH. Such DOM release by microbial activity under reductive condition as soluble organic metabolites, requires verification through follow-up of water soluble metabolites, e.g. with HPLC or more basically firstly through specific UV absorbance of DOM (Grybos et al., 2009; Hanke et al., 2013). On the other hand there could just as well be a direct coupling: i.e. both reductive dissolution of pedogenic oxides and rise in pH would bring DOM into solution. Because there was no correlation between C-emission and DOC level or DON release (Table 3.2), the entire correlation analysis presented in Tables 3.2 and 3.3 rather suggest a direct availability on shifts in pH and reduction of pedogenic Fe. The question remains which of both mechanisms is most important. Stronger correlations existed between rate of Fe release and DOC and DON-release than with shift in pH. But on the other hand, comparison of the timing of Fe dissolution (Fig. 3.3), DOC and DON buildup (Fig. 3.4) and change in pH (Fig. 3.2b) indicates closest synchrony between change in pH and DON release. Overall pH rise accompanying reduction was previously found to desorb DOM bound to Fe- and Mn-(hydr-)oxides or clay minerals (Grybos et al., 2009; Hanke et al., 2013). Regardless, the data suggest that abiotic mechanisms (dissolution of Fe and change in pH) are involved as intermediate steps in buildup of DON in soil solution.

The decreased DOC contents on 28DAS likely be coupled to increased MBC and MBN by their assimilation. The sudden drop off DOC on 42 DAS for most soils remains unexplained as final measurements of C-mineralization, Eh and Fe did not indicate sudden changes in

redox state or microbial activity towards 42DAS. Dissimilar to C mineralization, the modeled net mineralized N ($N_t$) for 28-42 days significantly connected (p<0.01) to DOC and DON levels (Table 3.3). This might confirm DON's role on soil organic N (SON) transformation possibly as an intermediate N pool during SOM mineralization or decomposition or depolymerization of non-DON fractions to low molecular weight DON by microbial extracellular enzyme (Li et al., 2010).

*3.4.1.3. Soil microbial biomass C (MBC) and N (MBN), and activity indicated by C emissions*

Flooding led to a substantial buildup of soil microbial biomass-C (139-582 mg kg$^{-1}$) and N (38-184 mg kg$^{-1}$) already within the first week of submergence. The total biomass of the microbial community was apparently quite well developed already after this early stage as MBC remained constant between 15 and 42DAS, just like in observations by Inubushi et al. (1999). Nevertheless the community structure may have changed during the incubations: with large variations throughout (average ranges MBC: 128-538 mg kg$^{-1}$, MBN: 30-137 mg kg$^{-1}$) between the sampling locations (Devêvre and Horwáth, 2000). The general decline in MBC and MBN contents between 7 and 14 DAS (-24.6 and -30.2±30.9 mg kg$^{-1}$ resp.; P<0.01 for a paired samples t-test between 7 and 14 DAS datasets) was probably due to shifts in microbial community structure from aerobes to facultative and obligate anaerobes after soil flooding (Lu et al., 2002). Likewise an elevation again in MBC and MBN (+64.0 and +26.5 mg kg$^{-1}$ resp.; P<0.01) towards 28DAS in majority of the higher Eh soils (Fig. 3.5), represented a shift towards well developed anaerobic populations. This establishment of an obligate anaerobic microbial community may possibly link to the higher amounts of exchangeable N on 28 DAS in the higher Eh soils (Fig. 3.7b) as anaerobic microbial metabolism is generally thought to require less N (Buresh, et al., 2008; Reddy and De Laune, 2008). In contrast the subsequent lowering of MBC and MBN between 28 and 42 DAS (- 48.7 and -32±49.2 mg kg$^{-1}$ resp.; P<0.01), especially in higher Eh soils, could be related to lower C-emission rates, perhaps due to depletion of easily available C-sources.

MBC and MBN contents (means for the entire incubation period) strongly positively (p<0.01) correlated with SOC, TN, DOC and DON. This probably illustrates the expected promotion of microbial biomass with enhanced substrate availability (Lu et al., 2002; Liu et al., 2009). Besides positive correlations between MBC and MBN and Fe release rate (p<0.05) are likely indirect, viz. increased microbial biomass is logically linked to enhanced anaerobic microbial activity, depending on Fe reduction.  The (p<0.01) positive correlations of MBN and MBC to apparent net mineralized N denotes that N mineralization is a microbially mediated process (Inubushi and Acquaye, 2004, Zhang et al., 2009).

An initial (5-8DAS) peak of total C efflux resulted mainly from higher $CO_2$ production from rapid microbial respiration and SOM decomposition. Overall the contribution of $CH_4$ to total C-emissions was low and we do not focus here on explaining patterns in $CH_4$-emissions. Suffice to mention that there were only negligible differences in $CH_4$ emissions of lower and higher Eh soils and indicated that Eh's control on $CH_4$ emission was not strong, instead DOC and SOC level and Fe-release rate were main predictors. From 15DAS a rapid decline in total C efflux could be the consequence of depletion of easily available C substrates, lack of alternative $e^-$ acceptors (e.g. $Fe_{ox}$ and $Mn_{ox}$), conversion to $CH_4$ or removal of $CO_2$ by precipitation as $FeCO_3$ and $MnCO_3$ (Ponnamperuma, 1972; Gao et al., 2002; Pan et al., 2014). A similar declining trends of soil organic C mineralization rate over time was observed by Li et al. (2010), who noticed higher rate during first week and rapid declined on 8 and 12 days after incubation (by 44% and 50%, respectively) compared to the rate on first day. Cumulative amount of emitted C during 42 days was only slightly different between higher and lower Eh soils (see Section 3.3.1.5), indicating that factors other than Eh controlled microbial activities. $C_t$'s insignificant correlations (r = 0.23 to 0.30) with SOC, MBC, DOC and Fe-release (Table 3.2) suggested no strong dependency of gross microbial activity on C or reducible Fe either.

*3.4.2. Temporal patterns in soil exchangeable N*

Under current study, the $NO_3^-$-N content in initial soil was minor (0.1-6.8 mg $kg^{-1}$) and quickly declined by N-reduction reactions with flooding. The asymptotic courses of soil mineral N build-up over time are typical in anaerobically incubated paddy soils (Li et al., 2003, Kader et al., 2013; Akter et al., 2016). Succeeding plateaued exchangeable N levels or minor fluctuations thereof were probably due to the slowing down of organic N mineralization process (Li et al., 2003, Kader et al., 2013). The decreased mineral N on 42 DAS in most soils with greater decline in higher Eh soils could firstly have been caused by several candidate processes:

1° Removal by biotic $NH_4^+$-N immobilization, seems unlikely here because MBN, MBC, DOC and DON for most soils also declined towards 42DAS and instead buildup of MBN was expected.

2° Secondly, rapid nitrification-dentrification could have removed $NH_4^+$-N towards 42 DAS. However, in the higher Eh soils, $NO_3^-$-N content was only 0.3-3.1 (mean of 1.2) mg $kg^{-1}$ on 42DAS, very small compared to the observed drops in exchangeable mineral N (approximately declined by 23 mg $kg^{-1}$) but of course $NO_3^-$ could have been rapidly lost by

73

denitrification (Patrick and Reddy, 1976). In an N fertilized continuously flooded paddy field, N loss by nitrifiication-denitrification was only ~0.5 kg ha$^{-1}$ over a period of 107 days (Dong et al., 2012). Tentatively assuming such average denitrification rate, the estimated amount of $NH_4^+$-N loss by nitrifiication-denitrification in this study per 15 days (28-42 DAS) might have been 0.8 mg kg$^{-1}$. Hence, ubstantial $NH_4^+$ loss by $N_2O$ emission seems unlikely given that low Eh, but we cannot exclude a probably much larger loss of N via $N_2$ gaseous loss. On the other hand, in this lab setups there was no rhizosphere from which $NO_3^-$ can diffuse into the anaerobic bulk soil and is denitrified, and so likely typical field measurement based emission rates like derived from Dong et al. (2012) would not apply here.

3° Loss of $NH_4^+$ by $NH_3$ volatilization appears at first also unlikely, as the soil pH remained at or below 7.2 for all soils during 28-42DAS and no N fertilizer was applied. There was no rise in pH during the 28-42DAS period and so a sudden increase in $NH_3$-volatilization after 28DAS is unlikely and could therefore not explain final dropping of soil exchangeable $NH_4^+$-N.

4° After flooding increased $NH_4^+$ by organic N mineralization and reduction and dissolution of Fe oxides coating on clay minerals' surfaces are expected to favor $NH_4^+$ diffusion from soil solution into interlayer of clay minerals (Zhang and Scherer, 2000). The increased negative charge in the interlayer of clay minerals induced by reduction of octahedral $Fe^{3+}$ to $Fe^{2+}$ under low redox condition after flooding could enhance $NH_4^+$ fixation in paddy soils (Scherer and Zhang, 2002). However, establishment of negative charge on clay minerals should have been stronger in soils with low Eh, while on the contrary lowering of soil exchangeable $NH_4^+$-N was larger in the high Eh soils. Also, the clay content in most higher Eh soils were in fact quite low (≤10%) and it seems less likely if a substantial dynamic 'clay interlayer $NH_4^+$ pool existed in the studied soils.

By absence of a plausible explanation for the late removal of $NH_4^+$ other processes than the ones discussed above would need to be further investigated. Given the limited information available, we here no further forward hypotheses on potential mechanisms. We do want to again point out the remarkable discrepancy in final $NH_4^+$removal (i.e. between 28 and 42DAS) between soils with 'high' and 'low' equilibrium Eh.


*3.4.2.1 Soil properties affecting paddy soil apparent net anaerobic N mineralization*


Stepwise regression analysis further confirmed that amount of apparent net mineralized N ($N_t$) predominantly controlled by SOC among the soil properties which explained 62% variability. Hence SOC was identified as the best predictor for $N_t$. This was in line with the findings of Dessureault-Rompré et al. (2015) who reported that soil TN is the best predictor for potentially mineralizable N (explained 56% variability) next to SOC (explained 45%

variability). Nonetheless, TN was not identified as predictor for $N_t$, suggesting its correlation with mineralized N was due to the relation to SOC (r= 0.79 and 0.62; P<0.01, resp.).

The influence of Eh and $pH_{KCl}$ on N mineralization rate seemed to be indirect, possibly by their impact on the release of easily decomposable OM (DOC and DON) interacting with pH change. As already mentioned before, under reduced condition OM bound to Fe- and Mn-(hydr-)oxides and minerals could be released into soil solution by reductive dissolution and desorption with pH rise (Grybos et al., 2009; Said-Pullicino et al., 2016), hence become available for mineralization. Although N mineralization rate constant ($k_f$) differed greatly between higher and lower Eh soils, net mineralized N ($N_t$) content (both observed and modeled) during 28 to 42 days varied only a minor degree (average $N_t$ differed by 6-7 mg kg$^{-1}$).

*3.4.2.2. Biochemical processes affecting apparent net anaerobic N mineralization in paddy soil*

Stepwise regression analysis, excluding SOC and TN, further disclosed that mostly DON (explained 53% variability) and to some extent $CH_4$ efflux, mean Eh, MBC and MBN impacted mineralized N among the biochemical processes, which generally explained 77% variability in $N_t$. Hence, DON release was identified as the best predictor for $N_t$ among studied proxies for biochemical processes. However, mean DOC level, Fe release rate and pH rise were not identified as predictors for $N_t$, suggesting that their correlations with mineralized N were probably manifested primarily via mutual correlations with SOC, DON release and $CH_4$ efflux. The significant (p<0.01) positive correlation of $N_t$ with Fe release rate (r = 0.49), indicated that $Fe^{3+}$ reduction would at first sight be a primary e$^-$ accepting process for SOM oxidation, and N mineralization (Sahrawat, 2004a). But since there was no correlation between C-efflux and Fe-release rate or SOC to $Fe_{ox}$ ratio, this analysis is probably invalid. The significant positive correlation of $N_t$ and $CH_4$ efflux (r = 0.56, p<0.01) may be indirect as well, namely substantial $CH_4$ emission demonstrates onset of strongly reducing conditions following abundant reduction of pedogenic Fe. The hypothesized absence of a direct biological interlink between methanogenesis and net mineral N-release would match with the fact that total C emission did not significantly correlated to $N_t$, DOC, DON, Fe release rate, $CH_4$ efflux and pH rise. The present analysis then implicates that DON is mostly released by abiotic processes, specifically by reductive dissolution of bound pedogenic Fe or desorption due to pH rise, and that in part buildup of exchangeable N depends on this process. We hypothesize that DON could play important role on anaerobic soil organic N mineralization by acting as an intermediate N pool, or through decomposition

or depolymerization of non-DON fractions into DON by microbial extracellular enzyme, and then low molecular weight DON entered microbial cell for next step catabolism (Li et al., 2010).

## 3.5. Conclusion

This study again confirms in line with **Chapter 2** that most studied biochemical processes, including mineral N buildup, generally are most rapid within a fortnight after onset of flooding. The rate and amount of measured and modeled mineralized N varied widely within the selected large paddy field and was found to best relate to SOC content and magnitude of DON-release. Surprisingly, a distinct spatial segregation in mean Eh reached within 21DAS existed in the paddy field, but this was not apparent for any of the other investigated variables, except for the sudden lowering of soil exchangeable N between weeks 5 and 6. We have no ready explanation for such a final 'loss' of exchangeable N, but can only take note of its connection to the equilibrium Eh reached.

Principal component analysis suggested two types of properties and biochemical processes, each with different influence on N mineralization. The modeled net mineralized N ($N_t$) had strongest (p<0.01) correlations with SOC and DON, followed by DOC, MBC, TN, $CH_4$ efflux, MBN, Fe release rate and pH rise, all of which were again significantly (p<0.05) inter-correlated. $N_t$'s significant correlations with Fe release rate, $CH_4$ efflux and pH rise might firstly logically be interpreted as follows: $Fe^{3+}$ reduction is a primary $e^-$ accepting process for SOM degradation and higher microbial activity enhanced mineral N release. However, given that total C emission did not correlate at all to $N_t$, DOC, DON, Fe release rate, $CH_4$ efflux, Eh and pH rise disproves this hypothesis. Instead strong correlations between pH-rise, Fe-dissolution rates, and DON and mean DOC levels (all p<0.01) would rather indicate that DOM is released by two parallel (a)biotic processes, namely DOM bound to Fe- and Mn-(hydr-)oxides or clay minerals released by reductive dissolution or by desorption due to pH rise. DON release rate's significant positive and negative correlations with SOC:$Fe_{ox}$ and %clay further suggested that less protection of OM by clay minerals or Fe(hydr-)oxides enhances decomposition of OM and DON release is perhaps mostly by Fe(hydr-)oxides dissolution. Hence a paddy soil's ability to supply DON, indicative probably of OM quality, might explicitly control net mineral N release (DON explained 53% variation in $N_t$) next to SOC level (explained 62% variation in $N_t$). Whether DON is mainly released abiotically with reductive dissolution of pedogenic (hydr-)oxides or is supplied by the enzymatic hydrolysis of labile SOM fractions would, however, be soil specific and so this conclusion should not be generalized. Ability of a soil to supply DOM may with other factors co-determine anaerobic

net N mineralization either by acting as intermediate N-pool or as general substrate for anaerobic microbial activity. Dedicated experiments still need to prove the relevance of both probably non-exclusive mechanisms but regardless a better prediction of potential DON release would serve to predict paddy soil N supply.

# Chapter 4

**Link between paddy soil mineral nitrogen release and iron and manganese reduction examined in a rice pot growth experiment**
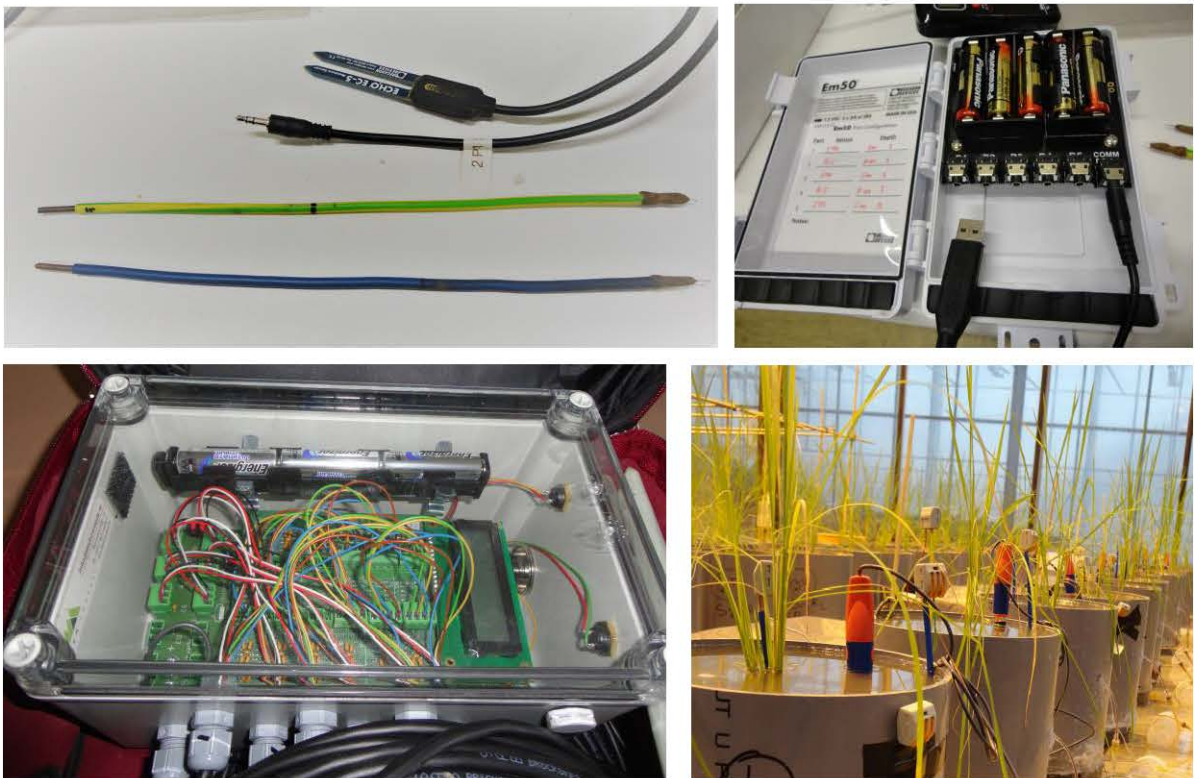


**Redrafted after:**

Akter M., Deroo H., De Grave E., Van Alboom T., Kader M. A., Pierreux S., Begum M.A., Boeckx P., Sleutel S., 2017. Link between paddy soil mineral nitrogen release and iron and manganese reduction examined in a rice pot growth experiment. Geoderma (submitted).

**Abstract**

Paddy soil indigenous N supply is often poorly related to N status and our aim was to assess its linkage to reduction of $Fe^{3+}$ and $Mn^{4+}$, primary terminal electron acceptors in submerged soils. Transplanted rice was grown in the greenhouse in four Bangladeshi paddy soils for 72 days firstly under continuous and then intermittent flooding. Solution buildup rates of Fe and Mn in the first 2-3 weeks of flooding correlated negatively with soil organic carbon (SOC) to $NH_4$-oxalate extractable Fe ($Fe_{ox}$) and Mn ratios (r: -0.82 to -0.84; p<0.01 and r:-0.83 to -0.93; p<0.01, resp.). Mössbauer analysis detected ferrihydrite and goethite in all soils and with $Mn_3O_4$ these are the likely source minerals. An electron ($e^-$) balance calculated from soil C-emission rates suggested reductive Fe and Mn dissolution to be a relevant $e^-$-accepting processes. But we hypothesize that reduction of abundantly present octahedral $Fe^{3+}$ in chlorites and vermiculite and their interstratified forms in these floodplain silty Inceptisols would partly also support microbial activity. Notwithstanding, a close temporal synergy existed between solution Fe and soil mineral N and their build-up rates were correlated (r: 0.77 to 0.90; p<0.01) and with that of dissolved OC (DOC) (r: 0.84 to 0.96; p<0.01), C emission rate (r: 0.99; p<0.01) and SOC:$Fe_{ox}$ (r: -0.71; p<0.01). Although pedogenic Fe was not identified as the single dominant $e^-$-acceptor, these correlations do suggest its reduction to be a relevant intermediary step in soil N mineralization, possibly through release of associated DOC, N or both. Switching to intermittent flooding lowered pH, and any dissolved Fe and Mn was oxidized or precipitated but, unexpectedly, DOC levels remained elevated. Clearly dissolution of Fe, Mn and DOC were then decoupled from mineral N release but since Eh remained in the Fe-reduction range in three out of four soils, possibly clay-$Fe^{3+}$ alternated with $O_2$ as $e^-$-acceptor. Most importantly, in all soils N release slowed or halted after only 2 weeks of flooding but recommenced with intermittent flooding. As a next step, field experiments could verify if indigenous soil N supply also benefits from non-continuous irrigation management. Release rates of exchangeable N could not be related to SOC or N level, and so quality of soil organic matter and its association with specifically pedogenic Fe as well as $Fe^{3+}$-bearing clay minerals needs to be further investigated. Lastly, experimental proof is pending for release of clay-bound N and interlayer $NH_4^+$ following reduction of octahedral $Fe^{3+}$ with consequent increased negative charge or structural destabilization, possibly an important process in floodplain paddy soils in Bangladesh.

## 4.1. Introduction

Irrigated rice systems account for half of the total rice area and contribute 75% of the world's annual rice production (IRRI, 2011) since most rice varieties exhibit maximum yield potential under sufficient water supply. Nitrogen stays the most yield limiting and difficult nutrient to manage due to its complex biogeochemical cycle, poor fertilizer use efficiency (usually just 30%) and rapid losses via different processes. The N availability to plants mainly results from the balance between soil organic matter (SOM) mineralization, microbial immobilization, plant uptake, $NH_4^+$-fixation, and losses via $NH_3$-volatilization. A number of studies reveal that N uptake by rice plants, 15 to 22kg N per ton rice (Dobermann and Cassman, 1996), originates mainly from soil organic N mineralization and not directly from fertilizer, even in sufficiently N-fertilized fields (Ando et al., 1992; Manguiat et al., 1994; Khaokaew et al., 2007). Previous studies, however, have shown very inconsistent dependencies of N mineralization rate on general soil properties and management (Narteh and Sahrawat, 1997; Adhikari et al., 1999; Sahrawat, 2006; Kader, 2012; Kader et al., 2013). Improved estimates of indigenous soil N supply would allow for adapted N fertilizer application, thereby optimizing N use efficiency as well as minimizing adverse environmental impacts of excessive N (Mikha et al., 2006, Sharifi et al., 2007). Under controlled conditions of often used lab incubations to asses N release, SOM decomposition evidently mainly depends on quality and quantity of SOM, but also very much on availability of oxidants (Cassman et al,. 1996; White and Reddy, 2001; Li et al., 2010; Gao et al., 2014). Thus empirical predictions of $NH_4^+$ production may be improved if co-based on contents of key oxidants, confirmed to drive anaerobic soil mineral N release. Usually $Fe^{3+}$ reduction is seen to dominantly capture electrons released from organic compounds, amounting up to 24% according to Jäckel and Schnell (2000), 66-84% according to Inubushi et al. (1984) and 58-79% according to Yao et al. (1999). Indeed, regression analysis indicated that inclusion of extractable Fe improved the prediction of mineralized N (Narteh and Sahrawat, 1997). For a set of 25 paddy fields in Bangladesh we found that anaerobic N mineralization correlated only with pH and pedogenic-Fe content and not with a myriad of other soil properties including soil C and N content (Kader et al., 2013). In our follow-up research (Akter et al., 2016) we instead found no correlations between anaerobic soil $NH_4^+$-release and pedogenic-Fe or Mn-levels. However, soil exchangeable-$NH_4^+$ and dissolved Fe demonstrated a remarkable co-evolution over time and were positively correlated. But causality would need to be elucidated and confirmed in a more realistic soil environment than in small scale bare soil lab incubations as used by Akter et al. (2016) and Kader et al. (2013). Firstly, rice root-derived $O_2$ input causes local rising of Eh, lowering of pH and re-oxidation and precipitation of Fe and Mn. Secondly, without plant N-uptake paddy soil $NH_4^+$-N contents likely become

inhibitive to further N-mineralization in bare soil setups. Thirdly, in a field setting, flooding is often not entirely continuous and frequent shorter periods of topsoil drying occur, deliberate or due to lack of irrigation water. Resulting variations of reduction or oxidation processes would strongly change the soil solution chemistry especially reductive dissolution of Mn and Fe (hydr-)oxides, OM degradation and N mineralization. Experiments with non-continuously flooded growing rice plants allow to further assess linkages between soil N supply and other soil processes under more realistic conditions. For instance, a fluctuating water table could not be implemented in the previous small soil cores experiments by Akter et al. (2016).

A first objective was to upscale our previous lab-incubations to rice pot-growth experiments and to complement recording of soil mineral N release with ancillary information on evolution of soil redox potential (Eh) and Fe and Mn reduction. Because the intensity of reduction processes in rice planted soils will differ strongly between soil layers vertically (Zschornack et al., 2011), we explicitly aimed to measure at a surface and underlying depth increment. We did not attempt to assess radial variation surrounding rice roots. A second objective was to investigate how transition to non-continuous soil wetting and resulting drying impacts Fe and Mn-reduction in relation to net mineral N supply (soil and plant mineral N). To address these objectives, we studied plant N-uptake, the progressive dissolution of Fe and Mn as well as change in mineral N content in four young floodplain paddy soils of North-Bangladesh with wide variations in soil C to oxalate extractable Fe ($Fe_{ox}$) ratio (1.6-4.9). We expected readily reducible $e^-$ acceptors ($Fe_{ox}$) would become limiting for net soil N supply at comparatively high soil C content and likely higher $e^-$ donation rate upon its microbial decomposition. If on the other hand, as mentioned in Chapter 3, the connection between soil $Fe_{ox}$ reduction and apparent soil N supply is mainly the result of co-release of DON then we expect an increasing apparent net N supply with increasing soil C to $Fe_{ox}$ ratio. We also monitored soil temperature, moisture, pH, Eh, DOC, $CO_2$ and $CH_4$ emission to obtain detailed insight in the evolution of soil reductive processes. For the initial first weeks after onset of flooding, when often a major part of soil mineral N release occurs, we estimated the potential share of donated electrons accepted by various soil oxidants. We used Mössbauer spectroscopy and assessed soil-specific relations between Fe and Mn solubility and pe + pH to identify source minerals of dissolved Fe and Mn.

## 4.2. Materials and Methods

### 4.2.1. Soils

Four typical floodplain young paddy soils were collected from farmers' fields in May 2014 in Northern Bangladesh (24°37´ N to 24°49´ N, 90°02´ to 90°25´ E). The subtropical monsoon climate is characterized by an annual mean temperature and rainfall of 25.8°C and 2427mm, respectively (BMD, 2015). Agricultural production is dominated by single or double rice cropping with rain-fed and supplemental irrigated production in the Aman season (Jul-Nov) and irrigated production in the dryer Boro season (Jan-Apr). Puddle layer (0-15cm) soil was collected from 15 spots per field by spade. The field-moist soils were broken, air dried, ground and sieved through a 2mm mesh sieve prior to shipment to the University of Ghent, Belgium. Previously determined general soil properties are shown in Table 4.1. In addition, plant-available macro (Ca, K, Mg and P) and micro (Cu, Fe, Mn, Zn and Mo) nutrients in air dried soils were determined by $NH_4$-lactate and DTPA (Diethylene triamine pentaacetic acid) extraction, respectively (Lindsay and Norvell, 1969) (Table 4.1). The pH-KCl of initial soils were measured by glass electrode in a 1:2.5 soil:KCl suspension. Before incubation, soil mineral N ($NH_4^+$-N and $NO_3^-$-N) content was determined in 1:5 soil:1M KCl extracts by means of a continuous flow auto analyzer (Skalar, The Nederlands).

The soils were specifically selected out of a larger set used by Kader et al. (2013) based on their differing soil organic C (SOC) to oxalate extractable Fe ($Fe_{ox}$) ratio (Table 4.1). The motivation was that while capacity to donate electrons and hence cause reduction of various species in soil is mainly a function of availability of a degradable C-substrate, the capacity to receive electrons depends on the availability of reducible Fe and Mn (Ponnamperuma et al., 1972). The ratio of SOC to oxalate extractable Fe or Mn may thus indicate proneness to lowering of Eh under submerged conditions. Four selected soils exhibited only ranges of ammonium oxalate extractable Fe and Mn ($Fe_{ox}$ and $Mn_{ox}$), while texture and pH-KCl were relatively invariable. SOC and soil N contents ranged widely from 5.5 to 23.6 g $kg^{-1}$ and 0.8 to 2.1 g $kg^{-1}$, respectively (Table 4.1). Following previously reported X-ray diffraction analyses, all four included soils contain mica, kaolinite, vermiculite, and, except for the Noaddah-2-sample, also chlorite. In the Sonatala-1 and Melandaho samples some crystalline goethite was also detected (Kader et al., 2013).

**Table 4.1** Physical and chemical properties of four Bangladeshi floodplain paddy soils used in the greenhouse rice growth pot experiment.

| Properties | Sonatala-1 | Melandoho | Balina | Noaddah-2 |
|---|---|---|---|---|
| Latitude (N)[a] | 24°43´14.5´´ | 24°48´42´´ | 24°49´28´´ | 24°37´19.2´´ |
| Longitude (E)[a] | 90°25´52.3´´ | 90°24´49´´ | 90°21´09´´ | 90°02´17´´ |
| Cropping Pattern[a] | Rice-Fallow-Rice | Rice-Fallow-Rice | Rice-Fallow-Fallow | Rice-Fallow-Rice |
| Soil Type[a] | Aeric Haplaquepts | Aeric Fluvaquents | Mollic Haplaquepts | Ultic Ustochrepts |
| SoilTexture[a] | Silt loam | Silt loam | Silty clay loam | Silt loam |
| SOC (g kg$^{-1}$) | 23.6 | 5.5 | 16.5 | 11.5 |
| Total N (g kg$^{-1}$) | 2.1 | 0.8 | 1.9 | 1.3 |
| pH-KCl | 5.5 | 4.2 | 4.0 | 4.2 |
| $Fe_{ox}$ (g kg$^{-1}$) | 4.8 | 3.5 | 8.4 | 4.5 |
| $Mn_{ox}$ (g kg$^{-1}$) | 0.20 | 0.05 | 0.22 | 0.25 |
| $SO_4^{2-}$(mg kg$^{-1}$)[a] | 19.3 | 17.5 | 58.2 | 12.6 |
| CEC (cmol$_c$ kg$^{-1}$)[a,b] | 44 | 25 | 43 | 35 |
| $NH_4^+$-N (mg kg$^{-1}$) | 7 | 16 | 13 | 6 |
| $NO_3^-$-N (mg kg$^{-1}$) | 4 | 8 | 12 | 2 |
| Ca-lac (mg kg$^{-1}$) | 1814 | 460 | 1652 | 401 |
| K-lac (mg kg$^{-1}$) | 24 | 32 | 61 | 22 |
| Mg-lac (mg kg$^{-1}$) | 554 | 95 | 339 | 42 |
| Na-lac (mg kg$^{-1}$) | 143 | 26 | 52 | 18 |
| P-lac (mg kg$^{-1}$) | 24 | 56 | 5 | 127 |
| Cu-DTPA (mg kg$^{-1}$) | 1.8 | 1.0 | 2.4 | 0.4 |
| Fe-DTPA (mg kg$^{-1}$) | 141 | 174 | 165 | 240 |
| Mn-DTPA (mg kg$^{-1}$) | 97 | 21 | 128 | 92 |
| Zn-DTPA (mg kg$^{-1}$) | 0.1 | 0.1 | 0.2 | 0.5 |
| Si-DTPA (mg kg$^{-1}$) | 43 | 21 | 40 | 35 |
| Mo-DTPA (mg kg$^{-1}$) | 0.1 | 0.1 | 0.1 | 0.1 |
| SOC:$Fe_{ox}$ | 4.9 | 1.6 | 2.0 | 2.6 |

[a]Data taken from Kader et al. (2013)

[b]CEC: Cation exchange capacity

*4.2.2. Greenhouse pot experiment*

A rice pot experiment was set up covering 4 soils × 3 replicates in the UGhent FBE-greenhouses from December 2014 to February 2015. The intent was to investigate the relation between release of mineral N and soil reductive processes. The soils were filled into PVC pots (25 cm H. × 18.5 cm Ø) forming cores of 20 cm height (Fig. 4.1a). The amount of dry soil per pot was 5.7 kg for Sonatala-1, 6.8 kg for Melandoho and Balina, and 7.8 kg for Noaddah-2, matching their bulk density in the field (1.05 Mg m$^{-3}$ for Sonatala-1, 1.26 Mg m$^{-3}$ for Melandoho and Balina, and 1.45 Mg m$^{-3}$ for Noaddah-2). In each pot, $Ca_3(PO_4)_2.H_2O$ powder and KCl grains, equalling doses of 27 kg P ha$^{-1}$ and 98 kg K ha$^{-1}$, were applied and mixed thoroughly during soil preparation. Per pot 4-5 twenty five days old seedlings of BINA Dhan7 (*Oryza sativa* L., maturity 120 days) were transplanted in a single hill per pot. Twelve pots were monitored for soil moisture level, soil pH, redox potential (Eh), temperature, soil solution chemistry and $CO_2$ and $CH_4$ emission (Fig. 4.1b and c). Twenty four additional pots were used to follow plant N-uptake and build-up of mineral N in soil (see Section 4.2.5). A specific irrigation scheme was laid out to represent the reality of field conditions with initial continuous flooding, regularly followed by temporary soil drying from heading until maturity rice growing stages, caused by progressively hotter and drier conditions along the Boro season and shortage of irrigation water. All pots were continuously flooded (CF) until 33 days after transplantation (DAT) to a 4-5cm standing level by regular addition of deionized water, that was degassed right before addition by purging with $N_2$ for one hour. From 34 till 72 DAT an alternate wetting and drying regime (AWD) was adopted by water application only every 3-4 days. The temperature in the greenhouse was maintained at 28°C.



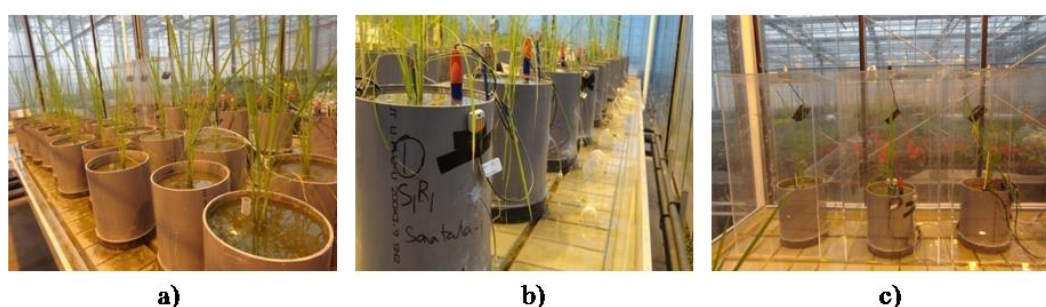a)                                    b)                                    c)

Fig.4.1 Experimental set up with rice plants grown in pots in the Ghent University Faculty of Bioscience Engineering greenhouses (a), pots with growing rice plants for nondestructive monitoring of different biochemical soil parameters (b) and (c) set-up of headspace gas sampling

### 4.2.3. Soil moisture, temperature, redox potential and pH

In a single pot per soil, volumetric water content ($\Theta_v$) at 0-4 and 4-14 cm and temperature at 4-14 cm depth were measured hourly with Decagon 5EC-5 and 5TM probes and data loggers. To monitor soil redox potential (Eh), in-house fabricated platinum (Pt) electrodes (Pt wire joined at the tip of insulated Cu wire with steel epoxy resin (Devcon Co., Netherlands)) were installed permanently at 4 and 14 cm depth in eight pots, i.e. 2 depths × 2 replicates × 4 soils. Per pot a reference Ag-AgCl-electrode was permanently installed and all probes were connected to a HYPNOS III data logger (MVH Consult, The Netherlands) to measure Eh every quarter until 72 DAT. Corrections were applied for the offset relative to a standard $H_2$-electrode. Soil pH was measured regularly by directly inserting a glass pH-electrode in the wet or saturated soil 2-3 cm deep.

### 4.2.4. Analysis of soil solution chemistry to monitor reductive Fe- and Mn-dissolution and release of dissolved organic matter

In each of the twelve fixed pots two micro-rhizon soil moisture samplers ((RSMS), pore size: 0.12-0.18µm, **5cm long** 2.5mm Ø **porous** part) (Rhizosphere Research Products, The Netherlands) were placed horizontally at 4 and 14 cm depth to regularly collect soil pore solution (Fig. 4.1b). At pH close to neutrality, any dissolved Fe and Mn is primarily $Fe^{2+}$ and $Mn^{2+}$ and by the evolution of their soil solution concentrations we inferred occurrence and rate of reductive dissolution of Fe and Mn in soil. Soil solution samples were extracted into 16.2 mg $K_3$EDTA-coated 9 ml plastic vacuum vials (Vacutest Kima srl : Arzergrande (PD), Italy) by piercing the vial's septum with the RSMS's needle. The $K_3$EDTA coating prevented re-precipitation of collected Fe and Mn from the sampled soil solution.

Log-normal models fitted well to the temporal evolutions of Fe and Mn concentration (*Fe(t)* and *Mn(t)*):

$$Fe(t) = Fe_{max}.\, e^{-c_{Fe}\left(1-\ln(\frac{t}{t_{max;Fe}})^2\right)}$$

$$Mn(t) = Mn_{max}.\, e^{-c_{Mn}\left(1-\ln(\frac{t}{t_{max;Mn}})^2\right)}$$

, with $Fe_{max}$ and $Mn_{max}$ the peak soil solution concentrations (in mg l$^{-1}$), and $t_{max;Fe}$ and $t_{max;Mn}$ the elapsed time in DAT to reach these maxima in dissolved Fe and Mn. The parameters $c_{Fe}$ and $c_{Mn}$ describe the shape of the log-normal curve.

Simultaneously, dissolved organic carbon (DOC) was quantified by collecting another set of soil solution samples into uncoated 9 ml vacuum vials (Vacutest Kima srl : Arzergrande (PD), Italy). Solutions were analyzed for their Fe and Mn contents by ICP-OES with a radial

plasma iCAP 6300 series spectrometer (Thermo Scientific, US). DOC levels were determined with a Shimadzu TOC-VCPN-analyzer (Shimadzu Corporation, Kyoto, Japan) with separate measurement of total C and inorganic C after acidification with 2M HCl.

### 4.2.5. Soil and plant sampling to determine soil mineral N release

Soil samples were collected by inserting a hollow PVC tube (1.5cm inner diameter × 16cm length) at 0-4 cm and subsequently in the same hole at 4-14 cm depth on 0, 7, 15, 21, 31, 46 and 58 DAT. Exchangeable-$NH_4^+$ was extracted from the collected 15g homogenized moist soil samples (equivalent to about 10g dry soil) by 1M KCl at a 1:5 soil to extract ratio. The slurries were shaken for 2 hours and filtered through 150mm diameter filter paper (MN 616 1/4). Derived extracts were analyzed for their $NH_4^+$-N and $NO_3^-$-N levels with a continuous-flow auto-analyzer (Skalar, The Nederlands). We calculated the amounts of N separately for the 0-4 cm and 4-14 cm layers by multiplying with soil mass and summed both to yield mg N pot$^{-1}$.

Rice plants were sampled destructively from the 24 dedicated pots on three occasions (31, 46 and 67 DAT), i.e. 2 replicates × 4 soils per sampling event. All above-ground plant parts were separated by cutting the rice plants at soil surface. The remaining roots were collected by gently removing the surrounding saturated soil and washing over a 2000μm mesh size sieve. Plant samples were oven-dried at 70°C for 72 hours and weighted. The dried materials were ground and analyzed for their C and N content with a Variomax CNS analyser (Elementar Analysen Systeme, Germany). A zero-order model was fitted to the total amount of N taken up by the plant per pot (with $R^2 > 0.93$) to calculate plant N uptake on the exact same dates of soil sampling (Fig. 4.7). The measured soil mineral N content in this study represents the balance between soil mineral N inputs, viz. soil organic N mineralization and clay interlayer defixation, and outputs, viz. plant N-uptake, microbial immobilization, clay interlayer fixation, and nitrification-denitrification (Dong et al., 2012; Hoque et al., 2002; Said-Pullicino et al., 2014). In the present paddy soil pot experiment with no hydraulic (mineral) N-fluxes, no alkaline pH, and no fertilizer applied, we assume that soil $NH_4^+$-N primarily stemmed from net organic N mineralization, i.e. ammonification - N immobilization, and was mainly consumed by rice plant (Zhang et al., 2009). Hence, we assumed that the evolution of summed amounts of soil exchangeable mineral N and plant N, equals net soil N supply. We assume that during the CF period defixation of $NH_4^+$ is minor because at low Eh the net negative charge of clays instead attracts $NH_4^+$ and gradual accumulation of exchangeable $NH_4^+$, given still limited plant N uptake, limits diffusion out of interlayers. Absence of clay defixation during 4 weeks of CF was furthermore evidenced

before for the Sonatala-1 and Melandoho soils by Akter et al. (2016). During CF, soil N supply thus mainly represents net SOM mineralization, of which some part may net clay-interlayer $NH_4^+$ exchange. The summed soil mineral N (0-14 cm) and plant N uptake per sampling time (in mg N pot$^{-1}$) was divided by the corresponding soil mass to obtain net soil N supply in mg kg$^{-1}$. A first-order kinetic model was then fitted to the evolution of net mineral N (summed soil plus plant N) with time during 0 to 31 DAT: $N_t = N_a(1 - e^{-k_f t})$, where $t$ is the time (in days), $N_t$ is the amount of mineral N released at time $t$ (mg N kg$^{-1}$), $N_a$ the amount of potentially mineralizable N, and $k_f$ is the first-order mineralization rate. A zero-order kinetic model was fitted to the evolution of net mineral N (soil and plant N) during the 31 to 58 DAT AWD period: $N_t = N_0 + k_0 t$, with $N_0$ the initial mineral N content, and $k_0$ is the linear N-release rate.

*4.2.6. Assessment of C mineralization via headspace $CO_2$ and $CH_4$ analysis*

Soil $CO_2$ and $CH_4$ emissions were monitored incrementally by means of a closed-chamber method (Fig. 4.1c). Acrylic Plexiglas chambers (34cm × 34cm × 70cm) were outfitted with a septum and a battery-operated fan. To collect gas samples, chambers were placed over the pots and the bottom was sealed by standing water on the supporting greenhouse bench. Then gas samples were drawn at 0, 15 and 30min by connecting 10ml pre-evacuated screw neck vials (VWR: 548-0247) via double-sided needles. Air temperature inside the chambers was recorded. The $CH_4$ and $CO_2$ concentrations of collected gas samples were analyzed by two Trace Ultra Gas Chromatographs (Thermo Electron Corporation, US), equipped with packed columns and a flame ionization detector and thermal conductivity detector and auto-sampler. Gas concentrations were converted to mass based levels by the ideal gas law and linear models were fitted to the accumulation of $CO_2$ and $CH_4$ with time. Derived linear C-flux rates were recalculated to mg C kg$^{-1}$ soil h$^{-1}$.

*4.2.7. Relationship between pe+pH and Fe and Mn solubility in flooded paddy soils*

The relation between pe+pH, a redox parameter, and dissolved Fe or Mn is mineral-specific and the comparison of their experimentally assessed values with theoretical equilibrium equations could indicate the source mineral of reduced $Fe^{2+}$ and $Mn^{2+}$ (Ponnamperuma et al., 1969; Brennan and Lindsay, 1996; Zhang et al., 2012). A short-term submerged soil incubation experiment (22°C, 25 days) was set up to generate variation in pH, Eh and dissolved Fe and Mn by anaerobic microbial activity. The soils were in duplicate filled into PVC pots (18 cm H × 12 cm Ø, i.e. 1358 cm³), with a similar preparation as in the pot

experiment, but without fertilizer application or growing rice plants. Per pot one RSMS was placed vertically, with the porous filter covering a 1-6 cm depth interval. Soil solution samples were collected regularly (see Section 4.2.4) and Eh and pH was measured (see Section 4.2.3).

### 4.2.8. Mössbauer spectroscopy of soil

Identification of the iron phases and their relative contents in four representative soils were determined using $^{57}$Fe Mössbauer spectroscopy at UGent's Dept. of physics and astronomy. The Mössbauer spectra (MS) were collected in transmission geometry using $^{57}$Co(Rh) sources with active diameter of 5 mm and initial activity of ~75 mCi (2.78 GBq), provided by Gamma-Lab Development S.L. The time-mode spectrometer was composed of Wissel GmbH drive, detection and data-acquisition (CMCA-550) modules, and operated in the constant acceleration mode with a triangular reference signal. The spectrometer exhibited excellent linearity and was calibrated using a standard α-Fe$_2$O$_3$ powder. All center shift (δ) values quoted hereafter are relative to α-Fe at room temperature. For all spectra the velocity (*v*) increment per channel was ~0.0442 mm/s and from the calibration spectra an instrumental line width of ~0.27 mm/s was observed for the innermost absorption lines of the calibration spectrum. The absorber thickness was not more than ca. 2 mg Fe per cm². Counts were accumulated in 1024 channels until an off-resonance count rate of ~$10^6$ per channel had been reached. Details on the spectrometer's performance are given in sub-section 4.3.9.

Typically, the low *T* (ca. 18 K) spectra were fitted with a superposition of two symmetric quadrupole doublets and two model-independent hyperfine-field distributions using in-house developed software based on the IMSL FORTRAN library optimizer routine ZXSSQ. All calculated subcomponents were composed of Lorentzian-shaped absorption lines. As commonly accepted, the relative content of different Fe phases present in these soils may be good approximation considered as being proportional to the fractional areas, *RA*, of the corresponding spectral components.

## 4.3. Results

### 4.3.1. Soil temperature and moisture content

During the entire follow-up period the average soil temperature remained close to 27°C, with clear diurnal fluctuations and similar patterns of evolution among the four soils (Fig. 4.2).

Volumetric moisture content ($\Theta_v$) ($m^3$ $m^{-3}$) varied considerably during intermittent flooding (34 to 72DAT), following continuous saturation during the preceding CF period. Drainage caused fast soil drying within 1-3 days to $\Theta_v$ as low as 0.2-0.3 $m^3$ $m^{-3}$ in the Balina and Noaddah-2 soils, while $\Theta_v$ dropped mostly to only 0.35-0.4$m^3$ $m^{-3}$ in case of Melandoho. Due to a malfunctioning of the dielectric probe 4cm depth $\Theta_v$ data was missing for Sonatala-1 from 44 to 66 DAT, but from the low Eh measured at 4cm depth (see Section 4.3.2) it seems unlikely that there were substantial drops in $\Theta_v$. Dielectric probe readings at 14cm depth indicated that the subsoil remained saturated, except for a final deep drainage around 68DAT in case of Balina.
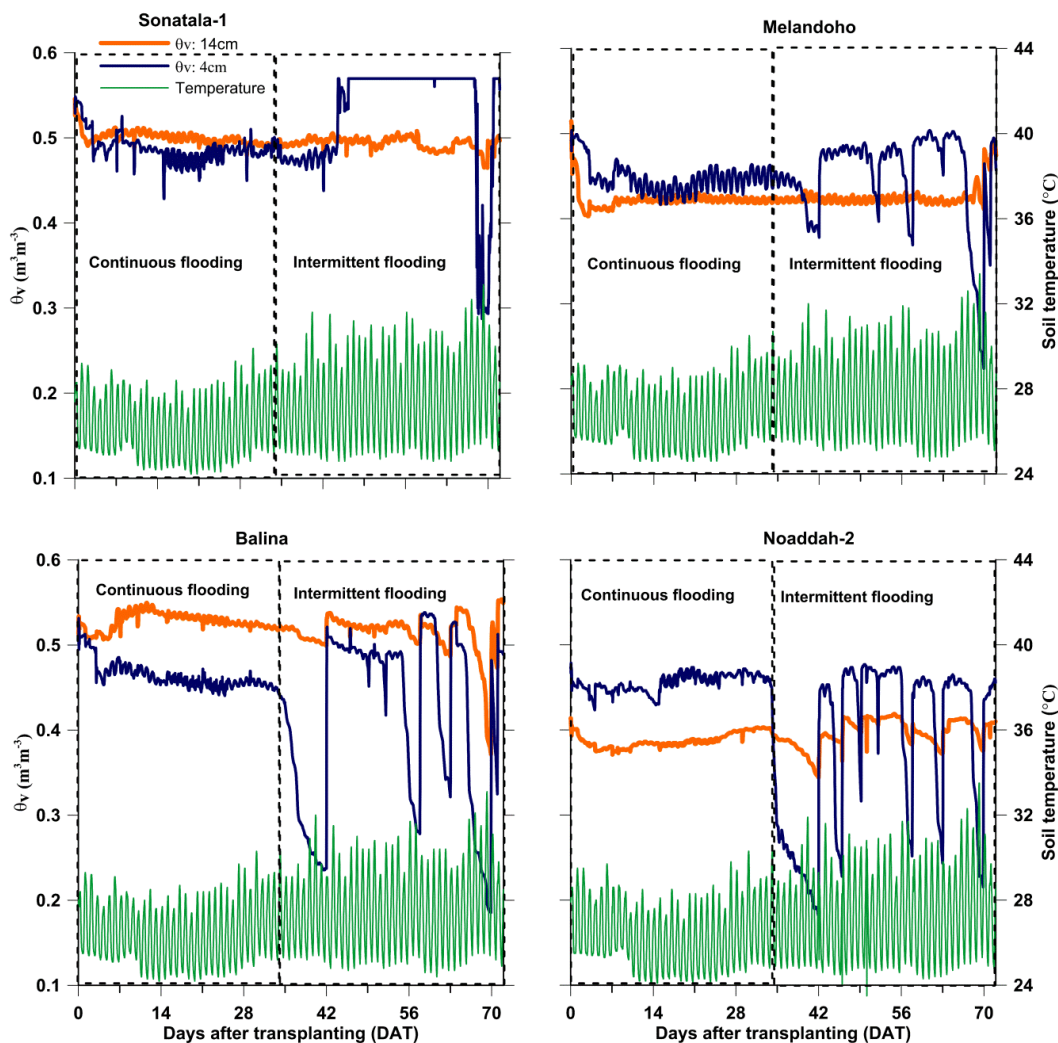


Fig. 4.2 Variations in soil temperature and volumetric moisture content ($\Theta_v$) of farmer's fields paddy soil with actively growing rice plants

*4.3.2. Soil pH and redox potential (Eh)*

Initial soil pH varied between 5.2 to 6.7 (Fig. 4.3), increased towards neutrality within 14DAT, and then stabilized during CF and fluctuated between 5.7 to 7.0 during intermittent flooding (34 to 72 DAT). In the Sonatala-1 soil, pH varied only slightly between 6.5 and 7.0 throughout the experiment, again suggesting that $\Theta_v$ at 0-4cm depth did not lower strongly during 34-66DAT. In all four soils Eh dropped sharply within the first 14DAT indicating reductive conditions both at 4 and 14cm depth (Fig.4.3). The extent of these declines in Eh varied widely: in Sonatala-1 from +300 mV to -144mV and -208mV at 4 and 14cm, respectively; in Melandoho from +334mV to -129mV and -140mV; in Balina from +321mV to -163mV and -175mV; and in Noaddah-2 from +281mV to -48mV and -73mV. Except for Noaddah-2, strongly reductive conditions persisted over the CF period.

During subsequent AWD irrigation management, Eh fluctuated in all soils at 4cm and to a lesser degree at 14cm depth. In the Sonatala-1 and Melandoho soils Eh stayed in Fe-reductive to methanic ranges (-94 to -199mV and -3 to -143mV, respectively). Instead, AWD caused Eh to rise up to a Mn- and Fe-reductive conditions in the Noaddah-2 (+152 to -148mV) soil. In clear contrast, Eh remained positive (+11 to +215mV) in the Balina soil at both depths.
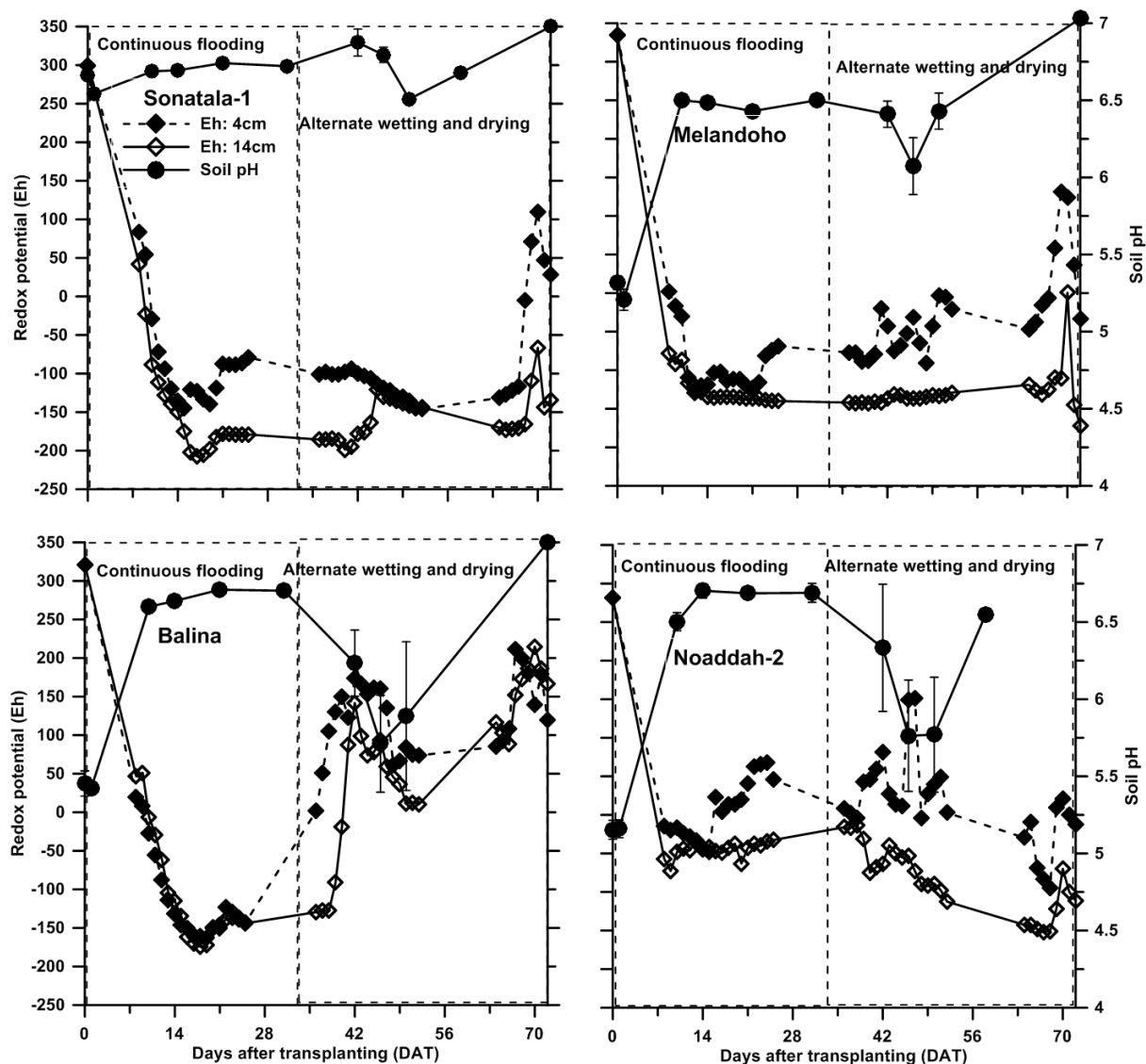
Fig. 4.3. Changes in soil pH and redox potential (Eh) in four Bangladeshi floodplain paddy soils (vertical bars indicate the standard errors around means, n=3 for pH; no bars for Eh with n=2)

### 4.3.3. Soil solution Fe and Mn and relation to initial drop in Eh following soil flooding

Solution Fe steeply increased in Melandoho and Balina soils, and already peaked around 14DAT, and the rise in dissolved Fe lasted till 21 and 29DAT, respectively (Fig. 4.4). While the rise in dissolved Fe was slower for the Sonatala-1 and Noaddah-2 soils (except at 14cm depth) (Fig. 4.4). Temporal patterns of soil solution Mn resembled those for Fe but a first fast rise at 4cm depth finished earlier, except in case of Balina. Concomitance Fe and Mn reduction is possible because $Mn^{4+/3+}$ and $Fe^{3+}$ can serve as $e^-$ acceptors at Eh ranges of +350 to +100 mV and +250 to -100mV, respectively (Patrick and Jugsujinda, 1986; Gao et

91

al., 2002). After peaking for several days soil solution Fe and Mn then more gradually dropped to low levels between 42-72DAT. For each of the four studied soils and at both depths, during the CF period Eh at individual measuring dates was well negatively correlated with solution Fe (mostly $p < 0.01$ and $r > 0.90$), logically denoting pronounced reductive dissolution of Fe-(hydr-)oxides following the initial fast Eh drop (Grybos et al., 2009; Zhang et al., 2012).

Parameters describing log-normal models fitted to these temporal evolutions are given in (Table 4.2). High $Fe_{max}$ levels were reached in the Balina (217-231 mg $l^{-1}$) and Melandoho (191-367 mg $l^{-1}$) soils, matching the most reductive conditions in these two soils (Eh lowered from +334 to -140 and +321 to -175mV in Balina and Melandoho, respectively). At 14cm depth as well, reductive Fe-dissolution was prominent in the Balina, Noaddah-2 and Melandoho soils. Elevated 4cm depth solution Mn levels in the Balina soil indicated that Mn-reduction was also a likely relevant process maintaining microbial activity in that soil. The same applies to the 14cm depth for Sonatala-1, Noaddah-2 and Balina soils (Fig. 4.4), where even higher Mn concentrations were reached. The ordination of $Mn_{max}$ was Balina > Noaddah-2 > Sonatala-1 > Melandoho.

These observations could be partly linked to $Fe_{ox}$ and $Mn_{ox}$ contents. Lowest Mn levels in the Melandoho soil match its lowest $Mn_{ox}$ content (Table 4.1). Highest the $Fe_{max}$ (66 mg $l^{-1}$) and $Mn_{max}$ (16 mg $l^{-1}$) at 4cm depth in the Noaddah-2 soil coincided with the less pronounced reductive conditions (average Eh: 22mV). Mostly trends in Eh and Fe and Mn were similar at both depths, but in the Noaddah-2 soil more prominent reductive conditions at 14cm depth were indicated from higher mean $Fe_{max}$ (229 mg $l^{-1}$) and $Mn_{max}$ (51 mg $l^{-1}$) and drop in Eh from +281 to -73mV during CF. Roughly summarized, the data suggest that Fe-reduction was predominant in Melandoho, Mn-reduction was predominant in Sonatala-1 and both processes were prominent in Noaddah-2 and Balina.

### 4.3.4. Fe and Mn/pe+pH diagrams

In all four soils, pe+pH dropped rapidly during 22days of anaerobic incubation, viz. from 12.4 to 4.2, from 12.3 to 4.4, from 11.8 to 4.0 and from 10.7 to 3.4 in the Sonatala-1, Melandoho, Balina and Noaddah-2 soils, respectively. Corresponding dissolved Fe and Mn/pe+pH diagrams differed greatly among the soils (Fig. 4.5). Fits with theoretical diagrams of pedogenic Fe- and Mn-(hydr-)oxides were poor and only tentatively indicated that in the Sonatala-1 and Melandoho soils levels of dissolved $Fe^{2+}$ might have been controlled primarily by reductive dissolution of amorphous- $Fe_3O_4$ or $Fe(OH)_3$. In the Noaddah-2 soil,

the solution $Fe^{2+}$ activity most closely followed the amorphous $Fe(OH)_3$ diagram. In clear contrast to all three other soils, the solution Fe in Balina soil might have most likely derived from diverse sources of Fe minerals and Fe(hydro-)oxides, possibly also including $\gamma$-FeOOH (lepidocrocite) and $\gamma$-$Fe_2O_3$ (maghemite) (Fig. 4.5). For Mn, experimental data did not match any of $logMn^{2+}+2pH/pe+pH$ diagrams of several common Mn-bearing minerals. The slope of $Mn_3O_4$'s diagram corresponded well with the data, however, with too low measured Mn concentrations.



Fig. 4.4 Evolution of soil solution Fe and Mn concentration at 4 and 14cm depth in four Bangladeshi floodplain paddy soils (vertical bars indicate standard errors around means, n=3)
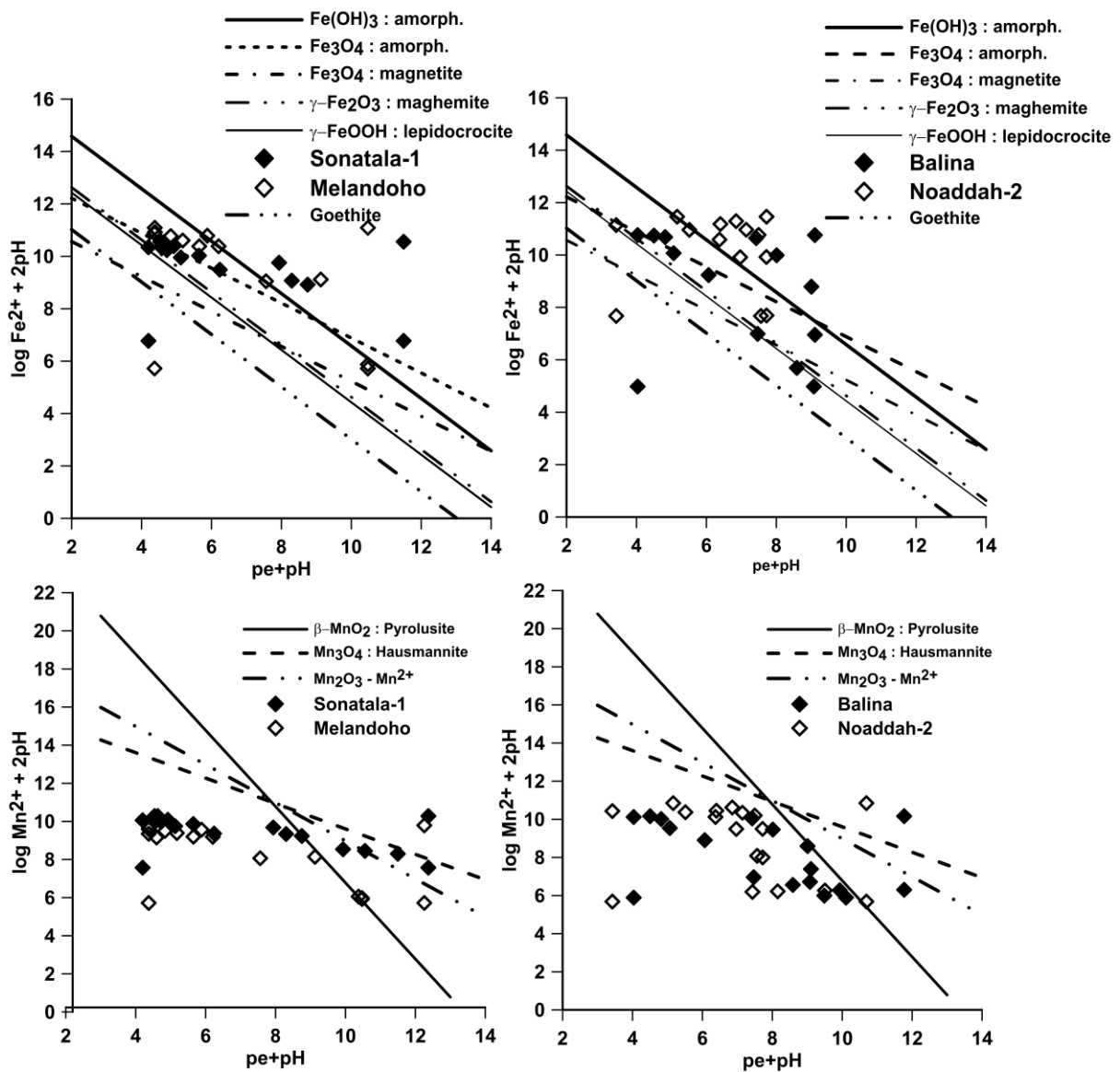
**Fig. 4.5** Activity of solution $Fe^{2+}$ and $Mn^{2+}$ in relation to pe+pH in four Bangladeshi floodplain paddy soils and theoretical solubility diagrams of various Fe and Mn (hydro-)oxides

*4.3.5. Temporal pattern of soil mineral N (NH$_4^+$-N and NO$_3^-$-N)*

Initial mineral N contents ranged from 8 to 25 mg kg$^{-1}$, with a considerable part under the form of NO$_3^-$-N. After flooding, however, any mineral N detected was NH$_4^+$-N. During 0 to 58DAT, exchangeable NH$_4^+$-N followed consistent patterns in each soil with relatively small standard deviations around means (Fig. 4.6). Generally, soil mineral N content went up linearly with time, peaked around 15DAT, and then declined gradually to very low levels at 58DAT. NH$_4^+$-N contents were nearly equal in both sampled depth increments and superior in the Melandoho and Balina soils. The overall order of calculated total soil mineral N build-up (in mg kg$^{-1}$) was Balina (65-77) > Melandoho (45-59) > Noaddah-2 (19-24) > Sonatala-1 (10-18).
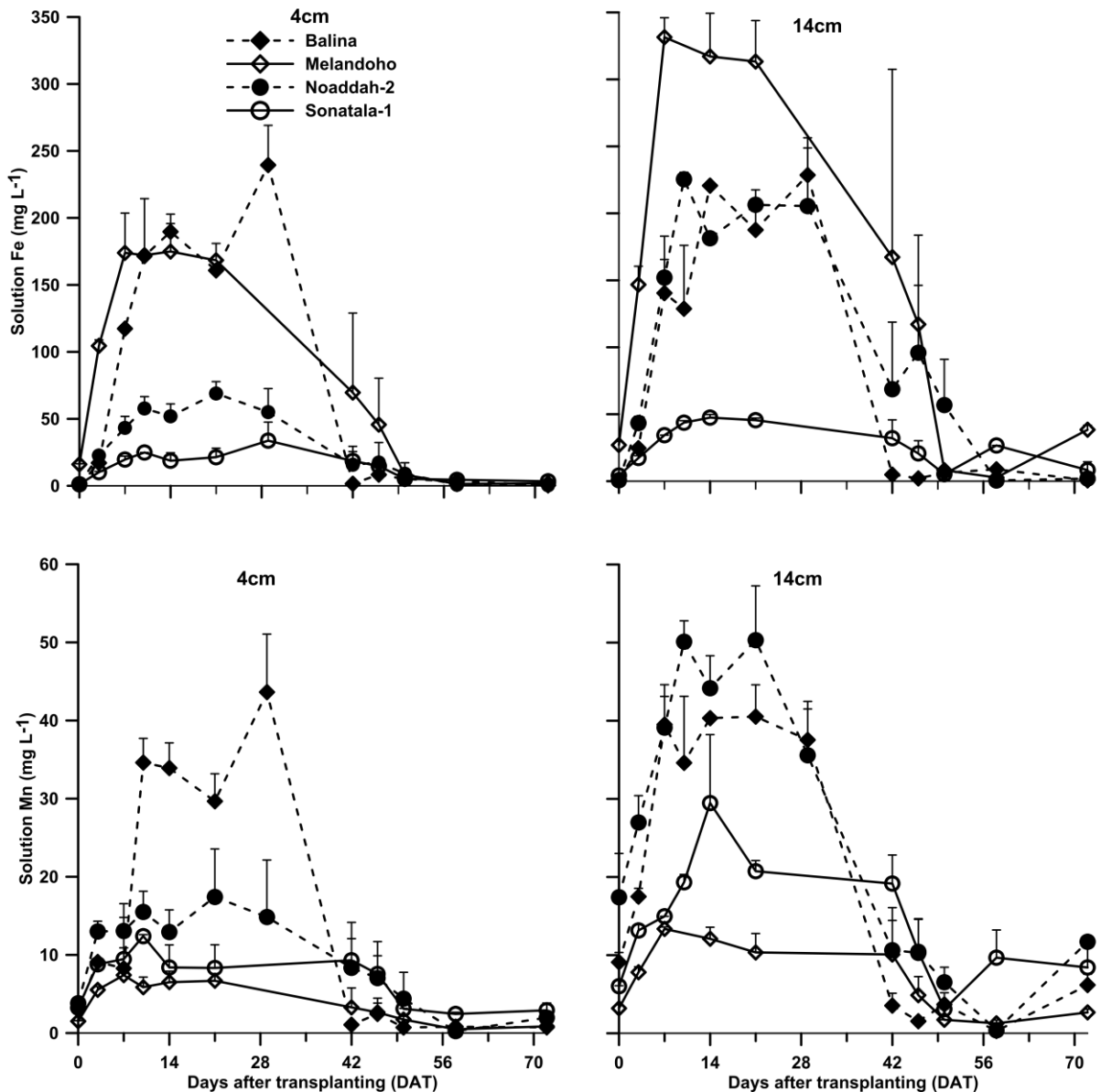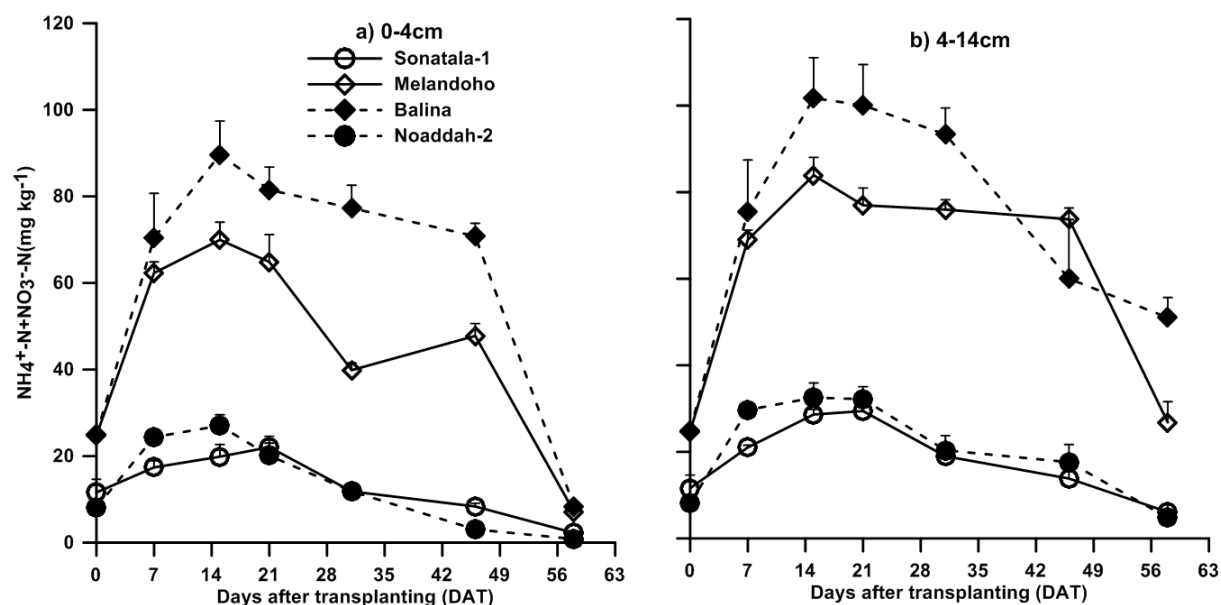


Fig. 4.6 Progression of soil mineral N content at 4 and 14cm depth in four Bangladeshi floodplain paddy soils (vertical bars indicate standard errors around means, n=3)

Table 4.2 Parameterization of log-normal models describing the temporal evolution of soil solution Fe and Mn

| Soil | $Fe_{max}$ (mg $L^{-1}$) | $t_{max;Fe}$ (day) | $C_{Fe}$ | $R^2$ | Fe rate (mg $L^{-1}$ day$^{-1}$) | $Mn_{max}$ (mg $L^{-1}$) | $t_{max;Mn}$ (day) | $C_{Mn}$ | $R^2$ | Mn rate (mg $L^{-1}$ day$^{-1}$) |
|---|---|---|---|---|---|---|---|---|---|---|
| Sonatala-1 (4cm): R1 | 16.6 | 9.6 | 1.5 | 0.55 | 1.7 | 10.9 | 10.6 | 1.8 | 0.73 | 1.0 |
| Sonatala-1 (4cm): R2 | 32.7 | 16.1 | 4.5 | 0.72 | 2.0 | 14.2 | 12.3 | 2.0 | 0.60 | 1.2 |
| Sonatala-1 (4cm): R3 | 22.5 | 10.7 | 3.0 | 0.92 | 2.1 | 10.6 | 6.9 | 1.1 | 0.92 | 1.5 |
| Sonatala-1 (4cm): mean | 23.1 | 12.4 | 2.8 | 0.82 | 1.9 | 11.6 | 9.8 | 1.5 | 0.79 | 1.2 |
| Melandoho (4cm): R1 | 231.0 | 10.9 | 2.9 | 0.78 | 21.1 | 9.2 | 10.0 | 1.8 | 0.70 | 0.9 |
| Melandoho (4cm): R2 | 219.3 | 9.0 | 3.5 | 0.95 | 24.5 | 8.1 | 7.6 | 2.1 | 0.95 | 1.1 |
| Melandoho (4cm): R3 | 128.2 | 7.9 | 2.3 | 0.76 | 16.1 | 5.0 | 5.1 | 0.7 | 0.72 | 1.0 |
| Melandoho (4cm): mean | 191.2 | 9.5 | 2.9 | 0.93 | 20.2 | 7.3 | 7.9 | 1.5 | 0.90 | 0.9 |
| Balina (4cm): R1 | 213.9 | 15.5 | 9.5 | 0.74 | 13.8 | 49.9 | 17.6 | 15.7 | 0.76 | 2.8 |
| Balina (4cm): R2 | 228.8 | 15.9 | 10.7 | 0.73 | 14.4 | 38.5 | 14.1 | 7.3 | 0.67 | 2.7 |
| Balina (4cm): R3 | 211.7 | 14.5 | 10.1 | 0.88 | 14.6 | 34.5 | 16.5 | 15.8 | 0.79 | 2.1 |
| Balina (4cm): mean | 217.3 | 15.3 | 10.0 | 0.78 | 14.2 | 40.9 | 16.6 | 13.1 | 0.75 | 2.5 |
| Noaddah-2 (4cm): R1 | 49.1 | 10.9 | 5.0 | 0.86 | 4.5 | 11.8 | 5.2 | 1.0 | 0.89 | 2.3 |
| Noaddah-2 (4cm): R2 | 80.6 | 20.6 | 11.5 | 0.76 | 3.9 | 19.0 | 6.9 | 1.8 | 0.91 | 2.8 |
| Noaddah-2 (4cm): R3 | 82.6 | 12.4 | 6.6 | 0.90 | 6.7 | 16.9 | 7.9 | 1.9 | 0.92 | 2.1 |
| Noaddah-2 (4cm): mean | 65.6 | 14.0 | 6.2 | 0.86 | 4.7 | 15.8 | 6.8 | 1.6 | 0.93 | 2.3 |
| Sonatala-1 (14cm): R1 | 46.6 | 15.6 | 3.4 | 0.65 | 3.0 | 20.4 | 18.1 | 1.8 | 0.66 | 1.1 |
| Sonatala-1 (14cm): R2 | 48.8 | 13.9 | 3.2 | 0.68 | 3.5 | 22.4 | 12.4 | 2.4 | 0.66 | 1.8 |
| Sonatala-1 (14cm): R3 | 48.1 | 13.0 | 5.2 | 0.81 | 3.7 | 19.7 | 11.8 | 2.3 | 0.86 | 1.7 |
| Sonatala-1 (14cm): mean | 47.2 | 13.9 | 3.6 | 0.84 | 3.4 | 20.5 | 13.3 | 2.1 | 0.79 | 1.5 |
| Melandoho (14cm): R1 | 308.5 | 9.5 | 2.3 | 0.75 | 32.4 | 11.0 | 6.8 | 0.9 | 0.67 | 1.6 |
| Melandoho (14cm): R2 | 396.0 | 11.2 | 4.5 | 0.92 | 35.2 | 15.3 | 11.3 | 3.2 | 0.85 | 1.4 |
| Melandoho (14cm): R3 | 404.0 | 10.5 | 3.7 | 0.91 | 38.4 | 15.5 | 8.8 | 3.0 | 0.93 | 1.8 |
| Melandoho (14cm): mean | 367.8 | 10.5 | 3.5 | 0.89 | 35.1 | 13.7 | 9.1 | 2.3 | 0.94 | 1.5 |
| Balina (14cm): R1 | 239.4 | 12.7 | 7.1 | 0.88 | 18.9 | 51.2 | 10.5 | 4.1 | 0.89 | 4.9 |
| Balina (14cm): R2 | 284.9 | 20.1 | 25.7 | 0.77 | 14.1 | 46.3 | 16.9 | 11.7 | 0.66 | 2.7 |
| Balina (14cm): R3 | 219.0 | 15.2 | 11.0 | 0.83 | 14.4 | 42.7 | 10.0 | 3.8 | 0.87 | 4.3 |
| Balina (14cm): mean | 231.5 | 15.8 | 11.4 | 0.80 | 14.6 | 43.9 | 11.3 | 4.3 | 0.82 | 3.9 |
| Noaddah-2 (14cm): R1 | 222.4 | 11.6 | 6.3 | 0.92 | 19.2 | 46.0 | 9.1 | 3.2 | 0.89 | 5.1 |

| | | | | | | | | | |
|---|---|---|---|---|---|---|---|---|---|
| Noaddah-2 (14cm): R2 | 263.7 | 19.3 | 8.4 | 0.78 | 13.7 | 56.1 | 12.8 | 4.0 | 0.73 | 4.4 |
| Noaddah-2 (14cm): R3 | 231.2 | 12.9 | 4.9 | 0.87 | 17.9 | 52.9 | 10.7 | 3.7 | 0.89 | 4.9 |
| Noaddah-2 (14cm): mean | 228.5 | 14.3 | 5.8 | 0.89 | 16.0 | 50.7 | 10.7 | 3.3 | 0.86 | 4.8 |

*4.3.6. Combined N release from soil into soil exchangeable N and plant N*

In the Sonatala-1 and Noaddah-2 soils, the summed amount of N taken up by the rice plant and the released N in soil increased almost linearly, between 0 to 15 DAT, stabilized until 31DAT and increased again linearly from 31 to 58 DAT. In the Balina and Melandoho soils, a fast build-up of mineral N in soil and plant between 0 to 15 DAT was followed by plateauing in the subsequent periods (15 to 58DAT) (Fig. 4.7). The evolution of net mineral N (soil-N and converted to plant N) over time was well modeled by first-order kinetic models during the 0 to 31 DAT CF period ($R^2$: 0.83-0.96) and by a zero-order model during the AWD period ($R^2$: 0.70-0.99) (Fig. 4.7). At any sampling event, the joint cumulative mineral N release differed significantly ($p<0.05$) between the soils with higher final total N-release (in mg kg$^{-1}$ after 58 days) from the Balina (86) soil than from Melandoho (76), Sonatala-1 (61) and Noaddah-2 (59) soils.
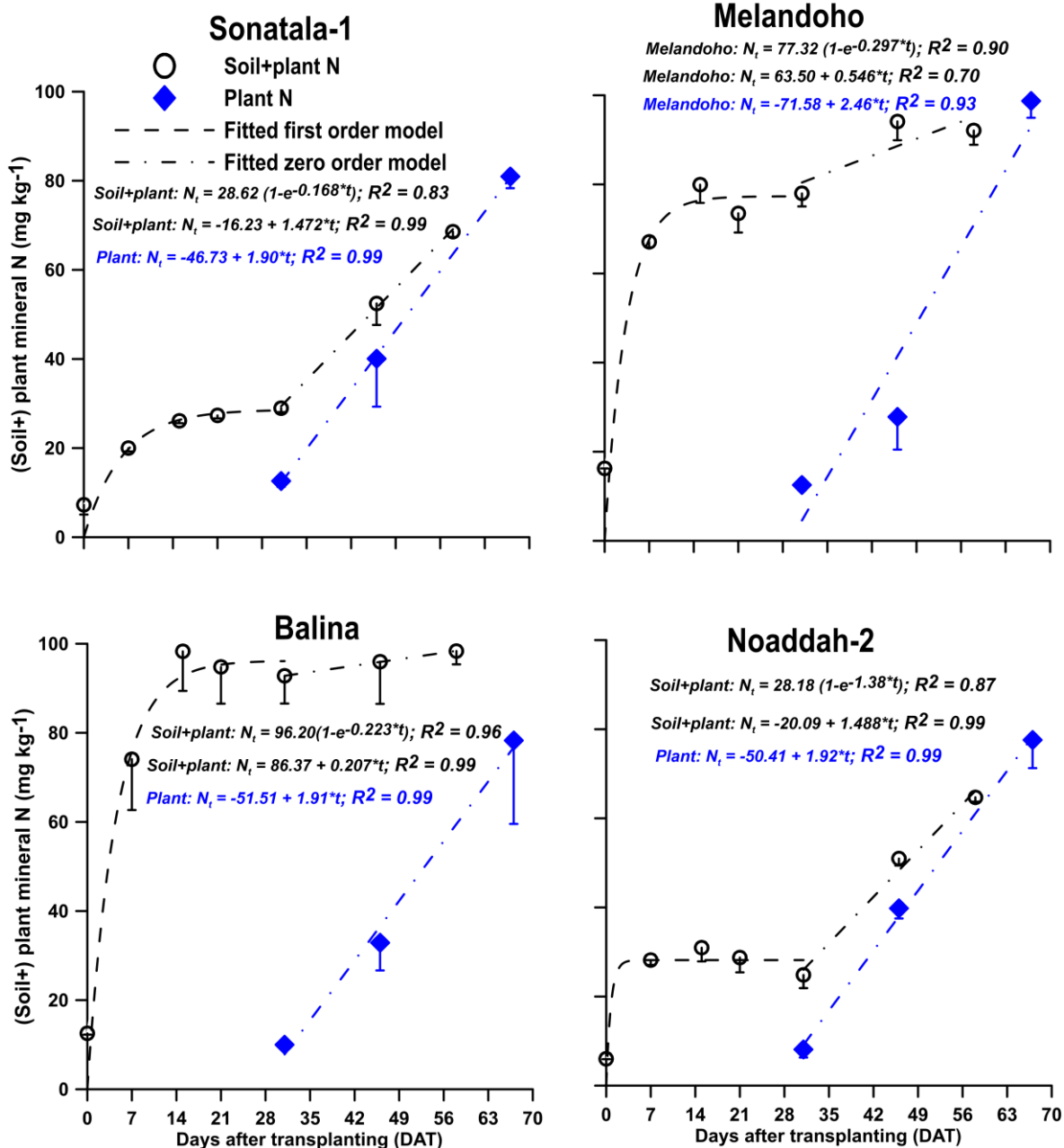
Fig. 4.7 Net evolution of mineral N in (soil+) plant in four Bangladeshi floodplain paddy soils (vertical bars indicate the standard errors of the means). Fitted first and zero order models are illustrated by dash lines (vertical bars indicate standard errors around means, n=3)

### 4.3.7. Evolution of DOC in soil solution and emission of $CH_4$ and $CO_2$

During the monitoring period, DOC concentrations increased at both sampled depths in the Sonatala-1, Melandoho and Noaddah-2 soils (Fig. 4.8a and b). In the Balina soil, the DOC concentrations increased sharply until 14DAT and then on decreased gradually until 42DAT (Fig. 4.8a and b). Within each soil, DOC concentrations at 14cm were always greater than at

4cm. Faster initial increases in DOC were also observed at 14cm depth for the Sonatala-1 and Melandoho soils. DOC levels in the Noaddah-2 soil were less than half than in the other soils. Calculated rises in DOC concentration, at 4 and 14 cm depth, respectively, were 326 and 488 mg $l^{-1}$ for Sonatala-1, 373 and 630 mg $l^{-1}$ for Melandoho, 456 and 667 mg $l^{-1}$ for Balina, and 87 and 272 mg $l^{-1}$ for Noaddah-2.

$CH_4$ emission rates remained minor throughout and strongly fluctuated in both the flooded and AWD periods (Fig. 4.8c). During CF mean $CH_4$ flux rates were indifferent between soils (Table 4.3). In the AWD period (42-72DAT) mean $CH_4$ fluxes varied significantly ($p < 0.01$) (Table 4.3) in the order: (in mg $CH_4$ $kg^{-1}$ $h^{-1}$) Melandoho (0.014) > Balina (0.0104) > Sonatala-1 (0.0103) > Noaddah-2 (0.005). $CO_2$ was digressively emitted from all soils and always dominated gaseous C emissions ($CO_2$-C + $CH_4$-C) (Fig. 4.8d). During the CF management (0-29DAT), the mean total C emission rates were 0.6, 0.7, 1.13 and 0.7 mg $kg^{-1}$ $h^{-1}$ from the Sonatala-1, Melandoho, Balina and Noaddah-2 soils, respectively (Table 4.3). Between 42-69 DAT total C emission rates declined and stabilized at 0-1 mg $kg^{-1}$ $h^{-1}$. A first-order kinetic model fitted well to the accumulative amount of C mineralized ($CO_2$-C + $CH_4$-C in mg $kg^{-1}$ soil) over time ($R^2 \geq 0.98$) (Fig 4.9).
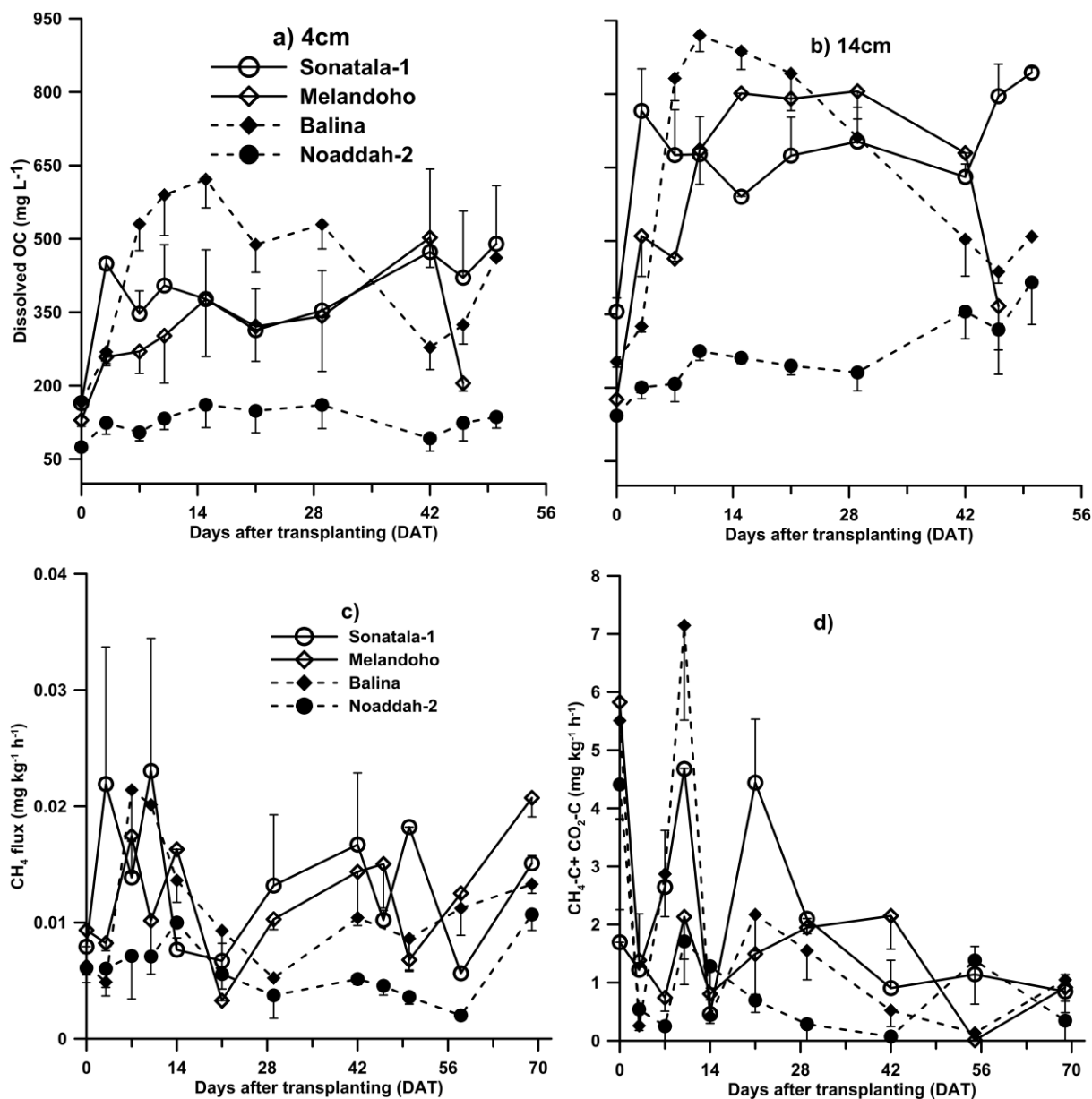
Fig. 4.8 Evolution of soil solution dissolved OC concentration (a, b), soil flux of $CH_4$ (c) and total C emission (d) rate for four Bangladeshi floodplain paddy soils (vertical bars indicate standard errors around means, n=3)
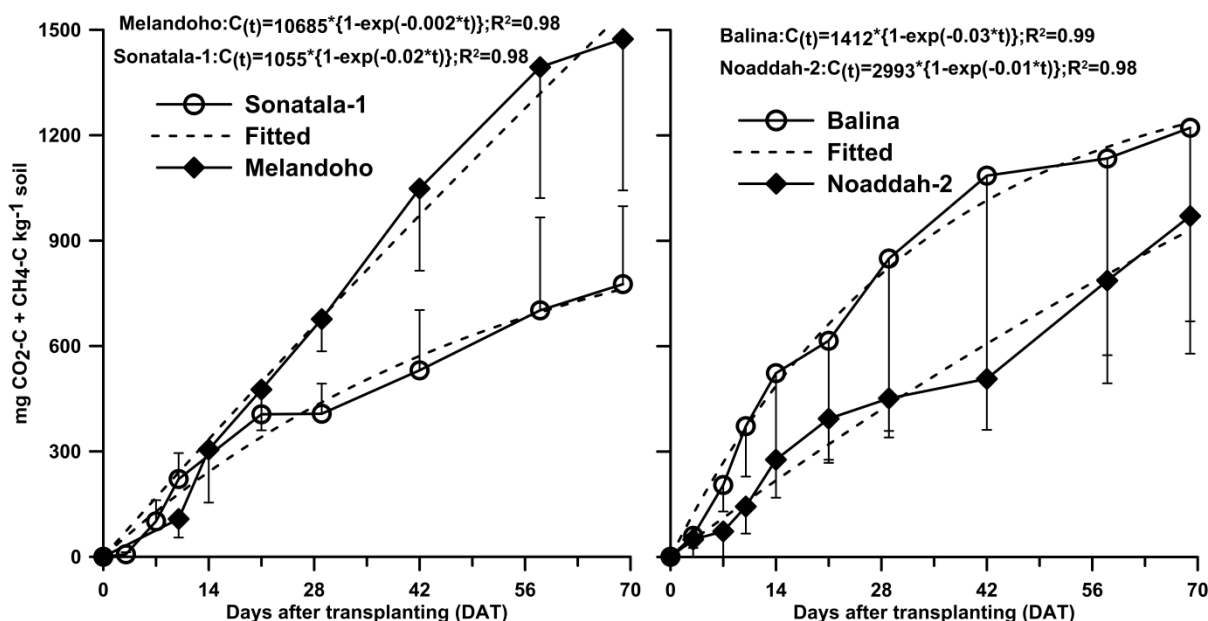
Fig. 4.9 Cumulative C mineralization (mg $CO_2$-C + $CH_4$-C $kg^{-1}$ soil) and fitted first order model in four farmer's fields paddy soil with actively growing rice plants as a function of transplanting time (vertical bars indicate the standard errors of the means, n=3)

*4.3.8. Correlation of net mineral N supply rate with soil properties, rate of DOC and C efflux, and reductive Fe- and Mn dissolution*

During both CF and AWD periods mineral N release rate correlated negatively with the initial soil pH-KCl (p<0.05) and the SOC:$Fe_{ox}$ ratio (p<0.01), while no relations were found with SOC, soil N, SOC:$Mn_{ox}$ ratio, $Mn_{ox}$ or $Fe_{ox}$ (Table 4.4). To investigate possible temporal co-variation of mineral N release and Fe and Mn dissolution rates among the soils we calculated the rates of mineral N build-up at corresponding time intervals DAT 0 to $t_{max;Fe}$ and $t_{max;Mn}$. Correlation coefficients were calculated between these mean short-term $NH_4^+$-N buildup rates (in soil and plant) on the one hand and release rates of solution Fe and Mn, and other relevant soil properties on the other (Table 4.4). During CF, the rate of net mineral N release was strongly and positively correlated with the build-up rates of soil solution Fe (p<0.01) and DOC (P<0.01) at both depths, and with total C efflux rate (p<0.01) (Table 4.4). C efflux rates also correlated negatively with initial soil pH-KCl and the SOC:$Fe_{ox}$ ratio (p<0.01). Within the CF period C efflux rates and release rates of soil solution Fe (p<0.01) and DOC (p<0.05) were correlated positively but only at 4cm depth. During AWD, the net mineral N release rate and C efflux rate did not correlate significantly with the mean DOC level (Table 4.4).

102

Table 4.3 Mean soil (± standard error) $CH_4$ and total C emission rates during continuously flooding (CF) and subsequent alternate wetting and drying (AWD) and model parameters of a 1st order kinetic model fitted to cumulative C mineralization data

| Soil | Mean $CH_4$ flux (mg $kg^{-1}$ $h^{-1}$) | | Mean $CO_2$ + $CH_4$ flux (mg C $kg^{-1}$ $h^{-1}$) | | 1st order C-model parameters | | |
|---|---|---|---|---|---|---|---|
| | CF | AWD | CF | AWD | $C_A$ (mg C $kg^{-1}$) | k ($day^{-1}$) | $R^2$ (-) |
| Sonatala-1 | 0.013 ± 0.0021 | 0.010 ± 0.0013b[a] | 0.551 ± 0.1053 | 0.449 ± 0.1442 | 1055 | 0.02 | 0.98 |
| Melandoho | 0.011 ± 0.0023 | 0.014 ± 0.0011a | 0.707 ± 0.1622 | 0.799 ± 0.4070 | 10685 | 0.002 | 0.98 |
| Balina | 0.012 ± 0.0005 | 0.010 ± 0.0003b | 1.1252 ± 0.6352 | 0.275 ± 0.2654 | 1412 | 0.03 | 0.99 |
| Noaddah-2 | 0.007 ± 0.0007 | 0.005 ± 0.0004c | 0.714 ± 0.2677 | 0.488 ± 0.2549 | 2993 | 0.01 | 0.98 |
| ANOVA[a] | N.S.[a] | p<0.01 | N.S. | N.S. | - | - | - |

[a] Significance of one-way ANOVA with 'Soil' as fixed-factor; N.S.: Not significant at p=0.05

[b] Different letters after group means indicate significant differences (p ≤ 0.01) according to Duncan's Multiple Range Test

**Table 4.4** Pearson's correlation coefficients (r) between C mineralization and mineral N build-up rate (soil + plant) and initial soil properties, soil solution Fe, Mn and DOC build-up rates during CF, the SOC:$Fe_{ox}$ and SOC:$Mn_{ox}$ ratios and mean DOC level

| Soil parameter | Mineral N release (in mg kg$^{-1}$ d$^{-1}$) | | C mineralization rate (in mg kg$^{-1}$ d$^{-1}$) | |
| --- | --- | --- | --- | --- |
| | CF | AWD | CF | AWD |
| SOC (g kg$^{-1}$) | -0.34 | -0.37 | -0.31 | -0.25 |
| Soil N (g kg$^{-1}$) | -0.16 | -0.20 | -0.12 | -0.06 |
| pH-KCl | -0.63[*a] | -0.60[*] | -0.64[*] | -0.61[*] |
| Fe-ox (g kg$^{-1}$) | 0.55 | 0.49 | 0.59[*] | 0.65[*] |
| Mn-ox (g kg$^{-1}$) | -0.36 | -0.44 | -0.32 | -0.26 |
| $SO_4^{2-}$ (mg kg$^{-1}$) | 0.75[**] | 0.71[**] | 0.79[**] | 0.83[**] |
| CF Fe build-up rate (mg l$^{-1}$ d$^{-1}$): 4cm | 0.90[**] | - | 0.80[**] | - |
| CF Fe build-up rate (mg l$^{-1}$ d$^{-1}$): 14cm | 0.77[**] | - | 0.48 | - |
| CF Mn build-up rate (mg l$^{-1}$ d$^{-1}$): 4cm | -0.18 | - | 0.18 | - |
| CF Mn build-up rate (mg l$^{-1}$ d$^{-1}$): 14cm | -0.41 | - | 0.03 | - |
| CF DOC build-up rate (mg l$^{-1}$ d$^{-1}$): 4cm | 0.96[*] | - | 0.66[*] | - |
| CF DOC build-up rate (mg l$^{-1}$ d$^{-1}$): 14cm | 0.84[**] | - | -0.14 | - |
| CF C mineralization rate (mg kg$^{-1}$ d$^{-1}$) | 0.99[**] | - | 1 | - |
| SOC : $Fe_{ox}$ ratio | -0.71[**] | -0.70[*] | -0.70[*] | -0.67[*] |
| SOC : $Mn_{ox}$ ratio | 0.05 | 0.12 | 0.03 | 0.02 |
| Mean DOC level (mg l$^{-1}$): 4cm | 0.59[*] | 0.48 | 0.60[*] | 0.40 |
| Mean DOC level (mg l$^{-1}$): 14cm | 0.62[*] | 0.13 | 0.62[*] | 0.01 |

[a] *: Significant at p=0.05; **Significant at p=0.01

### 4.3.9. Characterization of soil Fe by Mössbauer spectroscopy

Characterization of the initial soil Fe was performed using Mössbauer spectroscopy. A more detailed description and interpretation of experimental readings is given in 4.3.9.1. At room temperature, the MS were interpreted as several overlapping ferrous and ferric quadrupole doublets, which were insufficiently resolved to identify Fe phases. At 75 K, a magnetically split component was apparent and was attributed to ferric Fe in goethite (see further). At lower *T*, typically a second magnetic and very broad spectral component could additionally be resolved from the experimental spectra, which, on the basis of the extracted hyperfine parameters, in particular the magnetic hyperfine field $B_{hf}$, is believed to be due to ferric Fe in ferrihydrite (see further). The remaining and generally prominent doublet absorptions present

in these low T-spectra typically could be reproduced by one ferrous and one ferric doublet. In Table 4.5, the low T-results for the Mössbauer parameters of the four samples are listed. The related experimental and calculated MS are shown in Fig. 4.10. From the low T MS-analyses it is apparent that Balina, Sonatala-1 and Melandoho samples contain chlorite and/or vermiculite, as was confirmed by XRD previously by Kader et al. (2013). However, further identification of the chlorite was impossible. The magnetically split components resolved from the low-temperature spectra were typical for $Fe^{3+}$ and identified features were typical for poorly crystalline goethite. A final very broad magnetic component identified only at $T \approx 18$ K was assigned to ferrihydrite (Murad, 1998; Vandenberghe et al., 1990), indeed in many soil types closely associated with presence of poorly crystalline goethite. The MS of the Noaddah-2 sample are significantly different from those of the other samples, in the sense that the resonant γ-ray absorption in this sample is very weak in comparison with the former three samples. However, despite of the poor statistics, the calculated hyperfine parameters of the resolved magnetic components at low $T$ again indicate the presence of goethite and ferrihydrite in the Noaddah-2 soil. Contrary to the other three samples, however, the central absorption in the low T-MS could not be well adjusted by the combination of one $Fe^{3+}$ and one $Fe^{2+}$ doublet, but it is plausible that it originates from a chlorite or clay mineral as for the other samples.

*Details performance of the Mössbauer spectrometer and details on low temperature Mössbauer Spectra of the Balina, Sonatala-1 and Melandoho soils*

Balina, Sonatala-1 and Melandoho's low *T*-MS had comparable well-resolved quadrupole doublets, and Mössbauer parameters. The doublet with center shift $\delta \approx 1.25$ mm/s and quadrupole splitting $\Delta E_Q \approx 2.85$ mm/s is due to ferrous species in the involved mineral(s), while the doublet with $\delta \approx 0.48$ mm/s and $\Delta E_Q \approx 0.80$ - 0.87 mm/s is due to ferric cations in the respective sample structures. The ferrous doublet parameters, both at low *T* and *RT*, agree very well with those reported for chlorites and vermiculites (Ahmed et al., 2012; Kodama et al., 1982; Rozenson et al., 1979). At *RT*, the parameters for the ferric doublet in the present samples, $\delta \approx 0.38$ mm/s and $\Delta E_Q \approx 0.72 – 0.80$ mm/s, are close to the values of $\delta \approx 0.37$ mm/s and $\Delta E_Q \approx 0.65$ mm/s reported for chlorites (Ahmed et al., 2012; Kodama et al., 1982; Rozenson et al., 1979; Wagner and Wagner, 2004) and vermiculites (Ahmed et al., 2012; Ericsson et al., 1984). Low *T* parameters are not available for ferric species in chlorites and vermiculite, except for a few oxidized chlorites. For these last products, significantly higher ferric $\Delta E_Q \approx 1.30 – 1.44$ mm/s at low *T* especially, and $\Delta E_Q \approx 0.88 – 0.96$ mm/s at *RT*, are reported (Kodama et al., 1982).

The magnetically split components resolved from the low-temperature spectra are typical for $Fe^{3+}$. The subspectrum with $\delta \approx 0.46 - 0.47$ mm/s, quadrupole shift $2\varepsilon_Q \approx -0.23 - -0.24$ mm/s and hyperfine field $B_{hf} \approx 491 - 501$ kOe (highest probability value) observed at $T \approx 18$ K (see Table 4.5), is also present in the MS recorded at 75 K with compatible values for its hyperfine parameters, but does not appear as a magnetically split component in the *RT* spectrum. This latter feature, combined with the low-temperature values of the hyperfine parameters (Table 4.5), is typical for poorly crystalline goethite of which the MS is in most cases a doublet at *RT*, whereas its spectrum at lower temperatures, e.g., 80 K is generally magnetically splitted (Murad, 1998; Vandenberghe et al., 2000). The very broad magnetic component with $\delta \approx 0.44 - 0.56$ mm/s, $2\varepsilon_Q \approx 0.02 - -0.12$ mm/s and $B_{hf} \approx 427 - 439$ kOe (highest probability value, see Table 4.5) could only be resolved at the lowest applied temperature and its contribution to the total spectra is relatively weak and strongly overlapping with the goethite component. Consequently, its Mössbauer parameters are rather ill defined. Despite the large spread of its parameters for the three different samples, it is likely that this component has a common origin. On the basis of the parameter values as determined for the present samples, in particular the maximum-probability hyperfine field at ~18 K, and taking into account that magnetic splitting of the subspectrum only appears at temperatures below 75 K, the involved component is assigned to ferrihydrite (Murad, 1998; Vandenberghe et al., 1990), indeed in many soil types closely associated with presence of poorly crystalline goethite.

Table 4.5 Low temperature Mössbauer spectroscopy results for Balina, Sonatala-1, Melandoho and Noaddah-2 soil samples

| | $T$ | | Phase | $\delta$ | $\Delta E_Q$ | $2\varepsilon_Q$ | $B_{hf}$[a] | $\Gamma$ | RA |
|---|---|---|---|---|---|---|---|---|---|
| | (K) | | | (mm/s) | (mm/s) | (mm/s) | (kOe) | (mm/s) | (%) |
| Balina | 19 | $Fe^{2+}$ | Chlorite | 1.244 | 2.845 | | | 0.45 | 32.8 |
| | | $Fe^{3+}$ | Chlorite | 0.489 | 0.829 | | | 0.66 | 44.1 |
| | | $Fe^{3+}$ | goethite | 0.46 | | -0.23 | 494 | 0.27 | 14.7 |
| | | $Fe^{3+}$ | ferrihydrite | 0.45 | | -0.11 | 439 | 0.27 | 8.4 |
| Sonatala-1 | 17 | $Fe^{2+}$ | chlorite | 1.245 | 2.824 | | | 0.45 | 39.7 |
| | | $Fe^{3+}$ | chlorite | 0.487 | 0.863 | | | 0.61 | 39.1 |
| | | $Fe^{3+}$ | goethite | 0.47 | | -0.24 | 501 | 0.27 | 15.6 |
| | | $Fe^{3+}$ | ferrihydrite | 0.56 | | 0.02 | 427 | 0.27 | 5.6 |
| Melandoho | 19 | $Fe^{2+}$ | chlorite | 1.250 | 2.819 | | | 0.49 | 41.5 |
| | | $Fe^{3+}$ | chlorite | 0.484 | 0.872 | | | 0.62 | 41.3 |
| | | $Fe^{3+}$ | goethite | 0.46 | | -0.23 | 498 | 0.27 | 12.5 |
| | | $Fe^{3+}$ | ferrihydrite | 0.44 | | -0.12 | 435 | 0.27 | 4.7 |
| Noaddah-2 | 19 | $Fe^{2+}$ | chlorite | 1.180 | 2.766 | | | 1.565 | 26.7 |
| | | $Fe^{3+}$ | chlorite | 0.504 | 0.806 | | | 0.727 | 30.7 |
| | | $Fe^{3+}$ | goethite | 0.51 | | -0.19 | 491 | 0.27 | 29.0 |
| | | $Fe^{3+}$ | ferrihydrite | 0.60 | | 0.05 | 435 | 0.27 | 13.6 |

[a] Highest probability value of the evaluated model-independent hyperfine-field distribution
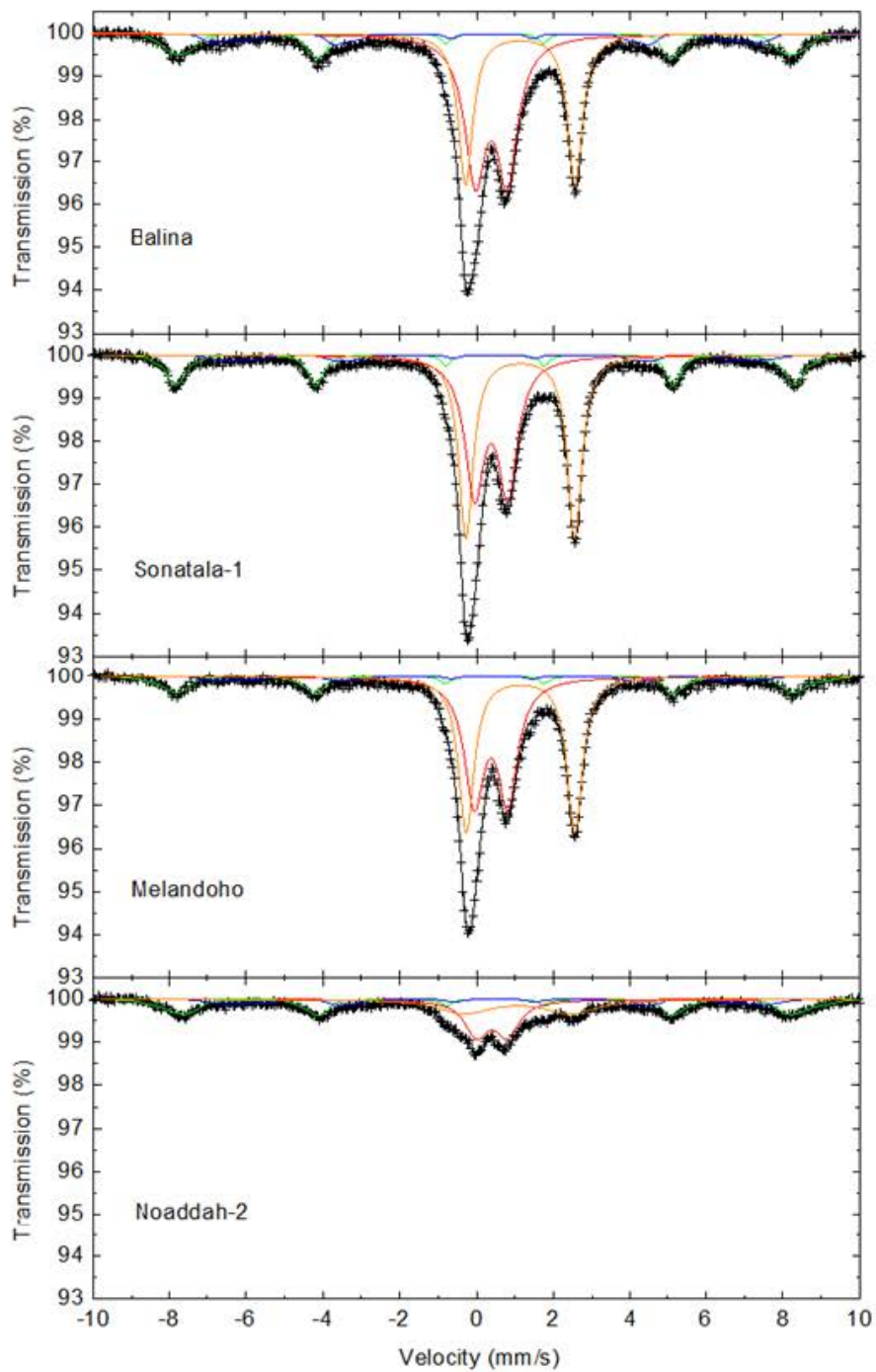
Fig. 4.10 Experimental (+) and calculated (black solid line) Mössbauer spectra for four Bangladeshi floodplain paddy soil samples. Green: goethite sub spectrum; blue: ferrihydrite sub spectrum; red: $Fe^{3+}$ doublet; orange: $Fe^{2+}$ doublet

## 4.4. Discussion

### 4.4.1. Soil redox reactions and microbial activity during continuous flooding

Eh (Fig. 4.3) (Munch et al., 1978) dropped quickly and steeply in all four studied young floodplain paddy soils. Soil temperatures were elevated, i.e. 27°C (Fig. 4.2), typical for field soils in late Boro and Aus seasons (Hossain et al., 2014), and resulting high soil microbial activity (Devevre and Horwath, 2000; Dommergues et al., 1978) likely caused this fast onset of soil reductive conditions. Indeed, the initial Eh drop and mean $CH_4$ emission rates during CF were greatest in the Sonatala-1 and then in the Balina soil with Eh < -150mV, followed by Melandoho and Noaddah-2 with less negative eventual Eh ranges (Fig. 4.3 and 4.8). Nevertheless, SOC content did not correlate to $CH_4$-emission rates nor to minimum Eh reached after several days of submergence. Also, cumulative total C-emissions during CF followed a different ordination than SOC level and the calculated maximal drop in Eh since onset of submergence (see Section 4.3.7). Hence, other factors than just SOC content must have co-determined gross microbial activity and digression of Eh.

Next to availability of a C substrate, course, rate and magnitude of Eh decrease are well known to also depend on nature and contents of oxidants ($NO_3^-$, $Mn^{4+}$, $Fe^{3+}$, $SO_4^{2-}$, $CO_2$) (Ponnamperuma, 1972; Narteh and Sahrawat, 1999; Sahrawat, 2005). Assuming that 1 meq of C mineralized corresponds to donation of 4 electrons, equivalent to oxidation of hexose carbohydrate units, electron ($e^-$) donation rate (in meq $e^-$ $kg^{-1}$ $day^{-1}$) during CF period was then greater in Balina (11-12) than in the Melandoho (8), Sonatala-1 (6) and Noaddah-2 (5) soils. This estimated $e^-$ donation (5-12 meq $e^-$ $kg^{-1}$ $day^{-1}$) during the first weeks (7-17 DAT) was derived from measured C effluxes (0.6-1.4 mg C $kg^{-1}$ $h^{-1}$). During this period the plant was at seedling stage with minor growth and net plant derived C-uptake was 0.08-0.12 mg C $kg^{-1}$ $h^{-1}$. Also the measurements of $CO_2$ were conducted during daytime in Perspex closed chamber. Hence, net plant C-fluxes sufficiently subordinate to C-emissions stemming from microbial activity and so net $CO_2$ build-up in the closed chambers is nearly representative to soil microbial activity. This as confirmed from incubations with bare soil (not presented here) which also revealed that soil C emissions strongly exceeded any plant-derived C-emission or net uptake. We then calculated the potential contribution of denitrification as counter-process to terminally accept these electrons, assuming all initially present $NO_3^-$ was completely reduced, requiring 5 meq $e^-$ per meq $NO_3^-$. If so, $NO_3^-$ reduction could have sustained but a less than 1% of anaerobic microbial activity. Sulphate reduction was not investigated, but initial soil $SO_4^{2-}$ contents and C mineralization rates correlated positively (p < 0.01) (Table 4.4). Assuming again complete reduction of all $SO_4^{2-}$ and acceptance of 8 meq $e^-$ per meq

$SO_4^{2-}$, again only about 4% (in Melandoho and Noaddah-2) and ~ 5-6 % (in Balina and Sonatala-1) of donated electrons could have maximally been consumed in sulphate reduction. The limited emission of $CH_4$ (1-2% of C emission) as well implicates that final reduction of $CO_2$ was also less relevant.

Iron reduction is usually the dominant processes in wetland paddy soils required to support anaerobic decomposition of SOM (Van Bodegom et al., 2003; Qu et al., 2004; Narteh and Sahrawat, 1997), so an improved relation between C emission and the proportionating of electron donators vs. acceptors matters would be logical. Indeed the least reductive conditions and lowest $CH_4$-emission rate were observed for the Noaddah-2 soil, with a SOC:$Fe_{ox}$ ratio of only 2.6. The lower minimal Eh at 4cm depth in Sonatala-1 compared to Balina could also be coupled with its higher SOC:$Fe_{ox}$ ratio (4.9 vs. 2.0) and SOC:$Mn_{ox}$ ratio (117 vs. 73). The ranking of cumulative C emission over 69 days (in mg C $kg^{-1}$) over the soils was also vice versa than the SOC:$Fe_{ox}$ ratio (Melandoho < Balina < Noaddah-2 < Sonatala-1) (Table 4.1 and Fig. 4.9). Notwithstanding, correlation of SOC:$Fe_{ox}$, and also SOC:$Mn_{ox}$, to the initial drop in Eh and C-emission during CF was weak, possibly because only a part of $NH_4$-oxalate Fe is readily utilizable by iron-reducers (Van Bodegom et al., 2003). Alternatively, the patterns of soil solution Fe and Mn were then considered to indirectly backtrack the contribution of reductive Fe and Mn dissolution among all $e^-$-accepting reactions.

The share of donated meq $e^-$ $kg^{-1}$ $day^{-1}$ then used for reductive dissolution of Fe and Mn, assuming that 1 meq of Fe (as amorphous $Fe(OH)_3$) and Mn (as $MnO_2$) corresponds to accept 1 and 2 meq $e^-$, respectively. In this estimation we neglect that part of dissolved $Fe^{2+}$ could have been re-oxidized in redox-couples with $SO_4^{2-}$ or precipitated as Fe-sulfides - carbonates or -phosphates (Zhang et al., 2012), or exchanged with $Ca^{2+}$ and $Mg^{2+}$. Thus the importance of reductive Fe and Mn dissolution as $e^-$-accepting processes might be underestimated. The overall contribution of reduction of $Fe^{3+}$, resulting in its dissolution (indicated as % of $e^-$ donated) was higher in the Melandoho soil (14-25%) than in the Noaddah-2 (5-17%), Balina (7%) and Sonatala-1 (2-4%) soils. Mn-reductive dissolution appeared a lesser relevant $e^-$ accepting process with a consumption of % of $e^-$ donated in the Noaddah-2 soil of only 3.2-6.7%, followed by the Balina (1.6-2.4%), Sonatala-1 (1.6-2.2%) and Melandoho (0.9-1.4%) soils. Clearly, between the four studied soils there were differences in the contribution of reductive Fe- and Mn-dissolution as redox-processes to maintain soil microbial activity. We then attempted to identify source Fe- and Mn-minerals firstly from the observed equilibria between soil solution and Fe and Mn(hydro-)oxides over a

range of pe+pH (Fig. 4.5). Visual inspection of the diagrams indicated most likely candidates to be amorphous $Fe_3O_4$ and $Fe(OH)_3$ for Sonatala-1 and Melandoho, $Fe(OH)_3$ for Noaddah-2, and diverse Fe minerals ($\gamma$-FeOOH, $\gamma$-$Fe_2O_3$ and amorphous $Fe_3O_4$) for Balina. In line, Ponnamperuma et al. (1967) suggested that the principal oxidant in flooded soils is $Fe(OH)_3$, because of its low crystallinity and related preferential reduction (Lindsay, 1979; Zhang et al., 2012). In addition Ponnamperuma et al. (1967) concluded a hydrated variant of $Fe_3O_4$ to be a common source of dissolved Fe too.

From the above it could be hypothesized that anaerobic microbial activity would be related to level of $Fe(OH)_3$. The quantitative Fe-distribution data obtained by Mössbauer spectroscopy (see Section 4.3.9), however, only identified goethite and ferrihydrite as prominent pedogenic forms of Fe. This consequently questions the validity of the empirically derived pe+pH/(log $Fe^{2+}$ + 2pH) diagrams, which may be skewed by re-precipitation of $Fe^{2+}$ and by dissolution of Fe from multiple source minerals. So instead, soil solution Fe would have mainly derived from low crystalline goethite and ferrihydrite in Balina, Sonatala-1 and Melandoho soils. Qu et al. (2004) found that ferrihydrite is preferentially used as electron acceptor in Italian paddy soils compared to goethite and hematite. In line, the highest and lowest recorded soil solution Fe levels were seen in the Balina and Sonatala-1 soils with the largest and lowest proportions of ferrihydrite-Fe (8.5% and 5.6% of Fe), respectively, in spite of a high proportion of goethite-Fe (15.6% of Fe) in the latter soil. But we cannot unequivocally confirm ferrihydrite-Fe as the primary source mineral of dissolved Fe. Likewise, specific minerals controlling Mn solubility could not be recognized in any of the studied soils. The pe and pH varied from +6 to -2 and 5.2 to 6.9, respectively, comparable to observations by Ponnamperuma et al. (1969), who found that the possible Mn systems are then $Mn_3O_4$-$Mn^{2+}$ and $Mn_3O_4$-$MnCO_3$. The $Mn_3O_4$-$Mn^{2+}$ equilibrium line's slope did match with the observed solution $Mn^{2+}$ activity and $Mn_3O_4$ thus tentatively remains the most likely source oxidant.

Most importantly, though, we infer from the above analysis that the majority of anaerobic microbial activity relies on reduction of still other soil oxidants than the ones discussed. A likely key alternative electron-accepting redox reaction may be reduction of $Fe^{3+}$ inside phyllosilicates, not accompanied by a substantial buildup of Fe in the soil solution. Bio-reduction of phyllosilicates was discovered 25 years ago (Pentráková et al., 2013) and since then often reconfirmed. Mössbauer spectroscopy identified silicate structural $Fe^{3+}$ to represent 31-44% of soil Fe, indeed a considerable pool of potentially reducible Fe but no relation existed between % of silicate $Fe^{3+}$ and soil C mineralization. Mössbauer spectra

from all four soils were characterized by large $Fe^{3+}$ and $Fe^{2+}$ doublets, characteristic of a chlorite or vermiculite. Brookshaw et al. (2016) recently demonstrated microbial reduction of chlorite. The co-occurrence of $Fe^{2+}$ and $Fe^{3+}$ would narrow the identification of chlorite present in these soils down to either chamosite, nimite or sudoite, but confirmation is complicated by the interstratification of chlorite and vermiculite in all four soils, as detected by X-ray diffraction (Kader et al., 2013).

*4.4.2. Soil mineral N (+ plant N) supply influenced by the reductive dissolution of Fe and Mn, and other relevant soil properties*

In all four soils, the soil exchangeable $NH_4^+$-N contents quickly rose, with the highest measured concentration in the Balina soil followed by Melandoho (Fig. 4.6), intermediate buildup in Noaddah-2 and lowest accumulation in Sonatala-1. Such fast increase of soil $NH_4^+$-N is likely the result of fast N mineralization and less immobilization in flooded soils (Ponnamperuma, 1972; Zhang and Scherer, 2000). The order of mineral N release rate (Fig. 4.7) did not correspond with that of SOC and total N content (see Section 4.3.6 and Table 4.1) in line with several previous studies (Zhu et al., 1984; Khaokaew et al., 2007; Kader et al., 2013). As an explanation, Cassman et al. (1996) and Adhikari et al. (1999) suggested that with increasing N content, paddy soils hold an increasing part of N, which is more resistant for anaerobic mineralization. Schmidt-Rohr et al. (2004) then confirmed that in continuously submerged paddy soils a large amount of amide N is bound to the aromatic rings of the lignin-rich SOM, possibly declining readily plant available N. In the present study, both rate of net soil N supply during CF and C mineralization rate correlated negatively with the $SOC:Fe_{ox}$ ratio (r = -0.71; p<0.01 and r = -0.70; p<0.01 respectively) (Table 4.4). A strong positive correlation also existed between the rate of soil solution Fe buildup and net anaerobic N mineralization (Table 4.4), with a remarkable synchrony of both in the first weeks of submergence (Fig. 4.4 and 4.6) and partly also later on. These results confirm the suggested contribution of Fe reduction to SOM decomposition and net N mineralization (Narteh and Sahrawat, 1999; Kögel-Knabner et al., 2010; Qu et al., 2004; Grybos et al., 2009; Pan et al., 2014; Akter et al., 2016).

The prompts the question just how Fe-reduction and microbial N mineralization relate. From our preliminary electron balance calculations (see Section 4.4.1), we infer that electron acceptance involved in reductive dissolution of Fe and Mn would not have dominantly controlled microbial activity in these soils. The temporal synchrony of buildup of soil solution Fe, Mn and soil exchangeable mineral N could instead be explained by release of mineral-bound OM from reduced pedogenic oxides, then made available for subsequent

mineralization (Grybos et al., 2009). Indeed, net N mineralization rates correlated positively with DOC release rates. Large release of DOC, as in the Balina and Melandoho soils, may have promoted net N mineralization, as observed from both soils. However, Hanke et al. (2013) concluded that shifts in pH and not in Eh or Fe-reduction dominantly drove DOC dynamics, but in their incubations lowest Eh reached was close to 0mV and highest solution Fe concentration only 5 mg $L^{-1}$, a factor 50 lower than levels reached here. So reductive Fe dissolution was a much more important process in the present pot experiment, while Hanke et al. (2013)'s soil slurry setup failed to establish reductive conditions typical for paddy fields.

One could alternatively hypothesize organic N release and later on mineralization to be caused by reduction of Fe in clay minerals, as silicate structural Fe-reduction might also be an important electron accepting process in the presently investigated soils. Sodano et al. (2016) found that electrostatic attraction of N-containing compounds by the negatively charged vermiculite surface is an important organic N binding mechanism. If so, reduction of silicate structural Fe would, however, have only resulted in a stronger clay surface negative charge and would not have caused specific N release. But care should be undertaken to extrapolate Sodano et al. (2016)'s findings, as the quality of applied DOM used could differ from the native DOM in the here studied soils. Lastly, of great importance is Brookshaw et al. (2016)'s recent observation that microbial reduction of the $Fe^{3+}$ in clay minerals causes a destabilization of the octahedral layer and release of K and Mg. All investigated soils were rich in vermiculite and interstratified vermiculite-chlorite and its reduction might then analogously result in fixed-$NH_4^+$ release. In addition, Scherer and Zhang (1999) suggested that reduction and dissolution of Fe-(hydr-)oxides coatings on clay surfaces at low Eh favors either release or fixation of $NH_4^+$, depending on $NH_4^+$ concentration in solution. Previous lab incubation experiments with two of the studied soils, however, did not confirm substantial release of fixed-$NH_4^+$ (Akter et al., 2016), but like in Hanke et al. (2013)'s study, solution Fe levels reached were much smaller than in the current pot experiment. So reductive conditions required to destabilize $Fe^{3+}$-clay or to dissolve covering pedogenic Fe-(hydr-)oxides may not have been reached in our previous study (Akter et al., 2016). It then remains plausible to hypothesize that reduction of vermiculite-$Fe^{3+}$ or Fe-(hydr-)oxides coatings on clay surfaces releases fixed $NH_4^+$. Only future experiments with a $^{15}N$-labelled fixed-$NH_4^+$ pool could help to test if and how soil reduction promotes its release and to what extent.

Finally, net N mineralization rate best correlated with total C emission rate ($CO_2$-C +$CH_4$-C) (r = 0.99 and p<0.01), demonstrating that regardless of the potential involvement of abiotic steps in organic N or fixed-$NH_4^+$ release, magnitude of microbial activity determines net N

113

mineralization. Yonebayashi and Hattori (1986a) as well found anaerobic N mineralization in waterlogged paddy soils to be greatly influenced by the presence and amount of easily degradable OM. Sahrawat (2004a) reported that soils having a high OC and reducible Fe were high in mineralizable N, whereas soils low in OC or reducible Fe had relatively lower contents of mineralizable N. The positive correlations between C and net N mineralization rates on the one hand, and on the other Fe-release rate and negatively with the $SOC:Fe_{ox}$ ratio do indicate a general connection between availability of Fe for reduction and microbial activity, but still this relation remains unresolved.

*4.4.3. Relation between soil solution chemistry, C-mineralization and net N-mineralization under alternating soil wetting and drying*

From 34 DAT onwards, in line with field practice, non-continuous flooding management was implemented with fast topsoil drying and lowered $\Theta_v$ (Fig. 4.2) at 4 cm depth and saturated conditions at 14 cm. These observations indicate that here the influence of soil drying on Eh did not reach until 14 cm depth, and was thus a relatively shallow process. Notwithstanding, Fe and Mn concentrations in all soils declined during AWD (Fig. 4.4) by re-oxidation and coupled to this, pH declined rapidly in Balina and Noaddah-2 soils, and slightly in Melandoho and Soantala-1 soils. These transitions to non-Fe or Mn reducing conditions or even to near-oxic conditions were expected to strongly affect C mineralization and N availability. During AWD (35 DAT onwards) C-emissions from the Balina and Noaddah-2 soils dropped by 78 and 31% compared to CF, respectively. Though aerobic C mineralization has been mostly assumed to exceed anoxic degradation, Hanke et al. (2013) demonstrated clearly that the paddy soil microbial community is well adapted to anoxic conditions, but less efficient in mineralizing OM during transient oxic periods. They measured much lower $CO_2$ emissions during oxic periods compared to non-paddy soils, and the drop in C-emissions from the Balina and Noaddah-2 soils may be explained likewise. In contrast, unaltered or minor changed C-emissions from the Sonatala-1 and Melandoho soils (Table 4.3 and Fig. 4.8d) designate that overall microbial activity remained at a par, most probably because in both soils AWD-induced topsoil drying was limited (Fig. 4.2) and Eh stayed negative for another month (Fig. 4.3). In all soils, methanogenesis did persist at a similar very low rate, likely then in the deeper still saturated soil (Fig. 4.2), though activity resulting in $CO_2$ production was the dominant $e^-$ donating process. The contrasting evolutions in $CO_2$-emissions and Eh after transition to AWD render the studied set of 4 paddy soils interesting model ecosystems for studying the still quite unknown effect of altering redox conditions on N turnover.

From the continued plateauing of plant N + soil exchangeable N after transition to AWD we infer that in the Balina soil little or no additional mineral N release occurred. The already substantial $NH_4^+$-N levels (90-100 mg N $kg^{-1}$) after just 15DAT under CF could have inhibited N mineralization and $NH_4^+$-diffusion from clay interlayer spaces. The plateauing could not be ascribed to plant N uptake, still minor around 21-28DAT. In the three other soils, switching to AWD instead reinitiated buildup of exchangeable mineral soil N and plant N (14 to 40 mg $kg^{-1}$), following a linear course (Fig. 4.7) with time ($R^2$= 0.70 to 0.99). Multiple explanatory mechanisms are explored for a recommencement of net mineral N supply after that CF-AWD transition:

1° Dissolved OM accumulated during CF, generally thought to stem from incomplete OM degradation and accumulation of water soluble intermediate metabolites (Sahrawat, 2004b), might have been mineralized and acted as N-source during subsequent less anoxic conditions during AWD. This seems improbable, however, because over the entire AWD period (33-50 DAT) DOC concentrations remained elevated, and also N release rates were not correlated with mean DOC levels between 31 to 58 DAT (Table 4.4). It should be noted though that DOC levels are furthermore the resultant of root-exudation and DOC removal by reabsorption. The latter process at least seems unlikely given the persistent low Eh during AWD.

2° A switch to AWD could not have caused sudden new desorption of OM and N because pH decreased during AWD and dissolved Fe and Mn re-oxidized. Apparently re-oxidation of Fe and Mn occurs very fast, perhaps by $O_2$ diffusion through rice roots (Li et al., 2008), which indeed started to vigorously grow simultaneously. In sum it cannot be excluded that DOC levels stayed high because evolving root exudation compensated DOC removal by mineralization. However, Said-Pullicino et al. (2016) found that over time the soil solution specific UV absorbance increases, indicating a larger degree of aromatics in DOM. This accumulation of more refractory C may explain why even after shifting to intermittent flooding, DOC was not readily bio-degraded, also in line with Hanke et al. (2013), who also found inert paddy soil DOC levels upon a shift from anoxic to oxic conditions.

3° Dying-off of anaerobic microbial biomass following transition to AWD could have instigated net mineral N release. Indeed, microbes in rice soils have been reported to be an important temporary sink for N (Said-Pullicino et al., 2014), especially with an external C-source applied. Unequivocal verification would require temporal follow-up of the soil microbial N pool, ideally with preceding microbial immobilization of $^{15}$N.

4° Plant growth promotes net buildup of inorganic N in submerged soils (Buresh et al., 2008), possibly in several concomitant ways. At 58DAT, all mineral N was mined from the upper soil increment and relocated to plant biomass. The resulting very low $NH_4^+$-N levels would favor diffusion from fixed-$NH_4^+$ pools and promote activity of co-enzymes involved in

ammonification, e.g. in terminal amino acid $NH_2$ hydrolysis. Mineral N depletion would furthermore have rendered microbial anabolism N-limited, forcing microorganisms to engage in mineralization of native SOM.

To summarize, there existed no link between DOC, Fe and Mn dynamics and net N mineralization during management with fluctuating water table. So in spite of still sustained low redox potential in three out of four soils, soil net mineral N release is not coupled anymore with Fe- and Mn reduction.


## 4.5. Conclusion

Net mineral N supply rate correlated with the rate of release of Fe in soil solution, DOC level and total C emission, but not with soil OC and total N, reconfirming previously reported weak relations between paddy soil microbial activity and SOM content. There appears to be a synchrony in timing and magnitude of reductive dissolution of Fe(hydro-)oxides and content of soil mineral N, suggesting a causal relation between both. However, strictly in their role as oxidants, pedogenic Fe and Mn oxides could not fully determine C and net N mineralization rates because electron uptake for Fe and Mn dissolution was less than 12% of all electrons donated. In an ancillary incubation experiment, reductive Fe and Mn dissolution was accompanied by a dissolution of an equal amount of $Mg^{2+}$ and $Ca^{2+}$ from the soil colloid surfaces. Assuming that this was caused by exchange with $Fe^{2+}$ and $Mn^{2+}$ the current approach may have underestimated pedogenic Fe-reduction by a factor 2. If so, then still other reductive processes, not quantified here, must have jointly supported anaerobic microbial activity.

The hypothesis that observed link between Fe and N cycles are due to co-release of bound organic N to Fe (hydr-)oxides via reductive dissolution and subsequent mineralization at present still seems a more plausible explanation, but this requires confirmation. Also, reductive dissolution of pedogenic Fe shielding clay interlayers and subsequent diffusion of fixed $NH_4^+$ could be a relevant mechanism. Unfortunately, it remains very difficult to unequivocally identify source minerals of dissolved Fe and Mn, but most likely candidates for young floodplain paddy soils in Northern Bangladesh appear ferrihydrite, poorly crystalline goethite and $Mn_3O_4$. From our tentative electron balance calculations and identification of substantial contents of $Fe^{3+}$ in phyllosilicates we postulate that reduction of octahedral $Fe^{3+}$ in chlorites, vermiculite and their interstratified forms would be a significant electron accepting process in Northern Bangladeshi paddy soils. Future experiments with $^{15}N$-labeling of the fixed $NH_4^+$-pool are required to test if such destabilization of the crystal structure furthermore releases $NH_4^+$ out of the clay minerals, in line with recent reports of release of other cations.

Lastly, temporal patterns in N supply from paddy soils can be very much soil dependent. In two soils we saw fast N release and then relocation of soil $NH_4^+$ to plant N. In the two other soils we saw a more gradual mineral N release, that slows after a few weeks but then is promoted again directly or indirectly by growing rice plant. But overall, it seems that initial differences that exist in N dynamics among soils fade in time and the rate of release of Fe and DOC may only have a large control on net N mineralization in the first two weeks after flooding. On the basis of this 2-month pot experiment, within season transition towards intermittent flooding at first sight appears to be a viable way to promote net soil N supply, pending confirmation in field experiments and further mechanistic elucidation.

# Chapter 5

# Abiotic drivers of paddy soil N supply and fertilizer efficiency in six farmers' fields during the Aman wet season

**Abstract**

In this Chapter a field study was completed with the aim to confirm hypothesized links between net N supply with releases of dissolved Fe, Mn and ON from a set of six Bangladeshi farmers' fields during the 2016 Transplant/T. Aman (wet) rice season. A second objective was to evaluate fertilizer N use efficiency and its ties to the array of investigated descriptors of soil reductive processes introduced in preceding chapters. Field experiments were laid out in six paddy fields in north-central Bangladesh with 80 or 60 kg N ha$^{-1}$ ($N_{80/60}$) or without ($N_0$) urea application. High soil temperature (29$^o$C), reduced conditions (Eh: 194 to -150 mV) and near neutral pH (6.4-7.2) till 70 or 84 days after transplantation (DAT) evoked reductive dissolution of Fe- and Mn- (hydr-)oxides and DON release. Despite variation between soils in these and in their exchangeable $NH_4^+$-N, all were only marginally affected by urea application. Net N supply (soil + plant N) throughout the Aman season on the contrary did vary between soils and with N treatments ($p<0.05$). Percent silt (r = 0.80 to 0.90) and sand (r = -0.86 to -0.90) ($p<0.05$) appeared to significantly determine soil N supply, and positive correlations also existed with $Fe_{ox}$, but not with solution Fe and Mn. DON further strongly correlated to soil $NH_4^+$-N (r = 0.88-0.92) and TN (r = 0.60-0.72), suggesting that level of DON, indicative of OM quality, may also control or at least be a predictor of soil N supply. Solution Fe's insignificant negative relations to N supply, DON and soil $NH_4^+$-N, contrary to previous chapters, perhaps due to the more openness of the N cycle in the field. N fertilizer recovery (28-56%), physiological (14-37 kg grain kg$^{-1}$ N uptake) and agronomic (4-14 kg grain kg$^{-1}$ N applied) efficiencies were in typical ranges for wetland rice. But, surprisingly, grain yield did not relate to N supply, neither in the $N_{80/60}$ nor in the $N_0$ plots. Also the N use efficiencies did not correlate to plant available nutrients, net N supply and with any other biochemical processes and soil properties including plant available P,K, Fe and Mn, except for positive ($p<0.05$) relation of $PE_N$ with %sand. It would thus appear that other constraints than N availability (variability in water, insect-pest and disease management) overridingly limit grain yield and N use efficiency.

## 5.1. Introduction

In Bangladesh rice is grown two to three seasons per year in an area of 11 million hectares (almost 80% of total agricultural land). Among the seasons monsoon-season (Aman: July-November, rain-fed with supplementary irrigation) rice contributes ~38% of the national rice production (Shelley et al., 2016). To keep pace with population growth, rice yields in both dry and wet season need to increase. One of the main constraints of rice cultivation in South

Asia including Bangladesh is low soil organic matter (SOM) content due to removal of crop residues, limited use of manures and enhanced SOM decomposition under hot and humid climatic condition with frequent tillage (Adhikari et al., 1999; Saha et al., 2007; Shelley et al., 2016). Among plant nutrients, N fertilizer use in Bangladesh has remarkably increased over the past 35 years, leading to nutrient imbalance in soil plant system. For instance, the average urea application rate in T. Aman season was 144 kg ha$^{-1}$ in 1999 and augmented to 168 kg ha$^{-1}$ in 2000 (Mustafi and Harun, 2002). Rice farmers have widely applied N fertilizer to maximize yield but often at lower or over rates depending on fertilizer price and availability, which either limits crop growth by N-deficiency or losses of N to adjacent water bodies and atmosphere and lowers farm profitability. Furthermore, half of the Bangladeshi government's fertilizer subsidies are dedicated to urea, and so efficient use of fertilizer-N is also crucial to save national investments (Miah et al., 2016).

Though total N (TN) was found to inconsistently relate to indigenous soil N supply (Cassman et al., 1996; Kader et al., 2013), N fertilizer recommendations in Bangladeshi paddy fields are typically made considering TN, crop N uptake and target yield goal, with in fact blanket N rate for most farmers' fields. Soil N supply between rice fields with similar soil types or in same field over time could vary (Cassman et al., 1996), however most past research has focused on the response of applied N rates to rice yield and mechanisms of loss instead of adjusting soil N supply based rates (Adhikari et al., 1999; Cassman et al., 1998; Saha et al., 2012; Zhao et al., 2010). The resulting imbalance contributes to low N-use efficiency and instigates negative N balance in both N fertilized and unfertilized paddy fields, including wet rice season in Bangladesh (Saha et al., 2007; Saha et al., 2012). Like other irrigated paddy fields (Adhikari et al., 1999; Cassman et al., 2002), N recovery efficiency (RE$_N$: 13-63%), physiological efficiency (PE$_N$: 34-52 kg grain kg$^{-1}$ N uptake) and agronomic efficiency (AE$_N$: 0.3-23.3 kg grain kg$^{-1}$ N applied) all were lower in wet (Transplant/T. Aman) rice season in Bangladesh (Saha et al., 2012). Soil N availability is a transient property and changes throughout season (Anh and Olk, 2002). Overall N-use efficiency would therefore be improved by balancing the amount and time of N fertilizer application based upon soil N supply and plant N status, but still lacking for most Bangladeshi paddy fields.

As described in preceding chapters: The inconsistent relations of mineralized N to soil properties along with variables involved in crop management like redox processes, length of inundation/fallow, crop rotation, residue management and temperature (Kader et al., 2013; Villaseñor et al., 2015; Watanabe et al., 1987), further challenge accurate prediction of paddy field *in-situ* soil N supply. Our previous rice growth pot experiment with four farmers' fields paddy soils disclosed strong positive correlations of mineral N build-up rate with rate of

solution Fe and DOC, rather than with TN and SOC, with pedogenic $Fe^{3+}$ not identified as leading $e^-$ acceptor (**Chapter 4**). Instead Fe reduction and DOC released (and as confirmed in **Chapter 3** pH rise and DON release) was hypothesized as intermediary step in N mineralization. Causality between Fe-reduction, change in pH and DOM release with soil N supply would need to be verified in real-field set ups for a rice growing season. Such systems are more complicated than pot and soil incubation setups used in previous chapters. Firstly, the temporal trends of paddy soil N supply is very much also influenced by the presence of growing rice plant and crop management like length of inundation or drying or fallow, crop rotation and temperature. Secondly, release rate of solution Fe and DOC only unraveled large controls on N mineralization during first 2-4 weeks of flooding which faded over time in **Chapters 4 and 3** (Akter et al., 2016; Inubushi, et al., 1985). In this initial phase of crop establishment, in fact crop N demand is still small (**Chapter 4**; Cassman et al., 1996), and the question then remains if any further control exists on gross soil N supply to rice and its growth. Thirdly, we hypothesize that with increasing indigenous soil N provision, fertilizer use efficiency would lower due to temporary occurrence of high mineral N levels, more prone be lost via various emission pathways. But this relation is not necessarily reversible: it is evident that a high fertilizer use efficiency is also attributable to absence of other constraints to rice growth in a particular paddy field, with no connection to indigenous soil N supply at all. Lastly, rice plant's N and soil mineral N status at different growth stages impact N supply from soil and fertilizer, hence improve N fertilizer use efficiency at real field-scale (Watanabe et al., 1987). A first objective was therefore to validate co-evolution of mineral N release with solution Fe and DON release attained by previous lab incubations and rice growth pot experiments at farmers' fields *in-situ*. A second objective was to explore predictor variables of total mineral N release from SOM and applied urea hydrolysis. A third objective was to evaluate N fertilizer use efficiency during T. Aman season. To address these objectives, we studied plant N-uptake, soil exchangeable N, and progressive dissolution of Fe and Mn throughout wet rice growing season in six farmers' paddy fields of Bangladesh with or without urea application. We also monitored pH, Eh and solution DON to attain detailed insight into evolution of soil reductive processes.

## 5.2. Materials and Methods

### 5.2.1. Experimental sites, soil properties and materials

Six individual field experiments were conducted in three districts (Mymensingh, Tangail and Gazipur) of north-central Bangladesh (23°59′ N to 24°49′ N, 90°02′ to 90°25′ E, average altitude of 19 to 30 m) during wet (Transplant Aman) rice growing season (Aug-Dec) in 2016.

The selected sites were: a long-term (from 1978 till now) experimental field at Bangladesh Agricultural University (BAU), Melandoho, Noaddah-2, Chhiata (at the Bangladesh Rice Research Institute, BRRI), and two from Sonatala-1 series here defined as Sonatala-1a and Sonatala-1b. The average (1979-2006) air temperature and rainfall during most period of wet rice growing season (Jun-Sep) were 28.5ºC and 1771 mm, respectively (Rahman et al., 2012). In spite of occurrence of 80-85% annual rainfall during T. Aman (Jun-Sep) season, sometimes one or more supplementary irrigations are obliged, depending on spread in rainfall episodes. Air temperature and rainfall data were obtained from the weather station 2 km away from the fields at BAU campus, and from Plant Physiology Division, at BRRI campus. The mean daily air temperature and rainfall during the experimental period (22 Aug-9 Dec) in 2016 are depicted in Fig. 5.1.

The main physical and chemical properties of the soils in puddle layer (0-15 cm) are given in Table 5.1. Plant-available macro (Ca, K, Mg and P) and micro (Cu, Fe, Mn, Zn and Mo) nutrients in air dried soils were determined by $NH_4$-lactate and DTPA (Diethylene triamine pentaacetic acid) extraction, respectively (Lindsay and Norvell, 1969) (Table 5.1). The pH-KCl was measured by glass electrode in 1:2.5 soil:KCl suspensions. The soils were explicitly selected out of a set of 25 farmers' paddy fields, used by Kader et al. (2013) based on their variation in SOC to pedogenic Fe ($Fe_{ox}$) ratio (Table 5.1). The motivation was that the extent of decline in redox potential, OM degradation and $NH_4^+$ production after flooding mostly depend on the kind and amount of easily decomposable OM and alternative $e^-$ acceptors, particularly reducible $Fe^{3+}$ and $Mn^{4+}$. Hence, mineral N release and reductive dissolution of Fe or Mn could link with the SOC to $Fe_{ox}$ or $Mn_{ox}$ ratio in flooded paddy fields. The selected soils and management are typical for the north-central part of Bangladesh and the study area is dominated by an annual Rice-Fallow-Rice cropping system. The soils at four sites (Sontatala-1a, Sonatala-1b, Melandoho, BAU long-term experimental site) belonged to the non-calcareous dark grey floodplain general soil type, while Noaddah-2 and Chhiata soils were in the red-brown and grey terrace soils in Madhupur Tract, respectively (Bangladeshi Soil Classification). The soil texture was silt loam for all sites except silty clay loam in case of Chhiata. The whole of all six soils exhibited wide ranges in SOC (0.6-2.5%) and TN (0.08-0.22%), but relatively narrow ranges in pH-KCl (4.2-5.7), ammonium oxalate extractable Fe ($Fe_{ox}$: 3.9-5.1 g $kg^{-1}$) and Mn ($Mn_{ox}$: 0.08-0.24 g $kg^{-1}$) (Table 5.1). Except for Mg and Ca in Noaddah-2, and K and Zn in all soils other than Chhiata, levels of puddle layer essential plant available nutrients remained above critical limits (BARC, 2012). The rice cultivar was BRRI dhan46 for all fields, except for BRRI dhan49 at the BAU long-term experimental site. Both cultivars were developed for the wet rice growing season by the Bangladesh Rice Research Institute. However, BRRI dhan46 is a photo-sensitive and late Aman (Aug-Dec)

season variety, developed especially for cultivation after recession of flood water or after harvest of Aus rice/Jute (could be transplanted till 15 September). BRRI dhan49 is photo-insensitive and an early T. Aman season (Jul-Oct) variety, but its adoption is increasing preferentially throughout the country for higher yield and grain quality (medium slender). The average yield, height and growth duration of BRRI dhan46 are 4.7 t ha$^{-1}$, 105 cm and 150 days, respectively, of which the vegetative stage is almost 85 days, reproductive stage 35 days and ripening stage 30 days. In case of BRRI dhan49, the height (100 cm) and growth duration (135 days) are shorter but the average yield is higher (5.5 t ha$^{-1}$), and vegetative stage is almost 70 days, reproductive stage 35 days and ripening stage 30 days.

Table 5.1 Physicochemical soil (0-15cm) properties of the six selected farmers' paddy fields in Bangladesh

| Soil series name | Sonatala-1a | Sonatala-1b | Melandoho | Noaddah-2 | BAU Long-term expt. | | Chhiata |
| | | | | | Control | NPKSZn | |
| | (-N/+N)PKSZn | | | | | | (-N/+N)PKSZn |
| %Sand[*] | 4 | 20 | 21 | 24 | 19 | 19 | 20 |
| %Silt[*] | 76 | 68 | 63 | 50 | 63 | 63 | 45 |
| %Clay[*] | 20 | 12 | 16 | 26 | 18 | 18 | 35 |
| Texture[*] | Silt Loam | Silt Loam | Silt Loam | Silt Loam | Silt Loam | Silt Loam | Silty Clay Loam |
| pH-KCl | 5.5 | 5.7 | 4.2 | 4.2 | 5.4 | 5.6 | 5.6 |
| $NH_4$-lactate extractable plant nutrients (mg kg$^{-1}$) | | | | | | | |
| Ca | 1825 | 1807 | 460 | 365 | 1818 | 2144 | 2739 |
| K | 37 | 26 | 32 | 25 | 29 | 29 | 66 |
| Mg | 543 | 574 | 95 | 49 | 489 | 468 | 489 |
| Na | 125 | 111 | 26 | 14 | 101 | 113 | 120 |
| P | 20 | 18 | 56 | 135 | 18 | 23 | 42 |
| DTPA-extractable plant micronutrients (mg kg$^{-1}$) | | | | | | | |
| Cu | 1.8 | 1.6 | 1 | 0.3 | 1.3 | 1.3 | 1 |
| Fe | 141 | 161 | 174 | 261 | 85 | 92 | 71 |
| Mn | 46 | 60 | 21 | 41 | 23 | 24 | 18 |
| Zn | 0.1 | 0.5 | 0.1 | 0.6 | 0.1 | 0.1 | 4 |
| Si | 54 | 51 | 21 | 42 | 63 | 63 | 131 |
| Mo | 0.1 | 0.1 | 0.1 | 0.1 | 0.1 | 0.1 | 0.1 |
| $Fe_{ox}$ (g kg$^{-1}$)[a] | 5.1 | 4.8 | 4.2 | 4.4 | 4.8 | 4.1 | 3.9 |
| $Mn_{ox}$ (g kg$^{-1}$)[a] | 0.2 | 0.2 | 0.1 | 0.2 | 0.1 | 0.1 | 0.2 |
| SOC (%) | 2.5 | 1.4 | 0.6 | 0.5 | 1.7 | 1.8 | 1.6 |
| Total N (%) | 0.2 | 0.2 | 0.1 | 0.1 | 0.2 | 0.2 | 0.1 |
| C:N (-) | 11.4 | 8.8 | 6.5 | 6.4 | 10.7 | 9.5 | 10.9 |
| SOC:$Fe_{ox}$ | 5 | 3 | 1 | 1 | 3 | 4 | 4 |
| SOC:$Mn_{ox}$ | 121 | 90 | 70 | 23 | 122 | 160 | 90 |

[*]Data taken from Kader et al. (2013) and Saha et al. (2007); [a]$NH_4$-oxalate extractable Fe and Mn

## 5.2.2. Experimental design and management practices

In all six sites, the experiment was laid out in a completely randomized block design with ($N_{80}$ or $N_{60}$: 80 or 60 kg urea N ha$^{-1}$) or without ($N_0$) N fertilizer application in three field replicates per N treatment. In all plots, except at BAU, P-K-S was applied at a rate of 20-50-10 kg ha$^{-1}$, respectively. At BAU only 60 kg urea N ha$^{-1}$ ($N_{60}$) was added plus P-K-S at the rate of 4-28-6 kg ha$^{-1}$, while the $N_0$ object had received no fertilizer at all for 38 years. In total thirty 20 m$^2$ plots (2 N treatments × 3 replicates × 5 sites) and six 74.75 m$^2$ plots at the BAU long-term experiment were established. Every plot was separated from each other by 50 cm-wide earthen bunds to prevent lateral exchange of water and nutrients across plots. The soils were plowed to a depth of 15 cm by means of a power tiller, puddled and leveled before transplanting. Except urea all other mineral fertilizers such as triple super phosphate (as P source), muriate of potash (as K source) and gypsum (as S source) were applied once as basal dose and incorporated on the day of transplanting. In N-treated plots, urea was applied into three equal splits in all sites (except Melandoho) with first top-dressing after 7-16 DAT, another one after 31-35 DAT (at tillering) and the remainder after 52-54 DAT, approximately before panicle initiation. The Melandoho site was overflowed between 28 and 52 DAT due to heavy rainfall caused water stagnation, and therefore a first third of the N was applied on 7 DAT and the rest only on 54 DAT. Once the fields were prepared, four to five 32-36 days old seedlings of BRRI dhan46 were transplanted per hill$^{-1}$ with spacing of 25 cm × 15 cm (26.66 hills m$^{-2}$) on 23 to 27 August, 2016 in all five sites, except at the BAU long-term experimental plots where 4-5 seedlings of BRRI dhan49 was transplanted at a spacing of 20 cm × 20 cm (25 hills m$^{-2}$) on 22 August, 2016. Mostly the plots were continuously flooded to a floodwater depth of 2-8 cm, either by supplementary irrigations or rain events until 84 DAT at four sites, and until 70 DAT at the Sonatala-1b and Chhiata sites. No irrigation water had to be applied from rice plant physiological maturity (from 84 DAT) until harvest. Control measures were taken when needed to avoid yield loss by disease, weeds and insect pests. All plots were manually weeded two times and insecticides (Malathion 57EC at the rate of 1L ha$^{-1}$ or Virtako 40WG at the rate of 1.7 g 10L$^{-1}$ water 120 m$^{-2}$) were applied once or twice at tillering and panicle initiation stages depending on the severity of insect infestation. Besides a fungicide (Nativo 75WG at the rate of 6g 10L$^{-1}$ water 120 m$^{-2}$) was applied twice from 44-48 DAT and 59-60 DAT at Chhiata, Sonatala-1a and Sonatala-1b sites to control rice blast disease. At maturity, the rice crop in $N_0$ and $N_{80}$ or $N_{60}$ plots of all sites were harvested on 100 to 107 DAT (from 3 to 7 December, 2016). To record grain and straw yields 125 or 134 hills (~ 5 m$^2$) and 16 hills (~ 0.6 m$^2$) were harvested per plot.

*5.2.3. Monitoring of soil redox potential (Eh) and solution pH*

Soil Eh was measured *in-situ* usually once per week by permanent installation of an in-house fabricated platinum (Pt) electrode per plot (a Pt wire joined at the tip of an insulated Cu wire with steel epoxy resin (Devcon Co., Netherlands) to a depth of 7-8 cm below the soil surface. In each field a reference electrode (3M KCl saturated with AgCl) was installed at 4-5 cm depth at least 2h before measuring the redox potential (mV) and Eh was recorded by connecting both redox and reference electrodes with multi-meter by cables. The redox potential (Eh) was then recalculated by adding measured potential ($E_m$) with Ag/AgCl reference electrode's potential ($E_{ref}$) ($E_h = E_m + E_{ref}$). Alongside, pH (see Section 5.2.4.) was measured by direct insertion of glass electrode into soil solution collected from all plots at 0-9 cm depth.

*5.2.4. Collection and analysis of soil solution to monitor dissolved organic N, Fe and Mn*

Soil solution from each plot was regularly sampled with Macro Rhizon soil moisture samplers (RSMS) (Rhizosphere Research Products, The Netherlands) to monitor dissolved organic N (DON) and Fe and Mn. Each macro RSMS was outfitted with a 9 cm long and 4.5 mm outer diameter porous part (pore size: 0.15 µm). A total of 36 macro RSMSs (2 N levels × 3 replicates × 6 experimental sites) were installed permanently vertically at 0-9 cm depth. Generally, soil solution was collected 8 times: approximately on 0-3, 7, 14, 28, 42, 58, 70 and 84-87 DAT by connecting a vacuumed isoprene latex 30 or 60 ml syringe with luer-lock fitted PVC/PE extension tubing connected to the RSMS. Luer locks were closed again immediately after sampling to avoid air entering the RSMS. A portion of the soil solution was transferred into 16.2 mg $K_3EDTA$-coated 9 ml plastic vacuum vials (Vacutest Kimasrl : Arzergrande (PD), Italy) by piercing the vial's septum with a needle connected to the syringe. The EDTA coating prevented re-precipitation of Fe and Mn in the sampled solutions. Simultaneously, the remaining soil solution was transferred into 9 ml glass vacuum vials and frozen for later on analysis of their dissolved organic N (DON) content. Soil pore solutions were analyzed for their Fe and Mn contents by ICP-OES on a radial plasma iCAP6300 spectrometer (Thermo Scientific, US). At near neutral pH practically any dissolved Fe and Mn exists as $Fe^{2+}$ and $Mn^{2+}$ and could be considered to equal total measured Fe and Mn in the soil solution. To determine DON concentration, soil solution was oxidized by the alkaline per sulfate digestion method (Koroleff, 1983). Briefly, 2 ml solution was taken into 12 ml disposable culture tube of 10 cm height × 1.6 cm diameter with 1 mm wall thickness and GL18 neck (Duran Group, Germany). Then 3 ml oxidizing reagent (mixture of purified $K_2S_2O_8$, $H_3BO_3$ and 3.75M NaOH) was added, and tubes were immediately closed with caps

126

(GL18, screw caps (PP) with rubber seal, Duran Group, Germany) to avoid $NH_3$ loss. Afterwards the samples were autoclaved for 30 minutes at 121°C and DON concentration (in mg $L^{-1}$) was measured as any produced $NO_3$ by means of a continuous-flow auto-analyzer (Skalar, The Nederlands).

### 5.2.5. Soil and plant sampling for mineral N analysis

To follow-up evolution of soil mineral N ($NH_4^+$-N and $NO_3^-$-N), soil from all 36 plots was sampled 2-3 cm close to rice hills in the puddle layer (0-15 cm) at regular intervals (around 0, 7, 14, 28, 42, 58, 70, 85 and 105 DAT) until harvest. After collection, samples were cooled and immediately transported to the laboratory and stored in the freezer at -20°C for later extraction. Fifteen g homogenized moist soil slurry (equivalent to ~10g dry soil) was extracted for 1h in Erlenmeyers on a shaker with 0.01M $CaCl_2$ at a 1:10 soil:extractant ratio. Filtered (Whatman no. 42) extracts were frozen (-20°C) until later analysis of their $NH_4^+$-N level by the indophenol blue method at 636 nm (Kempers, 1974) and for their $NO_3^-$-N content directly into the extracts at 210 and 275 nm wavelengths (Goldman & Jacobs, 1961) by spectrophotometer (GENESYS 5 UV-Vis Spectrophotometer, Thermo Spectronic, Waltham, MA, USA). For each sample, gravimetric moisture content was determined by oven drying a share of moist soil at 105°C for 24h to calculate mineral N concentrations on soil dry weight basis. Parallel to soil sampling, rice plants of 2 to 6 hills $plot^{-1}$ (depending on growth) were dug out around 7, 14, 28, 42, 58, 70, 85 and 105 DAT. The soil slurry adjacent to roots was gently removed by washing with tap water and then rinsing with distilled water. Plants were then oven-dried at 70°C for 72 hours, and the mass of shoots and roots were recorded separately. The dried plant materials were ground and analyzed for their total C and N contents by means of a TruMac CNS analyzer (LECO). Plant N uptake was recalculated into mg N $kg^{-1}$ soil and mineral N in soil (mg $kg^{-1}$) per sampling point both were then summed to attain net mineral N released. A first-order kinetic model was fitted ($R^2$ = 0.64 to 0.99) to the evolution of N buildup in soil exchangeable N and plant N ($N_t$) with time:

$N_t = N_0 + N_a(1 - e^{-k_f t})$ where $t$ is the time (in days), $N_0$ is the initial amount of mineral N, $N_a$ the potentially mineralizable N (mg $kg^{-1}$) and $k_f$ is the first-order mineralization rate constant.

### 5.2.6. Statistical analysis

Statistical tests were performed with IBM SPSS statistics 24.0 (SPSS Inc., USA). One-way ANOVA was carried out to detect differences between farmers' fields in grain yield and

mineral N build-up ($N_t$) jointly in soil and plant during all sampling points throughout the growing season. Non-linear regression was used to model net mineral N evolution in soil and plant over time. Correlation (Pearson correlation coefficient) and stepwise linear regression analyses were performed individually for $N_0$ and $N_{80/60}$ to investigate links of modeled amount of mineralized N ($N_t$) 84 days$^{-1}$ with soil properties, soil Eh, soil solution pH, Fe, Mn and DON levels, as well as to identify predictor variables of $N_t$.

## 5.3. Results

### 5.3.1. Seasonal variations in air temperature, rainfall, soil redox potential and solution pH

The daily average air temperature in the studied north-central parts of Bangladesh during earlier crop growing season (0-74 DAT) was around 29°C and thereafter gradually declined by 6°C reaching to ~23°C (75 to 107 DAT) (Fig. 5.1), i.e. typical Aman season temperature trend. Most of the rainfall events took place during the earlier rice growing season (0-70 DAT: 22Aug-31Oct) with total amounts of 454 mm and 492 mm at the Mymensingh and Gazipur districts, respectively (Fig. 5.1). Rainfall events were not uniformly distributed during earlier rice growing and almost absent in the later growing season (71 DAT till harvest), which obliged supplementary irrigation to avoid crop failure or yield loss.
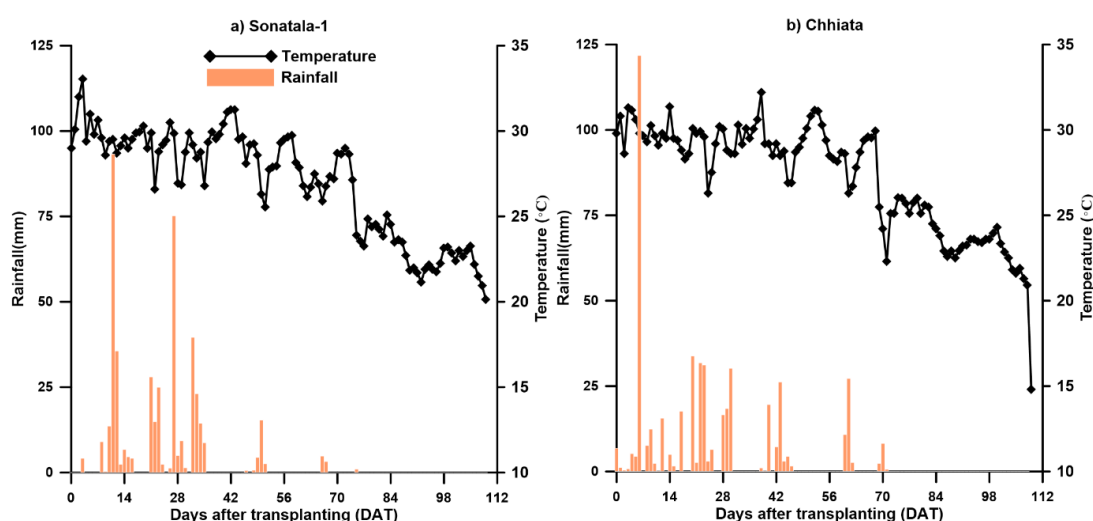


Fig. 5.1 Distribution of rainfall and trends in air temperature in the north-central part of Bangladesh during the 2016 wet rice (T. Aman) season (Aug-Dec)

Trends in soil redox potential (Eh) did not differ between N treatments, but they differed greatly between the soils (Fig. 5.2). Since fields were flooded or saturated before

transplanting by rain Eh range indicative of reductive conditions ranging from +160 mV (Melandoho) to -150 mV (BAU experimental plots) was already attained in the first week of transplanting (Fig. 5.2). The low Eh values at or below 0 mV sustained during most of the cropping season (0 to 70 or 84 DAT) for all soils. Exceptions were higher Eh values between 28 to 54 DAT in Melandoho (Fig. 5.2d) corresponding with an overflow of rain water (30-40 cm water level), and at several time points in Sonatala-1a (Fig. 5.2a) and Chhiata (Fig. 5.2f), due to shortage of rain events and irrigation water supply. The extent of Eh during 0 to 70 or 84 DAT varied in Sonatala-1a from +194 to -93 mV, in Sonatala-1b from +15 to -150 mV, at the BAU experimental site from +80 to -150 mV, in Noaddah-2 from +147 to -133 mV, in Melandoho from +160 to -73 mV and in Chhiata from 145 to -70 mV. From 75 to 87 DAT the Eh values increased to maxima of +208 to +433 mV in correspondence with field drying for harvest.



Fig. 5.2 Temporal evolutions of soil Eh in the puddle layer (8 cm depth) of studied paddy fields in Bangladesh during wet rice (T. Aman) season, 2016 with ($N_{60/80}$) or without ($N_0$) N fertilizer application (vertical bars indicate the standard errors of the means, n=3)

Similar to soil Eh, the soil solution pH did not differ greatly between N treatments within a soil, but some dissimilarity existed between the soils (Fig. 5.3). Generally the average soil solution pH stayed near neutrality (6.4-7.2) between 28 and 84 DAT in all five soils, except in

the Chhiata soil. The soil solution pH in Chhiata soil tended to sharply increase from neutral values on 28 DAT towards 7.8-8.2 on 58 DAT in $N_0$ and 73 DAT in $N_{80}$, with a subsequent decline (Fig. 5.3c).
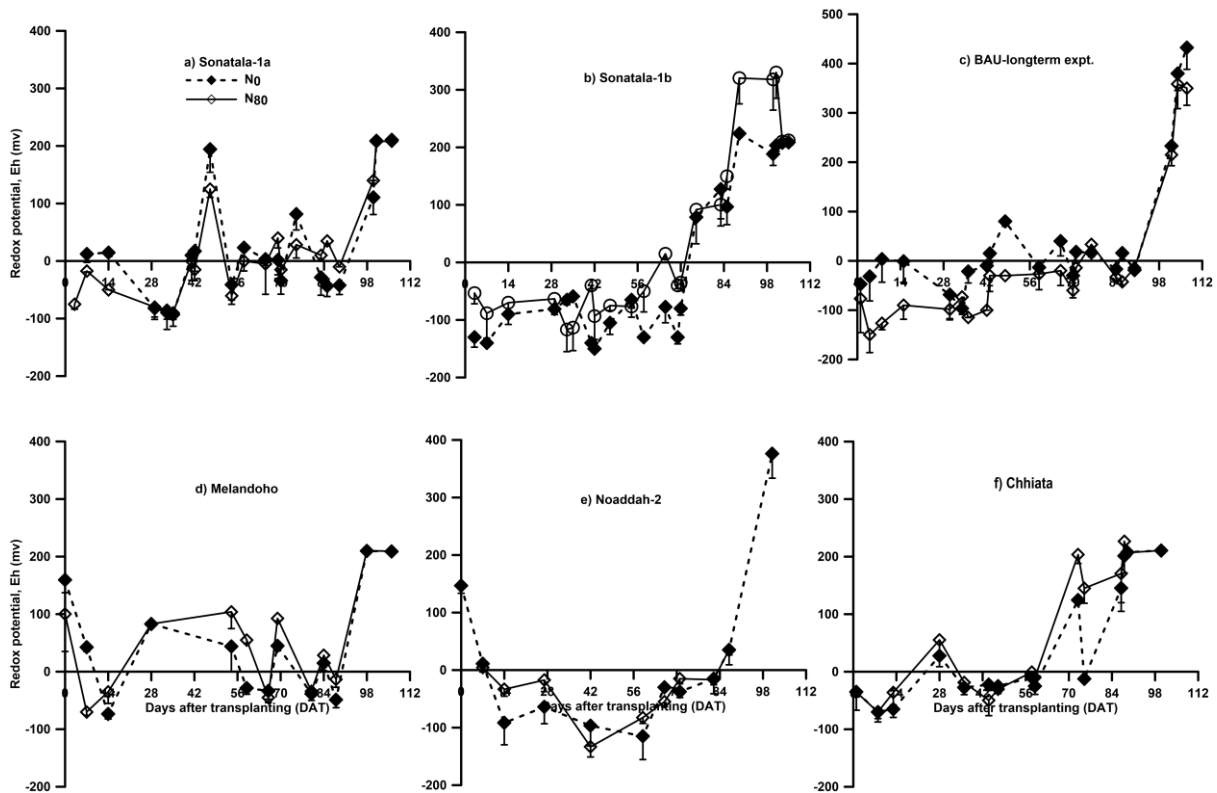


Fig. 5.3 Temporal evolutions of soil solution pH in the puddle layer (0-9 cm) of studied paddy fields in Bangladesh during wet rice (T. Aman) season, 2016 with ($N_{60/80}$) or without ($N_0$) N fertilizer application (vertical bars indicate the standard errors of the means, n=3)

### 5.3.2. Seasonal changes in soil solution Fe, Mn and dissolved organic N

In general the dissolved Fe and Mn concentrations over time varied remarkably between the soils, but the differences between $N_0$ and $N_{80}$ or $N_{60}$ treatments per soil were again minor (Fig. 5.4 and 5.5). Besides, temporal trends of solution Fe and Mn per soil resembled, except for Melandoho with dissimilar Fe and Mn patterns (Fig. 5.4 and 5.5). The higher solution Fe (20-30) and Mn (4-9) levels (in mg $l^{-1}$) in Sonatala-1a, Sonatala-1b and BAU experimental site were already reached in the first week since transplanting, and then solution Fe and Mn slowly declined to 12-16 mg Fe $l^{-1}$ and 2-5 mg Mn $l^{-1}$ on 30 DAT (Fig. 5.4a, 5.4b, 5.5a and 5.5b). Almost the same levels of dissolved Fe and Mn lasted in the former two sites, while in Sonatala-1a very low levels (in mg $l^{-1}$) of Fe (0.4-7.3) and Mn (1-3) were reached (42-85 DAT). In Melandoho soil dissolved Fe progressively increased from its initial low level (~ 10 mg $l^{-1}$) to 49 mg $l^{-1}$ in $N_{80}$ on 42 DAT and 51 mg $l^{-1}$ in $N_0$ on 69 DAT, and declined gradually thereafter (Fig. 5.4b). Unlike dissolved Fe, the solution Mn stayed around low range of 2-5 mg $l^{-1}$ in the Melandoho soil (Fig. 5.5b). In case of Noaddah-2 soil both dissolved Fe and Mn steeply increased, peaked already at 7 DAT (97-104 mg Fe $l^{-1}$ and 19-21 mg Mn $l^{-1}$), and then declined to low Fe (~ 30 mg $l^{-1}$) and Mn (3-5 mg $l^{-1}$) levels on 87 DAT (Fig. 5.4c and 5.5c). Both dissolved Fe and Mn in Chhiata soil sustained around same levels

of 9-13 mg Fe $l^{-1}$ and 2-3 mg Mn $l^{-1}$ until 44 DAT, and then declined to ≤ 1 mg $l^{-1}$ from 58 to 87 DAT, except for a small Fe peak on 73 DAT (Fig. 5.4c and 5.5c).
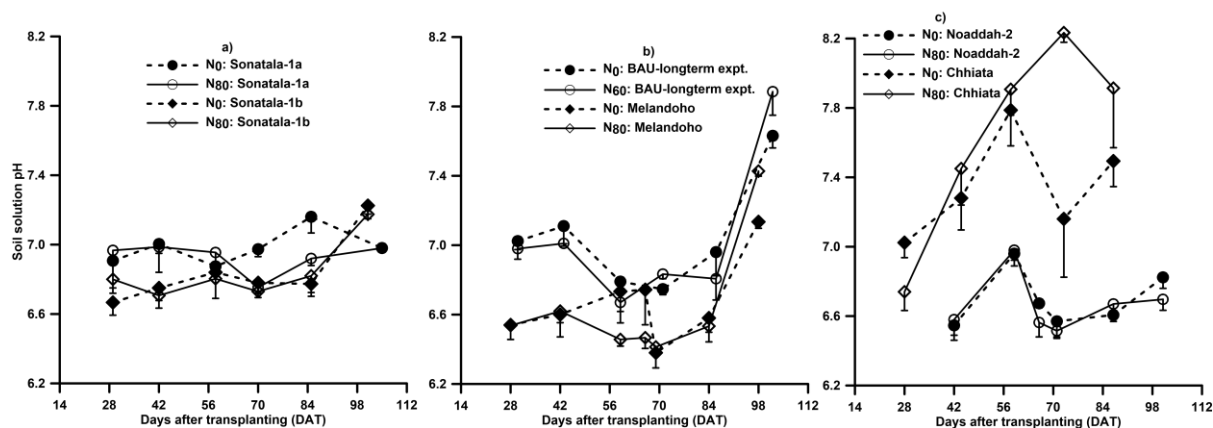


Fig. 5.4 Temporal evolutions of soil solution Fe in the puddle layer (0-9 cm) of studied paddy fields in Bangladesh during wet rice (T. Aman) season, 2016 with ($N_{60/80}$) or without ($N_0$) N fertilizer application (vertical bars indicate the standard errors of the means, n=3)

Regardless of N treatments, dissolved Fe and Mn did not correlate to $Fe_{ox}$ and $Mn_{ox}$ (data not shown). Instead, mean Fe correlated well to initial soil pH-KCl, SOC to $Fe_{ox}$ and $Mn_{ox}$ ratios (r = -0.81 to -0.91; p<0.05), and available phosphorus (P) (r = 0.92 to 0.97; p<0.05) (data not shown). Mean Mn- related only to $NH_4$-lactate extractable Fe and P (r = 0.82 to 0.90; p<0.05).
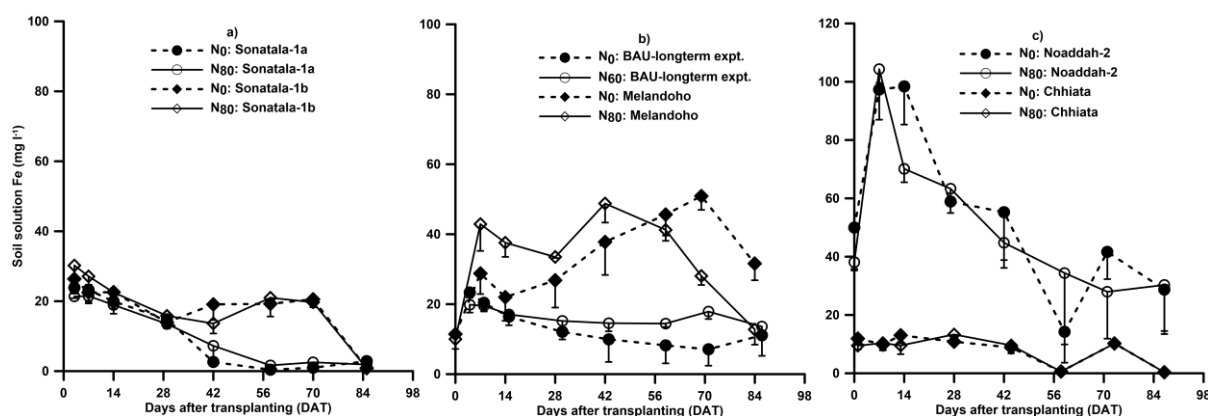


Fig. 5.5 Temporal evolutions of soil solution Mn in the puddle layer (0-9 cm) of studied paddy fields in Bangladesh during wet rice (T. Aman) season, 2016 with ($N_{60/80}$) or without ($N_0$) N fertilizer application (vertical bars indicate the standard errors of the means, n=3)

Overall, the temporal trends in dissolved organic N (DON) differed noticeably among the soils, but variations between $N_0$ and $N_{80}$ or $N_{60}$ treatments per soil were again incidental (Fig. 5.6). Generally, the DON concentrations (in mg $l^{-1}$) were higher (13-38 ~5-22 mg N $kg^{-1}$) during flooded (approximately till 70 or 84 DAT) than drained (with 7-13 around 100 DAT) period. The high DON levels (in mg $l^{-1}$) in Sonatala-1b (16-27) and Melandoho (15-23) soils continued from 28 to 70 DAT, and then lowered gradually (Fig. 5.6a and b). In the BAU long-term experiment (27-38) and Noaddah-2 (16-20) soils elevated DON levels lasted until 86 DAT, and only then declined (Fig. 5.6b and c). Despite slight lowering tendency from 28 till 58 DAT, the DON concentration in Chhiata soil fluctuated around same level of 13-26 mg N $l^{-1}$ during entire monitoring period (Fig. 5.6c). In case of Sonatala-1a, the DON level gradually declined from 28 DAT till 58 DAT, then increased linearly and sustained until harvest by unintended field flooding with drained out water from neighboring field for crop harvesting and seed-bed preparation (Fig. 5.6a). It is clearly seen that the DON levels in BAU experimental soil was greater than any other studied soils. The order of mean DON level during 28 to 70 or 84 DAT was BAU long-term experimental site > Sonatala-1a = Sonatala-1b > Melandoho = Chhiata = Noaddah-2. To summarize DON lowered in about 4 out of the six studied soils during the Aman season, but not always in a monotonous trend.



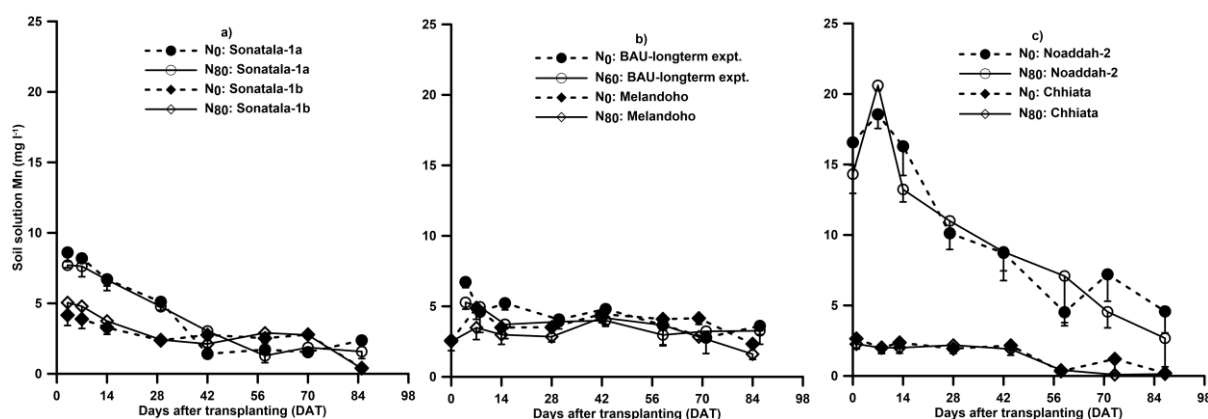Fig. 5.6 Temporal evolutions of solution DON in the puddle layer (0-9 cm) of studied paddy fields in Bangladesh during wet rice (T. Aman) season, 2016 with ($N_{60/80}$) or without ($N_0$) N fertilizer application (vertical bars indicate the standard errors of the means, n=3)

*5.3.3. Seasonal dynamics of soil mineral N, and net mineral N supply (N in soil plus plant)*

The initial soil exchangeable $NH_4^+$-N content ranged from 15 to 38 mg $kg^{-1}$, with no $NO_3^-$-N detected initially, nor throughout the season in any of the soils. Surprisingly variations between $N_0$ and $N_{80}$ or $N_{60}$ treatments per soil were in fact inconspicuous, except for greater

NH$_4^+$-N in the Sonatala-1a and Chhiata N$_{80}$ plots on 42 DAT and 13 DAT, respectively (Fig. 5.7). In case of BAU experimental site and Noaddah-2 soils a rise in NH$_4^+$-N contents were seen at 7 DAT, and then declined on 14 DAT to low levels lasting until harvest in Noaddah-2 and 59 DAT in BAU experimental soil (Fig. 5.7b and c). At BAU a further steep drop occurred from 70DAT on. In Sonatala-1b and Melandoho a fast initial decline (Fig. 5.7a and b) were followed by a stabilization of exchangeable NH$_4^+$-N till harvest except for small rise in Sonatala-1b on 42 DAT. Overall soil exchangeable NH$_4^+$-N contents remained high until 58 DAT in the Sonatala-1a and until 44 DAT in Chhiata soil (Fig. 5.7a and c), and declined later on and the low levels continued till harvest. The overall ranking of mean soil exchangeable NH$_4^+$-N during 0 to 84 DAT was BAU long-term experimental site > Sonatala-1a > Melandoho > Sonatala-1b > Chhiata > Noaddah-2.
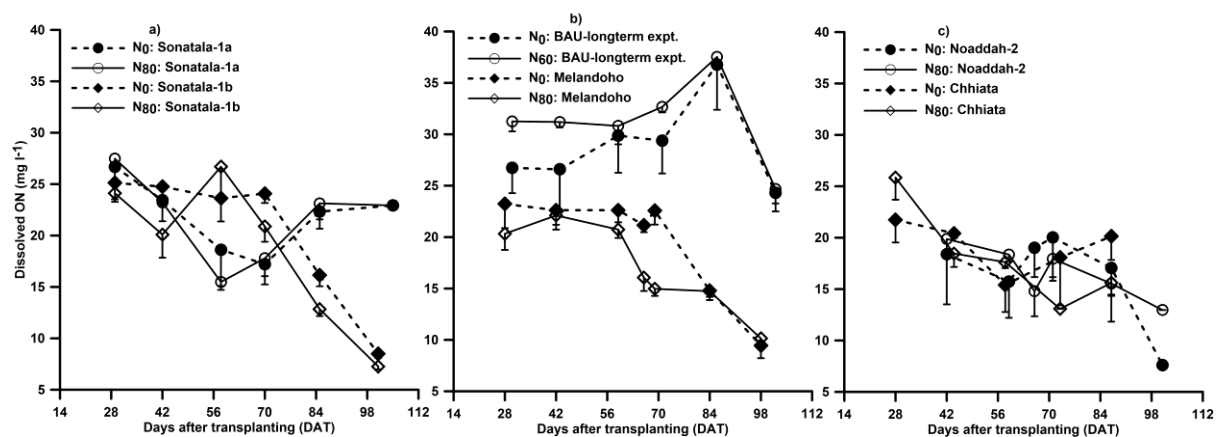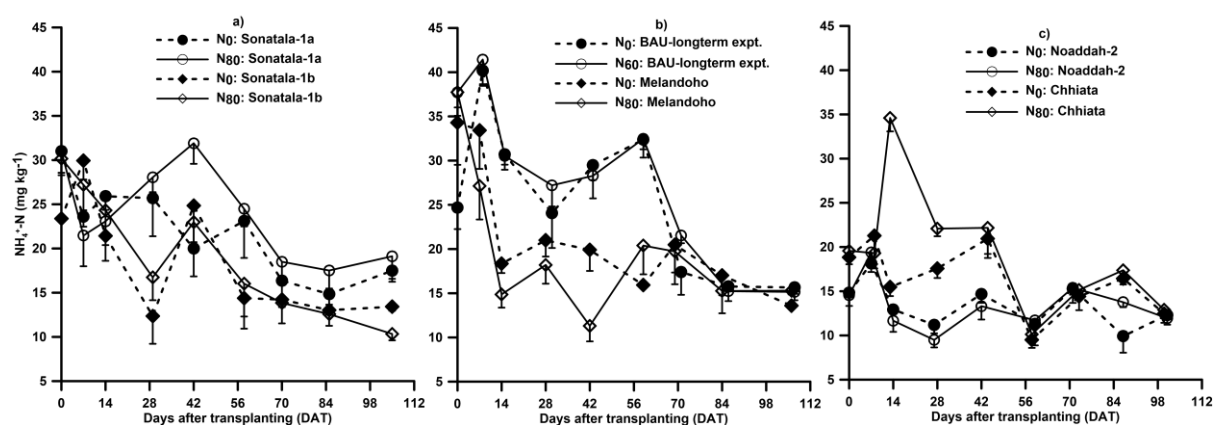


Fig. 5.7 Temporal evolutions of soil NH$_4^+$-N in the puddle layer (0-15 cm) of studied paddy fields in Bangladesh during wet rice (T. Aman) season, 2016 with (N$_{60/80}$) or without (N$_0$) N fertilizer application

The summation of soil exchangeable NH$_4^+$-N and plant N uptake, here defined as net mineral N supply over the season differed between the soils (p<0.01) (Table 5.2) and N treatments per soil (p<0.05) (Fig. 5.8). Plant N was a superior N pool than soil NH$_4^+$-N and its evolution primarily determined the inferred net soil N supply from 28 DAT till 84 DAT (Fig. 5.9) due to limited initial and final plant N uptake on the opposite soil exchangeable NH$_4^+$ instead did.

Regardless of N fertilizer application, net mineral N supply, slightly declined or stayed at same level until 14 DAT in five out of six soils (except Chhiata), then increased almost linearly from 14 DAT until 58 DAT, and then more or less plateaued until harvest (Fig. 5.8). The evolution of net mineral N supply over time was well modeled (R$^2$ = 0.67 to 0.92) by

133

first-order kinetics during 0 DAT until harvest for all soils with or without N fertilizer application (Fig. 5.8). The amount of net mineral N released was remarkably greater in N fertilized plots ($p < 0.05$) than in N unfertilized controls ($N_0$) from 28 DAT till harvest for all soils, except in Melandoho between 28 and 42 DAT and in Noaddah-2 on 28 DAT (Fig. 5.8; Table 5.2). In case of Chhiata soil net mineral N supply increased rather linearly (Fig. 5.8c). In $N_{80}$-Melandoho a minimum on 42 DAT (Fig. 5.8b) derives from the ineptitude to apply a second split of urea due to overflowed rainwater. Regardless of N treatments, generally the net mineral N supply was the highest in Sonatala-1a and lowest in Noaddah-2 soil ($p < 0.01$) for most sampling events (Table 5.2). While the released net mineral N supply in other four soils stood in between these two soils and were statistically identical to one another during most sampling points (Table 5.2). The overall ranking of net mineral N supply at harvest was Sonatala-1a > Sonatala-1b = BAU long-term experimental site = Melandoho = Chhiata ≥ Noaddah-2 for $N_0$, and Sonatala-1a = BAU long-term experimental site = Melandoho ≥ Sonatala-1b = Chhiata = Noaddah-2 for N fertilized treatment (Table 5.2).
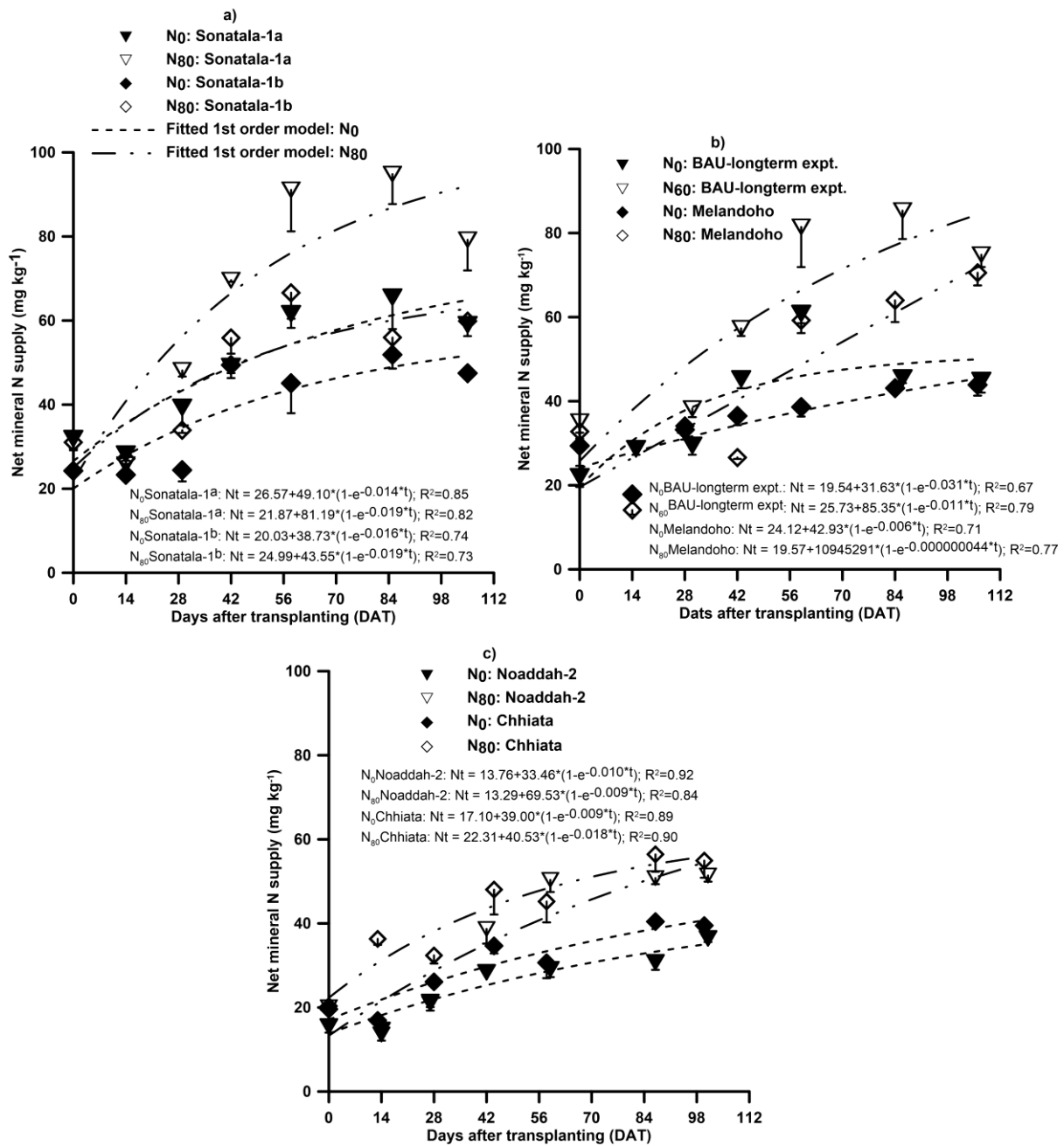
Fig. 5.8 Temporal evolutions net mineral N supply at the puddle layer (0-15 cm) of the studied paddy fields in Bangladesh during wet rice (T. Aman) season, 2016 with ($N_{60/80}$) or without ($N_0$) N fertilizer application (vertical bars indicate the standard errors of the means, n=3)
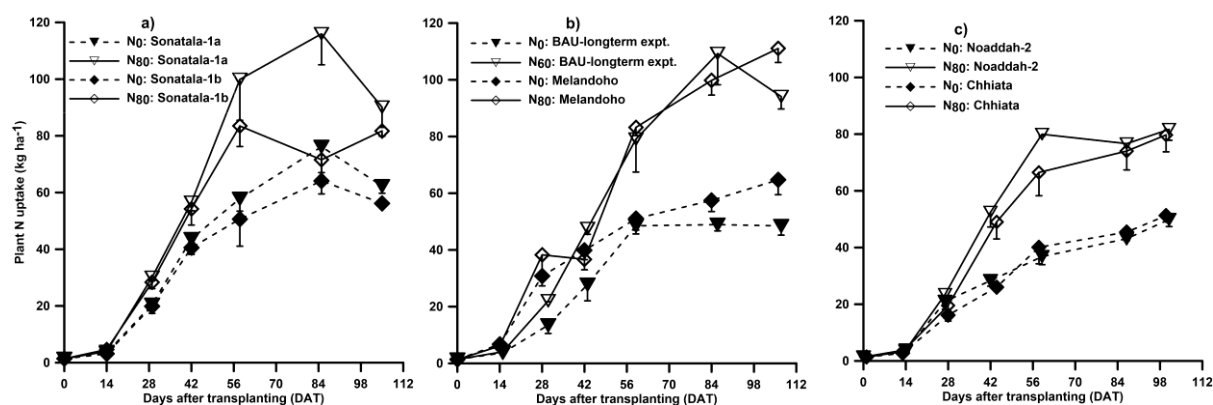
Fig. 5.9 Temporal evolutions of plant N uptake in the studied paddy fields of Bangladesh during wet rice (T. Aman) season, 2016 with ($N_{60/80}$) or without ($N_0$) N fertilizer application (vertical bars indicate the standard errors of the means, n=3)

Table 5.2 Effect of N fertilizer application on net mineral N supply (N jointly in soil and plant) for six farmers' paddy fields *in-situ* during wet rice growing season in 2016, Bangladesh

| Soils | Net mineral N supply (mg kg$^{-1}$) in $N_0$ | | | | | |
|---|---|---|---|---|---|---|
| | 0 DAT | 28 DAT | 42 DAT | 58 DAT | 84 DAT | At harvest |
| Sonatala-1a | 31a[*] | 39a[*] | 49a | 62a | 66a | 59a |
| Sonatala-1b | 23abc | 24bc | 49a | 45b | 52ab | 47b |
| BAU long-term expt. | 21abc | 30abc | 45a | 61a | 46bc | 45bc |
| Melandoho | 29ab | 33ab | 36b | 39b | 43bc | 44bc |
| Noaddah-2 | 15c | 21c | 28b | 29b | 31c | 36c |
| Chhiata | 19bc | 26bc | 35b | 31b | 40bc | 39bc |
| p-value | <0.01 | <0.01 | <0.01 | <0.01 | <0.01 | <0.01 |
| | Net mineral N supply (mg kg$^{-1}$) in $N_{80}$ or $N_{60}$ | | | | | |
| Soils | 0 DAT | 28 DAT | 42 DAT | 58 DAT | 84 DAT | At harvest |
| Sonatala-1a | 31a | 48a | 70a | 91a | 95a | 79a |
| Sonatala-1b | 30a | 34b | 56b | 67abc | 56b | 60bcd |
| BAU long-term expt. | 34a | 38b | 57ab | 81ab | 85a | 75ab |
| Melandoho | 32a | 34b | 27d | 59bc | 64b | 71abc |
| Noaddah-2 | 15b | 21c | 39bcd | 50bc | 51b | 51d |
| Chhiata | 20b | 32b | 48bc | 45c | 56b | 55cd |
| p-value | <0.01 | <0.01 | <0.01 | <0.01 | <0.01 | <0.01 |

[*]Different lower case letters denote significantly different mineral N (p<0.01) released among the farmers' paddy fields according to ANOVA and Duncan's Multiple Range Post-Hoc Test.

## 5.3.4. Grain yield and N use efficiency

Overall the grain yield in N treated plots ($N_{80/60}$) ranged from 3.08-5.01 t ha$^{-1}$ and was significantly ($p < 0.05$) greater (by 0.3 to 1.2 t ha$^{-1}$ equivalent increase of 11-60%) than in the $N_0$ counterpart plots (1.92 to 3.91 t ha$^{-1}$) (Table 5.3). Maximal ($p < 0.01$) grain yields were recorded at Noaddah-2 while the lowest yields were obtained in the BAU long-term experimental site. Grain yields at Sonatala-1b, Sonatala-1a, Melandoho and Chhiata were almost identical, regardless of N fertilizer application (Table 5.3).

Higher fertilizer N-recovery ($RE_N$) and agronomic ($AE_N$) efficiencies were attained in BAU long-term experimental soil (Table 5.3) than in the other treatments. But as an exception at BAU these actually represented the combined efficiencies of N, P, K and S fertilizers, because the $N_0$ plots in this site did not receive any other fertilizers (P, K, S), and the cultivated rice variety was also different from other five soils. Therefore, strict N use efficiencies are only obtained from the other five soils (Table 5.3). The recovery efficiency ($RE_N$) of applied N fertilizer by rice plant (grain + straw) ranged from 28% at Sonatala-1b to 56% in case of Melandoho. The physiological efficiency ($PE_N$: kg grain kg$^{-1}$ N uptake) was larger for Sonatala-1b (37) and Noaddah-2 (36) soils, and smaller for Sonatala-1a (14). Furthermore, the recorded agronomic efficiency ($AE_N$: kg grain kg$^{-1}$ N applied) was the minimum in Sonatala-1a (4) and the maximum in Melandoho and Noaddah-2 (14) soils.

Table 5.3 Paddy rice grain yield, N fertilizer recovery efficiency ($RE_N$), physiological efficiency ($PE_N$) and agronomic efficiency ($AE_N$) (means ± standard error) of the studied farmers' paddy fields during T. Aman, 2016 in Bangladesh

| Soil Series | Grain Yield (t ha⁻¹) | | Recovery Efficiency ($RE_N$) | Physiological Efficiency ($PE_N$) | Agronomic Efficiency ($AE_N$) |
|---|---|---|---|---|---|
| | $N_0$ | $N_{80/60}$ | % | kg grain kg⁻¹ N uptake | kg grain kg⁻¹ N applied |
| Sonatala-1a | 3.09 ± 0.22b* | 3.44 ± 0.12cd* | 30 | 14 | 4 |
| Sonatala-1b | 3.38 ± 0.12ab | 4.22 ± 0.23b | 28 | 37 | 10 |
| BAU long-term expt. | 1.92 ± 0.21c | 3.08 ± 0.16d | 62 | 31 | 19 |
| Melandoho | 2.97 ± 0.09b | 4.11 ± 0.05bc | 56 | 26 | 14 |
| Noaddah-2 | 3.91 ± 0.20a | 5.01 ± 0.24a | 38 | 36 | 14 |
| Chhiata | 2.91 ± 0.18b | 3.76 ± 0.09bcd | 33 | 32 | 11 |

*5.3.5. Relations of net mineral N supply to soil properties, Eh, soil solution pH, DON, Fe and Mn*

As mentioned before for most soils the solution pH stayed near neutral, soil Eh remained at lower levels and dissolved Fe, Mn and DON released though declined but still existed at notable levels till ~70 or 84 DAT. Hence, rather than using descriptors of their temporal evolutions, simple means for the Aman season were included in an analysis of predictors of net mineral N supply, described as the modeled net mineral N supply (soil exchangeable N + plant N) at 84DAT ($N_{84DAT}$). $N_{84DAT}$ correlated positively with %silt, $Fe_{ox}$, $SOC:Mn_{ox}$ and mean soil $NH_4^+$-N (r = 0.83 to 0.90; p<0.05) in the $N_0$ treatment, but negatively with %sand (r = 0.90; p<0.05) (Table 5.4). For the $N_{80}$ or $N_{60}$ treatment likewise relations were found but only significant correlations with %sand (r = -0.86) and soil $NH_4^+$-N (r = 0.81) (Table 5.4) (p<0.05).

Table 5.4 Pearson's correlation coefficients (r) between apparent net mineral N supply, initial soil properties, N fertilizer use efficiencies ($AE_N$, $PE_N$ and $RE_N$), soil $NH_4^+$-N and Eh, soil solution pH, Fe, Mn and DON during wet rice growing season in Bangladesh

| Soil parameter | Mineralized N ($N_t$) (mg kg$^{-1}$ 84 day$^{-1}$) | | N fertilizer efficiency | | |
| --- | --- | --- | --- | --- | --- |
| | $N_0$ | $N_{80/60}$ | $AE_N$ (kg grain kg$^{-1}$ N applied) | $PE_N$ (kg grain kg$^{-1}$ N uptake) | $RE_N$ (%) |
| SOC (%) | 0.72 | 0.69 | -0.53 | -0.49 | -0.40 |
| TN (%) | 0.75 | 0.74 | -0.42 | -0.40 | -0.33 |
| C:N | 0.44 | 0.36 | -0.52 | -0.30 | -0.52 |
| pH-KCl | 0.57 | 0.44 | -0.28 | -0.06 | -0.34 |
| Fe$_{ox}$ (g kg$^{-1}$) | **0.83***  | 0.52 | -0.71 | -0.48 | -0.54 |
| Mn$_{ox}$ (g kg$^{-1}$) | -0.06 | -0.15 | -0.54 | 0.02 | -0.73 |
| Sand (%) | **-0.90*** | **-0.86*** | 0.70 | **0.88*** | 0.30 |
| Silt (%) | **0.90*** | 0.80 | -0.37 | -0.60 | -0.04 |
| Clay (%) | -0.50 | -0.39 | -0.11 | 0.08 | -0.22 |
| SOC : Fe$_{ox}$ ratio | 0.54 | 0.57 | -0.34 | -0.33 | -0.29 |
| SOC : Mn$_{ox}$ ratio | **0.84*** | 0.78 | 0.14 | -0.33 | 0.32 |
| NH$_4$-lactate K (mg kg$^{-1}$) | -0.14 | -0.15 | -0.31 | -0.14 | -0.27 |
| NH$_4$-lactate P (mg kg$^{-1}$) | -0.77 | -0.53 | 0.26 | 0.31 | 0.09 |
| DTPA-Fe (mg kg$^{-1}$) | -0.36 | -0.31 | 0.02 | 0.17 | -0.08 |
| DTPA-Mn (mg kg$^{-1}$) | 0.36 | 0.15 | -0.44 | 0.07 | -0.58 |
| AE$_N$ | -0.49 | -0.26 | 1.00 | 0.55 | **0.84*** |
| Soil NH$_4^+$-N (mg kg$^{-1}$) | **0.87*** | **0.81*** | -0.12 | -0.38 | 0.04 |
| Soln. Fe (mg l$^{-1}$) | -0.60 | -0.50 | 0.25 | 0.32 | 0.09 |
| Soln. Mn (mg l$^{-1}$) | -0.42 | -0.26 | 0.1 | 0.21 | -0.08 |
| Soln. DON (mg kg$^{-1}$) | 0.70 | 0.73 | 0.28 | -0.14 | 0.38 |
| Soln. pH | 0.14 | -0.05 | -0.28 | 0.01 | -0.38 |
| Soil mean Eh (mV) | 0.03 | -0.16 | -0.27 | -0.48 | 0.05 |
| $N_t$ (mg kg$^{-1}$ 84day$^{-1}$) for $N_{80/60}$ | - | 1.00 | -0.26 | -0.76 | 0.15 |

## 5.4. Discussion

### 5.4.1. Seasonal evolutions of in-situ paddy field reductive processes

The daily average air temperature (around 29°C) and rainfall (7 mm day$^{-1}$) during 0 to 70 DAT (22 Aug-31 Oct) was analogous to the seasonal (Jun-Sep) average temperature (28.5°C) and rainfall (6-14 mm day$^{-1}$) during 1979-2006 in Bangladesh (Rahman et al., 2012). Soil Eh and solution pH are important properties to impact soil microbial activity and exhibit strong seasonal variability depended mostly on soil moisture, hence on the climatic

parameters likely rainfall and temperature. Therefore the prevailed higher temperature in the earlier wet season and field flooding even before transplanting favored anaerobic microbial activity and instantaneous development of reductive conditions. Until 70 or 84 DAT as expected this was accompanied by neutral soil solution pH (6.4-7.2) in all soils (except for Chhiata from 58 DAT). Rapid increasing trends in solution pH for Chhiata from 28 DAT onwards possibly linked to its higher available basic cations (Ca, K and Mg) (Table 5.1) along with field flooding by rain water containing more anthropogenic basic cations ($Ca^{2+}$, $Na^+$ and $K^+$) (Rajashekhara Rao and Siddaramappa, 2007; Shohel et al., 2016).

Continued low Eh levels (around 0 to -150 mV) during 0-70 or 84 DAT characterized all soils, except for Melandoho. Such changes in soil Eh during flooding were comparable to the in **Chapter 4** presented rice pot growth experiment, and previous published data for flooded rain-fed rice (around -100 mV) (Cha-un et al., 2017). The overall extent of soil Eh (194 to -150 mV) during flooding suggested mainly $Fe^{3+}$ (+250 to -150 mV at pH 6 to 8) and $Mn^{3+/4+}$ (+350 to +100 mV at pH 7) reduction (Atta et al., 1996; Gao et al., 2002; Haque et al., 2016; Hanke et al., 2013) as ongoing electron-accepting processes in all soils. Some Eh fluctuations from 28 DAT onwards could stem from inputs of $O_2$ into rhizosphere through rice's aerenchyma (Haque et al., 2016; Gao et al., 2002), and via $O_2$-rich rainfall or irrigation water. Rapid rise in soil Eh to positive values at several time points in Sonatala-1a (Fig. 5.2a) and Chhiata (Fig. 5.2f) before 84 DAT coincided with unintentional soil drying by lack of rain events and irrigation water supply. Likewise, although the plots were over flooded by rainwater during 28-54 DAT in Melandoho, the higher Eh values (44 to 104 mV) might be explained by the greater oxidizing power of rain water through dissolved oxidants like $O_2$ and $NO_3^-$ (Kasting, et al., 1985; Shohel et al., 2016). The onset of reduced condition in specific soil depth is microbially mediated and controlled by availability of alternative $e^-$ acceptors ($NO_3^-$, $Mn^{4+/3+}$, $Fe^{3+}$, $SO_4^{2-}$ and $CO_2$) and $e^-$ donors (particularly easily degradable OM) (Huang and Gambrell, 2011). Similar to previous pot experiment, the extent of Eh drop under current study, however, did not entirely follow the ordination of SOC and DON, implying that Eh change was directed by other interacting processes. For instance, the minimum attained Eh was 80 to -150 mV in Sonatala-1b and BAU experimental soils, which may logically be coupled to the relatively higher SOC (1.4 to 1.8%) and DON levels of these soils (see Section 5.3.2). But less negative Eh were recorded in the Sonatala-1a (194 to -93 mV), Chhiata (145 to -70 mV) and Melandoho (160 to -73 mV) soils although SOC contents in the first two soils were also high and 3 to 4 times higher than of the Melandoho soil (Table 5.1). Likewise mean Eh under current study neither correlate to any of the studied variables including reducible Fe ($Fe_{ox}$) and Mn ($Mn_{ox}$), nor to their ratios to SOC, dissolved Fe, Mn and DON levels. Temperature drop by 6°C and soil drying from ~75 or 87 DAT till harvest for

most soils tended to rise soil Eh (208 to 433 mV) by entry of $O_2$, decline microbial activity and solution Fe, Mn by precipitation or re-oxidation (Pan et al., 2014), and limit Fe- and Mn-(hydr-)oxides reductive dissolution (Fig. 5.4 and 5.5).

In this study pore water Fe and Mn at puddle layer (0-9 cm) was measured as indication of key reductive processes in flooded condition. In all soils N fertilizer application had inconsequential influence on puddle layer's dissolved Fe and Mn evolutions (Fig. 5.4 and 5.5). Almost the same was noticed for dry season continuously flooded Sonatala-1b paddy field *in-situ* (**Chapter 6**) and five fertilizer treatments (control, N, NP, NPK and N+FYM) in BAU experimental soils under laboratory incubation (Akter et al., 2016) (**Chapter 2**). Regardless of N fertilizer application, relatively higher dissolved Fe and Mn concentrations for all soils during earlier season with field flooding suggested reductive dissolution of Fe- and Mn- (hydr-)oxides, and use of $Fe^{3+}$ and $Mn^{4+/3+}$ as $e^-$ acceptors to oxidize SOM (Gao et al., 2002; Haque et al., 2016; Pan et al., 2014). Typically higher $Fe^{2+}$ concentration accomplished later than that of $Mn^{2+}$ (Gotoh and Yamashita, 1966), but in this study both dissolved Fe and Mn evolutions were fairly simultaneous and overlapped (Fig. 5.4 and 5.5), resembled to that observed by Gao et al. (2002). Overall, the dissolved Fe (1-104 mg $l^{-1}$) in all studied soils during flooding surpassed solution Mn (0.1-21 mg $l^{-1}$), which indeed suggested predominant role of $Fe^{3+}$ reduction than $Mn^{4+/3+}$ to mineralize SOM, hence mineral N release (**Chapter 4**; Narteh and Sahrawat, 1997; Van Bodegom et al., 2003). Even though $Fe^{3+}$ and $Mn^{4+/3+}$ reductions varied depending on soil type, substrate availability, concentration of products and pH (Haque et al., 2016; Gao et al., 2002; Wang et. al., 2017), solution Fe and Mn in these *in-situ* field experiments were not significantly correlated to oxalate extractable Fe ($Fe_{ox}$) and Mn ($Mn_{ox}$) (data not shown). Instead dissolved Fe correlated positively with $NH_4$-lactate extractable phosphorus (P) and negatively with pH-KCl, SOC:$Fe_{ox}$ and SOC:$Mn_{ox}$ ($p<0.05$) (data not shown), just identical to previous greenhouse pot experiment (**Chapter 4**). Positive correlations of solution Fe with $NH_4$-lactate extractable P and DTPA-extractable Fe (r = 0.92 to 0.97; $p<0.05$) indicated strong impact of P availability on Fe reduction and transformation, possibly by altering surface reactivity of poorly crystalline Fe (hydr-)oxides like ferrihydrite (Zhang et al., 2012; Willett and Higgins, 1978). Reductive dissolution of $Fe^{3+}$(hydr-)oxides caused by anaerobic microbial respiration could enhance P solubilization (Li et al., 2012). Accordingly Holford and Patrick (1979) observed that at pH 6.5, reduction (since Eh around -150 mV) released P previously occluded and precipitated with $Fe^{3+}$ compounds.

The strong negative correlation between Fe-release and the SOC to $Fe_{ox}$ ratio indicated the use of a share of $Fe_{ox}$ as $e^-$ acceptor by Fe reducers to oxidize OM. At neutral pH (~7), low

crystalline ferrihydrite reduction energetically predominates over the reduction of goethite with higher crystallinity (Wang et al., 2017). Both ferrihydrite and goethite were identified as prevalent forms of pedogenic Fe by Mössbauer spectroscopy in Sonatala-1a (5.6 and 15.6% of total Fe), Melandoho (4.7 and 12.5% of total Fe) and Noaddah-2 (13.6 and 29% of total Fe) soils in **Chapter 4** and we indeed estimated that an important share of donated $e^-$ were used for reductive Fe-dissolution in these three soils. Alternatively, strong negative correlations between Fe-release rate and the $SOC:Fe_{ox}$ ratio could be explained by an increasing adsorption of OC to the surface of hydrous Fe oxides (e.g. ferrihydrite and goethite in these soils) (Hanke et al., 2014), with consequent declined availability of Fe(hydr-)oxides for microbial reduction. However, such negative impact of OC loading on pedogenic Fe-reduction still needs to be confirmed experimentally. Other oxidants like $SO_4^{2-}$ and $CO_2$ could also have served as $e^-$ acceptors. But the near neutral pH and Eh range of +194 to -150 mV during flooding, should mostly not have favored extensive $SO_4^{2-}$ reduction (-120 to -180 mV) and $CH_4$ emission (-150 to -280 mV) (Sahrawat, 2004a; Wang et al., 1993).

*5.4.2. Seasonal evolutions of dissolved organic N*

Despite negligible differences in DON's temporal trends between $N_0$ and $N_{80}$ or $N_{60}$ per soil, noticeable variations (3-22 mg N $kg^{-1}$ ~8-38 mg $l^{-1}$) existed among the soils (Fig. 5.6). Comparable variation in DON content (3-18 mg $kg^{-1}$) with greater DON release in paddy soils with higher SOC and TN was reported by Li et al. (2010). The BAU, Sonatala-1a and Sonatala-1b soils had higher TN (~0.2%) and released more DON than the Melandoho, Noaddah-2 and Chhiata soils with only ~0.1% TN (see Section 5.3.2; Fig. 5.6). Elevated DON levels during flooding may be attributed to accumulation of organic metabolites under anoxic conditions (Sahrawat, 2004b) and DOM solubilization following reductive dissolution of Fe- and Mn- (hydr-)oxides, or OM desorption from clay minerals and Fe oxides via pH change (Grybos et al., 2009; Hanke et al., 2013). Identical to previous pot experiment's solution chemistry **(Chapter 4)**, solution Fe, Mn and DON all remained at higher levels during flooded period (~0 to 70 or 84 DAT) (Fig. 5.4, 5.5 and 5.6). DON's synchronized trends (Fig. 5.4, 5.5 and 5.6) and positive correlations with solution Fe and Mn per soil during flooding (r = 0.47 to 0.97; p = 0.002 to 0.43) in five soils, except the BAU long-term experimental soil would suggest a link between reductive Fe and Mn dissolution and DON release.

But we found insignificant or even negative correlations between mean DON and solution Fe and Mn concentrations (r = -0.32 to -0.64; p = 0.18 to 0.53), considering the flooded period

for all six soils, even for five soils if we eliminate BAU (r = -0.43 to -0.63; p = 0.25 to 0.47). This at least suggests that DON release is very soil specific and controlled by different overriding mechanisms per soil. Furthermore, DON removal mechanisms were not considered in the above discussion but evidently also impact DON dynamics and could differ in their extent among the studied soils. DOM can form complexes and co-precipitate with $Fe^{2+}$ or $Mn^{2+}$ under anaerobic condition (Akter et al., 2016; Kögel-Knabner et al., 2010; Sodano et al., 2017). Secondly, a part could have been mineralized. Thirdly, DON can be removed through electrostatic attraction of N-containing compounds by negatively charged vermiculite surface (Sodano et al., 2016) at low Eh. All investigated soils (except for Chhiata for which we have no mineralogical information) contained vermiculite and interstratified vermiculite-chlorite (Kader et al., 2013), which could both accumulate negative charge by acting as electron acceptor. Role of such temporary DON-removing processes on gross soil N supply to the rice plant is unclear and assessing their relevance would require further dedicated research.

*5.4.3. Soil mineral N and net mineral N supply influenced by soil properties, dissolved Fe, Mn and DON*

Soil mineral N in this *in-situ* field study is anticipated to derive from soil organic N mineralization and applied urea hydrolysis. Hence, soil $NH_4^+$-N content approximately represented the temporary balance between input (viz. soil organic N mineralization and urea hydrolysis) and output (viz. immobilization, plant N-uptake, clay fixation, nitrification-denitrification, leaching and volatilization) (Dong et al., 2012; Hoque et al., 2002; Said-Pullicino et al., 2014). Overall minor difference in soil $NH_4^+$-N between $N_0$ and $N_{80}$ or $N_{60}$ treatment per soil is surprising but does match with other reports in **Chapter 6**, and Zhang et al. (2009). Regardless of N fertilizer application, exchangeable $NH_4^+$-N in all soils remained at higher level from 0 to 7 DAT, likely from rapid mineralization of easily decomposable OM and temporary limited immobilization under anoxic conditions (Ono, 1989; Ponnamperuma, 1972; Zhang and Scherer, 2000). Rapid decline from the initial high soil $NH_4^+$-N by 5-23 mg $kg^{-1}$ between 7 to 14 or 28 DAT (Fig 5.7) for all soils (except in $N_{80}$ Chhiata on 13 DAT) seems to be typical for flooded paddy soils in North-central Bangladesh (**Chapter 4**) as this also connects to our observations in **Chapters 3 and 6**. Again since plant N uptake was only 3-7 kg $ha^{-1}$ (~1-4 mg $kg^{-1}$) until 14 DAT, and most N-uptake started only from 28 DAT (13-38 kg $ha^{-1}$ ~9-21 mg $kg^{-1}$) (Fig. 5.9) other removal processes are responsible for the initial drop in soil exchangeable mineral N. Likewise these same processes must also be responsible

for the remarkable limited impact of fertilization on course of soil exchangeable $NH_4^+$ (except for in Chhiata on 13DAT and on 42DAT for Sonatala-1a).

We here repeat candidate processes without going into details:

1° **$NH_4^+$ fixation** in clay interlayers induced by reductive dissolution of Fe(hydr-)oxides coatings on clay minerals or reduction of octahedral $Fe^{3+}$ at low Eh via flooding and buildup of negative charge thus attracting $NH_4^+$ (Scherer and Zhang, 1999; Scherer and Zhang, 2002).

2° $NH_4^+$-oxidation coupled to $Fe^{3+}$ reduction under water-logged condition might drive a part of $NH_4^+$ loss (8-61 kg $NH_4^+$ loss $ha^{-1}$ $year^{-1}$ by Ding et al., 2014) during 7-14 DAT, suggested also by elevated solution Fe and $O_2$ limiting Eh range (43 to -140 mV) (Fig. 5.2).

During 28-84 DAT, net mineral N supply (Fig. 5.8) was primarily a consequence of substantial plant N uptake (Fig. 5.9) and differed between soils ($p<0.01$) and N treatments ($p<0.05$) (Fig. 5.8). The net mineral N supply per soil itself followed asymptotic course (Fig. 5.8), comparable to previous laboratory incubation experiment (**Chapter 2** and Akter et al., 2016). Indigenous soil N supply by organic N mineralization (36-66 mg $kg^{-1}$) predominantly contributed (approx. 71%) to net mineral N supply than applied N fertilizer hydrolysis (15-29 mg $kg^{-1}$, approx. 29%). Besides, N fertilizer $RE_N$ was only 28-56% in all five soils other than the BAU long-term experimental soil. This confirms again a substantial loss of fertilizer N (44-72%) by different mechanisms, previously identified as possibly nitrification-denitrification, $NH_3$ volatilization, leaching and runoff, $NH_4^+$-oxidation etc. (Craswell and Vlek, 1983; Cucu et al., 2014; Dong et al., 2012).

Stepwise linear regression was used to identify predictor variables of modeled net mineral N supply ($N_t$) 84days$^{-1}$ separately for $N_0$ and $N_{80/60}$ including studied soil properties and biochemical processes as independent variables. This yielded the following models:

For $N_0$ : Net mineral N supply, $N_t$ (mg $kg^{-1}$ 84 days$^{-1}$)

$$= -126.68 + 0.89 \text{ Silt } (\%) + 17.15 \text{ mean pH (solution)}..........(1)$$

For $N_{80/60}$ : Net mineral N supply, $N_t$ (mg $kg^{-1}$ 84 days$^{-1}$)

$$= 73.61 - 1.37 \text{ Sand } (\%) + 1.49 \text{ DON (mg } kg^{-1})....................(2)$$

The models infer that %silt and solution mean pH had significant ($p<0.01$) positive partial correlation coefficient which together explained 99% of variation in $N_t$ for $N_0$, while %sand

and mean DON were identified to have significant (p<0.05) partial correlation coefficient which together explained 95% of variation in $N_t$ for $N_{80}$ or $N_{60}$. Among the physicochemical properties %silt and sand, $Fe_{ox}$, SOC, TN, SOC to $Mn_{ox}$ ratio, and solution DON best correlated to the modeled net mineral N supply (Table 5.4). Positive and negative impacts of percent silt (r = 0.80 to 0.90; p = 0.014 to 0.057) and sand (r = -0.86 to -0.90; p<0.05) on net mineral N supply should be indirect, as suggested by TN, $Fe_{ox}$ and DON's positive relations with %silt (r = 0.48 to 0.87; p = 0.03 to 0.34) and negative correlation with %sand (r = -0.35 to -0.81; p = 0.05 to 0.50). Faster fertilizer-N mobility and greater N loss by leaching and runoff in sandy than loamy or clay soils (Liu et al., 2016) could partly support the increase net mineral N supply with lower sand percent and vice-versa.

Li et al. (2010) revealed that DOM removal declined N mineralization (by ~7-27%) in paddy soils. A share of 21-52% of DON content is highly bio-available and played a key role in soil organic N mineralization, further signifying DON's positive impact on mineral N supply in the studied soils. Negative or insignificant correlations of net mineral N supply with dissolved Fe (r = -0.5 to -0.60; p = 0.21 to 0.31) in this *in-situ* study with six soils question our previous results on positive relations of solution Fe and soil mineral N release rates in laboratory and green-house pot experiments with three of these soils (**Chapters 2 & 4**) and Sri Lankan paddy soil (**Chapter 3**). Multiple transformation processes for mineral N, Fe and DOM (e.g. nitrification-denitrification, volatilization, leaching, runoff, $NH_4^+$-oxidation, DOM-$Fe^{2+}$-co-precipitation, $Fe^{2+}$-oxidation coupled to $NO_3^-$ reduction) may simultaneously/co-occur under field conditions. These may prompt insignificant or negative relations between net mineral N supply and dissolved Fe when considering all six paddy fields together. However, soil $NH_4^+$-N, solution Fe, Mn and DON disclosed temporal synchronized trends and positive correlations (r = 0.29 to 0.88; p = 0.011 to 0.64) per soil per sampling events in both N treatments for all soils (except soil $NH_4^+$-N vs. DON in BAU long-term experiment and $N_{80}$-Melandoho), just identical to that in controlled lab and green-house experiments. This temporal synchrony and net mineral N supply's positive correlations with $Fe_{ox}$, SOC:$Mn_{ox}$ , SOC, TN and DON, indicated that soil organic N mineralization in these paddy fields *in-situ* is still ultimately influenced by the quantity and quality of organic matter (particularly DON) and $e^-$ acceptors (mostly reducible Fe, $Fe_{ox}$).

*5.4.4. Grain yield and N use efficiency*

A significant increase in rice grain yield (by 0.3 to 1.2 t $ha^{-1}$) and N uptake (approx. by 15-29 mg $kg^{-1}$) in N fertilized over unfertilized plots shows that both net mineral N supply by soil

organic N mineralization and from applied urea hydrolysis is needed to achieve target yields for each soil. The recovery ($RE_N$: 28-56%), physiological ($PE_N$: 14-37 kg grain $kg^{-1}$ N uptake) and agronomic ($AE_N$: 4-14 kg grain $kg^{-1}$ N applied) efficiencies were almost comparable to that reported by Adhikari et al. (1999) ($RE_N$: 25-37%, $PE_N$: 29-34 kg grain $kg^{-1}$ N uptake, $AE_N$ : 6-11 kg grain $kg^{-1}$ N applied). Moreover the efficiencies are positively related to each other (r = 0.55 to 0.84; p = 0.04 to 0.26), but none of them significantly correlated with the studied soil properties and biochemical processes (Table 5.4), except for $PE_N$ with % sand (r = 0.88; p = 0.02). Instead they exhibited even negative correlations for most cases, and $PE_N$'s relation with net mineral N supply in $N_{80}$ (r = -0.76; p = 0.08) is the most striking. This correlation was not strong but would favor our hypothesized lowering of N-fertilizer efficiency at higher soil N supply, due to enhanced chance for N losses.

The estimated fertilizer N loss of 44-72% (at least temporary) is analogous to that reported (10-65%) by Cassman et al. (1998). Strikingly, the sequence of grain yield followed almost reverse order of net mineral N supply between the soils in both $N_0$ and $N_{80}$ or $N_{60}$ treatments (Tables 5.2 and 5.3). For instance, net mineral N supply in Sonatala-1a is greater than Noaddah-2 (Table 5.2), but the grain yield, $RE_N$, $PE_N$ and $AE_N$ were smaller in Sonatala-1a soil (Table 5.3). Irrespective of N fertilizer application net mineral N supply demonstrates insignificant correlations with grain yield (r = -0.35 to -0.78; p = 0.07-0.49) and N uptake (r = 0.30 to 0.46; p = 0.36-0.57). Also grain yield did not correlate with N uptake (r = -0.23 to 0.16; p = 0.66 to 0.77). These lacking significant correlations between net mineral N supply, grain yield and N uptake, even in the $N_0$ treatments question the validity of soil N supply concept as being a measure of efficient N fertilizer advice (Anh and Olk, 2002). Alternatively, grain yield in this study may have been influenced by factors other than N availability or N limitation and plant N uptake (Anh and Olk, 2002; Adhikari et al., 1999). Poor matching in time of soil and fertilizer N supply with crop N demand, (Anh and Olk, 2002; Casman et al., 1998), variability in water supply, insect-pest and disease management between the fields (Adhikari et al., 1999) are likely most important. Also the availability of other essential nutrients might not limiting to decline grain yield. Since we did not see any significant correlations of $AE_N$, $PE_N$ and $RE_N$ with plant available P, K, Fe and Mn (Table 5.4).

Also unquantified differences in N-losses via mainly $NH_3$-volatilization between the six soils may explain why the quantified net mineral N supply did not connect to yield and efficiency indicators. For instance, recently, Yao et al. (2017) found that urea deep placement (UDP) instead of surface urea broadcasting minimized N loss especially by $NH_3$-volatilization (92%) and increased $RE_N$ (by 55%), N uptake (by 28%) and grain yield (by 10%), with a better match in N availability and rice plants N demand. Increased N use efficiency (up to 50-70%)

146

and grain yield (by 15-20%), and reduced N fertilizer use (by 30-40%) by urea or NPK deep placement was as well reported by Miah et al. (2016). Average yield increase in urea briquettes and N-P-K briquettes over prilled urea broadcasted field was ~ 21–31% during wet (Aman) rice growing season in southern Bangladesh (Miah et al., 2016). Hence, continuing *in-situ* field research with improve nutrients, crop, water, weed, insect and disease managements should help to identify yield limiting factors.

## 5.5. Conclusions

Understanding how N supply from soil organic N mineralization and urea hydrolysis relate to SOC, TN, solution Fe, Mn and DON at field scale may help to optimize N fertilizer advice and improve N fertilizer efficiency. Reduced conditions with releases of solution Fe, Mn and DON appeared general in Bangladeshi paddy soils during the Aman season. Buildup of exchangeable $NH_4^+$-N, solution Fe, Mn and DON per soil demonstrate synchronizing trends but we could not unequivocally confirm the responsible mechanisms. Across all six studied soils, however, release of Fe/Mn and mineral N supply did co-vary. We hypothesize that multiple processes like release or fixation of $NH_4^+$ from/into clay minerals by reductive dissolution of Fe (hydr-)oxides coatings on clay surfaces, $NH_4^+$-oxidation coupled $Fe^{3+}$ reduction, DOM-$Fe^{2+}$-co-precipitation, $Fe^{2+}$-oxidation coupled $NO_3^-$ reduction all co-occur at varying levels under field conditions in these soils. This might explain these insignificant or even negative correlations.

Soil mineral N content throughout season significantly varied between soils but was remarkably unaffected by N fertilizer application, again confirming previous research that applied mineral N is quickly assembled into N-pools other than soil exchangeable N. DON and plant N were excluded. Gaseous or leaching losses were not quantified but might be relevant N-removal processes given the low $RE_N$ (28-56%) and predicted possible N fertilizer loss (44-72%). Future research by individual ^{15}N-levelled isotope setups may clarify if and which N-losses predominate in these fields. Neither N uptake nor net mineral N supply correlated significantly with grain yield in both $N_0$ and $N_{80/60}$, suggesting factors other than N availability impacted grain yield in wet season rice of north-central Bangladesh. Furthermore lack of significant correlations of $AE_N$, $PE_N$ and $RE_N$ with plant available P, K, Fe and Mn suggested that the limited N use efficiency did not stem from deficiency of these essential plant nutrients.

# Chapter 6

# Impact of irrigation management on paddy soil N supply and depth distribution of abiotic drivers

**Redrafted after:**

Akter M., Deroo H., Kamal A. M., Kader M. A., Verhoeven E., Decock C., Boeckx P., Sleutel S., 2017. Impact of irrigation management on paddy soil N supply and depth distribution of abiotic drivers. Agriculture, Ecosystems and Environment (submitted).

**Abstract**

In rice production, water-saving irrigation management is expanding and likely alters depth profiles of soil moisture, redox potential (Eh) and microbial activity. It is, however, unclear how such conditions then impact net soil N-release and availability to the rice crop, because we do not know well enough how water-saving management shapes depth-distribution of Eh and reductive processes, and microbial activity. A field experiment with rice was laid out on a typical young floodplain paddy soil of Bangladesh with three irrigation schemes, viz. continuous flooding (CF), safe alternate wetting and drying (AWD) and direct seeded rice (DSR), with 120 kg N ha$^{-1}$ ($N_{120}$) or without ($N_0$) urea application. We evaluated changes in soil mineral N and plant N uptake, $CH_4$ and $CO_2$ emissions and soil pH, and at multiple depths soil Eh and temperature, solution dissolved C, Fe and Mn throughout 2015 dry (Boro) season (Jan-Apr). Eh stayed at or above ~ +300 mV except for sudden drops to ~ -200 mV with irrigation events in DSR. Eh quickly dropped to methanogenic conditions, under both AWD and CF; rises to ~ +200 mV were observed during AWD-drainage events but were restricted to upper 5 or 12.5 cm depths. Throughout the growing season there was a pronounced increase in reductive dissolution of Fe and Mn (hydro-) oxides, buildup of dissolved C, and $CH_4$ effluxes under AWD and CF but not DSR, likely at least partially driven by the gradual soil warming from ~20ºC till 28°C. Predominant aerobic conditions under DSR lead to a nearly doubled C-emissions ($CO_2$+$CH_4$) compared to AWD and CF, suggesting more soil organic matter (OM) degradation in the former case, while soil mineral N plus plant N build-up rate followed an opposite order. Urea application did not raise soil exchangeable N levels, even prior to significant plant uptake from 28 DAT, and we forward temporal abiotic $NH_4^+$-fixation and N-removal processes as explanations. We conclude that regardless of some distinctions in temporal evolutions of puddle layer Eh, solution C, Fe and Mn, and $CH_4$-emission, soil N-supply was quite comparable under AWD and CF, as was rice yield. In the context of N availability, AWD could be safely adopted for rice growth in the Bangladeshi Boro season. The eventual fertilizer N recovery efficiency was higher for CF (42%) than for AWD (32%), but AWD saved 12% irrigation water. While DSR saved 45% water there was a large yield penalty, likely due to drought stress but also by poor germination caused by cold night temperatures in mid-January, while seedling transplantation in CF and AWD plots was only later on 28 January. Further research should be conducted to investigate the fast and pronounced removal of exchangeable inorganic N after initial N buildup by soil OM mineralization. At this moment most likely candidate processes appear clay-$NH_4^+$ fixation and anaerobic $NH_4^+$-oxidation.

## 6.1. Introduction

N fertilizer recovery is generally low for rice (*Oryza sativa*), approx. 31-40% (Cassman et al., 2002) and as a consequence compared to other crops, a substantial part (34 to 46%) of N taken up by rice plants derives from native soil supply. Hence organic matter (OM) mineralization (Zhu Zhaoliang, 1989) and possibly also $NH_4^+$-defixation are essential to meet the rice N demand. Understanding the patterns of soil mineral N and crop N uptake throughout the rice growing season are of particular interest to develop appropriate N fertilizer advice, while at present blanket N-doses are supplied regardless of the considerable cost to many South-East Asian farmers. Besides N, water supply is another important factor sustaining rice production because cultivated rice is highly sensitive to water shortage and requires 2500L water $kg^{-1}$ grain production (Bouman, 2009). Out of 75 million hectares of irrigated rice area, in Asia, 15-20 are expected to experience water shortage by 2025 (Tuong and Bouman, 2003). Dry season irrigated (Boro) rice contributes more than half of the national rice production in Bangladesh. Underground water is pumped up to keep paddy fields flooded during various growth stages (Parvin and Rahman, 2009; Price et al., 2013). This dependency on ground water reserves draws down the water table and makes irrigation water a costly input for farmers, approximating 25-30% of the production cost. Therefore the promotion of water-saving irrigation managements, especially alternate wetting and drying (AWD) and direct seeded rice (DSR), in South-East Asia and now also in Bangladesh is growing steadily. Both techniques could enhance water productivity, minimize non-beneficial water flows (i.e. seepage, percolation and evaporation) (Bouman et al., 2005; Tan et al., 2015), and N leaching losses from paddy fields.

Associated changes in alternation of aerobic and anaerobic conditions in paddy fields has, however, been reported to enhance gaseous N losses via nitrification-denitrification (Dong et al., 2012; Reddy and Patrick, 1975) and is expected to alter soil physicochemical properties like the use of oxidants for soil OM decomposition, level of dissolved OM, soil pH and Eh compared to continuously flooded, (CF) fields (Kögel-Knabner et al., 2010; Pan et al., 2014). Soil microbial activity and N supply processes are largely driven by these abiotic factors whose depth profiles are expected to differ strongly in continuously and non-continuously flooded fields. It is difficult to predict just how a rise in Eh and lowering of pH via re-aeration and concomitant decrease in methanogenesis (Minamikawa and Sakai, 2006; Moterle et al., 2013) and reduced species like $Fe^{2+}$ and $Mn^{2+}$ (Gotoh and Yamashita, 1966; Pan et al, 2014), will impact soil N-supply from non-continuously flooded paddy fields.

On the one hand it is generally assumed that net release under anaerobic conditions is higher due to lower metabolic N requirements of anaerobes under flooded (Kader et al., 2013; Ono, 1989; Patrick and Wyatt, 1964; Reddy and De Laune, 2008) than non-flooded or continuously aerated conditions. But flooding on the other hand could decline fertilizer derived and indigenous available N through enhanced immobilization (Cucu et al., 2014; Devêvre and Horwáth, 2000). Furthermore, in paddy soils facing short and frequent draining-rewetting events, SOM may decompose at a faster rate and $NO_3^-$ formed by nitrification may quickly lost by denitrification in subsequent wetting; together increasing C and N losses (Reddy and Patrick, 1975; Tan et al., 2015). Soil OM decomposition and consequent N mineralization in flooded paddy soils furthermore depends on the kind and amount of reducing and oxidizing agents, like $NO_3^-$, $Mn^{3+/4+}$, $Fe^{3+}$, $SO_4^{2-}$ and $CO_2$, with easily oxidizable substrates like dissolved OM and most abundant reducible agents like Fe- and Mn-(hydr-)oxides being most important (Li et al., 2010; Ponnamperuma, 1972). A link between N and Fe cycles was already suggested from our previous laboratory and greenhouse studies with Bangladeshi paddy soils (Akter et al., 2016; **Chapter 4**), where we found positive correlations and a close temporal synergy between dissolved Fe and soil mineral N buildup. OM adsorbed by clay minerals and Fe- and Mn- (hydr-)oxides is released as dissolved OM under reducing conditions by reductive dissolution or desorption via a pH rise and may be readily available for microbial degradation and thereby contribute to mineral N release, or act as an intermediate transitional pool for subsequent mineralization (Grybos et al., 2009; Huang et al., 2016; Li et al., 2010; Said Pullicino et al., 2016). Yet, net effects in the field could be complicated because Xu et al. (2013) for example, found that fluctuation in Eh due to multiple wet dry cycles increased dissolved OC content in the surface but decreased it in the deeper soil by diminishing leaching and percolation. Lastly, reduction of the $Fe^{3+}$ in clay minerals (e.g. vermiculite or interstratified vermiculite-chlorite) or dissolution of Fe-(hydr-)oxides coatings on clay surfaces at low Eh could also favor release of fixed $NH_4^+$, and hence influence soil exchangeable N levels (Brookshaw et al., 2016; Scherer and Zhang, 1999).

The majority of detailed studies on paddy soils' N mineralization have, however, been conducted in laboratories or green-houses under continuous flooding or draining conditions using soils from surface layers, with no ability to assess depth profiles of the dynamics of physicochemical variables affecting N mineralization from soil OM and applied N fertilizer in function of flooding. Therefore, a field experiment was conducted to test to what extent and depth, reductive dissolution of Fe and Mn, occurrence of anaerobic conditions and microbial activity differ between soils under continuous and water-saving irrigation alongside soil N supply. We expected that non-continuous flooding would lower soil N supply because 1°

aerobic OM degradation results in less net N-release than anaerobic microbial activity, 2°
$NH_4^+$-defixation would be limited and 3° release of dissolved OM is reduced compared to
under continuous flooding. We compared urea-fertilized and unfertilized paddy fields in
addition to compare urea fertilizer N-use efficiency in function of irrigation regime. We
conducted a depth-differentiated follow up of the dynamics of pH, Eh, dissolved C, solution
Fe and Mn *in-situ* under three irrigation managements (CF, AWD and DSR) in a young
floodplain paddy soil in Bangladesh during the Boro rice growing season. Simultaneously we
measured mineral N build-up in soil and plant, topsoil pH, and $CH_4$ and $CO_2$ emission as a
measure of general soil biological activity.

## 6.2. Materials and Methods

### 6.2.1. Site description, soil properties and materials

The field experiment was conducted in 2015 on a paddy field managed by the Soil Science
Dept. of Bangladesh Agricultural University (24°42′55″N, 90°25′47″E, average altitude 18 m).
The selected soil and management were typical for the North of Bangladesh: Rice-Fallow-
Rice cropping on a non-calcareous dark grey Floodplain soil, with a subtropical monsoon
climate, annual mean temperature of 25.8 °C and rainfall of 2427 mm (BMD, 2015) mostly
between April to October. We monitored soil biochemical properties, crop growth and N-
uptake during dry Boro rice growing season (January to May), where too low rainfall
necessitates flood irrigation of pumped-up ground water. Air temperature and rainfall data
were obtained from the weather station 2 km away from field, at the university campus.

The plow layer and plow pan extended from 0-15 cm and 15-21 cm depth, with bulk density
of 1.1 and 1.5 g $cm^{-3}$, respectively. The main physical and chemical properties of the initial
soil in surface (0-15 cm) and subsoil (15-25 cm) layers are given in Table 6.1. The soil
texture was silt loam with a neutral $pH(H_2O)$. Soil porosity, total C and N, ammonium oxalate
extractable Fe and Mn, and exchangeable $NH_4^+$ contents were greater in the surface soil
than in the subsoil. The levels of essential plant available nutrients in the puddle layer
remained above critical limits, except for K, Zn and Mo (BARC, 2012, Table 6.1). The rice
cultivar in this study was BRRI Dhan28 (developed by Bangladesh Rice Research Institute);
it is a predominant variety covering almost 33% of the total Boro rice area (out of 97%)
cultivating modern varieties. The average yield, height and growth duration was 6 t $ha^{-1}$, 90
cm, and 140 days respectively, of which the vegetative stage is almost 75 days, reproductive
stage 35 days and ripening stage 30 days.

Table 6.1 Relevant physico-chemical properties of the initial soil (n. d. not determined) and and critical soil nutrient limits in for rice cropping

| Soil properties | Surfacelayer (0-15 cm) | Subsoil (15-25 cm) | Critical limit in soil (mg $kg^{-1}$) (BARC, 2012) |
|---|---|---|---|
| Texture | Silt loam | Silt loam | |
| Bulk density (g $cm^{-3}$) | 1.1 ± 0.05 | 1.5 ± 0.04 | - |
| Porosity | 0.59 ± 0.02 | 0.47 ± 0.02 | - |
| Total C (% ± SE) | 1.41 ± 0.03 | 1.05 ± 0.14 | - |
| Total N (% ± SE) | 0.16 ± 0.01 | 0.12 ± 0.01 | - |
| pH-$H_2O$ (1:5) | 7.01 ± 0.1 | n.d. | - |
| $Fe_{ox}$ (g $kg^{-1}$) | 4.8 ± 0.4 | 2.4 ± 0.9 | - |
| $Mn_{ox}$ (g $kg^{-1}$) | 0.2 ± 0.0 | 0.1 ± 0.0 | - |
| CEC (meq 100 $g^{-1}$ soil) | 21 | 23 | - |
| Exchangeable $NH_4^+$ (mg $kg^{-1}$) | 14± 3 | 4.5 ± 0.5 | - |
| Ca-lac (mg $kg^{-1}$) | 1807 ± 56 | n.d. | 400 |
| K-lac (mg $kg^{-1}$) | 26 ± 1 | n.d. | 47 |
| Mg-lac (mg $kg^{-1}$) | 574 ± 19 | n.d. | 60 |
| Na-lac (mg $kg^{-1}$) | 111 ± 6 | n.d. | - |
| P-lac (mg $kg^{-1}$) | 18 ± 2 | n.d. | - |
| Si-lac (mg $kg^{-1}$) | 51 ± 2.5 | n.d. | - |
| Mo-lac (mg $kg^{-1}$) | 0.1 ± 0.0 | n.d. | 0.1 |
| Cu-DTPA (mg $kg^{-1}$) | 1.65 ± 0.02 | n.d. | 0.2 |
| Fe-DTPA (mg $kg^{-1}$) | 161 ± 6 | n.d. | 4.0 |
| Mn-DTPA (mg $kg^{-1}$) | 60 ± 6 | n.d. | 1.0 |
| Zn-DTPA (mg $kg^{-1}$) | 0.5 ± 0.05 | n.d. | 0.6 |

*6.2.2. Experimental design and management of water, nutrient and crop*

The field experiment was laid out in a split plot design with three water managements (DSR, AWD and CF) in the main blocks and two N levels ($N_0$: 0 and $N_{120}$: 120 kg N $ha^{-1}$) in the sub-plots with three field replicates per treatment (Fig. 6.1). Overall, 18, 20 $m^2$ subplots were established and main and sub plots were separated from each other by 50 cm and 30 cm earth bunds, respectively. To prevent exchange of water and fertilizer across plots, main blocks were separated by 2 m wide irrigation channels and plastic sheets till 45 cm depth. On CF plots ponded water was maintained at 1-8 cm above soil surface from transplanting until harvest (Fig. 6.3e). Plots under AWD regime were flooded from transplanting for two

weeks and then AWD was imposed from 15 to 52 DAT (approximately till panicle initiation stage). In each of the AWD plots, a PVC pipe of 30 cm length × 10 cm diameter with holes at the bottom 20 cm was installed. As soon as the water depth in the PVC tube reached at ~15 cm below soil surface (approximating soil water potential in the rooting zone between 0 to -10 kPa, Carrijo et al., 2017), irrigation was applied to a 4-7 cm flooded water level above soil surface and the plots were left to dry once again. Three consecutive cycles of AWD were required viz. lasting 7 (26-32 DAT), 5 (39-43 DAT) and 4 (49-52 DAT) days (Fig. 6.3e). From 52 DAT onwards again the plots were continuously flooded until harvest. On DSR plots BRRI Dhan28 was sown directly in dry soil 14 days before transplanting in case of AWD and CF. A nearly saturated soil moisture level was maintained for which only six times (on 7, 28, 45, 62, 77 and 99 DAT) irrigation water had to be supplied. From 62 DAT almost ponded water level was retained until harvest, except for soil saturation between 76-77 and 96-99 DAT (Fig. 6.3e). Underground water was pumped from a nearby irrigation channel and the irrigated volumes were recorded. No irrigation water had to be applied at all from rice plant physiological maturity (after 77 DAT in CF and AWD, from 99 DAT in DSR) until harvest, but heavy rain events flooded the plots.
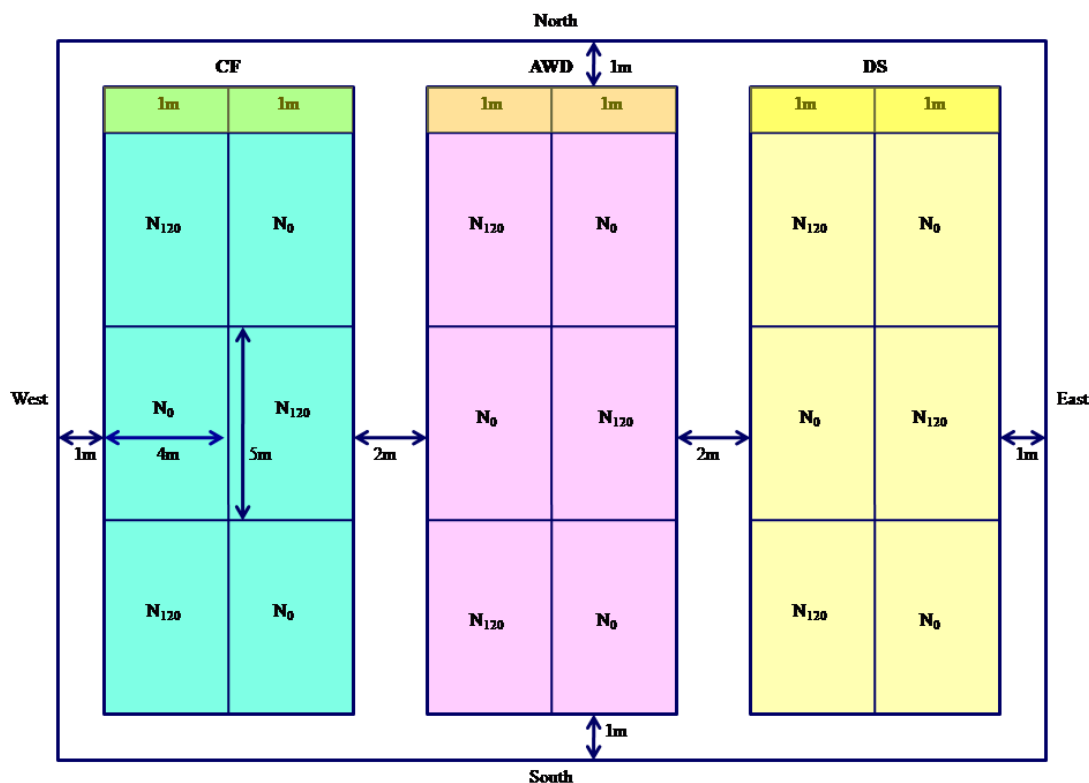


Fig. 6.1 Actual layout of the rice irrigation management field experiment with irrigation (3) x N management (2) combinations, the field was monitored between January to May, 2015 at the experimental field of Bangladesh agricultural University

155

The soils in all plots were prepared for rice cultivation by means of spade on 13 January, 2015 and leveled. Weeds and stubbles of the previous crop were manually removed from the field. After soil preparation, 5-7 pre-soaked and sprouted seeds of BRRI Dhan28 were sown per hill in DSR plots on January 14, 2015 with a spacing of 25 cm × 15 cm. Later on, CF and AWD plots were puddled on January 27, 2015 and 55 days aged seedlings of the same rice variety were transplanted on January 28, 2015 with a row-to-row distance of 25 cm and plant-to-plant distance of 15 cm. Basal fertilizers were broad-casted once one day prior to transplanting in all AWD and CF plots, and during sowing in all DSR plots at 20 kg P $ha^{-1}$, 70 kg K $ha^{-1}$, 10 kg S $ha^{-1}$ and 1 kg Zn $ha^{-1}$ as triple super phosphate (TSP), muriate of potash (MoP), gypsum and zinc sulphate, respectively. Nitrogen fertilizer was applied as urea into three equal splits in the $N_{120}$-AWD and $N_{120}$-CF plots (on 12, 32 and 45 DAT), and into four equal splits in the $N_{120}$-DSR plots (on the day of sowing, 32, 51 and 60 DAT). In DSR plots weeding was performed manually three times, while only twice in CF and AWD plots. To ensure uniform plant stand gap filling of missing hills was also performed once in all DSR plots on 43 DAT. An insecticide (Sabion60 EC: Diazinon 60%, McDonald Bangladesh Pvt. Limited) was applied once at tillering (36 DAT) and the application of insecticide was identical (50 ml per 20 liters water for all 18 plots) for CF, AWD and DSR treatments. At maturity, the rice crop in $N_0$- CF and AWD plots were harvested on April 27, 2015 (89 DAT), while those in $N_{120}$- CF and AWD were harvested on May 3, 2015 (95 DAT). Due to late maturity, all the DSR plots were harvested later on June 4, 2015 (127 DAT). To record grain and straw yields 134 (5.025 $m^2$) and 16 hills (0.60 $m^2$) per plot were harvested, respectively.

### 6.2.3. Monitoring of soil moisture, temperature, redox potential and pH

In two of the N-fertilized AWD and DSR plots, four PVC Tensiometer tubes were installed at plough layer (5 and 12.5 cm), plough pan (17.5 cm) and subsoil (28 cm) (Fig. 6.2a). Matric (h) potentials in head unit were measured frequently by means of an Electronic pressure sensor (SMS 2500 S), and the height of the water column in the tensiometer tubes above soil surface were recorded. During the drying cycle in two of the $N_{120}$- AWD (32 DAT) and DSR (44 DAT) plots, soil bulk density (by core method using metallic cores of 50 mm diameter × 52 mm height), porosity and moisture contents at puddle layer, plough pan and subsoil layers were determined. Soil water retention characteristic curves (pF) were deduced (data not shown) for pressure ranges of -10 to -100 cm and -100 to -15300 cm using the sandbox hanging-water column technique and pressure plate method at Ghent University. A quadratic regression model best fitted the pF-$\Theta_v$ data ($R^2 > 0.98$) and was used to convert measured matric potentials into $\Theta_v$ and % of water-filled pore space (WFPS) (Fig. 6.3c and d).

To acquire insight in the temporal evolution of depth profiles of redox potential (Eh) permanently installed soil Eh/T°-probes connected to a HYPNOS III-data logger (MVH Consult, The Netherlands) were used in two of the $N_{120}$-CF, AWD and DSR plots (Fig. 6.2b and c). Each probe was fitted with four platinum ring-shaped electrodes (measured Eh at 5.5, 12.5, 20.5 and 30.5 cm depth) and two temperature sensors (measured T⁰ at 8 and 28 cm depth). A single reference electrode (3M KCl saturated with AgCl) connected to the data logger was also installed permanently in the field. The Eh was recorded every 30 min for 84 days and corrected for the Ag/AgCl reference electrode's mV offset. Soil pH was measured *in-situ* by regular insertion of a portable pH-glass electrode (HACH sensION™ + pH1, USA) in the soil to depth of 2-4 cm.
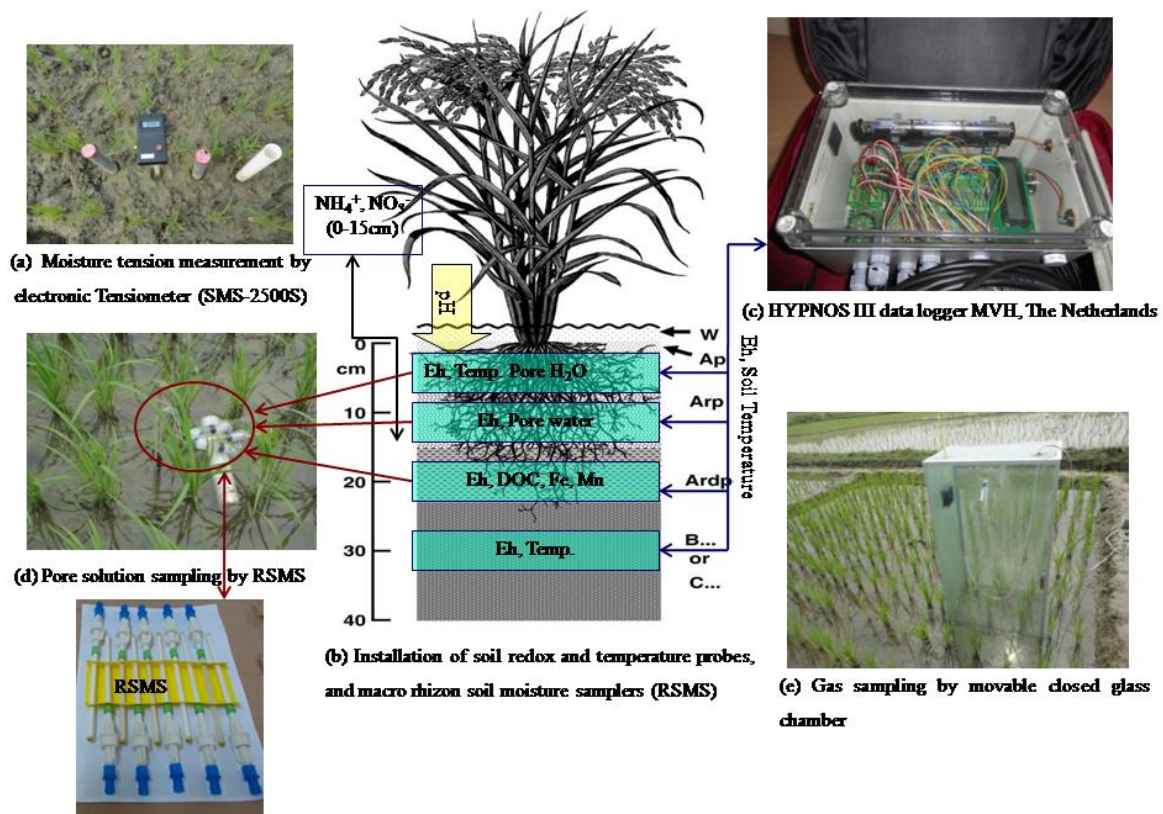


Fig. 6.2 Field monitoring of (a) soil moisture tension, (b) and (c) temperature and redox potential at different depths, (d) pore solution chemistry at three depths, (e) headspace gas sampling with large closed chambers to monitor $CO_2$ and $CH_4$ emission

*6.2.4. Collection and analysis of soil solution to monitor dissolved C, Fe and Mn*

To monitor dissolved C and occurrence of reductive dissolution of Fe and Mn, soil solution was sampled regularly with Macro Rhizon soil moisture samplers (RSMS) (Rhizosphere

Research Products, The Netherlands). Each macro RSMS was outfitted with a **9 cm long and** 4.5 mm outer diameter **porous** part (pore size: 0.15 μm). Macro RSMSs were installed permanently at 5.5 and 12.5 cm (horizontally), and 17.5 cm (diagonally) depth in 2 of the three replicate plots for each of the 2 N levels × 3 irrigation managements combinations, i.e. summing up to 36 RSMSs. Soil solution was then extracted at regular interval by connecting a vacuumed isoprene latex 30 or 60 ml syringe with luer-lock fitted PVC/PE extension tubing connected to the RSMS (Fig. 6.2d). Luer-locks were closed again immediately after sampling to avoid air entering the RSMS. A portion of the soil solution was transferred into 16.2 mg $K_3$EDTA-coated 9 ml plastic vacuum vials (Vacutest Kimasrl : Arzergrande (PD), Italy) by piercing the vial's septum with a needle connected to the syringe. The EDTA coating prevented re-precipitation of Fe and Mn from the sampled solutions. Simultaneously, the remaining soil solution was transferred into uncoated 9 ml vacuum vials (Vacutest Kimasrl, Italy) and frozen for later on dissolved C analysis. Soil pore solutions were analyzed for their Fe and Mn contents by ICP-OES on a radial plasma iCAP6300 spectrometer (Thermo Scientific, US). At near neutral pH practically any dissolved Fe and Mn exists as $Fe^{2+}$ and $Mn^{2+}$ and can be considered to equal total measured Fe and Mn in the soil solution samples. Total dissolved C contents were determined with a Shimadzu TOC-VCPN-analyzer (Shimadzu Corporation, Kyoto, Japan).

### 6.2.5. Soil and plant sampling for mineral N analysis

To follow-up the evolution of soil mineral N ($NH_4^+$-N and $NO_3^-$-N), soil was sampled 2-3 cm close to rice hills by a steel auger (2.5 cm inner diameter) at regular intervals until 89 DAT in AWD and CF plots, and up to 127 DAT in DSR plots. Separate samples were collected from the puddle layer (0-15 cm) and plough pan (15-21 cm). Soils were immediately transported to the laboratory and stored in the freezer at -20°C for later extraction. Fifteen g homogenized moist soil slurry (equivalent to about 10g dry soil) was extracted for 1h in Erlenmeyers on a shaker with 0.01M $CaCl_2$ at a 1:10 soil:extractant ratio. Filtered (Whatman no. 5) extracts were frozen (-20° C) until later analysis of $NH_4^+$-N and $NO_3^-$-N with a continuous-flow auto-analyzer (Skalar, The Nederlands). Simultaneous to soil sampling, rice plants of 3 to 4 hills plot[-1] were dug out on 0, 13, 28, 43, 62, 70 and 89 DAT in AWD and CF plots, and at the time points of, 62, 70, 84, 89 and 127 DAT in the DSR plots. Soil slurry surrounding roots was gently removed by washing with tap water and then distilled water. Plants were then oven-dried at 70°C for 72 hours, and the mass of shoots and roots were recorded separately per plot. The dried plant materials were ground and analyzed for their total C and N contents by means of a TruMac CNS analyzer (LECO). The net mineral N content in soil (mg kg^{-1}) and plant N uptake were recalculated into mg N kg^{-1} soil and then

summed. A zero-order kinetic model was then fitted to the evolution of N buildup in soil exchangeable N and plant N ($N_t$) with time: $N_t = N_0 + k*t$, where $t$ is the time (in days), $N_0$ the initial amount of mineral N and $k$ is the zero-order mineralization rate.

## 6.2.6. Assessment of total C mineralization via headspace $CO_2$ and $CH_4$ analysis

To assess the progression of soil C mineralization, $CO_2$ and $CH_4$ emissions were determined by the closed-chamber method (Fig. 6.2e) on all 18 plots. In addition soil $N_2O$ emissions were assessed simultaneously. Because of the ethereal nature of $N_2O$ emissions, a higher measuring frequency is required to robustly monitor seasonal $N_2O$ emissions. We therefore consider recorded $N_2O$-emissions just indicative of occurrence of soil denitrification and its order of magnitude and data are presented in the Fig. 6.11. Each glass closed-chamber consisted of a 100 cm × 50.5 cm × 30.2 cm chest covering 6 hills plot$^{-1}$ and was outfitted with a septum, two battery-operated (12 V) circulating fans to homogenize inner atmosphere and a thermometer on the top to record temperature inside the chamber during sampling. Gas sampling was performed weekly with extra samplings a day after N fertilizer top-dressings. To collect gas samples, a sampling chamber was placed and the bottom was sealed either by water or by saturated mud layer. Gas samples were drawn from the headspace after 0, 15 and 30 min by connecting 12 ml pre-evacuated glass vials (Exetainers®, Labco Limited Lampeter UK: 738W). The gas samples were analyzed for $CH_4$ content by injecting a 0.5 ml sample in a Thermo-Fisher Trace Ultra GC (Thermo Electron Corporation, US) equipped with packed columns and a FID. The $CO_2$ and $N_2O$ concentrations were analyzed by separately injecting 0.5 ml sample in another Trace Ultra GC equipped with a TCD for $CO_2$ and an ECD for $N_2O$. Gas standards were used to establish a linear calibration curve with each sample batch. The mass-based content of $CH_4$, $CO_2$ and $N_2O$ (mg chamber$^{-1}$) emission was calculated by the ideal gas law. C-Emission rates (mg m$^{-2}$ h$^{-1}$) were obtained by a linear equation between gas concentration and sampling time. For the DSR treatments a first-order model was fitted to cumulatively evolved C-emissions (in kg $CO_2$-C + $CH_4$-C emission ha$^{-1}$), while for the AWD and CF a parallel first- and zero- order kinetic model (Sleutel et al., 2005) used instead.

## 6.2.7. Statistical analysis

Statistical tests were performed with IBM SPSS statistics 23.0 (SPSS Inc., USA). Two-way ANOVA (N-fertilizer treatment × irrigation management) was carried out per sampling event to detect differences in mineral N build-up in soil and plant, Fe, Mn and dissolved C in solution. One-way ANOVA was also performed to detect differences in mineral N build-up in

soil and plant at harvest, grain yields and seasonal C emission. Linear and non-linear regression was used to model the net mineral N evolution in soil and plant, and cumulative C emission with time.

## 6.3. Results

### 6.3.1. Seasonal changes of rainfall, air and soil temperature, and percent water filled pore space

During the whole growing period of rice, rainfall amounted to 200 mm with intense precipitation between 61 to 84 DAT (March 30 to April 22, 2015) (Fig. 6.3a). The air temperature gradually increased from about 17 to 31°C over the growing season (Fig. 6.3a). Soil temperature followed a similar evolution with comparable daily variation at 8 cm depth, while diurnal fluctuation was absent at 28 cm depth. Soil temperature at 8 cm depth ranged from 16 to 31, 16 to 28 and 16 to 27 °C in the DSR, AWD and CF water regimes, respectively (Fig. 6.3a and b), i.e. with generally limited impact of irrigation management. At 28 cm soil depth temperature varied from 19 to 28 °C, across all treatments.

Measured $\theta_v$ in the puddle layer (5.5 and 12.5 cm) ranged from field capacity to saturation, i.e. between 0.45-0.57 and 0.48-0.61 $m^3$ $m^{-3}$ in $N_{120}$-AWD and $N_{120}$-DSR plots, respectively (data not shown). Throughout the season $N_{120}$-DSR plots' WFPS fluctuated from 81-100, 69-100 and 61-100%, with seasonal averages of 94, 95 and 98% at 5.5, 12.5 and 17.5 cm depth, respectively. In the $N_{120}$-AWD plots these WFPS ranges were 78-100, 84-100, 75-100 and 100-100% at 5.5, 12.5, 17.5 and 28 cm depth, respectively with seasonal averages of 96, 98, 99 and 100%. These observations indicate somewhat wetter soil conditions in the AWD than in the DSR plots, especially at 17.5 cm depth, while under DSR the extent of periodic soil drying was larger. Consecutive drying-re-flooding events were more frequent in the puddle layer (5.5 and 12.5 cm) than in the underlying plow pan and subsoil (Fig. 6.3c and d). Some very short-lived peaks (27, 61 DAT) in the DSR soil's moisture tension were observed at 17.5 cm depth coincided with subsoil drying and more frequent Eh readings did further indicate rises to oxic ranges (Fig. 6.4a), though the validity of the measurements were not beyond question.
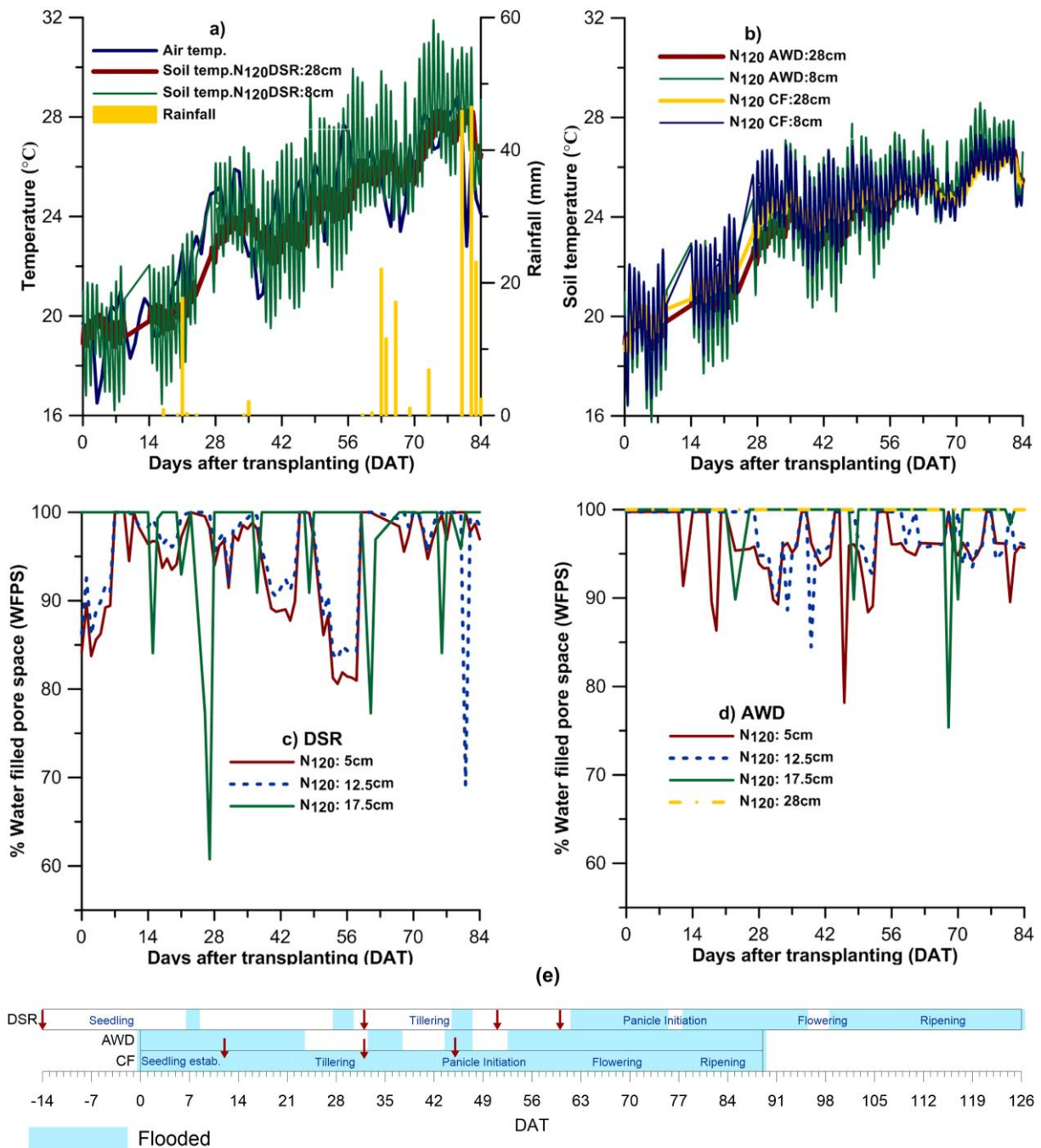
Fig. 6.3 Seasonal evolution of (a, b) rainfall, air and soil temperature, (c, d) WFPS % under water-saving irrigation management, and (e) flooded (blue zone), non-flooded (white zone) period with down arrows indicate urea top-dressed

### 6.3.2. Seasonal variations in soil pH and depth-distributed soil redox potential (Eh)

Throughout the season, soil pH remained at near-neutral ranges of 6.7-7.4 in CF and 6.9-7.8 in AWD, and very similar in $N_0$ and $N_{120}$ treatments (Fig. 6.4c and b). Topsoil pH was slightly

161

more alkaline under DSR, ranging from 7.1-8.1 (Fig. 6.4a). Water management markedly impacted evolution of soil Eh at different depths (Fig. 6.4). In DSR plots, the Eh in all soil depths stayed at or above ~ +300 mV during most of the growing season and suddenly decreased towards -200 mV in response to irrigation events at 28, 45 and 62 DAT (Fig. 6.4a). Under AWD and CF the initial Eh of +700 mV dropped within three weeks to almost -200 mV at all depths and these reductive conditions lasted in case of CF and at 30.5 cm in case of AWD until 75 and 72 DAT, respectively. Under AWD, Eh increased rapidly to about +200 mV during corresponding drainage episodes (26-32, 39-43 and 49-52 DAT) at 5.5 cm and to a lesser extent at 12.5 cm and sometimes at 20.5 cm depth, but also quickly decreased to ≤ -200 mV upon re-flooding. Hence compared to DSR, the response of Eh to drying-rewetting was smaller under AWD but more dissimilar for different soil depths and responses to drainage events were largely restricted to the puddle layer.
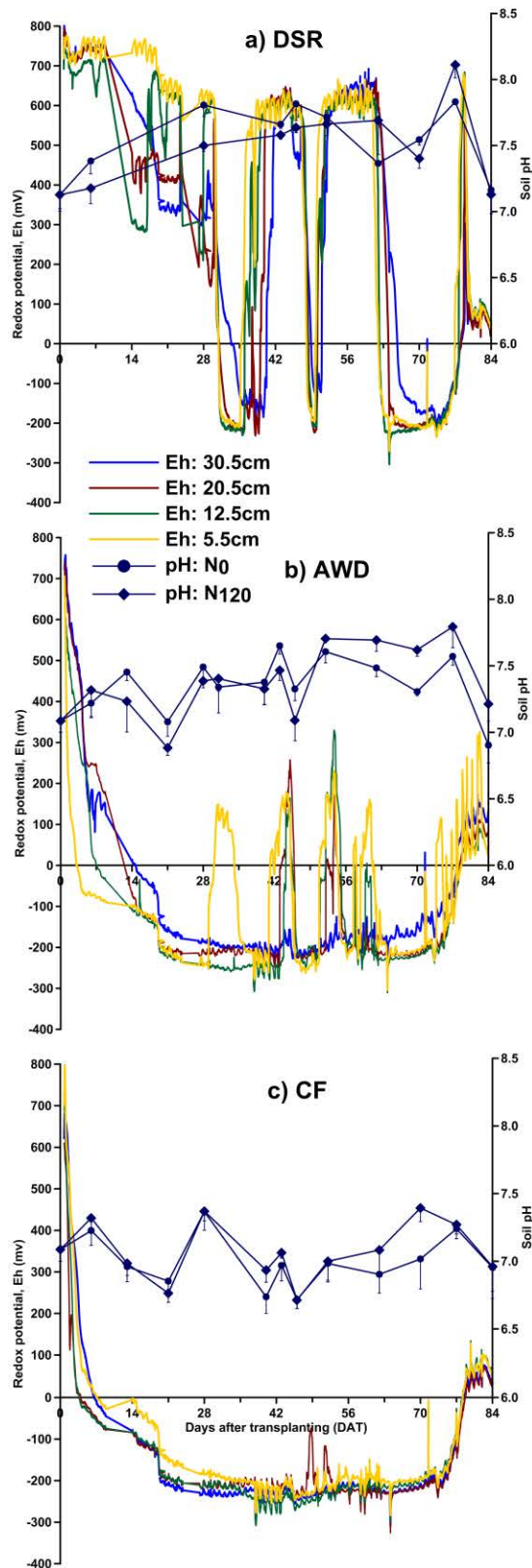
Fig. 6.4 Seasonal evolution of soil redox potential (Eh) and pH under different irrigation management with ($N_{120}$) or without ($N_0$) N-fertilizer application (vertical bars indicate standard errors around means, n=3)

*6.3.3. Seasonal evolutions of depth distributed soil solution Fe and Mn*

Overall, soil solution Fe and Mn concentrations (mg $l^{-1}$) at three different depths for both $N_0$ and $N_{120}$ treatments increased continuously across the season, but more under AWD and CF (Fig. 6.5). Levels lowered with depth in all N-fertilization and water management combinations. Except at 12.5 cm depth under $N_0$-CF, Fe levels exceeded Mn levels in the puddle layer, whereas the inverse was true for the plough pan (17.5 cm depth). Irrespective of N fertilizer application, Fe and Mn concentrations were negligible (0 to $\leq 1$ mg $l^{-1}$) in DSR plots until 52 DAT, after which they slightly increased. Linear release rates of solution Fe and Mn were 0.1-0.3 mg Fe $l^{-1}$ $d^{-1}$ ($R^2$: 0.6 to 0.9) and 0.04-0.09 mg Mn $l^{-1}$ $d^{-1}$ ($R^2$: 0.5 to 0.9) in the AWD and CF puddle layer (5.5 and 12.5 cm). At 17.5 cm the release rates of Fe and Mn were much lower: 0.004-0.01 mg Fe $l^{-1}$ $d^{-1}$ ($R^2$: $\geq 0.8$ except for $N_{120}$-CF) and 0.01-0.02 mg Mn $l^{-1}$ $d^{-1}$ ($R^2$: 0.4 to 0.8). Generally N-fertilizer application did not seem to have pronounced control on evolution of soil solution Fe and Mn under AWD or CF, an exception being lowered Fe levels at 12.5 cm in case of $N_0$-CF than in $N_{120}$-CF (Fig. 6.5c and f).
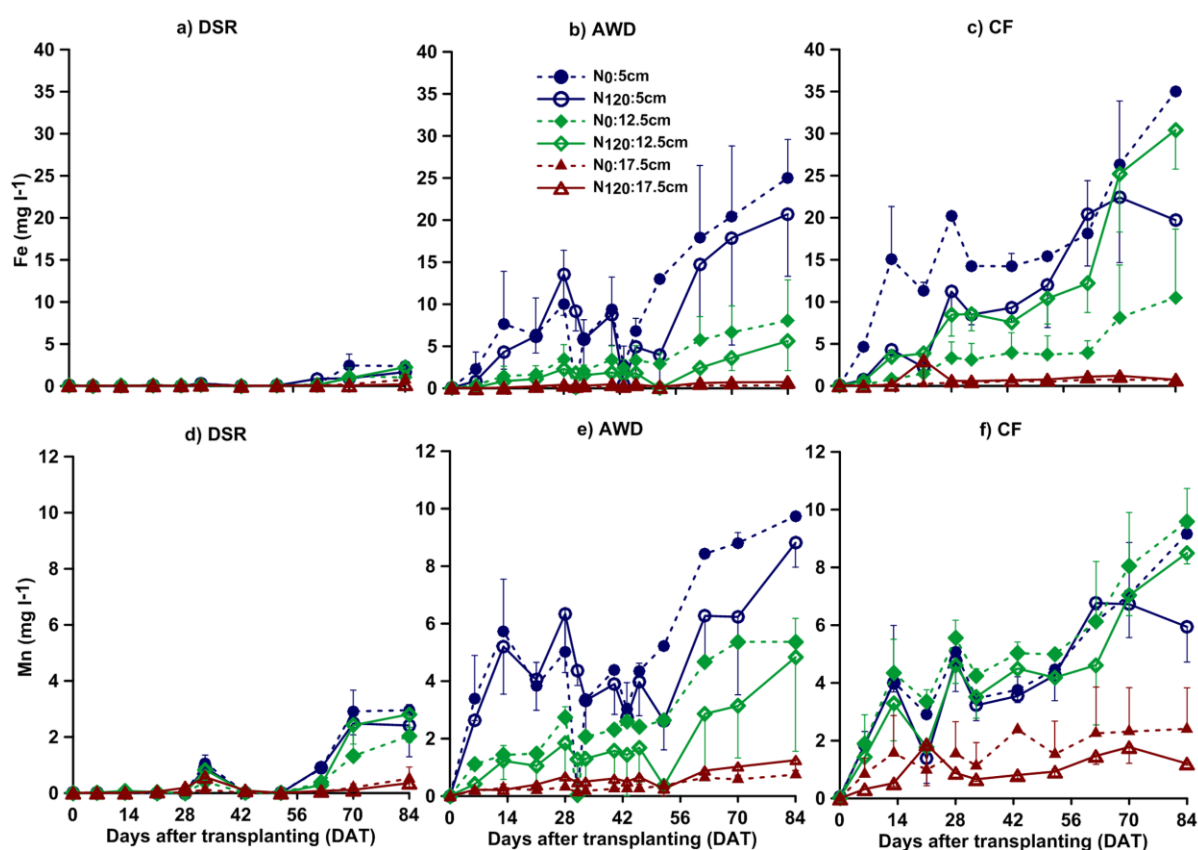


Fig. 6.5 Seasonal evolution of (a, b, c) Fe, and (d, e, f) Mn in soil solution at different depths and irrigation management with ($N_{120}$) or without ($N_0$) fertilizer application (vertical bars indicate standard errors around means, n=2)

*6.3.4. Seasonal patterns of gaseous C ($CO_2$-C + $CH_4$-C) emissions and soil solution dissolved C*

Methane and total $CO_2$ emissions were measured in all three irrigation managements as a measure of soil biological activity. Irrespective of N fertilizer application, the $CH_4$ effluxes from AWD and CF plots rose throughout the monitoring period and were minor (0 to ≤ 4 mg $m^{-2}$ $h^{-1}$) in case of DSR (Fig. 6.6). AWD events caused large fluctuations in $CH_4$ emission between 28-52 DAT. Mean $CH_4$ emission rates mostly did not differ between $N_0$ and $N_{120}$, but were significantly greater in case of $N_0$-CF compared to $N_{120}$-CF between 70-84 DAT (p<0.05). Significantly higher cumulative seasonal $CH_4$ emissions (kg $ha^{-1}$) were observed from plots under CF (275 in $N_{120}$ and 388 in $N_0$) than under AWD (164 in $N_{120}$ and 179 in $N_0$) and DSR (14 in $N_0$ and 23 in $N_{120}$) management (p<0.01).
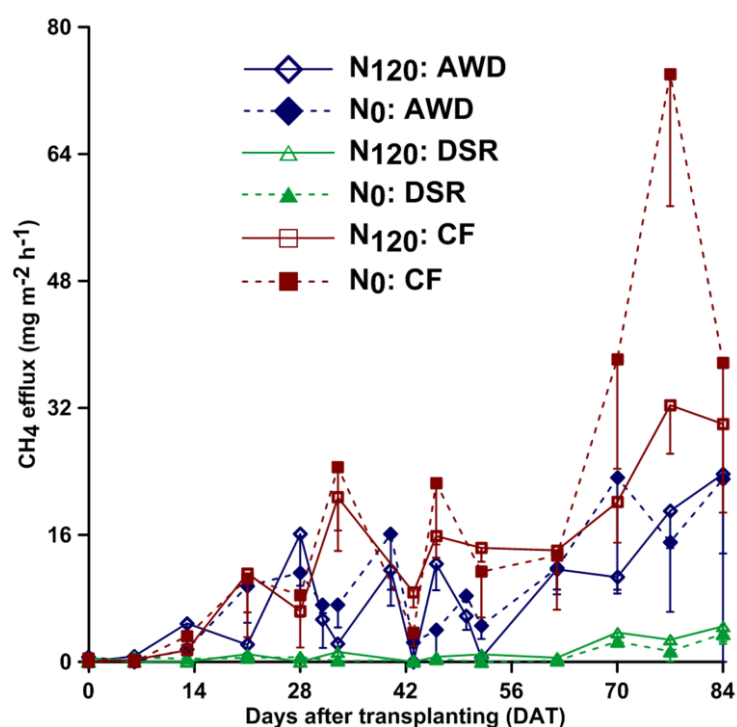


Fig. 6.6 Seasonal variations in $CH_4$ emissions under different irrigation management with ($N_{120}$) or without ($N_0$) fertilizer application (vertical bars indicate standard errors around means, n=3)

$CO_2$ efflux dominated the total gaseous C ($CO_2$-C + $CH_4$-C) emissions from the DSR and AWD treatments (Fig. 6.7), but was subordinate to $CH_4$ efflux in the CF treatment. Except for $N_0$-CF ($R^2$ = 0.80), first-order ($R^2$ ≥ 0.95, DSR) or parallel first- and zero- order kinetic models

(AWD and CF, $R^2 > 0.98$) fitted well to the cumulative $CO_2$-C + $CH_4$-C emission data (Fig. 6.7). The mean rate of $CO_2$-C + $CH_4$-C emission (in kg ha$^{-1}$ d$^{-1}$) was significantly greater under DSR than under AWD and CF ($p<0.01$) and there was no effect of N-application.



$N_0$AWD: C(t)=2.91*t+54.72*(1-e$^{-0.17*t}$); R2:0.99
$N_{120}$AWD: C(t)=3.38*t+69.17(1-e$^{-0.13*t}$); R2=0.98
$N_0$DSR: C(t)=1272.6*(1-e$^{-0.017*t}$); R2:0.99
$N_{120}$DSR: C(t)=1605.2(1-e$^{-0.007*t}$); R2=0.95
$N_0$CF: C(t)=2.41*t+833.25*(1-e$^{-0.000000012*t}$); R2:0.80
$N_{120}$CF: C(t)=3.04*t+32.09(1-e$^{-0.37*t}$); R2=0.99
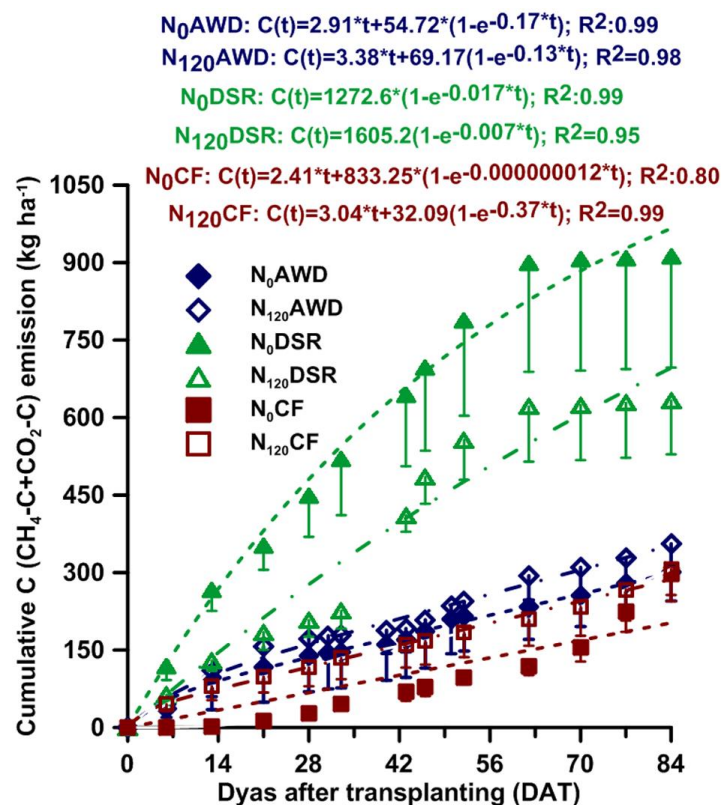
Fig. 6.7 Seasonal variations in observed and predicted ($N_0$ Fitted: - - - - - and $N_{120}$ Fitted: - · - · -) cumulative C emission ($CO_2$-C+$CH_4$-C) under different irrigation management and N-fertilizer application combinations (vertical bars indicate standard errors around means, n=3)

Soil solution dissolved C followed remarkably similar temporal patterns among the three considered soil depths in all treatments (Fig. 6.8). Overall, the temporal patterns in dissolved C were almost identical for the AWD and CF water managements, particularly between 6 to 84 DAT (Fig. 6.8b and c). Dissolved C varied from 120-196 mg C l$^{-1}$ on 6 DAT and increased gradually till 199-254 mg C l$^{-1}$ on 84 DAT. In the case of DSR, initially higher (184-439 mg l$^{-1}$) dissolved C levels declined rapidly within 13 DAT till 107-136 mg C l$^{-1}$, and stabilized (Fig. 6.8a).
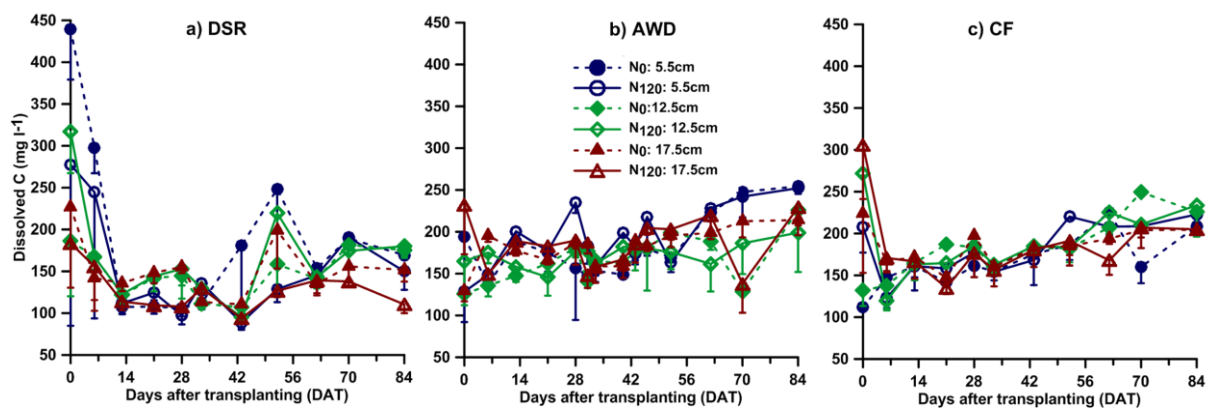
Fig. 6.8 Seasonal variations in dissolved C in soil solution at different depths under different irrigation management with ($N_{120}$) or without ($N_0$) fertilization (vertical bars indicate standard errors around means, n=2)

### 6.3.5. Seasonal patterns of soil mineral N evolution

The initial exchangeable N content in AWD and CF plots was 14 mg $NH_4^+$-N $kg^{-1}$. Higher contents with a substantial part as $NO_3^-$ were present in DSR plots due to earlier irrigation and urea application. Evolutions throughout the season were influenced by irrigation management (Fig. 6.9). Under DSR the soil $NH_4^+$-N remained at 4-15 mg $kg^{-1}$, while soil $NO_3^-$-N content declined from 13-23 mg $kg^{-1}$ to 0.1-4 mg $kg^{-1}$ after one week (Fig. 6.9a). During the first 13 DAT soil $NH_4^+$-N remained at higher levels of 14-23 and 14-31 mg $kg^{-1}$ under AWD and CF, respectively and then lowered to 3-21 and 5-17 mg $kg^{-1}$ (Fig. 6.9b and c). Soil $NO_3^-$-N contents were mostly negligible (~ 0 mg $kg^{-1}$), aside from minor $NO_3^-$-N peaks (0.1-0.8 mg $kg^{-1}$) in case of AWD.



Fig. 6.9 Seasonal variations of paddy soil puddle layer $NH_4^+$-N and $NO_3^-$-N under different irrigation management and N-fertilizer application combinations (vertical bars indicate standard errors around means, n=3)

### 6.3.6. Seasonal evolutions of soil exchangeable-N and N taken up by the rice plant

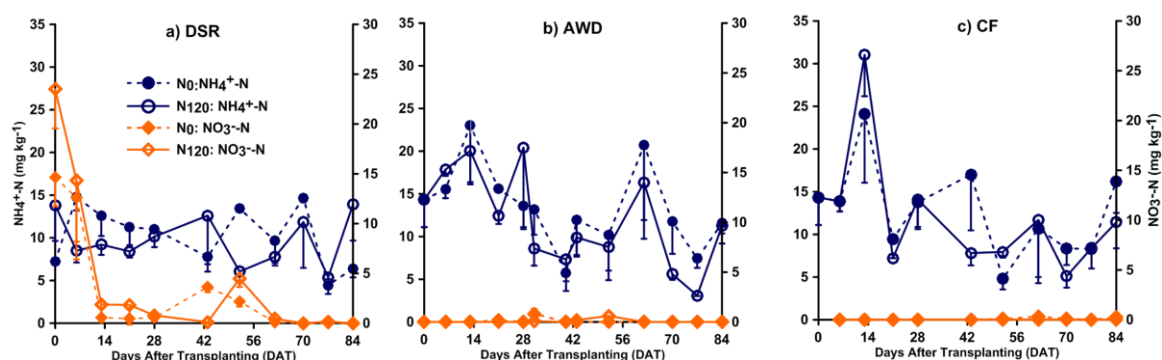Both irrigation and N management impacted the seasonal rate of net soil N-supply, defined here as apparent net N mineralization and quantified as the sum of N taken up by the rice plants and soil mineral N content (Fig. 6.10). The rice N-uptake predominantly shaped the net mineral N supply. Considerable plant N-uptake started primarily after 28 DAT in case of AWD and CF, and was delayed until 62 DAT under DSR (Fig. 6.10). In case of $N_0$ and $N_{120}$ treatments, total N uptake (at harvest) was significantly greater under AWD and CF than DSR, and the contents were identical for AWD and CF (Table 6.2) (p<0.01). Net mineral N supply was significantly greater under AWD and CF compared to DSR and no differences existed between AWD and CF (p<0.05). Nitrogen fertilizer application ($N_{120}$) enhanced net mineral N supply at most points in time, with significantly higher values (p<0.01) compared to $N_0$ between 62-89 DAT in the case of AWD and CF, and between 70-127 DAT in case of DSR. The final (at harvest) net mineral N supply (in mg kg$^{-1}$) were in the order: $N_{120}$-CF (54) = $N_{120}$-AWD (51) > $N_{120}$-DSR (41) > $N_0$-AWD (28) = $N_0$-CF (25) = $N_0$-DSR (22) (p<0.01). The grain yield (in t ha$^{-1}$ at oven dry basis) in $N_{120}$-CF (4.8 ± 0.2) and $N_0$-CF (1.6 ± 0.05) were statistically identical with those in $N_{120}$-AWD (4.1 ± 0.1) and $N_0$-AWD (1.6 ± 0.09), but significantly greater than in $N_{120}$-DSR (3.3 ± 0.4) and $N_0$-DSR (1.4 ± 0.01) (p<0.05) (Table 6.2). The attained grain yields were statistically similar in $N_{120}$-AWD and $N_{120}$-DSR, but significantly lower in $N_0$-DSR than $N_0$-AWD (p<0.05).
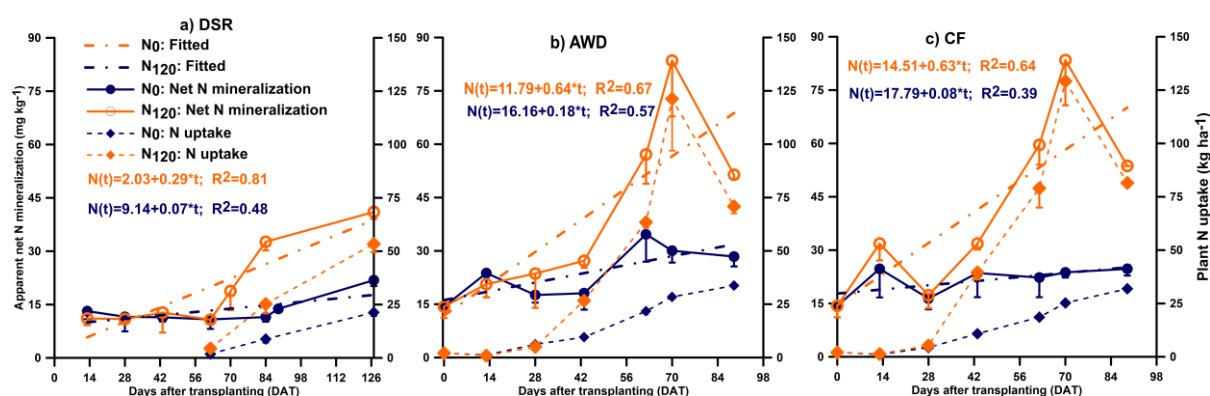


Fig. 6.10 Seasonal variations in plant biomass N and net mineral N supply (soil mineral N + plant biomass N) for different irrigation management and N-fertilizer application combinations (vertical bars indicate standard errors around means, n=3)

Table 6.2 Paddy rice grain yield, total biomass yield (oven dry basis) and N uptake (means ± standard error, n=3), and amount of water applied under different irrigation management during dry season, 2015 in Bangladesh

| Treatment | | Grain yield | Total biomass | N uptake | N recovery efficiency | Water applied (L ha$^{-1}$) | |
|---|---|---|---|---|---|---|---|
| | | (t ha$^{-1}$) | (t ha$^{-1}$) | (kg ha$^{-1}$) | (%) | Irrigation | Rainfall |
| DSR | $N_0$ | $1.4 \pm 0.01b^1$ | $2.9 \pm 0.06$ | $21 \pm 1.7b^1$ | 25 | 2371000 | |
| | $N_{120}$ | $3.3 \pm 0.37b^2$ | $7.4 \pm 0.72$ | $53 \pm 3.8b^2$ | | | |
| AWD | $N_0$ | $1.6 \pm 0.09a^1$ | $3.9 \pm 0.12$ | $34 \pm 1.3a^1$ | 32 | 5211000 | 2220000 |
| | $N_{120}$ | $4.1 \pm 0.09ab^2$ | $8.9 \pm 0.29$ | $71 \pm 3.3a^2$ | | | |
| CF | $N_0$ | $1.6 \pm 0.05a^1$ | $3.6 \pm 0.16$ | $32 \pm 1.8a^1$ | 42 | 6192000 | |
| | $N_{120}$ | $4.8 \pm 0.15a^2$ | $9.4 \pm 0.24$ | $81 \pm 0.6a^2$ | | | |

[2 & 1] Water management indicated by different letters within each N fertilized (p<0.01) and unfertilized (p<0.05) treatment are statistically different from each other

## 6.4. Discussion

### 6.4.1. Seasonal changes of soil temperature, moisture and Eh as influenced by irrigation management

Less frequent or absent rainfall during earlier crop growth stages (23 mm from 0 - 61 DAT: transplanting till heading) and rising air temperature (from 17 till eventually 31°C) typecast the measured growing season. Consistently during 1979-2006, the observed mean seasonal (Dec-Feb) rainfall was 41 mm, while the average seasonal temperature increased from 20.3°C (Dec-Feb) to 27.4ºC (Mar-May) (Rahman et al., 2012). Therefore conversion of non-continuously flooded irrigation systems should strongly impact soil moisture profiles and possibly soil temperature, both major drivers of microbial activity. Soil temperature, however, increased gradually by approximately 8°C towards the end of cropping season (Fig. 6.3a and b), regardless of irrigation management. Alongside $CH_4$ emissions and Fe in soil solution, indicators of anaerobic microbial activity, increased across all treatments, suggesting a general temperature control (Fig. 6.6 and 6.5).

Soil moisture was only measured in the two water saving treatments, as the CF was continuously flooded and expected to be at saturation throughout the growing season. Measured moisture contents ($m^3$ $m^{-3}$) fluctuated mostly only in the puddle layer, ranging from

field capacity to saturation. A first observation is that with both water-saving options, soil drying was relatively limited and near saturated soil conditions mostly persisted. A second observation is that soil drying remained shallow, as in the plough pan unsaturated conditions occurred only trice under AWD, and eight times under DSR, comparable to an experiment by Xu et al. (2013) with 11 wet-dry cycles where WFPS cycled between 60 and 100%. The confinement of AWD's impact to the puddle layer moisture also resulted in shallow effects on soil Eh and pH (Fig. 6.4). The only occasional rise in Eh at 20.5 cm depth and continuously low Eh at 30.5 cm (~ -200 mV) confirm that AWD management primarily only lifted soil reductive conditions in the puddle layer.

Soil Eh remained quite similar between depths in the case of CF and DSR, while a clear downward depth-gradient was conspicuous under AWD during drainage events. An evolution to generally positive Eh ($\geq$ 0 mV) from 77 DAT onwards occurred regardless of irrigation management and at all depths, likely due to entry of dissolved $O_2$ via unusually intense rainfall during the ripening phase in 2015. An initial rapid decline of soil Eh till -200 mV in AWD and CF fields at all depths likely resulted from fast microbial consumption of existing easily degradable C (Munch et al., 1978) and quick depletion of $O_2$ and $NO_3^-$ (Pan et al., 2014; Ponnamperuma, 1972). But also later in the growing season, Eh also dropped quickly to ~ -200 mV even within a day after re-flooding events in AWD and even in DSR treatments, as also seen by Minamikawa and Sakai (2005), but in contrast with a two-year monitoring of an Italian AWD-managed paddy field by Said-Pullcino et al. (2016). High dissolved C levels (> 5 mg dissolved C $g^{-1}$ SOC) were recorded throughout (Fig. 6.8) and this may have fueled rapid microbial activity and excess $e^-$-donation. Akter et al. (2016) showed that in the present soil about a third of dissolved C is OC, and if so dissolved OC levels were high, e.g. double than in Chinese paddy soils incubated by Hanke et al. (2013). In contrast to AWD, DSR's impact on Eh extended into the underlying plough pan and was much more pronounced (Eh rises till +600 mV), demonstrating temporary aerobic conditions. Much variation exists in actual implementation of AWD among studies depending on climate and soil texture. Here, only a limited number of three prominent drying cycles were imposed, which is probably not representative for lighter textured soils, but nevertheless not unrealistic as Bouman et al. (2007) and Howell et al. (2015) for instance implemented similar AWD management. Thus our results may apply to similar alluvial silt loam paddy fields, common in large parts of SE-Asia. The flooding of DSR plots later on in the Boro season (62-84 DAT) was not deliberate but caused mostly by unusual intensive precipitation and so dropping of Eh from about 60 DAT onwards is not typical (Fig. 6.4).

170

*6.4.2. Effects of irrigation and N managements on soil reductive processes*

Besides $O_2$, the contents and form of other inorganic oxidants (e.g. $NO_3^-$, $Mn^{4+}$, $Fe^{3+}$, $SO_4^{2-}$ and $CO_2$) determines their sequential or simultaneous contribution to the oxidation of OM after flooding (Gao et al., 2002; Mansfeldt, 2004; Hou et al., 2000). Occurrence of main soil reductive processes was quantified through monitoring of pore water Mn and Fe levels, and $CH_4$ efflux. Negative correlations between solution Fe and Mn and Eh at different depths, and positive correlations of solution Fe with soil temperature (r = 0.66 to 0.90; p<0.05) and dissolved C concentrations (r = 0.38 to 0.91; p<0.05 for most cases, Table 6.3) in the puddle layer in case of CF and AWD confirm patterns in solution Fe and Mn to indeed stem from reductive dissolution of Fe- and Mn- (hydr-)oxides under anoxic conditions (Pan et al., 2016; Said-Pullicino et al., 2016). Generally, soil solution Fe and Mn concentrations were greatest in CF followed by AWD, and then DSR, irrespective to N fertilizer treatments. In case of DSR, the positive Eh (usually > +300 mV) during the larger part of the growing season, should have been limiting for Mn and Fe reduction, and methanogenesis. This was confirmed by minor $CH_4$ effluxes (0 to ≤ 4 mg $m^{-2}$ $h^{-1}$) and solution Fe and Mn concentrations (0 to ≤ 3 mg $l^{-1}$). Regardless of N fertilizer application, drop off puddle layers' solution Fe and Mn on 21DAT in both AWD and CF (Fig. 6.5) possibly due to the sequential reduction of $SO_4^{2-}$ after $Mn^{4+}$ and $Fe^{3+}$ reductions, as well as forming precipitation with solution $Fe^{2+}$ and $Mn^{2+}$, under favourably reduced (Eh: -100 to -200mV) condition. In case of AWD on the other hand, fluctuating Eh between +200 to -200 mV during 28-58 DAT was as expected accompanied by relatively high but fluctuating Fe concentrations, and compared to CF low $CH_4$ efflux. The slightly lowered solution Fe and Mn at 5.5 cm depth on 33, 43 and 52 DAT coincided with AWD topsoil drying events, and so these drops were likely caused by re-oxidation of $Fe^{2+}$ to $Fe^{3+}$-oxides and precipitation of $Mn^{2+}$ to $MnO_2$ (Pan et al., 2014; Ponnamperuma, 1972). When considering the gradual cumulative evolution of $CH_4$-C + $CO_2$-C-emissions (Fig. 6.7) it becomes clear that further late increases in solution Fe and Mn (± from 55 DAT onwards) did not result from a generally enhanced microbial activity during the rice reproductive stage. Instead the increasing soil temperature thus appeared to specifically promote activity of Fe- and Mn reducers towards the end of the growing season.

Regardless of N fertilizer application and water management, much greater dissolution of Fe and Mn occurred at 5.5 and 12.5 cm depths than in the underlying plough pan at 17.5 cm depth, pointing out stronger microbial activity in the puddle layer. Also, this demonstrates that leaching of Fe and Mn and likely other solutes through the plough pan must have been

very limited. As expected, the overall concentrations of Fe (0-35 mg $l^{-1}$) exceeded those of Mn (0-10 mg $l^{-1}$) at 5 and 12.5 cm depths in all water regimes, indicating Fe reduction to be the dominant electron accepting process (Yao and Conrad, 2000) to support SOM decomposition in the puddle layer. However the opposite result was found at 17.5 cm depth, likely because preferential Mn reduction sufficed to maintain the more limited anaerobic microbial activity.

Table 6.3 Pearson correlations coefficient between $CH_4$ efflux, solution Fe and dissolved C

| Treatment | | Dissolved C 5 cm (mg l$^{-1}$) | Dissolved C 12.5 cm (mg l$^{-1}$) | Dissolved C 17.5 cm (mg l$^{-1}$) | $CH_4$ efflux (mg m$^{-2}$ h$^{-1}$) |
|---|---|---|---|---|---|
| $N_0CF$ | Fe : 5 cm (mg l$^{-1}$) | 0.68$^{*a}$ | 0.88$^{**}$ | 0.22 | 0.82$^{**}$ |
| | Fe : 12.5 cm (mg l$^{-1}$) | 0.61$^{*}$ | 0.87$^{**}$ | 0.37 | 0.89$^{**}$ |
| | Fe : 17.5 cm (mg l$^{-1}$) | 0.78$^{**}$ | 0.86$^{**}$ | 0.33 | 0.64$^{*}$ |
| | $CH_4$ efflux (mg m$^{-2}$ h$^{-1}$) | 0.40 | 0.80$^{**}$ | 0.20 | 1 |
| $N_{120}CF$ | Fe : 5 cm (mg l$^{-1}$) | 0.66$^{*}$ | 0.38 | -0.067 | 0.76$^{**}$ |
| | Fe : 12.5 cm (mg l$^{-1}$) | 0.63$^{*}$ | 0.38 | 0.03 | 0.87$^{**}$ |
| | Fe : 17.5 cm (mg l$^{-1}$) | 0.04 | -0.06 | -0.46 | 0.31 |
| | $CH_4$ efflux (mg m$^{-2}$ h$^{-1}$) | 0.50 | 0.24 | -0.17 | 1 |
| $N_0AWD$ | Fe : 5 cm (mg l$^{-1}$) | 0.79$^{**}$ | 0.55 | 0.75$^{**}$ | 0.89$^{**}$ |
| | Fe : 12.5 cm (mg l$^{-1}$) | 0.81$^{**}$ | 0.56 | 0.75$^{**}$ | 0.92$^{**}$ |
| | Fe : 17.5 cm (mg l$^{-1}$) | 0.81$^{**}$ | 0.59 | 0.67$^{*}$ | 0.81$^{**}$ |
| | $CH_4$ efflux (mg m$^{-2}$ h$^{-1}$) | 0.77$^{**}$ | 0.36 | 0.60 | 1 |
| $N_{120}AWD$ | Fe : 5 cm (mg l$^{-1}$) | 0.91$^{**}$ | 0.46 | 0.09 | 0.95$^{**}$ |
| | Fe : 12.5 cm (mg l$^{-1}$) | 0.86$^{**}$ | 0.62$^{*}$ | 0.11 | 0.91$^{**}$ |
| | Fe : 17.5 cm (mg l$^{-1}$) | 0.87$^{**}$ | 0.51 | 0.07 | 0.94$^{**}$ |
| | $CH_4$ efflux (mg m$^{-2}$ h$^{-1}$) | 0.83$^{**}$ | 0.5 | -0.03 | 1 |
| $N_0DSR$ | Fe : 5 cm (mg l$^{-1}$) | -0.08 | 0.50 | 0.00 | 0.95$^{**}$ |
| | Fe : 12.5 cm (mg l$^{-1}$) | -0.06 | 0.53 | 0.03 | 0.94$^{**}$ |
| | Fe : 17.5 cm (mg l$^{-1}$) | -0.10 | 0.40 | 0.01 | 0.89$^{**}$ |
| | $CH_4$ efflux (mg m$^{-2}$ h$^{-1}$) | -0.14 | 0.50 | -0.05 | 1 |
| $N_{120}DSR$ | Fe : 5 cm (mg l$^{-1}$) | 0.06 | 0.01 | -0.06 | 0.87$^{**}$ |
| | Fe : 12.5 cm (mg l$^{-1}$) | 0.06 | 0.09 | -0.16 | 0.92$^{**}$ |
| | Fe : 17.5 cm (mg l$^{-1}$) | -0.09 | -0.06 | -0.15 | 0.75$^{**}$ |
| | $CH_4$ efflux (mg m$^{-2}$ h$^{-1}$) | 0.11 | 0.13 | -0.07 | 1 |

[a] *Significant at the 0.05 level; **Significant at the 0.01 level

Fe and Mn levels were mostly lower at 12.5 than at 5.5 cm depth in CF and AWD plots. For AWD this depth gradient was reverse to expectation, as the more frequent and pronounced soil drying and lifting of Eh at 5.5 cm depth was thought to limit reductive dissolution of Fe and Mn. Apparently, regardless of mostly shallow AWD drying events, anaerobic microbial activity and Fe and Mn reduction still digresses with depth even within the puddle layer. These observations of a moderate depth differentiation in soil reductive processes with

irrigation management could be useful for validation of biogeochemical computer models like DNDC.

N fertilizer application had a subordinate impact on evolution of solution Fe and Mn. Higher Fe at 12.5 cm depth in $N_{120}$-CF than $N_0$-plots is likely due to stimulated anaerobic microbial activity indicated by higher C emissions (see Section 6.4.3), probably driven by enhanced crop growth (3-6 t ha$^{-1}$ more biomass yield) and root exudation (0.5 t ha$^{-1}$ more root yield) from 62 to 89 DAT (Table 6.2) in the N-fertilized plots. However, on the contrary N-application to AWD plots lowered Mn and Fe levels during transition from the vegetative to reproductive phase (52-70 DAT). Root growth was substantially greater (+0.49 t ha$^{-1}$ on 70 DAT) with N-application and so enhanced transport of $O_2$ to the rhizosphere might have restricted Fe and Mn-reduction, in line with Haque et al. (2015) and Haque et al. (2016).

*6.4.3. Seasonal dynamics of gaseous C ($CO_2$+$CH_4$) emission, as affected by irrigation and N-fertilization managements*

The intent of $CH_4$ and $CO_2$ emission monitoring was to measure of how irrigation and fertilizer application management impacted biological activity in the soil. Seasonal methane effluxes were strongly influenced by water regime; compared to CF, reductions of 47% and 93% under AWD and DSR were observed, respectively ($p<0.01$). This is in line with a lowering of $CH_4$ emission by 45% under intermittent flooding (Yagi et al., 1996) and by 36% with Eh-control irrigation (> -150 mV) (Minamikawa and Sakai, 2006). Levels in dissolved C did not follow the same ordination as $CH_4$ or total C emissions across treatments and were equal under AWD and CF, while in contrast, Said-Pullicino et al. (2016) found dissolved organic C levels to be clearly influenced by water regime. It should be noted though that high variation in dissolved inorganic C may have masked trends in dissolved OC. Probably though with the sufficient supply of dissolved OC, the higher $CH_4$ efflux in CF than in AWD and DSR is attributed to the continued maintenance of low Eh (~ -200 mV), a prerequisite for methanogenesis (Cai et al., 2003), in the entire 0-20 cm layer (Fig. 6.4 and 6.6). Temporal lowering of $CH_4$ effluxes between 28 and 52 DAT under AWD mostly coincided with drying events and a rise in Eh of the puddle layer, although the deeper soil layers remained anoxic (Fig. 6.3d, Fig. 6.4b and Fig. 6.6). The oxic soil conditions indicated by higher Eh values (~ +300 mV) in the DSR plots explain the consistently low $CH_4$ efflux (approximately ≤ 1 mg m$^{-2}$ h$^{-1}$). In conclusion, irrigation-control on $CH_4$-emissions was largely manifested by alteration of topsoil Eh, which indeed correlated negatively to $CH_4$-efflux (r = -0.13 to -0.81; p: 0.001 to 0.67).

Seasonal total $CO_2$-C+$CH_4$-C emissions were lower (p<0.01) under CF and AWD than in DSR (Fig. 6.7) in line with observations by Ma et al. (2017). Overall, greater dissolved C concentrations under AWD and CF relative to DSR might be associated with a temporal accumulation of intermediate metabolites under anoxic conditions (Hanke et al., 2013) or to release of C bound to Fe- and Mn- (hydr-) oxides, as across the season rises in soil solution Fe, Mn and C were concurrent in case of AWD and CF. It thus appears that differences in dissolved C dynamics between irrigation managements do not explain our observed trends in microbial activity, but perhaps instead slower and incomplete degradation of SOM in submerged soils logically explains the observed patterns (Devevre and Horwath, 2000). Across the Boro season rising soil temperature between January and March appears also to be a factor for the concomitant increase in $CH_4$ effluxes, as both factors were positively correlated for all CF and AWD treatments (r = 0.66 to 0.81; p<0.05). Such a general climatic control could have effected methanogenic activity both directly and indirectly through rising C-substrate availability. In case of CF and AWD, the continual rise of $CH_4$ efflux towards growing season are also expected to link equally (as identical biomass yield) to vigorously growing rice plant serving more C substrates by root exudates and sloughed plant parts, and well developed aerenchyma to transport $CH_4$. It should be noted though that inferred soil biological activity via day time static chamber-measured C-emissions includes plant $CO_2$ fluxes. Rice photosynthesis and respiration may have been different across the laid out irrigation and fertilizer combinations, with for instance faster root respired $CO_2$ efflux from the drier DSR soil and larger root biomass in case of AWD and CF. Also, some produced $CO_2$ and $CH_4$ could have stored into the soil in flood water, thus lowering $CO_2$ efflux to the atmosphere (Liu et al., 2013). Regardless of these limitations to our approach, C-emission patterns do suggest more than double C-mineralization under DSR than under AWD and CF with strikingly comparable total emissions. Across several years, adoption of DSR instead of current CF management may thus lead to a loss of soil C.

The contribution of $CH_4$ and $CO_2$ to total C emission largely depended on water managements with 98% of emissions coming from $CO_2$ under DSR, while the opposite was seen in case of CF, with 83% of emissions coming from $CH_4$. Under AWD the contribution of $CO_2$-C and $CH_4$-C to total C emission were 60% and 40% respectively. The acetoclastic pathway is usually most important and results in equal $CO_2$ and $CH_4$ production, and so the high share of C-emitted as $CH_4$ is surprising. Two potential explanations may be forwarded: 1° most CH4 was produced by the hydrogenotrophic pathway; 2° part of $CO_2$ emitted into the closed chambers was removed by photosynthesis. The disappearance of flood water level also stimulated $CO_2$ release relative to CF, as found by Liu et al. (2013) and Yang et al. (2017), resulting in comparable total C emission from AWD and CF plots (Fig. 6.7).

Nitrogen fertilizer application to CF and AWD plots did not affect seasonal $CO_2$+$CH_4$-C emission, in line with Zheng et al. (2007) and the comparable patterns in Fe, Mn, dissolved C and Eh with or without N-fertilizer applied. Under DSR, N-fertilizer application strikingly reduced C-emissions ($p<0.05$) ($N_{120}$-DSR vs. $N_0$-DSR), may be because a higher N availability to soil microbes (Chen et. al., 2014) then limited extracellular enzymatic activity and coupled decomposition of SOM (Cheng-Fang et al., 2012). The overall $CH_4$ efflux decreased by 29% in $N_{120}$-CF and 8% in $N_{120}$-AWD compared to $N_0$ counterpart treatments, much like Cai et al. (1997) found. In case of CF, greater effluxes between 70 and 84 DAT caused the total higher $CH_4$ emission from the $N_0$-CF plots, possibly due to depletion of soil $NH_4^+$ at the growing season's end, limiting activity of methanotrophs (Cai et al., 1997; Sun et al., 2016). Soil $NH_4^+$-N levels were, however, not lower in $N_0$-CF than in $N_{120}$-CF plots, but conditions in the rhizosphere may have differed strongly from our bulk soil measurements.

*6.4.4. Seasonal dynamics of soil mineral N, and net mineral N supply as influenced by irrigation, N fertilizer and relevant soil physicochemical properties*

Water management may impact a number of N transformation processes including gaseous N losses by volatilization and nitrification-denitrification, immobilization, plant N-uptake, clay interlayer fixation, and leaching (Craswell and Vlek, 1983; Li et al., 2015; Said-Pullicino et al., 2014). This field experiment was designed to follow-up the course of plant-available N in soil, and N taken up by plants, and N was expected to derive mainly from net soil organic N mineralization and fertilizer urea-N hydrolysis.

*6.4.4.1. Direct seeded rice (DSR) vs. transplanted rice*

Over the growing season, puddle layer (0-15 cm) $NH_4^+$- and $NO_3^-$-N contents did not differ greatly between AWD and CF, analogous to findings by Dong et al. (2012) but patterns under DSR deviated (Fig. 6.9). A first distinction was that only under DSR significant $NO_3^-$-N was initially formed (13-23 mg kg$^{-1}$), likely by nitrification given the oxic Eh (0-6 DAT). Soil $NO_3^-$-N levels quickly dropped to 0-4 mg kg$^{-1}$ at 13 DAT. Likely this was due to loss from the puddle layer because plant N assimilation was actually lower under DSR compared to AWD and CF until as long as 62 DAT (1-3 mg kg$^{-1}$ N in only 0.1-0.2 t biomass ha$^{-1}$). This failed crop establishment was due to a mismatch of the BRRI Dhan28 rice cultivar and the relatively dry topsoil conditions at time of seeding, while a variety suited to cooler temperatures and drier soil would likely have fared better. Though several $N_2O$ emission peaks were observed from both $N_0$- and $N_{120}$-DSR treated soils with maximum efflux on 46

DAT (Fig. 6.11), cumulative $N_2O$-N emission was only 1.3-2.0 kg ha$^{-1}$ which equaled to ~0.7-1.1 mg kg$^{-1}$. Hence $N_2O$ emission was not a significant N-removal process. $N_2$ emission peaks may have occurred but their detection *in-situ* is very challenging (Dong et al., 2012). Under DSR, the prevailing puddle layer WFPS fluctuated between 81-100% and Eh was mostly very positive, conditions under which complete denitrification or dissimilatory $NO_3^-$ reduction to $NH_4^+$ should have been negligible. Instead, much $NO_3^-$-N loss might have been caused by leaching with percolated water after rewetting of the DSR plots (Tan et al., 2013) but we did not quantify drainage. Given the nearly double C-emissions from DSR plots with limited crop growth until 62 DAT, a lower net mineral N supply compared to the AWD and CF plots might otherwise be logically caused by enhance biotic N-immobilization. Lastly, reductive Fe and Mn dissolution was much lower under DSR than CF and AWD and so would any release of Fe-bound dissolved organic N but this was not suggested from the almost comparable patterns of total dissolved C (Fig. 6.8).
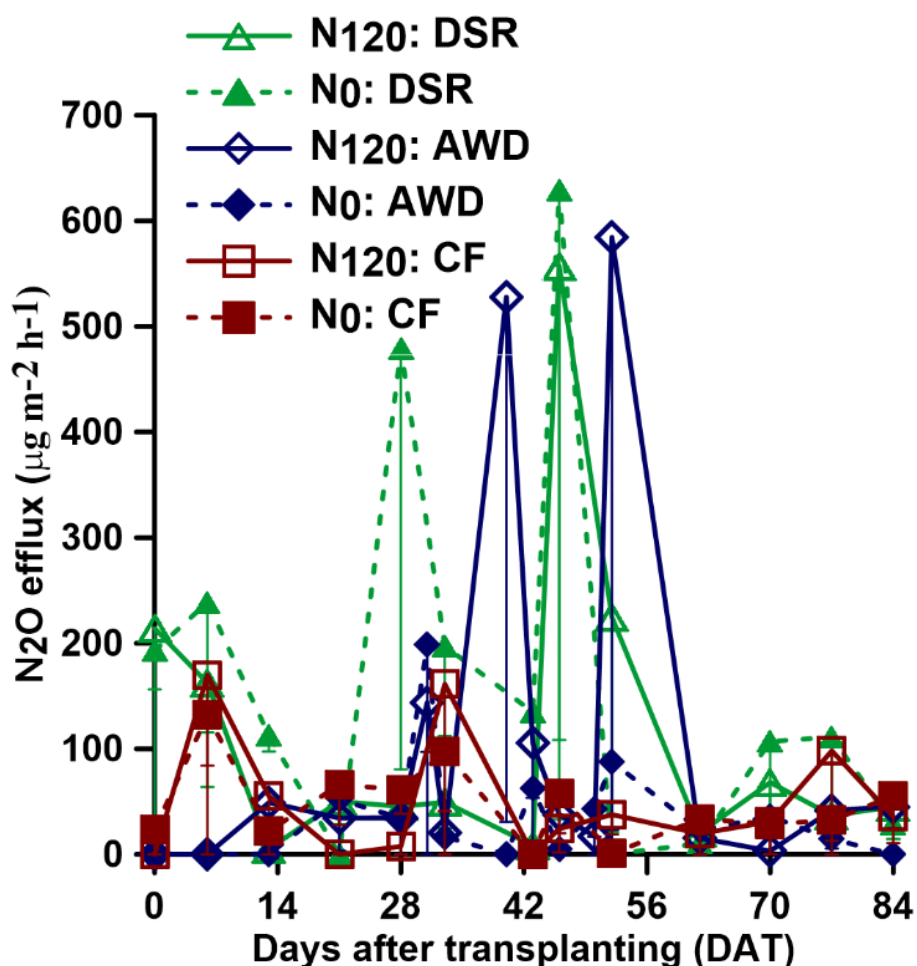


Fig. 6.11 Seasonal variations in $N_2O$ efflux in paddy field under different irrigation and N fertilizer managements (vertical bars indicate the standard errors of the means, n=3)

*6.4.4.2. Alternate wetting and drying (AWD) vs. continuous flooding (CF)*

Temporal evolutions of soil mineral N (+ plant N) were remarkably similar in AWD and CF managed plots. We discern two phases:

An overall rapid increase of soil $NH_4^+$-N during first 13 DAT in both AWD and CF plots stems likely from net N mineralization of initially present labile OM (Ponnamperuma, 1972; Zhang and Scherer, 2000). This initial peak was followed by a gradual decline of $NH_4^+$-N levels till 42 DAT by about 10-15 mg $kg^{-1}$. Notable plant N uptake started only from 28 DAT (2.6 to 4.0 mg $kg^{-1}$ ~4-6 kg $ha^{-1}$) and increased linearly until 70 DAT in $N_{80}$ (121-129 ± 11-24 kg $ha^{-1}$) and 89 DAT in $N_0$ (32-34 ± 1.5 kg $ha^{-1}$) (Fig 6.10). Development of the rooting system also mainly commenced from 28 DAT (data not shown). This offset between plant N uptake and lowering of soil mineral N matches with findings in a rice pot-growth study using soil from a nearby paddy field (Sonatala-1) (**Chapter 4**). Parallel monitoring of exchangeable-N in unplanted $N_0$-CF plots (data not shown) confirmed a decline of about 10-20 mg N $kg^{-1}$ between 7 and 21 DAT, just like in the planted experimental plots. Hence, the pronounced plummeting of quickly accumulated topsoil $NH_4^+$-N in all CF and AWD plots is apparently general in North-Bangladeshi paddy soils and suggests substantial transformation of $NH_4^+$- after several weeks of submergence.

Firstly, we consider abiotic N-immobilization. In previous incubation experiments with four Bangladeshi paddy soils similar to the present field, Akter et al. (2016) confirmed a consistent rise in non-exchangeable soil $NH_4^+$ by as much as 75 mg N $kg^{-1}$ within 2-4 weeks (approximately 120 kg N $ha^{-1}$). Initial fixed $NH_4^+$ of the present field experiment's soil was 200 mg N $kg^{-1}$ and it seems plausible that in the AWD and CF plots abiotic fixation accounted for the 10-20 mg N $kg^{-1}$ drop in exchangeable $NH_4^+$ between 14-28 DAT. These trends were very clear in the same experimental plots amended with 120 kg N $ha^{-1}$ in the 2014 growing season (Fig. 6.12), confirming clay interlayer-$NH_4^+$ to act as an important dynamic reservoir of fertilizer-derived $NH_4^+$ in the early growing season, with defixation afterwards. In support, reductive dissolution of Fe- and Mn-(hydr-)oxides occurred concomitantly in the first weeks after submergence and this has been thought to be a prerequisite for diffusion into otherwise partly shielded clay interlayer space and subsequent $NH_4^+$ fixation (Nieder et al., 2011). Furthermore, we recently calculated tentative electron balances for four floodplain paddy soils (**Chapter 4**) and inferred that temporary reduction of phyllosilicate structural $Fe^{3+}$ could be a relevant electron acceptation process in Bangladeshi paddy soils, as Mössbauer spectroscopy revealed typically high proportions of $Fe^{3+}$-containing chlorites and vermiculite. Bio-reduction of silicate-$Fe^{3+}$ has been confirmed by

many studies, as reviewed by Pentráková et al. (2013), and would in addition raise the negative charge of clays and thereby enhance $NH_4^+$-fixation. Since Eh was equally low and patterns in solution Fe and Mn comparable between CF and AWD in first weeks of the experiment, there is no reason to assume that N-fixation under both managements would differ.
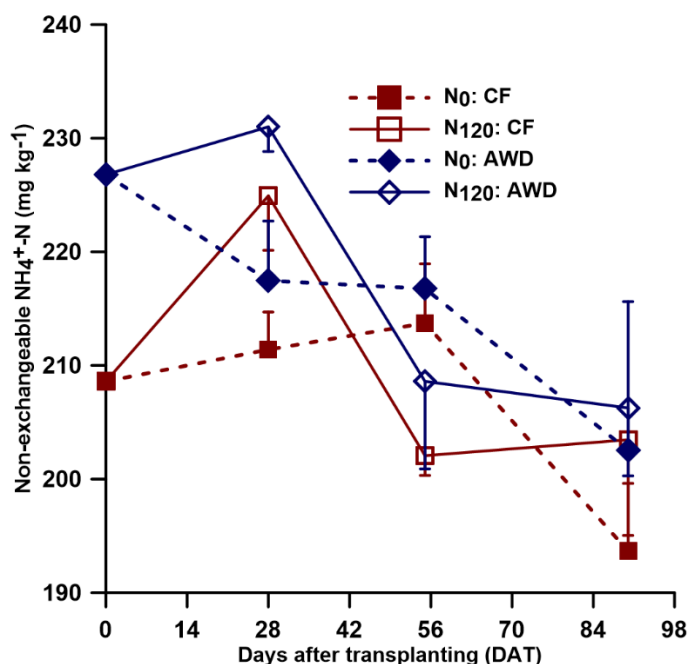


Fig. 6.12 Seasonal variations in non-exchangeable $NH_4^+$-N content for N fertilized and unfertilized continuously (CF) and intermittently (AWD) flooded paddy field during 2014 dry rice growing season (vertical bars indicate the standard errors of the means, n=3)

Secondly, gaseous N-emissions might partially explain early growing season lowering of soil exchangeable-N. However, substantial $NH_3$-volatilization seems unlikely because soil pH rose to only ca. 6.7 after several DAT. At this pH and 30°C, about 7.8% of dissolved $NH_4^+$ is under the form of $NH_3$ (or about 0.14 mg $NH_3$ $l^{-1}$) which is still far below the solubility maximum. Drying-rewetting cycles in AWD temporarily raised topsoil Eh to ~ +200 mV (Fig 6.4b), surprisingly not followed by any increase in soil $NO_3^-$-N. $N_2O$-N losses of any $NO_3^-$ or $NO_2^-$ produced by nitrification-denitrification were as under DSR, again relatively minor (0.4-1.3 kg $ha^{-1}$, Fig. 6.11). Given the lower Eh in the AWD soil $Fe^{2+}$-oxidation coupled to reduction of $NO_3^-$ (Wang et al., 2016) might as well have prevented its accumulation and in support of this abundantly present dissolved $Fe^{2+}$ did drop between 28 and 52 DAT. In any case seasonal $N_2O$-N effluxes from the field plots were about 0.3-0.8 mg $N_2O$-N $kg^{-1}$ and thus even to double these figures to account for possible $N_2$ losses, such emissions could

have caused only a fraction of the 10-20 mg $NH_4^+$-N $kg^{-1}$ loss between 14-42 DAT. As well Dong et al. (2012) observed quantitatively insignificant seasonal N loss by nitrification-denitricantion in N fertilizer applied AWD and CF paddy fields (4.0 and 0.5 kg $ha^{-1}$ $season^{-1}$ resp.).

Lastly, biotic N-immobilization seems another plausible explanation for initial drops in soil exchangeable N under CF and AWD. Cucu et al. (2014) reported immediate, by both biotic and abiotic immobilization of about half of applied fertilizer N in incubated Italian paddy soils, the greater part of which was released later on again. Analogously, biotic immobilization could explain in part why 120 kg urea-N amendment was followed by but a small rise in exchangeable $NH_4^+$ (Fig. 6.9). However, there is no reason to assume that after two weeks of intense net biotic N-release, suddenly microbial metabolism becomes N-limited resulting in N-immobilization between 14-28 DAT. Hence we hypothesize, that in the present experiment with no addition of exogenous C-rich OM like rice straw biotic N-immobilization does not explain lowering of soil exchangeable N after a first period of build-up, but this needs to be confirmed through microbial N monitoring.

From 28 DAT onwards soil $NH_4^+$-N levels remained more or less similar in both $N_0$- and $N_{120}$-AWD and CF treatments and this is likely explained by vigorous plant N-uptake as almost 80 to 90% of total N uptake occurred between 28-70 DAT. Inorganic N losses by biological oxidation of $NH_4^+$ to $N_2O$, by $Fe^{3+}$ or $SO_4^{2-}$, or reduction of nitrite to $N_2O$ by $Fe^{2+}$ or elemental S (Wang et al., 2017) might have also taken place given the ambient low Eh and substantial release of Fe in soil solution. The higher soil $NH_4^+$-N levels at 62 DAT under AWD than CF would well match projected lower Fe or S-reduction coupled $NH_4^+$-oxidation rates due to a rise in soil Eh, which was observed to be about +100 mV at 5 and 12.5 cm in the AWD at this time. From 28 DAT onwards plant N uptake competed with other N transformation processes (Craswell and Vlek, 1983; Dong et. al., 2012) and so summed amounts of soil exchangeable N and plant N at different growth stages approximated net mineral N supply (Fig. 6.10). The limitedness of differences in here investigated indicators of microbial activity and reductive processes between AWD and CF connect with also almost identical patterns of net mineral N supply (soil mineral N plus plant N). For instance, drainage in AWD during 28 to 52 DAT was insufficient to establish oxic soil conditions as Eh did not rise above ~ +230 mV (Fig. 6.4b). It is then not surprising that AWD drainage did not impact N cycling compared to CF, with just as well anoxic conditions. The clearly deviating patterns of Eh, WFPS%, evolutions of dissolved C, Fe and Mn under DSR compared to AWD and CF were also accompanied by lower release of mineral N in the DSR (see Section 6.3.6), and as

discussed earlier, despite much larger C-emissions. The question emerges if less net mineral N supply under DSR resulted from a lower N requirement by the rice crop that was clearly limited in its growth or if instead N-supply was limiting crop growth or a combination of both.

*6.4.4.3. Grain yield, fertilizer N-use efficiency and irrigation water use*

Despite resembling soil $NH_4^+$ evolutions of $N_0$ and $N_{120}$ counterparts, final grain yield and N-uptake was always significantly ($p<0.01$) greater with all N applied irrigation treatments (Table 6.2). Apparent fertilizer N recovery efficiency was higher in CF (42%) compared to AWD (32%) and DSR (25%), which re-confirms the vital role of indigenous paddy soil N supply for rice growth in all water managements (Table 6.2). So, while DSR saved 45% water relative to CF, there was however a significant impact on N-use efficiency because rice grain yield was 13 to 31%, and 16 to 19% lower than in case of $N_0$- and $N_{120}$- CF and AWD management, respectively (Table 6.2). We assume limited water supply to have mainly resulted in yield loss for DSR (Table 6.2); similarly Carrijo et al. (2017) reported that adoption of a severe AWD (soil water potential at rooting zone < -20 kPa) irrigation scheme, i.e. similar with the DSR treatment imposed here, declined yield by 23% and water use by 33% compared to CF. In this trial the applied 'safe AWD' saved only 12% water and it is then not very surprising that there were just marginal non-significant effects on indicators of soil reductive processes and microbial activity, N-availability, and grain yield. Howell et al. (2015) also found "no yield penalty" for AWD, but did reach 57% reduced water use. Our present observations for AWD and DSR may not be entirely representative as fierce late season precipitation interfered with the experimental setup. In more typical drier Boro seasons DSR yield and N-use efficiency could be even lower, but on the other hand irrigation water savings and yield may be higher in case of AWD. In fact several reports exist of significant yield increases with AWD, likely due to soil drying during grain filling stage by promoting faster C remobilization and root enlargement for maximum nutrient uptake (Carrijo et al., 2017).

**6.5. Conclusion**

Understanding how water management affects soil Eh, pH, reductive processes, microbial activity and total C emission should help in comprehending irrigation-impacts on paddy soil N supply. A first observation is that regardless of irrigation management dissolved C, Fe and Mn levels and $CH_4$ emissions all progressed over the Boro growing season. We hypothesize the typical gradual warming of soil by as much as 8°C had an overriding control on soil

microbial activity and solution chemistry. Our results indicated that safe alternate wetting and drying (AWD) caused Eh fluctuations between ~ +300 to -200 mV, and that these fluctuations were confined to the puddle layer only (0-15 cm). In spite of temporal oxidation events, soil conditions under AWD remain apparently sufficiently anoxic to result in a nearly continual rising of solution Fe, Mn and dissolved C much as under CF. In contrast, direct seeding and maintenance of a nearly saturated soil (DSR) produced temporarily more oxic soil conditions down to the underlying plough pan and subsoil and appeared to clearly limit reductive dissolution of Mn and Fe as well as $CH_4$-emission. Lower seasonal $CH_4$ emissions in $N_{120}$-CF (by 29%) and AWD (by 8%) than in their unfertilized counterparts might indicate rhizosphere methanotrophic activity was N-limited, though this was not confirmed from bulk soil exchangeable N analysis. In line with the observed comparable evolutions of indicators of soil reductive processes and gross microbial activity under CF and AWD, summed evolutions of soil mineral N and N taken up by the rice plant appear to be strikingly unaffected by these two irrigation managements. In contrast, C-emissions doubled, and N-use efficiency and rice yield were significantly lowered by adopting DSR irrigation management. In the conditions of North Bangladesh, inadequate rainfall during the early Boro growing season makes it imperative to apply enough irrigation water to dry seeded rice such that germination and seedling establishment is not inhibited, but ensuring that water is still saved. This field experiment confirmed the previously reported absence of soil exchangeable mineral N build-up with N fertilizer application. We hypothesize both abiotic and biotic immobilization mainly lead to fast N-removal. A dynamic equilibrium between 'fixed' $NH_4^+$, microbially 'immobilized' N and mineral N then implies that measures derived from monitoring of soil exchangeable N do not well represent the actual plant-available mineral N pool. Such fast N-transfers have been demonstrated previously, e.g. by Said-Pullcino et al. (2014), and our monitoring suggests a strong similarity between CF and safe-AWD. Further minimization of water use seems possible through adoption of AWD with no or acceptable yield loss, but this requires experimental confirmation. There does appear to be risk for crop failure under direct seeding in Northern Bangladesh but we found no direct indication that this is related to a limitation of N availability.

# Chapter 7

## General Discussion and Conclusions

## 7.1. Introduction

In natural wetlands including paddy fields whether fertilized or not, N release from soil organic N mineralization is a crucial process to control biomass production and yield. But N supply in wetland rice soils is the result of multiple processes, rendering it as one of the most complex biogeochemical cycles in agro-ecosystems. Both biotic and abiotic mechanisms are responsible for (bio)availability of soil (organic) N and consequent mineral N release. An extensive number of studies focused on the relation of anaerobic N mineralization with soil properties only, without indicators of relevant reductive processes and easily decomposable OM. Study of just N transformations in function of environmental and edaphic factors does not advance mechanistic insight. In reality such factors determine rates of soil processes like soil microbial activity, changes in pH, lowering of Eh to specific equilibria, availability and reactions of electron acceptors (reducible $Fe^{3+}$) and bioavailable OM. In this PhD we set forward to link anaerobic N mineralization with $Fe^{3+}$ and $Mn^{4+/3+}$ reduction, microbial activity and release of dissolved OM in young floodplain paddy soils. A series of experiments were performed to recognize dominant drivers of anaerobic N mineralization. Firstly we evaluated soil N release in the laboratory with or without artificial soil amendment by pedogenic oxides, and soils under natural variability, then we followed up net mineral N release in rice growth pot experiment. Finally we conducted field-scale experiments with or without N fertilizer application during wet season and during the dry season under various irrigations. The main findings of this PhD-research are discussed below thematically for relevant research questions and striking observations that motivate further research.

## 7.2. Does availability of reducible Fe and Mn limit anaerobic microbial activity and N mineralization?

$Fe^{3+}$ and $Mn^{4+/3+}$ have been previously identified as the two most important terminal electron acceptors supporting soil organic N mineralization in wetland paddy soils. Restricted availability of reducible Fe- and Mn- (hydr-)oxides might limit microbial activity in young floodplain paddy soils with relatively limited weakly crystalline (i.e. here quantified as $NH_4$-oxalate extractable) Fe ($Fe_{ox}$) and Mn ($Mn_{ox}$) oxides contents as opposed to well-developed terrace or upland soils (Kader et al., 2013). Addition of Hematite or Mn/Al mixed oxides (**Chapter 2: Objective O1**) to soil did not strongly impact temporal patterns of solution Fe and soil exchangeable $NH_4^+$-N. In all soils and treatments both Fe and Mn reduction and N-release were limited to a relatively short period of 2-4 weeks. However, the source of Fe

used, hematite, may not well represent the natural condition in which Fe is constantly reduced and re-oxidized (Qu et al., 2004). Hematite instead is more crystalline (~4.5% of added Fe was $NH_4$-oxalate extractable) and so this setup was not entirely fit to test if lack of reducible Fe would form a bottleneck for anaerobic N mineralization. Addition of Mn/Al mixed oxides did increase solution Mn levels and lowered or delayed $CH_4$ emission, pointing to preferential reduction of the applied Mn instead of other electron acceptors. Regardless, evolutions of exchangeable $NH_4^+$-N remained unaffected. In a Sri Lankan paddy soil (**Chapter 3**) mineralized N, levels of DOC and DON, $CH_4$ efflux, Fe release rate and pH rise were all positively interrelated (p<0.05), but none of these related to total C emission (Table 7.1)**.** This result therefore also disputes that $Fe^{3+}$ reduction as $e^-$ accepting process would constrain anaerobic microbial activity. In response to **research question Q1**: This leads us to conclude that lack of reducible-Fe or Mn did not form a bottleneck for soil mineral N release in the studied paddy soils.

In Chapter 4's rice growth pot experiment net mineral N supply rate did, however, positively relate to total C emission rate and rate of buildup of Fe (Table 7.1) **(research question Q3a).** Preliminary electron balance calculations, however, indicated Fe and Mn reductive dissolution as lesser $e^-$-accepting processes and accept only 2-25% and 1-7% of electron donated by mineralized C resp. for Noaddah-2, Melandoho and Sonatala-1a soils (**Chapter 4**). However, follow-up of just solution $Fe^{2+}$ may not have fully represented all release of $Fe^{2+}$ by reduction due to exchange with $Ca^{2+}$ and $Mg^{2+}$ on colloid surfaces, or by precipitation with carbonates, phosphates and sulphate. It is nearly impossible to experimentally quantify rate of formation of FeS, siderite and vivianite in a natural soil. With respect to FeS, information could have been inferred from $SO_4^{2-}$ levels in solution but then still assumptions would have to be made about the equilibrium between solution and solid phase. $SO_4^{2-}$ formation mainly starts at pe<4 and such conditions were not observed except in some of the investigated soils in **Chapter 3**. Regardless of the above we assumed that Fe precipiration became significant only as soon as solution Fe levels began to drop after reaching maxima. Rates of reductive Fe-dissolution were accordingly only based on kinetics describing the initial sigmoidal increase in solution $Fe^{2+}$ (and $Mn^{2+}$). Therefore the quantified kinetics of initial reductive Fe and Mn dissolution should not have been strongly offset by precipitation reactions.

Exchange of $Ca^{2+}$ and $Mg^{2+}$ by $Fe^{2+}$ was not quantified in this PhD research. Additional soil incubations with the soils used in **Chapter 4** displayed a similar trend in release of $Ca^{2+}$ and $Mg^{2+}$. From the evolution of molar concentration in solution we can roughly assume that a nearly equal amount of solution Fe was removed by ion exchange. If so, the actual rate of

reduction of pedogenic Fe was double than what was estimated on the basis of observation of trends in solution Fe. Reduction of pedogenic Fe's contribution to $e^-$ acceptation inferred in Ch4's $e^-$ balance then increased to 4-49%, which is still lower than ranges reported (66-84%) by Inubushi et al. (1984). This outcome still points out that other processes then pedogenic $Fe^{3+}$ reduction are involved as $e^-$ accepting process, one being possibly reduction of phyllosilicate $Fe^{3+}$.

In a field-scale *in-situ* study (**Chapter 5)** we again found temporal synchrony between soil $NH_4^+$-N, solution Fe, Mn and DON. However, net mineral N supply's negative and insignificant correlations with dissolved Fe (Table 7.1) in **Chapter 5** was in contrast with relations found throughout **Chapters 2, 3 & 4 (research question Q4)**. This lack of a clear relation between Fe reduction and N-release in the field in **Chapter 5** may be explained by the co-occurrence of multiple unquantified N-transformation processes like $NH_3$-volatilization and $NO_3^-$ leaching. Also, the duration of a field experiment surpasses that of incubation and pot trials. After the fast buildup of soil mineral N and release of Fe and Mn, a prolonged period of constant or lowering of soil exchangeable $NH_4^+$ (**Chapter 6**) and dissolved Fe and Mn and DOC or DON followed. It is then logical that for an experimental period spanning a full growing season mean concentrations or buildup rates of Fe and exchangeable $NH_4^+$ do not necessarily correlate anymore. This does not mean that Fe and N cycles no longer intersect after about one month of flooding: some unquantified N-transformations probably also are linked to Fe cycling, viz. $NH_4^+$-oxidation coupled to $Fe^{3+}$ reduction, DOM-$Fe^{2+}$-co-precipitation, $Fe^{2+}$-oxidation coupled to $NO_3^-$ reduction.

Per soil there were very similar temporal patterns of dissolved Fe and 1M KCl-extractable-$NH_4^+$, and both were positively related (Table 7.1), still suggesting direct or indirect ties between N-release and Fe reduction **(Objective O2)**. Next to Fe's role as electron acceptor, multiple mechanisms have been hypothesized for the connection between Fe reductive dissolution and $NH_4^+$ release. Reductive dissolution of Fe-(hydr-)oxide coatings on clay surfaces (2:1 phyllosilicates) would facilitate release or fixation of $NH_4^+$ from or into clay interlayers by diffusion, depending on the exchangeable $NH_4^+$ content (Scherer and Zhang, 1999). Given the general abundance of 2:1 clay minerals (e.g. vermiculite) (Kader et al., 2013) this mechanism may be relevant in Bangladeshi young floodplain soils. Gradual increase of both exchangeable and non-exchangeable-$NH_4^+$ during the 4-weeks anaerobic incubation indicated that flooding actually favored $NH_4^+$ fixation rather than its net release, in four farmers' fields soils (**Chapter 2**). And so we did not find proof that Fe-reduction would

stimulate soil exchangeable-N buildup by enabling diffusion of $NH_4^+$ out of 2:1 clay mineral interlayer spaces.

In sum relations of net (an)aerobic N mineralization to general soil properties and physicochemical processes applicable across paddy soils and at different scales is one of the greatest challenges being faced, as also clearly observed in this thesis's outcomes (Table 7.1). Despite lack of impact of added hematite and $Mn^{4+}$ as $e^-$ acceptors on soil exchangeable $NH_4^+$ for each soil **(Chapter 2),** the similarity between exchangeable $NH_4^+$ and dissolved Fe and DOC or DON were consistent accross **Chapters 3 to 5**. This generally indicated the (in)direct association of Fe(hydr-)oxides reductive dissolution and DOM (DOC/DON) release to apparent net anaerobic N mineralization, next to other soil properties or processes. Overall, our results demonstrated that only in Chapter 3 SOC and TN were important properties explaining net anaerobic N mineralization. Inconsistent with this, $SOC:Fe_{ox}$ and pH-KCl in rice growth pot experiment **(Chapter 4)**, as well as %silt and $Fe_{ox}$ content during wet rice season **(Chapter 5)** seemed to be the most striking soil characteristics related to apparent net anaerobic N mineralization, along with DON release. But Chapter 3 was conducted on Sri Lankan paddy soils and so these results are not really in contradiction with each other but just likely based on different soil types.

Table 7.1 Regression and Pearson's correlation coefficients (r) representing amount or rate of apparent net anaerobic N mineralization tie-ups with studied (Fe reductive) processes and soil properties for the investigated paddy soils at diffenerent scales

| Soil parameter | Amount ($N_t$) or rate of apparent net anaerobic N mineralization | | | |
|---|---|---|---|---|
| | **Chapter 2** | **Chapter 3** | **Chapter 4** | **Chapter 5** |
| | ($N_t$: mg kg$^{-1}$) | ($N_t$: mg kg$^{-1}$) | (rate: mg kg$^{-1}$ d$^{-1}$) | ($N_t$: kg ha$^{-1}$) |
| Sand (%) | | | | **-(r: 0.90\*)** |
| Silt (%) | | +(0.04) | | **+(r: 0.90\*)** |
| SOC | | **+(r: 0.79\*\*)** | -(0.34) | +(r: 0.72) |
| TN | | **+(r: 0.62\*\*)** | -(0.16) | +(r: 0.75) |
| C:N | | **+(r: 0.72\*\*)** | | |
| pH-KCl | | | **-(r: -0.63\*)** | +(r: 0.57) |
| Fe$_{ox}$ (g kg$^{-1}$) | | +(r: 0.08) | +(r: 0.55) | **+(r: 0.83\*)** |
| SOC to Fe$_{ox}$ ratio | | **+(r: 0.34\*)** | **-(r: -0.71\*\*)** | +(r: 0.54) |
| SOC to Mn$_{ox}$ ratio | | | | **+(r: 0.84\*)** |
| SO$_4^{2-}$ (mg kg$^{-1}$) | | | **+(r: 0.75\*\*)** | |
| Solution Fe (mg l$^{-1}$) | **+(r: 0.34-0.94)** **(p:0.002-0.7)** | | | -(r: 0.60) |
| Fe release rate (mg l$^{-1}$ d$^{-1}$) | | **+(r: 0.49\*\*)** | **+(r: 0.77-0.90\*\*)** | |
| DON content (mg kg$^{-1}$) | | **+(r: 0.73\*\*)** | | +(r: 0.70) |
| Mean DOC (mg kg$^{-1}$ or mg l$^{-1}$) | | **+(r: 0.71\*\*)** | **+(r: 0.59-0.62\*)** | |
| DOC release rate (mg l$^{-1}$ d$^{-1}$) | | | **+(r: 0.84-0.96\*\*)** | |
| MBC (mg kg$^{-1}$) | | **+(r: 0.66\*\*)** | | |
| MBN (mg kg$^{-1}$) | | **+(r: 0.50\*\*)** | | |
| C emission rate (mg kg$^{-1}$ d$^{-1}$) | | | **+(r: 0.99\*\*)** | |
| Mean CH$_4$ efflux (µg g$^{-1}$ h$^{-1}$) | | **+(r: 0.56\*\*)** | | |
| pH rise | | **+(r: 0.29\*)** | | |
| Chapter 3 | Eq.1 Nt(mg kg$^{-1}$) = 6.8SOC(g kg$^{-1}$)+666.3CH$_4$ efflux(µg g$^{-1}$ h$^{-1}$)-21.1; (R$^2$:0.67) | | | |
| | Eq. 2 N$_t$ (mg kg$^{-1}$) = 4.6DON(mg kg$^{-1}$)+0.1MBC(mg kg$^{-1}$)+0.04Eh(mV) -0.2MBN(mg kg$^{-1}$)+508.9CH4 efflux(µg g$^{-1}$ h$^{-1}$)-0.1; (R$^2$ = 0.77) | | | |
| Chapter 5 | N$_0$:N$_t$(mg kg$^{-1}$ 84 days$^{-1}$) = - 126.68+0.89Silt(%)+17.15mean pH; R$^2$:0.99) | | | |
| | N$_{80/60}$:N$_t$(mg kg$^{-1}$ 84 days$^{-1}$) = 73.61-1.37Sand(%)+1.49DON(mg kg$^{-1}$); (R$^2$:0.95) | | | |

*Significant at the 0.05 level; **Significant at the 0.01 level; non-significant: not bold

## 7.3. Sources of reducible Fe and Mn (research question Q3b)

The magnitude of $Fe^{3+}$ reduction is very much soil specific and logically depends on the changes in redox potential linked to content and availability of electron donors (SOM), but also to forms of pedogenic Fe. The temporal trends of exchangeable $NH_4^+$-N and dissolved Fe concentration per soil was identical in Chapter 2. We hypothesized that release of organic N bound to pedogenic oxides by reductive dissolution could promote subsequent mineralization. This instigated to identify the source of dominant $e^-$ accepting $Fe^{3+}$-bearing minerals. In **Chapter 4** an attempt was made to infer source minerals of dissolved Fe and Mn by establishment of relations between Fe and Mn solubility and pe + pH (objective O3). The theoretical $Mn_3O_4$-$Mn^{2+}$ equilibrium line's slope best matched the experimental data and suggested $Mn_3O_4$ as the most likely source oxidant for dissolved $Mn^{2+}$ (Ponnamperuma et al., 1969). Likewise, the empirical pe+pH values and dissolved Fe with theoretical equilibria suggested that amorphous $Fe_3O_4$ and $Fe(OH)_3$ for Sonatala-1 and Melandoho, $Fe(OH)_3$ for Noaddah-2, and diverse Fe minerals ($γ$-FeOOH, $γ$-$Fe_2O_3$ and amorphous $Fe_3O_4$) for Balina were the most likely oxidants, in line with Ponnameruma et al. (1967). Mössbauer spectroscopy, however, only identified goethite and ferrihydrite as prominent pedogenic Fe forms, contradicting our analysis of pe+pH/(log $Fe^{2+}$ + 2pH) diagrams. Possibly the latter were skewed by re-precipitation or re-oxidation of $Fe^{2+}$ and $Mn^{2+}$ and distorted by simultaneous dissolution of multiple source Fe minerals.

The Mössbauer spectroscopy analysis suggests that low crystalline goethite and ferrihydrite should be the main reducible pedogenic Fe minerals (**research question Q3b**). This matches with Qu et al. (2004)'s analysis that ferrihydrite is the preferential $e^-$ acceptor in Italian paddy soils. The highest and lowest soil solution Fe maxima were attained in the Balina and Sonatala-1 soils in line with the highest and lowest proportions of ferrihydrite-Fe (8.5% and 5.6% of Fe) in these two soils respectively. The high proportion of goethite-Fe (15.6% of Fe) in Sonatala-1 remarkably coincided with the lowest soil solution Fe buildup, suggesting that it was less available for reduction. The $e^-$ balance calculation demonstrated that $e^-$ acceptance involved in reductive dissolution of Fe and Mn should have received just 2-25% of all donated $e^-$. If this estimate is correct then pedogenic Fe reduction should not dominantly control microbial activity, C and N mineralization in these floodplain paddy soils (**Chapter 4**). However, it is unclear to what extent reduction of ferrihydrite and weakly crystalline goethite proceeds without discernible buildup of Fe in solution. Indeed dissolved $Fe^{2+}$ may be removed from soil solution by re-oxidation or by formation of insoluble siderite ($FeCO_3$), vivianite ($Fe_3(PO_4)_2$) or iron sulfide. The latter process seems less relevant because it may only occur in soils with Eh<-220mV when supply of Fe is limited (Zhang et

al., 2012). Formation of vivianite may also be limited since pore water P concentrations (measured in another lab incubation using 4 soils in Chapter 4) were minor (0.1-0.9 mg $l^{-1}$). Formation of siderite may have limited Fe buildup in soil solution. Follow-up of dissolved $CO_2$ and ortho-phosphate next to $Fe^{2+}$ could help to estimate these processes. Solution $Fe^{2+}$ might exchange with cations like $Ca^{2+}$ and $Mg^{2+}$, and so follow-up of Fe in solution only may lead to underestimation of pedogenic Fe-reduction. Maximum soil solution $Ca^{2+}+Mg^{2+}$ concentrations were 2, 4 and 6 mmol $l^{-1}$ in Noaddah-2, Melandoho and Balina soils, respectively, as assessed in additional 4-weeks lab incubation. These preliminary data suggest that possibly in **Chapter 4**, but perhaps also in other experiments we underestimated reduction of pedogenic Fe by a factor 2. The absolute quantification of $Fe^{3+}$-reduction is mainly important for correct assessment of $e^-$ balances, as in **Chapter 4**, while a probably more or less systematic underestimation of this process is less crucial when exploring correlations between rate of pedogenic Fe and Mn-reduction and net soil N supply and $CO_2$ emission as was done in **Chapters 2, 3, 5 and 6.**

### 7.4. Bio-reduction of $Fe^{3+}$ in clay phyllosilicates

From the analysis in **Chapter 4** and section **7.3** we postulated that overall anaerobic microbial activity may in part rely on the reduction of other silicate-$Fe^{3+}$ as well. Recently, Brookshaw et al. (2016) proved that chlorite and biotite can both be bio-reduced. Mössbauer spectroscopy in **Chapter 4** demonstrated that the Balina, Sonatala-1 and Melandoho soils contain chlorite and/or vermiculite, as previously confirmed via X-ray diffraction (Kader et al., 2013). Silicate structural $Fe^{3+}$ was found to represent 31-44% of soil Fe and so could be a relevant alternative $e^-$ acceptor **(research question Q3b)**. We, however, found no correlation between % of silicate $Fe^{3+}$ and C mineralization and could not yet confirm this hypothesis based on this study of only four soils.

### 7.5. Fe/Mn-reductive dissolution and pH shift as drivers of DOC/DON release

Dissolved OM (viz. DOC and DON) is generally regarded a bioavailable fraction of soil OM and could therefore play an important role in C and N cycling under anoxic conditions. Typical involved reactions are the production of soluble organic metabolites by microbes during soil reduction, release of OM bound to Fe- and Mn-(hydr-)oxides through reductive dissolution, desorption of OM from soil minerals due to changes in pH, and removal via DOM-$Fe^{2+}$-co-precipitation/complex formation (Grybos et al., 2009; Hanke et al., 2013; Kögel-Knabner et al., 2010). In **Chapter 3** pH-rise, Fe- and DON buildup rates, and mean DOC level were all strongly interrelated but none of these related to total C emission

(**Chapter 3**). This would suggest that general SOM decomposition is not the primary source of DOM. Possibly, in the currently studied soils DOM mainly originated from OM-release from soil minerals. Two parallel mechanisms i.e. release of DOM bound to Fe- and Mn-(hydr-)oxides or clay minerals by reductive dissolution or by desorption due to pH rise likely co-occur. Stronger correlations of DOC and DON-releases were found with Fe release rate than with shift in pH after submergence. Build-up rates of solution Fe and DOC were strongly correlated to each other, and both were further related to net mineral N released rate and C mineralization rate during flooded period in rice growth pot experiment (**Chapter 4**). Likewise in the field (**Chapter 5**)*,* DON's temporal trend synchronized and positively correlated with solution Fe and Mn per soil during flooding (except for the BAU site). This suggests DON release via reductive Fe and Mn dissolution is a more likely process rather than change in pH, particularly so because pH stayed at almost neutral level throughout. Considering all six soils together insignificant or even negative correlations were found between mean DON and solution Fe and Mn concentrations. This then suggests that between soils, solution DON is not just determined by release through reductive dissolution of Fe and Mn **(research question Q4)**. One candidate process could be DON removal through electrostatic attraction by negatively charged vermiculite surface (Sodano et al., 2016), which is abundant in the studied soils. In **Chapter 6**, we observed slightly greater dissolved C concentrations under AWD and CF than under DSR in spite a somewhat higher pH in the latter case **(research question Q5)**. Again, extra release of C bound to Fe- and Mn- (hydr-) oxides by reductive dissolution in case of AWD and CF explains these trends. In sum the most likely processes for solution DOC/DON in Bangladeshi paddy soils is reductive dissolution of Fe- and Mn-(hydr-)oxides, rather than pH rise, while both are likely equally responsible in the studied Sri Lankan paddy soil in **Chapter 3**.

### 7.6. Is DON release a relevant intermediate step in soil N supply?

DON has been thought to constitute a highly bio-available organic N pool and found to play a vital role in anaerobic N mineralization (Li et al., 2010; Said-Pullicino et al., 2014). As already mentioned in section **7.5** DOC and DON are most likely co-released by reductive dissolution of Fe- and Mn- (hydr-)oxides and to a lesser extent by pH rise. The modeled net mineralized N correlated with DON levels and C:N ratio in **Chapter 3** (Table 7.1). Net N mineralization rate also positively correlated with DOC release rate in **Chapter 4** (Table 7.1). In **Chapter 5** DON was also positively related to net mineral N supply and identified as one of the few predictor variables of modeled net mineralized N ($N_t$) in N-fertilized plots (Table 7.1). Temporal synchronized trends in soil $NH_4^+$-N, solution Fe, Mn and DON were found in **Chapter 2, 4 and 5.** So a paddy soil's ability to supply DON, indicative of soil OM quality,

may be a suited predictor of net soil mineral N release (**Chapter 3) (research question Q2b).** But **regardless,** the question remains if DON release itself is a relevant intermediate step for anaerobic N mineralization in Bangladeshi floodplain paddy soils. Causal relations between reduction of pedogenic Fe, release of DON and net soil N supply cannot be proven with the experimental setups used in this PhD. Indeed, DON could just as well be a product of soil organic N mineralization, and may or may not modulate finale mineral N release (Li et al., 2010). Also DON is perhaps just co-released through reductive dissolution of Fe- and Mn-(hydr-)oxides (Grybos et al., 2009) without being a substantial source of mineral N after its mineralization. In **Chapter 3**, C mineralization did not relate at all to net mineral N-release, while DON release did (Table 7.1): so the mindset that DON release is just a side product of gross microbial activity was not supported. Use of $^{15}$N-labeled DON bound to pedogenic Fe or Mn would be needed to unequivocally demonstrate the relevance of reductive Fe and Mn dissolution in soil N supply. However, pedogenic oxide bound OM is the resultant of a long-term sequence of growing seasons. Therefore any short-term experiment may not really be representative.

**7.7 Early growing season lowering of soil exchangeable N**

A rapid increase in soil exchangeable $NH_4^+$-N within the first two weeks of flooding seems to be very typical for all studied paddy soils (**Chapters 2, 3, 4, 5 and 6)** and stems likely from net N mineralization of initially present labile OM and limited immobilization under anoxic conditions. Afterwards declining soil $NH_4^+$-N levels were observed between 28-42 DAS/DAT in **Chapters 3, 5 and 6** (in CF and AWD). In **Chapter 3** there was no actively rice grown so plant N uptake can be excluded. But just as well also in **Chapters 5** and **6** the development of a rooting system and notable plant N uptake recommenced only from 28 DAT. Likewise in **Chapter 4** we saw already a 10-25 mg kg$^{-1}$ decline in soil exchangeable N from 14 till 31DAT (especially in Melandoho) while significant plant N uptake started only around 28DAT. This partial offset between plant N uptake and lowering of soil mineral N therefore seems to be general in the studied paddy soils. The most likely candidate processes are:

**1° Abiotic N-immobilization**: Fixed $NH_4^+$-N increased by 121 mg kg$^{-1}$ in Sonatala-1a and 41 mg kg$^{-1}$ in Melandoho after two weeks of submergence in **Chapter 2.** In the preceding year of **Chapter 6**'s irrigation management field experiment 5-15 mg $NH_4^+$-N kg$^{-1}$ was stored into clay-interlayer non-exchangeable $NH_4^+$ between 0 and 28DAT. Thus it seems plausible that the drops in exchangeable $NH_4^+$-N by about 5-20 mg kg$^{-1}$ between 14-28DAT could be at least partially be caused by abiotic $NH_4^+$-N fixation in clay interlayers. This process is furthermore thought to be pending on reductive dissolution of Fe(hydr-)oxides coatings on

clay minerals, which was always apparent in the first weeks after flooding. In addition, bio-reduction of silicate-$Fe^{3+}$ (Pentráková et al., 2013) at low Eh leads to buildup of negative charge, thereby enhancing $NH_4^+$-fixation (Scherer and Zhang, 1999; Scherer and Zhang, 2002).

Striking, however, is the observation in **Chapter 6** that the initial storage of $NH_4^+$-N in clay interlayers was followed by a steady drop of up to 30 mg N $kg^{-1}$ till 84DAT. So it seems that the previously termed 'fixed $NH_4^+$' pool is in fact dynamic and can act as a temporary reservoir for excess soil exchangeable $NH_4^+$. Possibly this release was driven by rice plant mining of exchangeable $NH_4^+$. Again, quantifying clay interlayer $NH_4^+$ defixation's share to net soil mineral N supply will require a stable isotope approach. But in such experiments it will be challenging to create a soil with a representative $^{15}N$-labeled fixed $NH_4^+$ pool because $NH_4^+$ 'fixed' on the outskirts and inner parts of clay interlayers differ in their proneness to be released into soil solution.


**2⁰** Gaseous N-emissions may partially explain early growing season lowering of soil exchangeable-N. In this PhD $NH_3$-volatilization was not quantified, as it is a difficult to capture process, especially in the field. Soil or solution pH fluctuated around neutral pH range ca. 6.7 to 7.4 in **Chapters 3, 5 and 6**. At pH 6.7 and 30°C, about 7.8% of dissolved $NH_4^+$ is under the form of $NH_3$, accounting for ~0.14 mg $NH_3$ $l^{-1}$, which is still far below the solubility maximum. Under these conditions $NH_3$ fluxes were likely minor. Though we did not measure $NH_3$ volatilization, at the very same season in a nearby (120m) field (**Chapter 6**) Gaihre et al (2016) indeed found only very minor $NH_3$-N loss by volatilization in AWD, ranging from 0.09 (unfertilized plot) to 3.21 (prilled urea broadcasted plot) kg $NH_3$-N $ha^{-1}$ $season^{-1}$. But other researchers (Dong et al., 2012; Yao et al., 2017) found much higher $NH_3$-losses (e.g. 17 and 27 kg $ha^{-1}$ $season^{-1}$ in N fertilized AWD and CF, resp. by Dong et al., 2012) from paddy fields and so we cannot exclude a considerable gaseous loss of N. We did not measure floodwater pH, but these authors did find floodwater pH to increased from 7.4 up to 8.4 after urea application.

Secondly, denitrification can lead to loss of soil N. In **Chapter 6** $N_2O$ emissions were monitored and found to constitute only 0.4-1.3 kg $ha^{-1}$. Despite temporary rising of Eh up to +100 to + 200mV soil $NO_3^-$-N (in mg N $kg^{-1}$) were ranged from 0.1-0.8 in AWD and 0.1-4.0 in DSR (**Chapter 6**), and 0.3-3.1 in **Chapter 3**, minor compared to the observed drops in exchangeable mineral N (by about 10-15 mg N $kg^{-1}$ in **Chapter 6** and 23 mg $kg^{-1}$ in **Chapter 3**. Nevertheless, complete denitrification could have been responsible for fast $NO_3^-$ removal and remains an uncertain flux in most soil N-cycling studies, including this PhD. $N_2$

emissions were not quantified though but likely strongly exceed $N_2O$-N losses and could significantly have been responsible for an important fraction (31.2-194 g ha$^{-1}$ d$^{-1}$ and 245-333 g ha$^{-1}$ d$^{-1}$) of early season dropping of soil (exchangeable) mineral N (Dong et al., 2012; Verhoeven, 2017).

$3^0$ $NH_4^+$-oxidation coupled to $Fe^{3+}$ reduction under water-logged condition at low Eh has been forwarded as a $NH_4^+$ removal process responsible of 8-61 kg $NH_4^+$ loss ha$^{-1}$ yr$^{-1}$ by Ding et al. (2014). Elevated solution Fe levels and clearly absence of $O_2$ and sufficiently low Eh ranges (+43 to -140mV) were standard conditions in the first 2-4 weeks after flooding throughout all experiments conducted in this PhD. So it could be reasonably hypothesized that Fe-ammox is a relevant N-removal process in young floodplain paddy soils in Bangladesh. Since the main product is $N_2$ it is, however, again difficult to quantify or even detect this N-transformation process in the lab, let alone in the field.

$4^0$ Lastly, **biotic N-immobilization** could have caused drops in soil exchangeable N after several weeks of submergence in **Chapters 6 and 3.** However, we see no immediate reason to assume that after two weeks of intense net biotic N-release, suddenly microbial metabolism becomes N-limited, then resulting in N-immobilization between 14-28 DAT. Also, biotic $NH_4^+$-N immobilization seems unlikely in **Chapter 3**, because MBN, MBC, DOC and DON for most soils declined towards 42DAS, while instead buildup of MBN would be expected.

## 7.8. Limited response of evolutions in soil exchangeable N and indicators of soil reduction to N fertilizer application

N fertilizer application may be evidently expected to alter temporal evolution of soil exchangeable N at least for some part of the rice growing season. Soil exchangeable N did, however, not differ between fertilized and unfertilized plots per soil in **Chapter 5** and per irrigation regime **in Chapter 6** for AWD and CF. These observations are in line with previous research that applied mineral N is quickly assembled into N-pools other than soil exchangeable N. Mechanisms described in **7.7** could also have led to fast removal of hydrolyzed $NH_4^+$-N from urea-applied soils in **Chapters 5 and 6.** We repeat 7.7s sub-conclusion that clay interlayer-$NH_4^+$ could act as an important dynamic reservoir of fertilizer-derived $NH_4^+$ in the early growing season (Said-Pullicino et al., 2014).

It is less clear how general anaerobic microbial activity and progression of soil reductive processes would be impacted by mineral N application. In general, N fertilizer application

had a subordinate effect on evolution of solution Fe and Mn: their overall trends did not differ greatly between N fertilized and unfertilized plots in **Chapters 5** and **Chapter 6.** Fe and Mn-reductive dissolution seemed to have been mainly limited during 52-70 DAT (Haque et al., 2015; Haque et al., 2016) by N-fertilizer application. The substantially greater root growth (+0.49 t ha$^{-1}$ on 70 DAT) in N-applied than in $N_0$-AWD plots could have enhanced transport of $O_2$ to the rhizhosphere, explaining less Fe and Mn reduction. In the case of DSR irrigation management, however, N-fertilizer application strikingly reduced C-emissions compared to $N_0$-DSR. Possibly the higher N availability to soil microbes (Chen et. al., 2014) may have limited extracellular enzymatic activity along with SOM decomposition (Cheng-Fang et al., 2012). N fertilizer application declined overall $CH_4$ efflux by 29% in $N_{120}$-CF and 8% in $N_{120}$-AWD compared to their $N_0$ counterparts. The greater $CH_4$ effluxes in $N_0$-CF between 70 and 84 DAT possibly result from depletion of soil $NH_4^+$ at the growing season's end, limiting activity of methanotrophs (Cai et al., 1997; Sun et al., 2016). Though soil $NH_4^+$-N levels were not lower in $N_0$-CF than in $N_{120}$-CF plots, conditions in the rhizosphere may have differed strongly from bulk soil measurements.

To summarize: We also conclude that impact of N-fertilizer application on bulk soil Fe and Mn reduction is relatively limited, probably because fertilizer N, as previously demonstrated, is quickly transported to other soil N pools, like clay interlayer $NH_4^+$. Clear fertilizer effects on crop growth did not directly result in changed evolutions of Fe and Mn either.

## 7.9. Impact of transition to water-saving irrigation on net mineral N supply and fertilizer use efficiency (research question Q5)

Water management is expected to impact net mineral N supply by influencing the degree of several N transformation processes such as volatilization, nitrification-denitrification, immobilization, plant N-uptake, clay interlayer fixation, and leaching (Craswell and Vlek, 1983; Li et al., 2015). In the designed field experiment with three water managements in **Chapter 6** overall buildup of soil exchangeable $NH_4^+$ was strikingly alike in case of AWD and CF. In line there were also just limited differences in indicators of microbial activity and reductive processes between AWD and CF in spite of AWD caused Eh fluctuations between ~ +300 to -200 mV in the puddle layer. Apparently under AWD still sufficiently anoxic conditions were maintained with no noticeable impact on Fe and Mn reductive dissolution, patterns in dissolved C or soil (exchangeable) mineral N. More severe soil drying under DSR did impact these patterns alongside Eh, soil $NH_4^+$-N level and net mineral N supply.

Apparent N fertilizer recovery efficiency was higher in CF (42%) compared to AWD (32%) and DSR (25%). So, while DSR saved 45% water relative to CF, there was however a

significant impact on N-use efficiency because rice grain yield was 13 to 31%, and 16 to 19% lower than in case of $N_0$- and $N_{120}$- CF and AWD management, respectively. In **Chapter 5** the attained recovery ($RE_N$: 28-56%), physiological ($PE_N$: 14-37 kg grain $kg^{-1}$ N uptake) and agronomic ($AE_N$: 4-14 kg grain $kg^{-1}$ N applied) efficiencies were comparable to previously reported values for paddy soils in South Asia. In both dry and wet rice seasons in North Bangladesh (**Chapters 6 and 5**) huge apparent losses of fertilizer N were seen. Future research should now address the question if this fertilizer N is truly lost from the puddle layer (gaseous, leaching and runoff losses) or partially stored in other soil N pools. Anyway, this again further signifies the role of soil N supply for rice crop N uptake. Finally, it should be noted that neither N uptake nor N supply related significantly with wet-season grain yield in both $N_0$ and $N_{80/60}$ in **Chapter 5**. Hence, likely other factors than N availability co-determined grain yield. Even if so, adapted N fertilizer dosage based on improved predictions of indigenous soil N supply will still at least reduce unnecessary costs for farmers and limit N-losses to the environment.

## 7.10. Recommendations for future research

Firstly lack of impact of Mn and Fe availability on net anaerobic N mineralization in hematite powder amended soils in **Chapter 2** may have been due to limited reducibility. This experiment could be repeated with soil amendment with more soluble Fe (hydr-)oxides (e.g. ferrihydrite) but ideally after mixing several oxidation and reduction cycles follow, so that realistic pedogenic Fe minerals form *in-situ.*

After initial soil $NH_4^+$-N buildup the rapid declining levels from 14-28/42 days after flooding, may be owed to clay interlayer fixation as negative charge builds up and any shielding pedogenic Fe has been dissolved (**Chapters 3, 5 and 6**). Fixation of $NH_4^+$ into clay interlayers is dynamic and might act as a temporary reservoir for excess (fertilizer)soil exchangeable $NH_4^+$ (**Chapter 5 and 6**). We also found steady drops of initially fixed $NH_4^+$ till growing season's ends in **Chapter 6.** Measurement of this non-exchangeable $NH_4^+$ pool clearly is needed in any future research on paddy soil N cycling. More fundamental investigations are needed to quantify clay interlayer $NH_4^+$ (de)fixation's contribution to net mineral N supply. But this would probably require a $^{15}$N-labeled isotope approach.

Based upon tentative $e^-$ balance calculation and identification of substantial $Fe^{3+}$ in structural phyllosilicates in Chapter 4, we found an indication that octahedral $Fe^{3+}$ reduction in chlorites, vermiculite and their interstratified forms might be a significant $e^-$ accepting

process in Bangladeshi paddy soils. Chronoamperometry could at least be used to assess the ability of clays in these soils to accept electrons.

Thirdly quantification of gaseous N losses via $NH_3$-volatilization and coupled nitrification-denitrification are crucial to explain early growing season lowering of soil exchangeable-N (**Chapter 3, 5 and 6)** and lower N fertilizer recovery efficiency **(Chapter 5 and 6)**. Despite difficulties to capture, a modified dynamic chamber method for ammonia volatilization and direct measurement of $^{15}N_2$ emission in $^{15}N$-labeled urea applied micro-plots at field scale was used previously by Dong et al. (2012) and such seems necessary to quatify these important gaseous N losses.

Fourthly, rice cultivation may enrich microbially reducible $Fe^{3+}$ and cause potential N loss by $NH_4^+$-oxidation coupled to $Fe^{3+}$ reduction under water-logged condition. This process also requires further research by $^{15}N$-labeled ammonium-based isotopic tracing and acetylene inhibition techniques.

Further attention is required on the release of DON/DOC and their impact on net anaerobic N mineralization. A potential approach may be use of $^{15}N$-labeled DON bound to pedogenic Fe to elucidate if DON acts as intermediate step for anaerobic N mineralization or just co-releases with Fe- and Mn-(hydr-)oxides reductive dissolution without being a source for mineral N following mineralization. Absence (**Chapter 3)** or presence (**Chapter 4)** of C emission's significant relations with interrelated net N mineralization, solution Fe and DOC/DON, indicated that DOM was released mostly by Fe(hydr-)oxides reductive dissolution and/or pH rise. Which one of both processes predominates across paddy soils deserves further attention.

Last but not least removal of an important share of dissolved $Fe^{2+}$ from soil solution by exchange with other cations (mostly $Ca^{2+}$ and $Mg^{2+}$), re-oxidation or by formation of insoluble siderite, vivianite or iron sulfide, need to be assessed to unequivocally evaluate the importance of $Fe^{3+}$ reduction as $e^-$ accepting process. Further measurement of dissolved $CO_2$ and other ions (mostly $Ca^{2+}$, $Mg^{2+}$, $K^+$, P and $SO_4^{2-}$) along with Fe and Mn will be required to that end.

# References

Adhikari, C., Bronson, K.F., Panuallah, G.M., Regmi, A.P., Saha, P.K., Dobermann, A., Olk, D.C., Hobbs, P.R., Pasuquin, E., 1999. On- farm soil N supply and N nutrition in the rice-wheat system of Nepal and Bangladesh. F. Crop Res. 64, 273-286.

Ahmed, M.A., Sharshar, T., Hassan, H.E., da Costa, G.M., De Grave, E., 2012. Measurements of natural radioactivity and mössbauer effect in some soil samples collected from the new campus of taif university, saudi arabia. J. Physics. 1, 31-37.

Akter, M., Kader, M.A., Pierreux, S., Gebremikael, M.T., Boeckx, P., Sleutel, S., 2016. Control of Fe and Mn availability on nitrogen mineralization in subtropical paddy soils. Geoderma. 269, 69-78.

Alam, M.L., Miyauchi, N., Shinagawa, A., 1994. Study on clay mineralogical characteristics of calcareous and noncalcareous soils of Bangladesh. Clay Science, 9, 81-97.

Alam, M.S., Hossain, M., 1998. Farmers' perceptions on yield gaps, production losses and priority research problem areas in Bangladesh. Bangladesh J. Agric. Econs. 21, 21-38.

Ando, H., Aragones, R.C., Wada, G., 1992. Mineralization pattern of soil organic N of several soils in the tropics. Soil Sci. Plant Nutr. 38, 227-234.

Anh, T.T.N., Olk, D.C., 2002. Prediction of crop nitrogen uptake and grain yield by soil nitrogen availability tests for irrigated lowland rice-Correlations between seasons for grain yield, plant nitrogen uptake, soil properties and soil availability indices. Omonrice 10, 67-73.

Armstrong, W., 1979. Aeration in higher plants. Adv. Bot. Res. 7, 226–332.

Atta, S.K., Mohammed, S.A., Van Cleemput, O., Zayed, A., 1996. Transformations of iron and manganese under controlled Eh, Eh-pH conditions and addition of organic matter. Soil Technol. 9, 223-237.

Bangladesh Meteorological Department (BMD), 2015. Available at: http://www.bmd.gov.bd/Document/climateofbangladesh.doc (accessed 29/06/2015).

BARC, Fertilizer Recommendation Guide (FRG), 2012. Bangladesh Agricultural Research Council, Dhaka, Bangladesh.

Bishwajit, G., Sarker, S., Kpoghomou, M.A., Gao, H., Jun, L., Yin, D., Ghosh, S., 2013. Self-sufficiency in rice and food security: a South Asian perspective. Agriculture & Food Security, 2(1), p.10.

Blakemore, L.C., Searle, P.L., Daly, B.K., 1987. Methods for chemical analysis of soils. Newzealand Soil Bur. Scientific Rep. 80, 103p.

Bouman, B. A. M., 2009. How much water does rice use. Rice Today. 8, 28–29.

Bouman, B.A.M., Lampayan, R.M., Tuong, T.P., 2007. Water Management in Irrigated Rice: Coping with Water Scarcity.

Bouman, B.A.M., Peng, S., Castaneda, A.R., Visperas, R.M., 2005. Yield and water use of irrigated tropical aerobic rice systems. Agric. Water Manage. 74, 87-105.

Brennan, E. W., Lindsay, W. L., 1996. The role of pyrite in controlling metal ion activities in highly reduced soils. Geochim. Cosmochim. Acta. 60.19, 3609-3618.

Brookshaw, D.R., Lloyd, J.R., Vaughan, D.J., Pattrick, R.A., 2016. Effects of microbial Fe (III) reduction on the sorption of Cs and Sr on biotite and chlorite. Geomicrobiol. J. 33, 206-215.

BRRI (Bangladesh Rice Research Institute), 2010. Proceedings of the BRRI Annual Research Review for 2008–2009, held on 1–6 January 2010, Gazipur, Bangladesh.

BRRI (Bangladesh Rice Research Institute), 2017. Modern Rice Cultivation. 20th edition.

Buresh, R.J., Reddy, K.R., van Kessel, C., 2008. Nitrogen transformations in submerged soils. In: Schepers JS, Raun WR (eds) Nitrogen in agricultural systems. Agron. Monograph 49. ASA, CSSA, and SSSA, Madison, WI, USA, 401-436.

Cai, Z., Tsuruta, H., Gao, M., Xu, H., Wei, C., 2003. Options for mitigating methane emission from a permanently flooded rice field. Glob. Chang. Biol. 9, 37-45.

Cai, Z., Xing, G., Yan, X., Xu, H., Tsuruta, H., Yagi, K., Minami, K., 1997. Methane and nitrous oxide emissions from rice paddy fields as affected by nitrogen fertilisers and water management. Plant Soil, 196, 7-14.

Carrijo, D.R., Lundy, M.E., Linquist, B.A., 2017. Rice yields and water use under alternate wetting and drying irrigation: A meta-analysis. Field Crop Res. 203,173-180.

Cassman, K. G., Peng, S., Olk, D.C., Ladha, J.K., Reichardt, W., Dobermann, A., Singh U., 1998. Opportunities for increased nitrogen-use efficiency from improved resource management in irrigated rice systems. F. Crop Res. 56, 7-39.

Cassman, K.G., Dobermann, A., Sta Cruz, P.C., Gines, G.C., Samson, M.I., Descalsota, M., Alcantara, J.M., Dizon, M.A., Olk, D.C., 1996. Organic matter and the indigenous nitrogen supply of intensive irrigated systems in the tropics. Plant Soil. 182, 267-278.

Cassman, K.G., Dobermann, A., Walters, D.T., 2002. Agroecosystems, nitrogen-use efficiency, and nitrogen management. Ambio: J. Human Environ. 31, 132-140.

Cha-un, N., Chidthaisong, A., Yagi, K., Sudo, S., Towprayoon, S., 2017. Greenhouse gas emissions, soil carbon sequestration and crop yields in a rain-fed rice field with crop rotation management. Agric. Ecosyst. Environ. 237, 109-120.

Chen, X., Wang, X., Liebman, M., Cavigelli, M., Wander, M., 2014. Influence of Residue and Nitrogen Fertilizer Additions on Carbon Mineralization in Soils with Different Texture and Cropping Histories. PLoS ONE. 9, e103720.

Cheng, Y.Q., Yang, L.Z., Cao, Z.H., Yin, S., 2009. Chronosequential changes of selected pedogenic properties in paddy soils as compared with non-paddy soils. Geoderma. 151, 31–41.

Cheng-Fang, L., Dan-Na, Z., Zhi-Kui, K., Zhi-Sheng, Z., Jin-Ping, W., Ming-Li, C., Cou-Gui, C., 2012. Effects of Tillage and Nitrogen Fertilizers on $CH_4$ and $CO_2$ Emissions and Soil Organic Carbon in Paddy Fields of Central China. PLoS ONE. 7, e34642.

Cho, D.W., Chon, C.M., Jeon, B.H., Kim, Y., Khan, M.A., Song, H., 2010. The role of clay minerals in the reduction of nitrate in groundwater by zero-valent iron. Chemosphere. 81,611–616.

Choudhury, A.T.M.A., Khanif, Y.M., Aminuddin, H., Zakaria, W., 2002. Effects of copper and magnesium fertilization on rice yield and nitrogen use efficiency: A $^{15}N$ tracer study. In Proceedings of the 17th World Congress of Soil Sciences, CD Transactions; Kheoruenromne, I, ed.; Symposium No. 50, Paper No. 226. August 14–21. Bangkok, Thailand, 1–10.

Choudhury, A.T.M.A., Zaman, S.K., Bhuiyan, N.I., 1997. Nitrogen response behavior of four rice varieties under wetland culture. Thailand J. Agric. Sci. 30, 195–202.

Craswell, E.T., Vlek, P.L.G., 1983. Fate of fertilizer nitrogen applied to wetland rice. In Gaseous loss of nitrogen from plant-soil systems. Springer Netherlands. pp. 237-264.

Cucu, M. A., Said-Pullicino, D., Maurino, V., Bonifacio, E., Romani, M., Celi, L., 2014. Influence of redox conditions and rice straw incorporation on nitrogen availability in fertilized paddy soils. Biol. Fertil. Soils. 50, 755-764.

Dessureault-Rompré, J., Zebarth, B.J., Burton, D.L., Georgallas, A., 2015. Predicting soil nitrogen supply from soil properties. Can. J. Soil Sci. 95, 63-75.

Devêvre, O.C., Horwáth, W.R., 2000. Decomposition of rice straw and microbial carbon use efficiency under different soil temperatures and moistures. Soil Biol. Biochem. 32, 1773-1785.

Ding, L.J., An, X.L., Li, S., Zhang, G.L., Zhu, Y.G., 2014. Nitrogen loss through anaerobic ammonium oxidation coupled to iron reduction from paddy soils in a chronosequence. Environ. Sci. Technol. 48, 10641-10647.

Dobermann, A., Cassman, K. G., 1996. Precision nutrient management in intensive irrigated rice systems–the need for another on-farm revolution. Better Crops Int. 10.2, 21.

Dobermann, A., Wltt, C. 2000. The potential impact of crop intensification on carbon and nitrogen cycling in intensive rice systems. In: Kirk GJD, Olk DC (Eds). Carbon and Nitrogen Dynamics in Flooded Soils, International Rice Research Institute, Los Baños, Philippines.

Dommergues, Y.R., Belser, L.W., Schmidt, E.L., 1978. Limiting factors for microbial growth and activity in soil. In Adv. microbial ecology. 49-104. Springer US.

Dong, N.M., Brandt, K.K., Sørensen, J., Hung, N.N., Van Hach, C., Tan, P.S., Dalsgaard, T., 2012. Effects of alternating wetting and drying versus continuous flooding on fertilizer nitrogen fate in rice fields in the Mekong Delta, Vietnam. Soil Biol. Biochem. 47, 166-174.

Ekanayake, H.K.J., 2009. The impact of fertilizer subsidy on paddy cultivation in Sri Lanka. Staff Studies, 36.

Ericsson, T., Linares, J., Lotse, E., 1984. A Mössbauer study of the efect of dithionite/citrate/bicarbonate treatment on a vermiculite, a smectite and a soil. Clay Miner. 19, 85-91.

Gaihre, Y.K, Singh, U., Huda, A., Islam, S.M.M., Islam, M.R., Biswas, J. C., DeWald, J., 2016. Nitrogen use efficiency, crop productivity and environmental impacts of urea deep placement in lowland rice fields. Proceedings of the 2016 International Nitrogen Initiative Conference, "Solutions to improve nitrogen use efficiency for the world", 4 – 8 December 2016, Melbourne, Australia. www.ini2016.com

Gao, H., Bai, J., He, X., Zhao, Q., Lu, Q. Wang, J., 2014. High temperature and salinity enhance soil nitrogen mineralization in a tidal freshwater marsh. PloS one, 9(4), 95011.

Gao, S., Tanji, K.K., Scardaci, S.C., Chow, A.T., 2002. Comparison of redox indicators in a paddy soil during rice-growing season. Soil Sci. Soc. Am. J. 66, 805-817.

Gee, G.W., Or, D., 2002. Particle Size Analysis. In: Dane, J.H., Topp, G.C., Eds., Methods of Soil Analysis, Part 4, Physical Methods, Soils Science Society of America, Book Series No. 5, Madison, 255-293.

Goldman, E., Jacobs, R., 1961. Determination of Nitrates by Ultraviolet Absorption. American Water Works Association 53 (2), 187-191.

Gong. Z.T., 1983. Pedogenesis of paddy soil and its significance in soil classification. Soil Sci. 135: 5–10.

Gotoh, S., Yamashita, K., 1966. Oxidation-reduction potential of a paddy soil in situ with special reference to the production of ferrous ikon, manganous manganese and sulfide. Soil Sci. Plant Nutr. 12, 24-32.

Griffiths, B.S., Spilles, A., Bonkowsk, M., 2012. C:N:P stoichiometry and nutrient limitation of the soil microbial biomass in a grazed grassland site under experimental P limitation or excess. Ecol. Process. 1, 6.

Grybos, M., Davranche, M., Gruau, G., Petitjean, P., Pédrot, M., 2009. Increasing pH drives organic matter solubilization from wetland soils under reducing conditions. Geoderma. 154, 13-19.

Hanke, A., Sauerwein, M., Kaiser, K., Kalbitz, K., 2014. Does anoxic processing of dissolved organic matter affect organic–mineral interactions in paddy soils? Geoderma, 228, 62-66.

Hanke, A., Cerli, C., Muhr, J., Borken, W., Kalbitz, K., 2013. Redox control on carbon mineralization and dissolved organic matter along a chronosequence of paddy soils. Eur. J. Soil Sci. 64, 476–487.

Haque, K.S., Eberbach, P.L., Weston, L.A., Dyall-Smith, M., Howitt, J.A., 2016. Variable impact of rice (Oryza sativa) on soil metal reduction and availability of pore water $Fe^{2+}$ and $Mn^{2+}$ throughout the growth period Chem. Ecol. 32, 182-200.

Haque, K.S., Eberbach, P.L., Weston, L.A., Dyall-Smith, M., Howitt, J.A., 2015. Pore $Mn^{2+}$ dynamics of the rhizosphere of flooded and non-flooded rice during a long wet and drying phase in two rice growing soils. Chemosphere. 134, 16-24.

Haque, S.A., 2006. Salinity problems and crop production in coastal regions of Bangladesh. Pakistan J. Botany. 38, 359–1365.

Holford, I.C.R., Patrick, W.H., 1979. Effects of reduction and pH changes on phosphate sorption and mobility in an acid soil. Soil Sci. Soc. Am. J. 43, 292-297.

Hoque, M.M., Inubushi, K., Miura, S., Kobayashi, K., Kim, H.Y., Okada, M., Yabashi, S., 2002. Nitrogen dynamics in paddy field as influenced by free-air CO2 enrichment (FACE) at three levels of nitrogen fertilization. Nutri. Cycl. Agroecosyst. 63, 301-308.

Hossain M. J, Kuri, S.K., Islam, M.S., Mondal, D.U., 2014. Estimating the effect of climate change on rice production: a study from Mymensingh district of Bangladesh using quantile regression method. Int. J. Sustain. Crop Prod. 9, 1-7.

Hossain, M., Bose, M.L., Mustafi, B.A.A., 2006. Adoption and Productivity Impact of Modern Rice Varieties in Bangladesh. The Developing Economics, XLIV-2: 149–166.

Hou, A.X., Chen, G.X., Wang, Z.P., Van Cleemput, O., Patrick, W.H., 2000. Methane and nitrous oxide emissions from a rice field in relation to soil redox and microbiological processes. Soil Sci. Soc. Am. J. 64, 2180-2186.

Howell, K.R., Shrestha, P., Dodd, I.C., 2015. Alternate wetting and drying irrigation maintained rice yields despite half the irrigation volume, but is currently unlikely to be adopted by smallholder lowland rice farmers in Nepal. Food Energy Secur. 4, 144-157.

Huang, B., Gambrell, R.P., 2011. Redox condition and nitrate change in a newly flooded rice soil under percolation as influenced by oxidative iron and manganese. Soil Sci. Plant Nutr. 57, 759-764.

Huang, X., Zhu-Barker, X., Horwath, W.R., Faeflen, S.J., Luo, H., Xin, X., Jiang, X. 2016. Effect of iron oxide on nitrification in two agricultural soils with different pH. Biogeosciences. 13, 5609–5617.

Huq, S. M. I., Shoaib, J. U. M., 2013. The Soils of Bangladesh. World Soils Book Series 1, DOI: 10.1007/978-94-007-1128-0_2.

http://irri.org/rice-today/rice-in-south-asia

Inglett, P.W., Reddy, K.R., Corstanje, R., 2005. Anaerobic Soils. University of Florida, Gainesville, FL, USA. Ed. Elsevier Ltd.

Inubushi, K., Acquaye, S., 2004. Role of microbial biomass in biogeochemical processes in paddy soil environments. Soil Sci. Plant Nutr. 50, 793-805.

Inubushi, K., Cheng, W., Chander, K., 1999. Carbon dynamics in submerged soil microcosms as influenced by elevated CO2 and temperature. *Soil Sci. Plant Nutr. 45*, 863-872.

Inubushi, K., Wada, H., Takai, Y., 1985. Easily decomposable organic matter in paddy soil. VI. Kinetics of nitrogen mineralization in submerged soil. Soil Sci. Plant Nutr. 31,563-572.

Inubushi K., Wada, H., Takai, Y., 1984. Easily decomposable organic matter in paddy soil. Soil Sci. Plant Nutr. 30:2, 189–198.

IRRI, 2011. Rice production and processing. http://irri.org/about-rice/rice-facts/rice-production-and-processing (accessed 14.11.11).

Jackel, U., Schnell, S., 2000. Suppression of methane emission from rice paddies by ferric iron fertilization. Soil Biol. Biochem.32:1811-1814.

Jäckel, U., Schnell, S., 2000a. Role of microbial iron reduction in paddy soil. In Non-CO2 Greenhouse Gases: Scientific Understanding, Control and Implementation (pp. 143-144). Springer Netherlands.

Jahan, M.S., Khanif, Y.M., Omar S.R, Sinniah, U.R., 2013. Effects of low water input on rice yield: Fe and Mn bioavailability in soil. Pertanika J. Trop. Agric. Sci. 36 (1): 27- 34. John, A., Fielding, M., 2014. Rice production constraints and 'new'challenges for South Asian smallholders: insights into de facto research priorities. Agric. Food Security. 3, 18p.

John, A., Fielding, M., 2014. Rice production constraints and 'new'challenges for South Asian smallholders: insights into de facto research priorities. Agric. Food Security. 3, 18p.

Juang, T.C., Wang, M.K., Chen, H.J., Tan, C.C. 2001. Ammonium fixation by surface soils and clays. Soil Sci. 166, 345–352.

Kader, M.A., 2012. Nitrogen mineralization in sub-tropical paddy soils in relation to soil properties, soil organic matter fractions, and fertilizer management. Ph.D. thesis, Faculty of Bioscience Engineering, Ghent University, Ghent, Belgium, 208 pp.

Kader, M.A., Sleutel, S., Begum, S.A., Moslehuddin, A.Z.M., 2013. Nitrogen mineralization in sub-tropical paddy soils in relation to soil mineralogy, management, pH, carbon, nitrogen and iron contents. Eur. J. Soil Sci. 64, 47-57.

Kasting, J.F., Holland, H.D., Pinto, J.P., 1985. Oxidant abundances in rainwater and the evolution of atmospheric oxygen. J. Geophys Res. 90, 0497-510.

Keeney, D.R., Sahrawat, K.L., 1986. Nitrogen transformations in flooded rice soils. Fert. Res. 9,15–38.

Keerthisinghe, G., Mengel, K., De Datta, S.K., 1984. The release of nonexchangeable ammonium (15N labelled) in wet-land rice soils. Soil Sci. Soc. Am. J. 48, 291-294.

Kempers, A.J., 1974. Determination of sub-microquantities of ammonium and nitrates in soils with phenol, sodiumnitroprusside and hypochlorite. Geoderma. 12, 201-206.

Khaokaew, W., Attanandana, T., Chanchareonsook, J., Sripichitt, P., Yost, R., 2007. Nitrogen mineralization and different methods of ammonium determination of some paddy soils in the north, central, and northeast regions of Thailand. Kasetsart J. p.96.

Khatun, M. A., Rashid, M.B., Hygen, H.O., 2016. Climate of Bangladesh: Climate. MET Report. Norwegin Meteoorological Institute. ISSN 2387-4201. Report no. 08/2016.

King, G.M., Klug, M.J., Lovley, D.R., 1983. Metabolism of acetate, methanol, and methylated amines in intertidal sediments of Lowes Cove. Maine. Appl. Environ. Microbiol. 45,1848-1853.

Kodama, H., Longworth, G., Townsend, M.G., 1982. Mössbauer investigation of some chlorites and their oxidation products. Can. Mineral. 20, 585-592.

Kögel-Knabner, I., Amelung, W., Cao, Z., Fiedler, S., Frenzel, P., Jahn, R., Kalbitz, K., Kölbl, A., Schloter, M., 2010. Biogeochemistry of paddy soils. Geoderma. 157, 1-14.

Koroleff, F., 1983. Simultaneous oxidation of nitrogen and phosphorous compounds by persulfate. p. 168-169. In K.Grasshoff, M. Eberhardt, and K. Kremling (ed) Methods of seawater analysis. 2$^{nd}$ ed. Verlag Chemie, Weinheim, FRG.

Kraemer, S.M., 2004. Iron oxide dissolution and solubility in the presence of siderophores. Aquat. Sci. 66, 3–18.

Leinweber, P., Schulten, H.R., 2000. Nonhydrolyzable forms of soil organic nitrogen: Extractability and composition. J. Plant Nutr. Soil Sci. 163, 433–439.

Li, H., Han, Y., Cai, Z., 2003. Nitrogen mineralization in paddy soils of the Taihu Region of China under anaerobic conditions: dynamics and model fitting. Geoderma, 115, 161-175.

Li, Y., Šimůnek, J., Zhang, Z., Jing, L., Ni, L., 2015. Evaluation of nitrogen balance in a direct-seeded-rice field experiment using Hydrus-1D. Agric. Water Manage. 148, 213-222.

Li, Y., Yu, S., Strong, J., Wang, H., 2012. Are the biogeochemical cycles of carbon, nitrogen, sulfur, and phosphorus driven by the "FeIII–FeII redox wheel" in dynamic redox environments?. J. Soils Sediments. 12, 683-693.

Li, Z.P., Han, C.W., Han, F.X., 2010. Organic C and N mineralization as affected by dissolved organic matter in paddy soils of subtropical China. Geoderma. 157, 206–213.

Lindsay, W.L., 1979. Chemical equilibria in Soils. New York: John Wiley & Sons.

Lindsay, W.L., Norvell, W.A., 1969. Equilibrium relationships of $Zn^{2+}$, $Fe^{3+}$, $Ca^{2+}$, and $H^+$ with EDTA and DTPA in soils. Soil Sci. Soc. Am. J. 33, 62-68.

Liu, M., Hu, F., Chen, X., Huang, Q., Jiao, J., Zhang, B., Li, H., 2009. Organic amendments with reduced chemical fertilizer promote soil microbial development and nutrient availability in a subtropical paddy field: the influence of quantity, type and application time of organic amendments. *Applied Soil Ecol, 42*, 166-175.

Liu, X., Wang, H., Zhou, J., Hu, F., Zhu, D., Chen, Z., Liu, Y., 2016. Effect of N Fertilization Pattern on Rice Yield, N Use Efficiency and Fertilizer–N Fate in the Yangtze River Basin, China. PloS one, 11(11), p.e0166002.

Liu, Y., Wan, K.Y., Tao, Y., Li, Z.G., Zhang, G.S., Li, S.L., Chen, F., 2013. Carbon dioxide flux from rice paddy soils in central China: effects of intermittent flooding and draining cycles. PLoS ONE. 8, e56562.

Lovley, D.R., Phillips, E.J.P., 1986. Organic matter mineralization with reduction of ferric iron in anaerobic sediments. Appl. Environ. Microbiol. 51, 683-689.

Lu, Y., Watanabe, A., Kimura, M., 2002. Contribution of plant-derived carbon to soil microbial biomass dynamics in a paddy rice microcosm. Biol. Fertil. Soils. 36, 136-142.

Ma, Y., Xu, J.Z., Wei, Q., Yang, S.H., Liao, L.X., Chen, S.Y., Liao, Q., 2017. Organic carbon content and its liable components in paddy soil under water-saving irrigation. Plant Soil Environ. 63, 125–130.

Manguiat, I.J., Mascarina, G.B., Ladha, J.K., Buresh, R.J, Tallada, J., 1994. Prediction of nitrogen availability and rice yield in lowland soils: Nitrogen mineralization parameters. Plant Soil. 160, 131-137.

Manguiat, I.J., Watanabe, I., Mascariña, G.B., Tallada, J.G., 1996. Nitrogen mineralization in tropical wetland rice soils: I. Relationship with temperature and soil properties. Soil Sci. Plant Nutr. 42, 229-238.

Mansfeldt, T., 2004. Redox potential of bulk soil and soil solution concentration of nitrate, manganese, iron, and sulfate in two Gleysols. J. Plant Nutr. Soil Sci. 167, 7-16.

Matsuoka, K., Moritsuka, K., 2011. Dynamics of clay-fixed ammonium as a sink or source of exchangeable ammonium in a paddy soil. Soil Sci. Plant Nutr. 57, 751-758.

Miah M.A.M., Gaihre Y.K., Hunter G., Singh U., Hossain S.A., 2016. Fertilizer deep placement increases rice production: evidence from farmers' fields in Southern Bangladesh. Agron. J. 108, 805-812.

Mikha, M.M., Rice, C.W., Benjamin, J.G., 2006. Estimating soil mineralizable nitrogen under different management practices. Soil Sci. Soc. Am. J. 70, 1522–1531.

Minamikawa, K., Sakai, N., 2005. The effect of water management based on soil redox potential on methane emission from two kinds of paddy soils in Japan. Agric. Ecosyst. Environ. 107, 397-407.

Minamikawa, K., Sakai, N., 2006. The practical use of water management based on soil redox potential for decreasing methane emission from a paddy field in Japan. Agric. Ecosyst. Environ. 116, 181-188.

Minh Khoi, C., 2000. Nitrogen mineralization in relation to soil organic carbon and its C: N ratio in acid sulfate soils from the Mekong Delta area–Vietnam. Sveriges lantbruksuniversitet, Institutionen för markvetenskap, avd. för växtnäringslära.

Moterle, D.F., Silva, L.S.D., Moro, V.J., Bayer, C., Zschornack, T., Avila, L.A.D., Bundt, Â.D.C., 2013. Methane efflux in rice paddy field under different irrigation managements. Rev. Bras. Ciênc. Solo. 37, 431-437.

Munch, J.C., Hillebrand, T., Ottow, J.C.G., 1978. Transformations in the Feo/Fed ratio of pedogenic iron oxides affected by iron-reducing bacteria. Can. J. Soil Sci. 58, 475-486.

Munch, J.C., Ottow, J.C.G., 1980. Preferential reduction of amorphous to crystalline iron oxides by bacterial activity. Soil Sci. 129, 14-21.

Murad, E., 1998. Clays and clay minerals: What can Mössbauer spectroscopy do to help understand them? Hyperfine Interact. 117, 39-70.

Mustafi, B. A. A., Harun, M. E., 2002. Contract Research Project on Rice crop cultivation practices: Input-Output relationship. BRRI, Gazipur. Feb. 2002. Submitted to BARC.

Narteh, L.T., Sahrawat, K.L., 1997. Potentially mineralizable nitrogen in West African lowland rice soils. Geoderma. 76, 145-154.

Narteh, L.T., Sahrawat, K.L., 1999. Influence of flooding on electrochemical and chemical properties of West African soils. Geoderma. 87, 179-207.

Nealson, K.H., Myers, C.R., 1992. Microbial reduction of manganese and iron: new approaches to carbon cycling. Appl. Environ. Microbiol. 58, 439-443.

Nieder, R., Benbi, D.K., Scherer, H.W., 2011. Fixation and defixation of ammonium in soils: a review. Biol. Fertil. Soils. 47, 1-14.

Nierop, K.G.J., Jansen, B., Verstraten, J.A., 2002. Dissolved organic matter, aluminium and iron interactions: precipitation induced by metal/carbon ratio, pH and competition. Sci. Total Environ. 300, 201–211.

Nishimura, S., Sawamoto, T., Akiyama, H., Sudo, S., Yagi, K., 2004. Methane and nitrous oxide emissions from a paddy field with Japanese conventional water management and fertilizer application. Global Biogeochem. Cycl. 18, GB2017.

Olk, D.C., Cassman, K.G., Schmidt-Rohr, K., Anders, M.M., Mao, J.D., Deenik, J.L., 2006. Chemical stabilization of soil organic nitrogen by phenolic lignin residues in anaerobic agroecosystems. Soil Biol. Biochem. 38, 3303–3312.

Ono, S.I., 1989. Nitrogen mineralization from paddy and upland soils under flooded and non-flooded incubation. Soil Sci. Plant Nutr. 35, 417-426.

Pan, Y., Koopmans, G.F., Bonten, L.T., Song, J., Luo, Y., Temminghoff, E.J., Comans, R.N., 2014. Influence of pH on the redox chemistry of metal (hydr) oxides and organic matter in paddy soils. J. Soils Sediments. 14, 1713-1726.

Pan, Y., Koopmans, G.F., Bonten, L.T., Song, J., Luo, Y., Temminghoff, E.J., Comans, R.N., 2016. Temporal variability in trace metal solubility in a paddy soil not reflected in uptake by rice (Oryza sativa L.). Environ. Geochem. Health. 38, 1355-1372.

Panabokke, C.R., 1996. Soils and agro -ecological environments of Sri Lanka. Natural recourses, energy and science authority. Sri Lanka.

Parvin, L., Rahman, M. W., 2009. Impact of irrigation on food security in Bangladesh for the past three decades. J. Water Resource and Protection. 3, 216-225.

Patrick Jr, W.H., Jugsujinda, A., 1986. Redox and pH chemistry and nutrient uptake by rice in flooded oxisols of Sitiung Area of Sumatra, Indonesia (No. 1). A Technical Report.

Patrick, Jr. W.H., Reddy, C.N., 1978. Chemical changes in rice soils. In Soil and Rice, pp 361- 379 International Rice Research Institute: Manila, Philippines.

Patrick, Jr. W.H., Reddy, K.R., 1976. Nitrification-denitrification reactions in flooded soils and sediments: Dependence on oxygen supply and ammonium diffusion. J. Environ. Qual. 5, 469-472.

Patrick, W.H., Wyatt, R., 1964. Soil nitrogen loss as a result of alternate submergence and drying. Soil Sci. Soc. Am. J. 28, 647-653.

Pentráková, L., Su, K., Pentrák, M., Stucki, J.W., 2013. A review of microbial redox interactions with structural Fe in clay minerals. Clay Miner. 48, 543-560.

Ponnamperuma, F. N., Teresita A. L., Estrella M. T., 1969. Redox equilibria in flooded soils: ii. the manganese oxide systems. Soil Sci. 108.1, 48-57.

Ponnamperuma, F.N., 1972. The chemistry of submerged soils. Adv. Agron. 24, 29–96.

Ponnamperuma, F.N., 1977. Physicochemical properties of submerged soils in relation to fertility. IRRI Research Paper Series (IRPS), 5.

Ponnamperuma, F.N., Tianco, E.M., Loy, T., 1967. Redox equilibria in flooded soils: The iron hydroxide systems. Soil Sci. 103, 374–382.

Price, A.H., Norton, G.J., Salt, D.E., Ebenhoeh, O., Meharg, A.A., Meharg, C., Islam, M.R., Sarma, R.N., Dasgupta, T., Ismail, A.M., McNally, K.L., 2013. Alternate wetting and drying irrigation for rice in Bangladesh: Is it sustainable and has plant breeding something to offer?. Food Energy Secur. 2, 120-129.

Qiu, S., Peng, P., Rong, X., Liu, Q. and Tang, Q., 2006. Dynamics of soil microbial biomass and dissolved organic carbon and nitrogen under flooded condition. J. *Applied Ecol. 17*, 2052-2058.

Qu, D., Ratering S., Schnell, S., 2004. Microbial reduction of weakly crystalline iron (iii) oxides and suppression of methanogenesis in paddy soil. Bull. Environ. Contam. Toxicol. 72, 1172–1181.

Rahman, M. M., Ferdousi, N., Sato, Y., Kusunoki, S., Kitoh, A., 2012. Rainfall and temperature scenario for Bangladesh using 20 km mesh AGCM. Int. J. Climate Change Strategies and Management. 4, 66-80.

Rajashekhara Rao, B.K., Siddaramappa., R., 2007. Influence of tree leaf litters and paddy straw on the nutrient availability in two paddy soils of South Karnataka, India. Archiv. Agron. Soil Sci. 53, 405-422.

Reddy, K.R., 1982. Nitrogen cycling in a flooded-soil ecosystem planted to rice (Oryza sativa L.) Florida Agricultural Experiment Station J. series No. 3855.

Reddy, K.R., De Laune, R.D., 2008. Biochemistry of Wetlands: Science and Applications. CRC Press, Taylor and Francis Group, Boca Raton, Florida, USA, 774 p.

Reddy, K.R., Patrick, W.H. 1984. Nitrogen transformations and loss in flooded soils and sediments. Crit. Rev. Environ. Control. 13, 273–309.

Reddy, K.R., Patrick, W.H., 1975. Effect of alternate aerobic and anaerobic conditions on redox potential, organic matter decomposition and nitrogen loss in a flooded soil. Soil Biol. Biochem. 7, 87-94.

Roth, P.J., Lehndorff, E., Zhuang, S., Bannert, A., Wissing, L., Schloter, M., Kögel-Knabner, I., Amelung, W., 2011. Accumulation of nitrogen and microbial residues during 2000 years of rice paddy and non-paddy soil development in the Yangtze River Delta, China. *Global Change Biology. 17*(11), pp.3405-3417.

Rozenson, I., Bauminger, E.R., Heller-Kallai, L., 1979. Mössbauer spectra of iron in 1: 1 phyllosilicates. Am. Mineral. 64, 893-901.

Saha, P. K., Miah, M. A. M., Hossain, A. T. M. S., Rahman, F., Saleque, M. A., 2009. Contribution of rice straw to potassium supply in rice-fallow-rice cropping pattern. Bangladesh J. Agril. Res. 34, 633-643.

Saha, P.K., Ishaque, M., Saleque, M.A., Miah, M.A.M., Panaullah, G.M., Bhuiyan, N.I., 2007. Long-Term Integrated Nutrient Management for Rice-Based Cropping Pattern: Effect on Growth, Yield, Nutrient Uptake, Nutrient Balance Sheet, and Soil Fertility. Commun. Soil Sci. Plant Anal. 38, 579-610.

Saha, P.K., Islam, S.M.M., Akter, M., Zaman, S.K., 2012. Nitrogen response behaviour of developed promising lines of T. Aman rice. Bangladesh J. Agric. Res. 37, 207-213.

Sahrawat, K.L., 1979. Ammonium fixation in some tropical rice soils. Commun. Soil Sci. Plant Anal. 10, 1015–1023.

Sahrawat, K.L., 1983. Nitrogen availability indexes for submerged rice soils. Advances in Agronomy. 36, 415- 451.

Sahrawat, K.L., 2003. Organic matter accumulation in submerged soils. Adv. Agron. 81, 169–201.

Sahrawat, K.L., 2004a. Ammonium production in submerged soils and sediments: The role of reducible iron. Commun. Soil Sci. Plant Anal. 35, 399- 411.

Sahrawat, K.L., 2004b. Organic matter accumulation in submerged soils. Adv Agron. 81,169–201.

Sahrawat, K.L., 2005. Fertility and organic matter in submerged rice soil. Curr. Sci. 88, 735–739.

Sahrawat, K.L., 2006. Organic matter and mineralizable nitrogen relationships in wetland rice soils. Commun. Soil Sci. Plant Anal. 37, 787- 796.

Sahrawat, K.L., 2006. Organic matter and mineralizable nitrogen relationships in wetland rice soils. Commun. Soil Sci. Plant Anal. 37, 787- 796.

Sahrawat, K.L., 2008. Soil fertility advantages of submerged rice cropping systems: A review. J. Sustainable Agric. 31, 5-23.

Sahrawat, K.L., 2010. Nitrogen mineralization in lowland rice soils: The role of organic matter quantity and quality. Arch. Agron. Soil Sci. 56, 337-353.

Sahrawat, K.L., 2012. Soil fertility in flooded and non-flooded irrigated rice systems. Achives of Agronomy and soils science. International Crops Research Institute for Semi-Arid Tropics. 58(4): 423-436.

Sahrawat, K.L., Narteh, L.T., 2001. Organic matter and reducible iron control of ammonium production in submerged soils. Commun. Soil Sci. Plant Anal. 32, 1543–1550.

Sahrawat, K.L, Narteh, L.T., 2003. A chemical index for predicting ammonium production in submerged rice soils. Commun. Soil Sci. Plant Anal. 34, 1013-1021.

Said-Pullicino, D., Cucu, M.A., Sodano, M., Birk, J.J., Glaser, B., Celi, L., 2014. Nitrogen immobilization in paddy soils as affected by redox conditions and rice straw incorporation. Geoderma. 228-229, 44-53.

Said-Pullicino, D., Miniotti, E.F., Sodano, M., Bertora, C., Lerda, C., Chiaradia, E.A., Romani, M., de Maria, S.C., Sacco, D., Celi, L., 2016. Linking dissolved organic carbon cycling to organic carbon fluxes in rice paddies under different water management practices. Plant Soil. 401, 273-290.

Scherer, H.W., Zhang, Y., 2002. Mechanisms of fixation and release of ammonium in paddy soils after flooding III. Effect of the oxidation state of octahedral Fe on ammonium fixation. J. Plant Nutr. Soil Sci. 165, 185-189.

Scherer, H.W., Zhang, Y.S., 1999. Studies on the mechanism of fixation and release of ammonium in paddy soils after flooding. I. Effect of iron oxides on ammonium fixation. J. Plant Nutr. Soil Sci. 162, 593–597.

Schmidt-Rohr, K., Mao, J.D., Olk, D.C., 2004. Nitrogen-bonded aromatics in soil organic matter and their implications for a yield decline in intensive rice cropping. Proceedings of the National Academy of Sciences of the United States of America, 101, 6351–6354.

Schneiders, M., Scherer, H.W., 1998. Fixation and release of ammonium in flooded rice soils as affected by redox potential. European J. Agron. 8, 181–189.

Schwertmann, U., Cornell, R.M., 1991. Iron oxides in the laboratory. VCH, Weinheim.

Sharifi, M., Zebarth, B.J., Burton, D.L., Grant, C.A., Cooper, J.M., 2007. Evaluation of some indices of potentially mineralizable nitrogen in soil. Soil Sci. Soc. Am. J. 71, 1233–1239.

Shelley, I.J., Takahashi-Nosaka, M., Kano-Nakata, M., Haque, M.S., Inukai, Y., 2016. Rice cultivation in Bangladesh: present scenario, problems, and prospects. J. Intl. Cooper. Agric. Dev. 14: 20–29.

Shohel, M., Ullah, M., Akter, F., Salam, A., 2016. Chemical Composition of Rain Water Collected at Urban and Rural Areas in Bangladesh. 16th Asian Chemical Congress (16ACC),16-19 March 2016, Dhaka, Bangladesh.

Silva, J.A., Bremner, J.M., 1966. Determination and isotope-ratio analysis of different forms of nitrogen in soils. 5. Fixed ammonium. Soil Sci. Soc. Am. J. 30, 587-594.

Sleutel, S., De Neve, S., Prat Roibas, M.R., Hofman, G., 2005. The influence of model type and incubation time on the estimation of stable organic carbon in organic materials. Eur. J. Soil Sci. 56, 505-514.

Sleutel, S., Kader, M.A., Demeestere, K., Walgraeve, C., Dewulf, J., De Neve S., 2013. Subcritical water extraction to isolate kinetically different soil nitrogen fractions. Biogeosciences 10, 7435-7447.

Sodano, M., Lerda, C., Nistico, R., Martin, M., Magnacca, G., Celi, L., Said-Pullicino, D., 2017. Dissolved organic carbon retention by coprecipitation during the oxidation of ferrous iron. Geoderma. 307, 19-29.

Sodano, M., Said-Pullicino, D., Fiori, A.F., Catoni, M., Martin, M., Celi, L., 2016. Sorption of paddy soil-derived dissolved organic matter on hydrous iron oxide–vermiculite mineral phases. Geoderma. 261, 169-177.

SSSA, 2008. Methods of Soil Analysis Part 5—Mineralogical Methods, SSSA Book Series 5.5Eds. A.L. Ulery, L.R. Drees. Soil Science Society of America, Madison, WI.

Steffens, D., Sparks, D.L., 1999. Effect of residence time on the kinetics of nonexchangeable ammonium release from illite and vermiculite. J Plant Nutr Soil Sci. 162, 599–604.

Stucki, J.W., 1988. Structural iron in smectite. In Iron in Soils and Clay Minerals. Stucki, J.W., Goodman, B.A., Schwertmann, U.(Eds.), D. Reidel, Dordrecht, The Netherlands,pp. 625-675.

Stucki, J.W., Golden, D.C., Roth, C.B., 1984. Effects of reduction and reoxidation of structural iron on the surface charge and dissolution of dioctahedral smectites. Clays and Clay Minerals. 32, 350–356.

Stumm, W., Sulzberger, B., 1992. The cycling of iron in natural environments: Considerations based on laboratory studies of heterogeneous redox processes. Geochim. Cosmochim. Acta 56, 3233–3257.

Sun, B.F., Hong, Z.H.A.O., Lü, Y.Z., Fei, L.U., Wang, X.K., 2016. The effects of nitrogen fertilizer application on methane and nitrous oxide emission/uptake in Chinese croplands. J. Integr. Agr. 15, 440-450.

Takeda, K., Furusaka, C., 1970. J. Agr. Chem. Soc. Jap. 44, 343-355.

Tan, X., Shao, D., Gu, W., Liu, H., 2015. Field analysis of water and nitrogen fate in lowland paddy fields under different water managements using HYDRUS-1D. Agric. Water Manage. 150, 67-80.

Tan, X., Shao, D., Liu, H., Yang, F., Xiao, C. and Yang, H., 2013. Effects of alternate wetting and drying irrigation on percolation and nitrogen leaching in paddy fields. Paddy Water Environ. 11, 381-395.

Tuong, T.P., Bouman, B.A.M., 2003. Rice production in water scarce environments, in: Water Productivity in Agriculture: Limits and Opportunities for Improvement" (J.W. Kijne, R. Barker and D. Molden, Eds.). CABI Publishing, Wallingford, UK, pp. 53-67.

van Bodegom, P.M., van Reeven, J., Denier van der Gon, H.A.C., 2003. Prediction of reducible soil iron content from iron extraction data. Biogeochemistry. 64, 231-245.

Vance, E.D., Brookes, P.C., Jenkinson, D. S., 1987. An extraction method for measuring soil microbial biomass C. Soil Biol. Biochem. 19, 703-707.

Vandenberghe, R.E., Barrero, C.A., Da Costa, G.M., Van San, E., De Grave, E., 2000. Mössbauer characterization of iron oxides and (oxy) hydroxides: the present state of the art. Hyperfine Interact. 126, 247-259.

Vandenberghe, R.E., De Grave, E., Landuydt, C., Bowen, L.H., 1990. Some aspects concerning the characterization of iron oxides and hydroxides in soils and clays. Hyperfine Interact. 53, 175-195.

Verhoeven, E., 2017. Agricultural management effects on nitrogen cycling and nitrous oxide emissions across the soil profile. Ph.D. thesis, Department of Environmental Systems Sciences, Institute of Agricultural Sciences, Swiss Federal Institute of Technology, ETH-Zurich, Zurich, Switzerland., 153pp

Villaseñor, D., Zagal, E., Stolpe, N., Hirzel, J., 2015. Relationship between mineralized nitrogen during anaerobic incubations and residual effect of nitrogen fertilization in two rice paddy soils in Chile. Chilean J. Agric. Res. 75, 98-104.

Villegas-Pangga, G., Blair, G., Lefroy, R. 2000. Measurement of decomposition and associated nutrient release from straw (Oryza sativa L.) of different rice varieties using a perfusion system. Plant and Soil. 223, 1–11.

Wagner, F.E., Wagner, U. 2004. Mössbauer Spectra of Clays and Ceramics. Hyperfine Interact.154, 35-82.

Wang, C., Lai, D.Y., Sardans, J., Wang, W., Zeng, C., Peñuelas, J., 2017. Factors Related with CH4 and N2O Emissions from a Paddy Field: Clues for Management implications. PLoS ONE. 12, e0169254.

Wang, M., Hu, R., Zhao, J., Kuzyakov, Y., Liu, S., 2016. Iron oxidation affects nitrous oxide emissions via donating electrons to denitrification in paddy soils. Geoderma, 271,173-180.

Wang, W.J., Chalk, P.M., Chen, D., Smith, C.J., 2001. Nitrogen mineralisation, immobilisation and loss, and their role in determining differences in net nitrogen production during waterlogged and aerobic incubation of soils. Soil Biol. Biochem. 33, 1305-1315.

Wang, X.N., Sun, G.X., Yong-Guan Zhu, Y.G. 2017. Thermodynamic energy of anaerobic microbial redox reactions couples elemental biogeochemical cycles. J. Soils Sediments. DOI 10.1007/s11368-017-1767-4.

Wang, Z.P., Delaune, R.D., Patrick, W.H., Mascheleyn, P.H., 1993. Soil redox and pH effects on methane production in a flooded rice soil. Soil Sci. Soc. Am. J. 57, 382-385.

Watanabe, I., De Datta, S.K., Roger, P.A., 1987. In: Advances in nitrogen cycling in agricultural ecosystems. Edited by: JR Wilson. Proc. Symposium on Advances in Nitrogen Cycling in Agricultural Ecosystems, Brisbane, Australia, 11-15 May 1987. CAB International, UK, pp. 239-256.

Weerahewa, J., Kodithuwakku, S.S., Ariyawardana, A., 2010. The fertilizer subsidy program in Sri Lanka. Food policy for developing countries: Case studies.

White, J.R., Reddy, K.R., 2001. Influence of selected inorganic electron acceptors on organic nitrogen mineralization in everglades soils. Soil Sci. Soc. Am. J. 65, 941–948.

Wijewardena, J.D.H., 2005. Improvement of plant nutrient management for better farmer livelihood, food security and environment in Sri Lanka. Proceedings of a regional workshop on improving plant nutrient management for better farmer livelihoods, food

security and environmental sustainability .12-16 December, 2005, Beijing, China. PP:73-93.

Willett, I.R., Higgins, M.L., 1978. Phosphate sorption by reduced and reoxidized rice soils. Soil Res. 16, 319-326.

Xu, J., Yang, S., Peng, S., Wei, Q., Gao, X., 2013. Solubility and leaching risks of organic carbon in paddy soils as affected by irrigation managements. Scientific World J.

Yagi, K., Tsuruta, H., Kanda, K.I., Minami, K., 1996. Effect of water management on methane emission from a Japanese rice paddy field: Automated methane monitoring. Glob. Biogeochem. Cycles. 10, 255-267.

Yang, S., Liu, X., Liu, X., Xu, J., 2017. Effect of water management on soil respiration and NEE of paddy fields in Southeast China. Paddy Water Environ. 1-10.

Yao Y., Zhang M., Tian Y., Zhao M., Zhang B., Zhao M., Zeng K., Yin B., 2017. Urea deep placement for minimizing $NH_3$ loss in an intensive rice cropping system. Field Crops Res. (in press).

Yao, H., Conrad, R., 2000. Effect of temperature on reduction of iron and production of carbon dioxide and methane in anoxic wetland rice soils. Biol. Fertil. Soils. 32, 135-141.

Yao, H., Conrad, R., Wassmann, R., Neue, H.U., 1999. Effect of soil characteristics on sequential reduction and methane production in sixteen rice paddy soils from China, the Philippines, and Italy. Biogeochemistry. 47, 269–295.

Yi, W., Wang, B., Qu, D., 2012. Diversity of isolates performing Fe (iii) reduction from paddy soil fed by different organic carbon sources. African J. Biotechnology. 11(19): 4407-4417.

Yonebayashi, K., Hattori, T., 1986a. Distribution of organic forms of nitrogen in paddy soils in tropical and temperate regions. Soil Sci. Plant Nutr. 32, 189-200.

Yonebayashi, K., Hattori, T., 1986b. Patterns and factors controlling nitrogen mineralization in paddy soils in tropical and temperate regions. Soil Sci. Plant Nutr. 32, 407-420.

Yoshida, 1981. Fundamentals of Crop Science. International Rice Research Institute. Los Banos Philippines: 269.

Yoshida, T., Ancajas, R.R., 1973. Nitrogen-fixing activity in upland and flooded rice fields. Soil Sci. Soc. Am. Proc. 37, 42–46.

Yu, K., Böhme, F., Rinklebe, J., Neue, H.U., DeLaune, R.D., 2007. Major biogeochemical processes in soils-a microcosm incubation from reducing to oxidizing conditions. Soil Sci. Soc. Am. J. 71, 1406–1417.

Zhang, C., Ge, Y., Yao, H., Chen, X., Hu, M., 2012. Iron oxidation-reduction and its impacts on cadmium bioavailability in paddy soils: a review. Front. Environ. Sci. Eng. 6, 509–517.

Zhang, J., Qin, J., Yao, W., Bi, L., Lai, T., Yu, X., 2009. Effect of long-term application of manure and mineral fertilizers on nitrogen mineralization and microbial biomass in paddy soil during rice growth stages. Plant Soil Environ. 55, 101–109.

Zhang, X., Li, L., Pan, G., 2007. Topsoil organic carbon mineralization and $CO_2$ evolution of three paddy soils from South China and the temperature dependence. J. Environ. Sci.19, 319-326.

Zhang, Y., Scherer, H.W., 2000. Mechanisms of fixation and release of ammonium in paddy soils after flooding II. Effect of transformation of nitrogen forms on ammonium fixation. Biol. Fertil. Soils. 31, 517-521.

Zhang, Y., Xu, W., Duan, P., Cong, Y., An, T., Yu, N., Zou, H., Dang, X., An, J., Fan, Q., Zhang, Y., 2017. Evaluation and simulation of nitrogen mineralization of paddy soils in Mollisols area of Northeast China under waterlogged incubation. PloS one, 12, p.e0171022.

Zhao, L., Wu, L., Dong, C., Li, Y., 2010. Rice yield, nitrogen utilization and ammonia volatilization as influenced by modified rice cultivation at varying nitrogen rates. Agric. Sci. 1, p.10.

Zheng, J., Zhang, X., Li, L., Zhang, P., Pan, G., 2007. Effect of long-term fertilization on C mineralization and production of CH4 and CO2 under anaerobic incubation from bulk samples and particle size fractions of a typical paddy soil. Agric. Ecosyst. Environ. 120, 129-138.

Zhou, S., Sakiyama, Y., Riya, S., Song, X., Terada, A., Hosomi, M., 2012. Assessing nitrification and denitrification in a paddy soil with different water dynamics and applied liquid cattle waste using the 15 N isotopic technique. Sci. Total Environ. 430, 93-100.

Zhu, Z., 1989. Dynamics of soil nitrogen and its management. In International Rice Research Conference, Hangzhou, China, 21-25 Sep, 1987. IRRI.

Zhu, Z.L., Liu, C.Q., Jiang, B.F., 1984. Mineralization of organic nitrogen, phosphorus and sulphur in some paddy soil of China. *In*: Organic matter and rice. International Rice Research Institute. Los Baños, Philipinnes, pp. 259-272.

Zschornack, T., Bayer, C., Zanatta, J. A., Vieira, F. C. B., Anghinoni, I., 2011. Mitigation of methane and nitrous oxide emissions from flood-irrigated rice by no incorporation of winter crop residues into the soil. Rev. Bras. Ciênc. Solo. 35, 623-634.

# Curriculum Vitae

**Personal data**

| | |
|---|---|
| Name: | Masuda Akter |
| Address: | Senior Scientific Officer |
| | Soil Science Division |
| | Bangladesh Rice Research Institute, |
| | Gazipur-1701 |
| | Bangladesh |
| Place of birth: | Tangail |
| Date of birth | 15-08-1982 |
| Nationality: | Bangladeshi |
| Phone no: | +32467610687, +8801912732621 |
| E-mail: | masudabrri@gmail.com |
| | Masuda.Akter@UGent.be |

**Education**

| | |
|---|---|
| 2013-2017: | PhD in Bioscience Engineering, Department of Soil Management, Faculty of Bioscience Engineering , Ghent University |
| 2011-2013: | M.Sc. in Physical Land Resources (Soil Science), Ghent University |
| 2006-2007: | M.Sc. in Entomology, Bangladesh Agricultural University, Bangladesh |
| 2001-2005: | B.Sc. Ag. (Hons.), Bangladesh Agricultural University, Bangladesh |

**Professional Career**

| | |
|---|---|
| 2007-2012: | Scientific Officer, Soil Science Division, Bangladesh Rice Research Institute, Gazipur, Bangladesh |
| 2012 to present: | Senior Scientific Officer, Soil Science Division, Bangladesh Rice Research Institute, Gazipur, Bangladesh |

**Scientific publications**

*Publications in international journals with peer review cited in the Science Citation Index (IF = impact factor for 2017)*

**Akter M**., Deroo H., Kamal A. M., Kader M. A., Verhoeven E., Decock C., Boeckx P., Sleutel S., 2017. Impact of irrigation management on paddy soil N supply and depth distribution of abiotic drivers. Agric. Ecosys. Environ. (submitted).

**Akter, M.**, Deroo, H., De Grave, Eddy., Van Alboom, T., Kader, M., A., Boeckx, P., Sleutel, S. Link between paddy soil mineral nitrogen release and iron and manganese reduction examined in a rice pot growth experiment. Geoderma (submitted).

**Akter, M**., M A Kader, S Pierreux, M T Gebremikael, P Boeckx, S Sleutel. 2016. Control of Fe and Mn availability on nitrogen mineralization in subtropical paddy soils. Geoderma. 269, 69-78. IF = 4.036

*Publications in national peer-reviewed journals*

**Akter, M.,** M. A. Haque, M. A. Monsur, M. K. Quais, H. Begum. 2009. Biological activity of celaflor against pulse beetle, *Callosobruchus maculatus* (Fab.). Bangladesh j. entomol. 19, 79-89.

Saha, P. K., **M. Akter**, M. Hossain, S. K. Zaman. 2012. Zinc and nitrogen interaction in hyv rice grown in calcarious soil. Bangladesh Rice J. 16, 41-45.

Saha, P. K., S M M Islam, **M. Akter,** S. K. Zaman. 2012. Nitrogen response behavior of developed promising lines of T. Aman rice. Bangladesh J. Agril. Res. 37, 207-213.

Saha, P. K., **M. Akter,** M. A.M. Miah, S. K. Zaman. 2011. Effects of organic and inorganic sources of k on rice yield and soil k balance in the rice-rice cropping system. Bangladesh J. Agril. Res. 36, 305-311.

Rahman, M. Z., M. A. A. Mamun, M. P. Ali, **M. Akter**. 2010. Integrated use of cowdung and acacia leaves with inorganic nitrogenous fertilizer in rice cultivation. Bangladesh J. Prog. Sci. & Tech. 8, 275-278.

Rahman, M. Z., M. A. A. Mamun, M. P. Ali, **M. Akter**. 2010. Nutrient uptake and soil properties as influenced by integrated use of organic manures and inorganic fertilizers in rice cultivation. Bangladesh J. Prog. Sci. & Tech. 8, 291-294.

M. K. Quais, K. S. Islam, M. Jahan, M. A. Monsur, **M. Akter**. 2010. Evaluation of neem, mahogoni and karanja oils for their residual effect against pulse beetle, C*allosobruchus chinensis* and seed viability. Bangladesh j. entomol. 20, 99-108.

Rahman, F., A .T. M. S. Hossain, **M. Akter,** R. Khanam. 2009. Effect of different aged poultry litter on growth, yield and economics of wetland boro rice. Eco-friendly Agril. J. 2, 920-925.

Saha, A. K., I. Hossain, M. A. Monsur, M. K. Quais, **M. Akter** 2009. Effect of amistar and garlic extract in controlling purple blotch and storage diseases of onion. Bangladesh J. Plant Pathol. 25, 67-70.

## Scientific activities

### *Participation in symposia with oral presentation*

**Akter M.,** Sleutel, S., Kader, M. A., Pierreux, S., Kamal, A. M., Boeckx, P., 2017. Evaluating the Performance of Water Conserving Technologies in Rice Cultivation to Mitigate Greenhouse Gas Emission. Oral presentation at the 2nd Conference on Conservation Agriculture for Smallholders (CASH-II), 14-16 February 2017, Mymensingh, Bangladesh.

**Akter M.,** M. A., Kader, S., Pierreux, A. M., Kamal, P., Boeckx, Sleutel, S., 2016. Depth distribution of abiotic drivers of N mineralization from a continuously and intermittently flooded Bangladeshi paddy soil. Oral presentation at the 5th National Convention and International Agricultural Conference, 29-30 September 2016, Dhaka, Bangladesh.

**Akter, M.**, Kader, M. A., Pierreux, S., Boeckx, P., Kamal, A. M., Sleutel, S., 2016. Depth distribution of abiotic drivers of N mineralization and methane emission from a continuously and intermittently flooded Bangladeshi paddy soil. Oral presentation at the European Geosciences Union General Assembly. 17-22 April, 2016, Vienna, Austria.

Sleutel S., **Akter, M**., Kader, M. A., Begum, S. A., De Neve, S., 2014. Is there a link between reduction of Fe and Mn and anaerobic N mineralization in floodplain paddy soils in Bangladesh? In: Proceedings of the Paddy soils international workshop: Biogeochemistry of submerged agro-ecosystems: properties, processes, cycles and functions. 21-25 September, 2014, Freising, Germany.

### *Participation in symposia with poster presentation*

**Akter, M.,** Thilakarathna, E. M. S.K., Deroo, H., Kader, M. A., Boeckx, P., Sleute**l**, S., **2017.** Controls of organic N mineralization in paddy soil of Sri Lanka with spatial variation in

edaphic factors. Poster presentation at the 6th International symposium on Soil Organic Matter. 3-7 September, 2017. Harpenden, United Kingdom.

Pierreux, S., Verhoeven, E., **Akter, M.**, Sleutel, S., Said-Pullicino, D., Romani, M., Boeckx, P., 2016. Evaluating the relative contribution of methane oxidation to methane emissions from young floodplain soils under alternative irrigation management. Poster presentation at the European Geosciences Union General Assembly. 17-22 April, 2016, Vienna, Austria

**Akter, M.**, Kader, M. A., Pierreux, S., Boeckx, P., Kamal, A. M., Sleutel, S., 2015. Greenhouse gas emissions from a continuously and intermittently flooded Bangladeshi paddy field in relation to redox potential, soil moisture and soil solution chemistry depth profiles. Poster presentation at the 5th International symposium on Soil Organic Matter. 20-24 September, 2015. Goerg-August-Universitat, Göttingen, Germany.

**Akter, M**., Sleutel, S., Kader, M. A., 2014. Effect of N and water management on greenhouse gas emission and N availability in paddy soils of Bangladesh. Poster presentation at the Paddy Soils international workshop on Biogeochemistry of submerged agro-ecosystems: properties, processes, cycles and functions. 21-25 September, 2014, Freising, Germany.